MECHANICAL AND TRIBOLOGICAL CHARACTERIZATION OF RED MUD AND TUNGSTEN CARBIDE PARTICLE REINFORCED ALUMINIUM METAL MATRIX HYBRID COMPOSITES

A Dissertation work
Submitted in partial fulfilment of the requirements for
the award of Degree of

DOCTOR OF PHILOSOPHY

in

MECHANICAL ENGINEERING

Submitted by

NEELIMA DEVI CHINTA

(Roll No. 701111)

DEPARTMENT OF MECHANICAL ENGINEERING

NATIONAL INSTITUTE OF TECHNOLOGY

WARANGAL, T.S, INDIA - 506004

APRIL – 2017

MECHANICAL AND TRIBOLOGICAL CHARACTERIZATION OF RED MUD AND TUNGSTEN CARBIDE PARTICLE REINFORCED ALUMINIUM METAL MATRIX HYBRID COMPOSITES

A Dissertation work
Submitted in partial fulfilment of the requirements for
the award of Degree of

DOCTOR OF PHILOSOPHY
in
MECHANICAL ENGINEERING

Submitted by

Neelima Devi Chinta
(Roll No. 701111)

Under the Guidance of

Prof. N. Selvaraj
Supervisor
Mechanical Engineering Department
National Institute of Technology
Warangal – 506004
&
Prof. V. Mahesh
Co-Supervisor
Mechanical Engineering Department
S.R. Engineering College
Warangal – 506371

DEPARTMENT OF MECHANICAL ENGINEERING
NATIONAL INSTITUTE OF TECHNOLOGY
WARANGAL, T.S, INDIA - 506004
APRIL - 2017

DEPARTMENT OF MECHANICAL ENGINEERING
NATIONAL INSTITUTE OF TECHNOLOGY
WARANGAL-506004 (T.S), INDIA.

CERTIFICATE

This is to certify that the dissertation work entitled "**MECHANICAL AND TRIBOLOGICAL CHARACTERIZATION OF RED MUD AND TUNGSTEN CARBIDE PARTICLE REINFORCED ALUMINIUM METAL MATRIX HYBRID COMPOSITES**", which is being submitted by **Mrs. Neelima Devi Chinta(Roll No.701111)**, is a bonafide work submitted to the Department of Mechanical Engineering, National Institute of Technology, Warangal in partial fulfilment of the requirement for the award of the degree of **Doctor of Philosophy in Mechanical Engineering.**

To the best of our knowledge, the work embodied in this thesis has not been submitted to any other university or institute for the award of any other degree.

Prof. V.Mahesh
Co-Supervisor
Department of Mechanical Engineering
S.R. Engineering College
Warangal-506371

Prof. N.Selvaraj
Supervisor
Department of Mechanical Engineering
National Institute of Technology
Warangal-506004

THESIS APPROVAL FOR Ph.D.

This thesis entitled **"Mechanical and Tribological Characterization of Red mud and Tungsten Carbide particle reinforced Aluminium Metal Matrix Hybrid Composites"** by **Mrs. Neelima Devi Chinta** is approved for the degree of Doctor of Philosophy.

Examiners

_____

_____

_____

Supervisor(s)

Dr. V.Mahesh
(External Supervisor)

Professor, Mechanical Engineering Department, S.R Engineering College Warangal

Dr. N. Selvaraj

Professor, Mechanical Engineering Department, NIT Warangal

Chairman

Prof. S. Srinivasa Rao

Head, Mechanical Engineering Department, NIT Warangal

DECLARATION

This is to certify that the work presented in the thesis entitled. **"MECHANICAL AND TRIBOLOGICAL CHARACTERIZATION OF RED MUD AND TUNGSTEN CARBIDE PARTICLE REINFORCED ALUMINIUM METAL MATRIX HYBRID COMPOSITES"** is a bonafide work done by me under the supervision of Prof.N.Selvaraj and Prof. V.Mahesh. It was not submitted elsewhere for the award of any degree. I declare that this written submission represents my ideas in my own words and where others' ideas or words have been included, I have adequately cited and referenced the original sources. I also declare that I have adhered to all principles of academic honesty and integrity and have not misrepresented or fabricated or falsified any idea / data / fact / source in my submission. I understand that any violation of the above will be a cause for disciplinary action by the Institute and can also evoke penal action from the sources which have thus not been properly cited or from whom proper permission has not been taken when needed.

Place: C.Neelima Devi

Date: (Roll No: 701111)

ABSTRACT

Aluminium metal matrix hybrid composites have evoked a keen interest in recent times for potential applications in aerospace and structural applications owing to their superior strength-to-weight ratio and high temperature resistance. Using high performance materials, it is possible for the modern aircraft to rotate larger degree while retaining its strength in both the airframe and propulsion systems. To obtain continual performance, designers are constantly searching for lighter and stronger materials.

The attractiveness of aluminum is that it is a relatively low cost, light weight metal that can be heat treated to fairly high strength levels and it is one of the most easily fabricated high performance materials. Metal matrix hybrid composites have the future of fulfilling these requirements. The present work is focussed on the characterisation of the mechanical and wear behaviour of red mud and tungsten carbide particle reinforced aluminium through conventional sintering.

The objective of this research work is aimed at finding out utilization of industrial byproducts such as red mud for value added applications and also helps to solve the environmental problems. In the current work, aluminium is mixed with red mud at micro as well as nano level and tungsten carbide to form metal matrix hybrid composites, synthesized by powder metallurgy, which exhibit superior mechanical and tribological properties and applications.

An environmental hazardous waste material, red mud is obtained from bayer's process during the processing of alumina. Red mud received from NALCO (National Aluminium Corporation) has been subjected to sieve analysis for micron level of 100 μm, 150 μm and 200 μm and milled to nano level of 42 nm using high energy ball mill. Hardness and compression strength properties are improved for nano level red mud with pure aluminium test specimen at 42 nm size and 6% weight fraction of red mud. As compared to micro level, nano level has achieved the highest wear resistance due to the interfacial area between the aluminium matrix material and reinforced red mud material.

The mechanical property such as hardness is found at normal condition and heat treatment conditions, for which mathematical modeling is done by regression analysis. Further compression test and validation of compression test is performed with Deform -2D Software. An increase in hardness and compression strength is observed with increase in the amount of percentage weight fraction of red mud. Hardness values variation depicts the information that nano red mud specimens have more hardness when compared with micro nature specimens.

Micro structural observation such as Scanning Electron Microscope (SEM) analysis and Energy Dispersive X-Ray Spectroscopy (EDX) are performed. The work also investigates on tribological characterization such as wear behavior of pure aluminium with red mud at normal and heat treatment conditions with varying 2%, 4% and 6% weight fractions of red mud, particle size of 100 μm and 42 nm and 200 rpm, 400 rpm and 600 rpm speed of pin-on-disc wear testing machine at 10N, 20N and 30N load.

The mathematical modeling is done by regression analysis for prediction of wear behaviour at normal and heat treatment conditions. The predicted equations at normal and heat treatment conditions are significant in nature with near unity R square values. The predicted mathematical modeling results of wear rate using regression analysis and experimental values are within the limits of 1-4% error difference of pure aluminium-red mud metal matrix composites and pure aluminium-red mud-tungsten carbide hybrid metal matrix composites.

CONTENTS

NOMENCLATURE/ABBREVIATIONS

Al - Aluminium

RM - Red mud

WC - Tungsten Carbide

P/M –Powder Metallurgy

μm - micro meter

nm - nano meter

VHN - Vickers Hardness Number

Φ - Diameter

% - Percentage

MPa - Mega Pascals

ρ – Density, kg/m³

m_1 - Initial mass, gm

m_2 - Final mass, gm

Δm - Initial mass – Final mass, gm

Vs - Sliding velocity, m/sec

t – Time, sec

F_f - Average frictional force, kgf

F_n - Applied load, kgf

μ - Co-efficient of friction = F_f / F_n

R.D - Rolling / Sliding distance (L), m

W_r - Wear rate = $\Delta m/L$, N/m

W_v - Volumetric Wear rate = $\Delta m / \rho t$, m^3/sec

W_s - Specific Wear rate = $W_v / (V_s F_n)$, $m^3/N\text{-}m$

RPM - Revolutions Per Minute

μ - Co-efficient of friction

XRD - X - Ray Diffraction

SEM - Scanning Electron Microscope

EDX – Energy Dispersive X-Ray Spectroscopy

^0C – Degree Centigrade

N/m – Newton per metre

Kgf – Kilogram force

LIST OF FIGURES

LIST OF TABLES

CHAPTER 1

INTRODUCTION

The beginning of the history with stone age followed by bronze, iron, aluminium and its alloys are significant for the growth of science and technology. The capabilities of higher strength, light weight, and cost effective composites are pioneered in the world of advanced materials [1-3]. Nowadays there is a tremendous usage of composites with good structural properties, better thermal, tribological, electrical and environmental applications. The present chapter is describing composites, types of composites and their manufacturing methods.

1.1 ENGINEERING MATERIALS AND THEIR APPLICATIONS

Many of the modern technologies require new engineering materials with exceptional combinations of properties that cannot be met by the conventional metal alloys and polymeric materials. This is especially true for engineering materials that are needed for automobile, aerospace, underwater and structural applications. Automobile and aircraft engineers are tremendously searching for new engineering materials that have low densities, strong, abrasion, corrosion and impact resistant.

In engineering, an accomplishment design depends on upon the selection of materials having the most desirable properties for a given application. While at the same time, the cost is also an important consideration for the selection of materials [5]. Nowadays, the scientists, researchers and engineers have ingeniously mixed various metals, ceramics and polymers to develop a new generation of extraordinary materials. Most of the engineering materials have been created in the form of composites to improve the wear behaviour and mechanical characteristics such as hardness, compression strength, stiffness, toughness and high-temperature resistance [5]. The new engineering materials are used in automotive industry, aerospace, sporting goods and construction purpose etc., [6-8].

1.2 ALUMINIUM COMPOSITES

A composite material consists of two or more distinct physical and/or chemical in nature constituents with separating interface / interphase between them. The constituents of composite materials are named as matrix and reinforcement materials. Composite materials are broadly classified into Metal Matrix Composites (MMC), Polymer Matrix Composites (PMC) and Ceramic Matrix Composites (CMC) [81-84]. The polymer matrix composites have poor high-temperature capabilities, low strength, and stiffness. The ceramic matrix composites have very low toughness and difficult to machine [9].

1.2.1 Salient features of Metal Matrix Composites (MMC)

The metal matrix composites (MMC) are having good strength, ductility, high toughness, magnetic properties, electrical and thermal conductive [85-86]. According to the type of reinforcement, particle, laminar, flake, fiber and filler varieties are reinforced matrix composites [78]. The various types of composites based on reinforcement are shown in Figure 1.1.

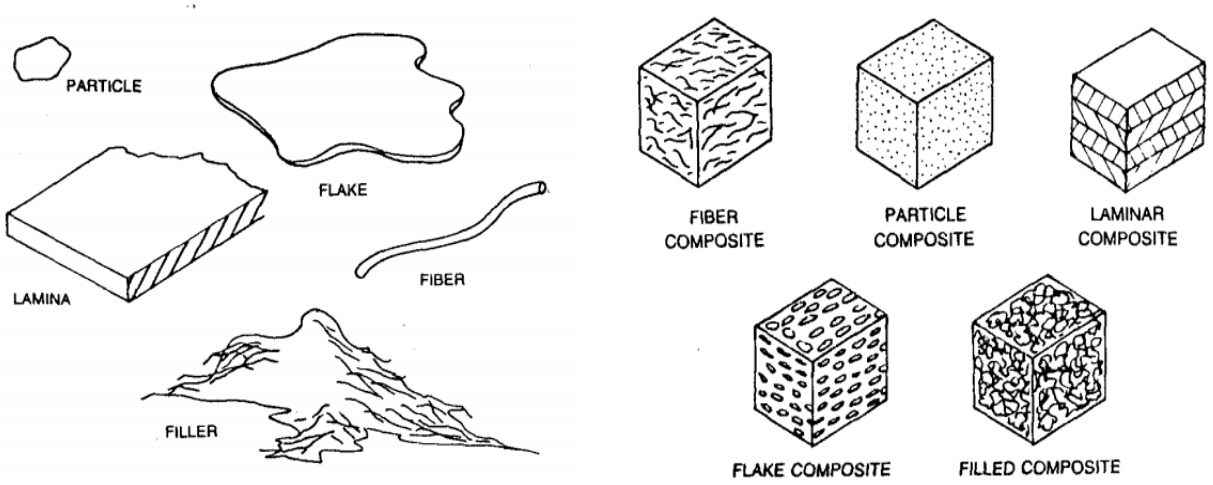

Figure 1.1: Various types of composites based on reinforcement

Aluminium is a soft, light, gray metal that resists corrosion when pure, regardless of its chemical activity because of a thin surface layer of oxide [90]. Aluminium has a wide range of applications in the aerospace and automotive industries due to better strength-to-weight ratio. The reduction in weight saves the fuel requirements and emissions which in turn affects the cost problems and environmental advantages [18 and 88].

Aluminium metal matrix composites have the more impact and potential to be utilized in various applications of engineering fields such as aerospace, automobile, naval, mechanical, structural and defence organizations [11, 13-14, 21-22]. The various applications of aluminium composites are as shown in Figure 1.2.

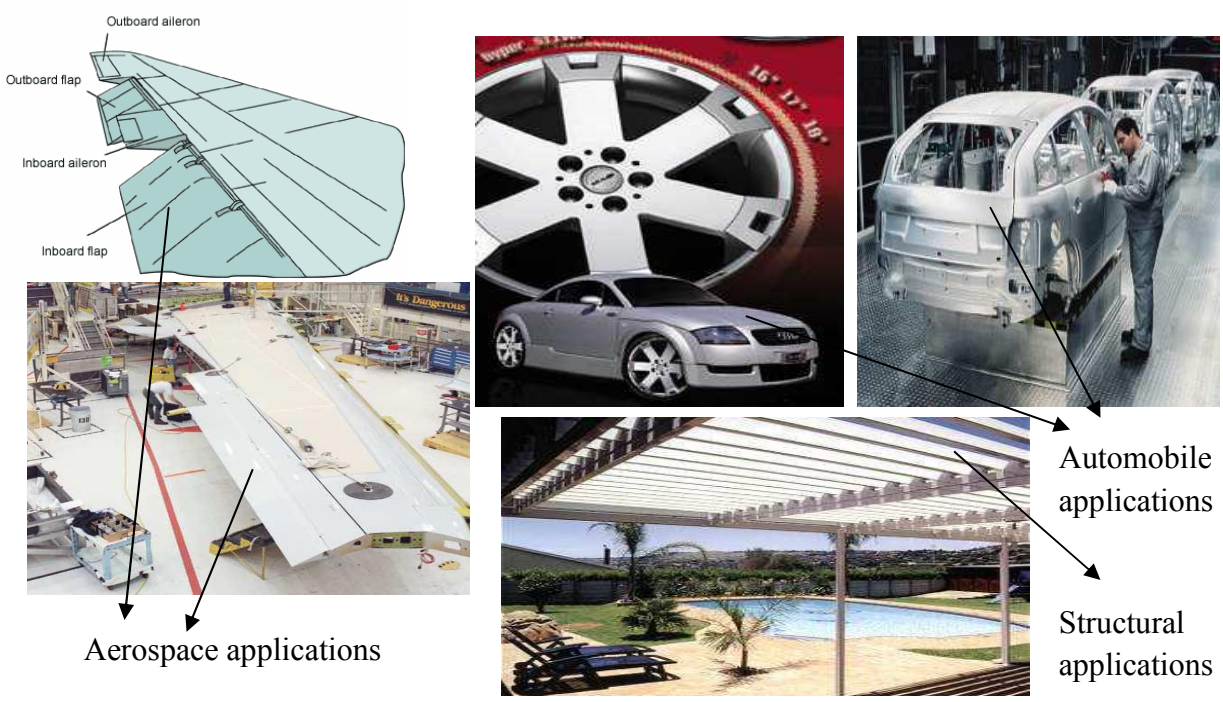

Figure 1.2: Various applications of aluminium composites

The main limitation of aluminium composites is not satisfying the combination of desired needs for advanced engineering applications such as manufacturing of Boeing 767, Airbus A 380 and race cars etc.

1.3 ALUMINIUM HYBRID COMPOSITES

Aluminium hybrid composites are finding increased demand and usage in new aircraft designs due to their higher strength capabilities. Aluminium metal matrix hybrid composites have considerable importance since their mechanical and tribological properties are superior over non-reinforced alloys [4-6]. Aluminium-red mud-tungsten carbide hybrid composites will become alternative materials for different engineering applications with their excellent qualities like light weight, environment friendliness, quality, performance with superior mechanical properties, wear characteristics and low cost [10, 19-20]. Therefore, the innate ability of aluminium hybrid composites with a wide variety of applications are lying in various research activities all over the world [58, 62, 70].

The potential demands are met with a number of performance capabilities such as improved mechanical characteristics and better tribological behaviour etc., using hybrid composites. The applications of aluminium hybrid composites are shown in Figure 1.3.

Figure 1.3: Applications of aluminium hybrid composites

1.4 MANUFACTURING METHODS

The suitability of various manufacturing methods for composite materials depends on engineering applications, synthesis of the material, characteristics of the matrix material, reinforcement material, and heat treatment conditions.

1.4.1 Solid state manufacturing methods

There are many ways to manufacture metal matrix composites by solid state techniques.

1.4.1.1 Diffusion Bonding

Diffusion bonding is defined as common solid state welding method used to join similar or dissimilar metals. There are many variants of the basic diffusion bonding process; however, all of them involve a step of simultaneous application of pressure and high temperature. Interdiffusion of atoms from clean metal surfaces in contact at an elevated temperature leads to welding. Matrix alloy foil and fiber arrays, composite wire, or monolayer laminae are stacked in a predetermined order. Figure 1.4 shows diffusion bonding technique, also called the foil-fiber-foil process.

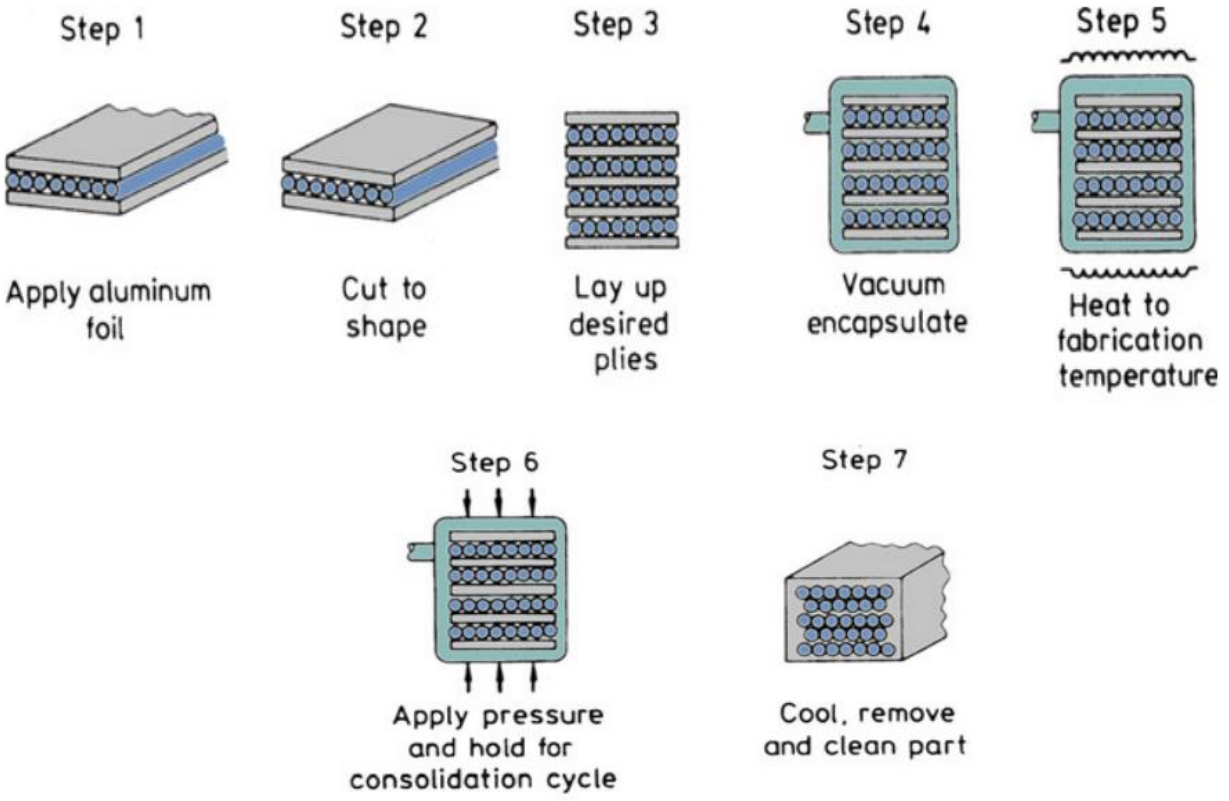

Figure 1.4: Diffusion bonding technique [Courtesy of J. Baughman]

1.4.1.2 Powder Metallurgy Route

The processing of powder metallurgy can be divided into four stages. Preparation of the powder, mixing or blending of powders in desired proportions, compacting the powders into desired shapes in suitable dies at specified pressures and sintering the compacted components in furnaces provided with controlled atmospheres. For the preparation of powders, mechanical pulverization, atomization, chemical reduction process and electrolytic process are used. Sintering involves the heat treatment of powder compacts at elevated temperatures, in the temperature range where diffusion mass transport is appreciable [10-11, 72]. The different stages involved in the sintering process are as shown in Figure 1.5.

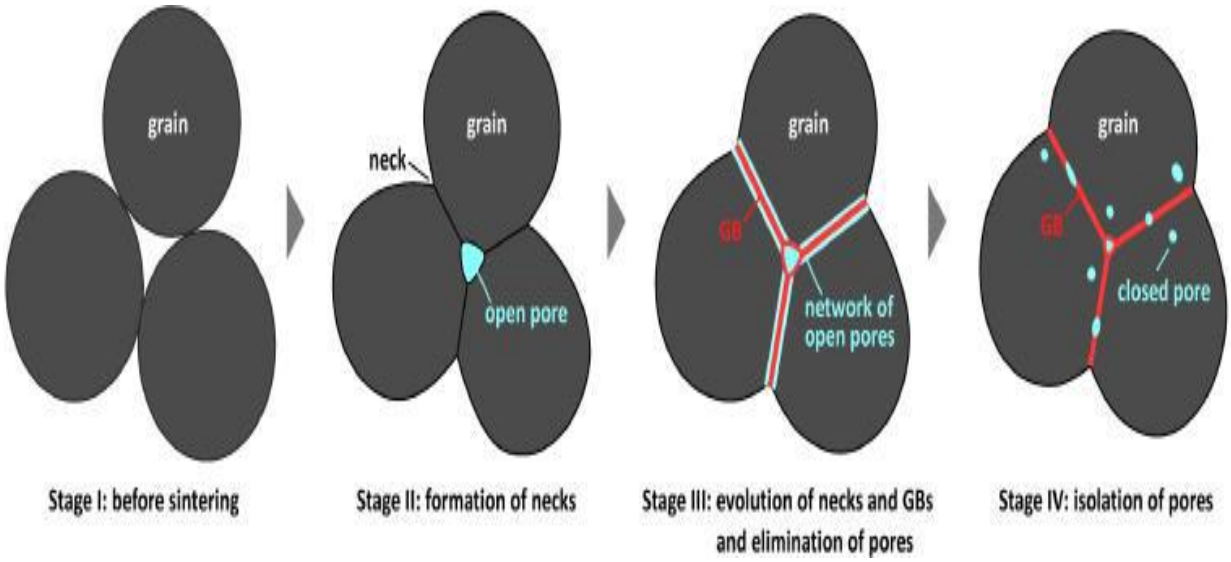

Figure 1.5: Different stages involved in sintering process

1.4.2 Liquid state manufacturing methods

There are different methods to manufacture metal matrix composites by liquid state techniques.

1.4.2.1 Liquid Infiltration method

Liquid-phase infiltration faces difficulties mainly with ceramic reinforced material in wet condition to prepare MMCs. Before infiltration, fiber coatings are applied which increases the wettability and control reactions.

1.4.2.2 Squeeze Casting

The squeeze casting process is shown in Figure 1.6. In this process, application of pressure can be done upto solidification. The molten metal is imposing through tiny pores of the fibrous material. Better wettability between the reinforced material and matrix can be obtained in squeeze casting [44].

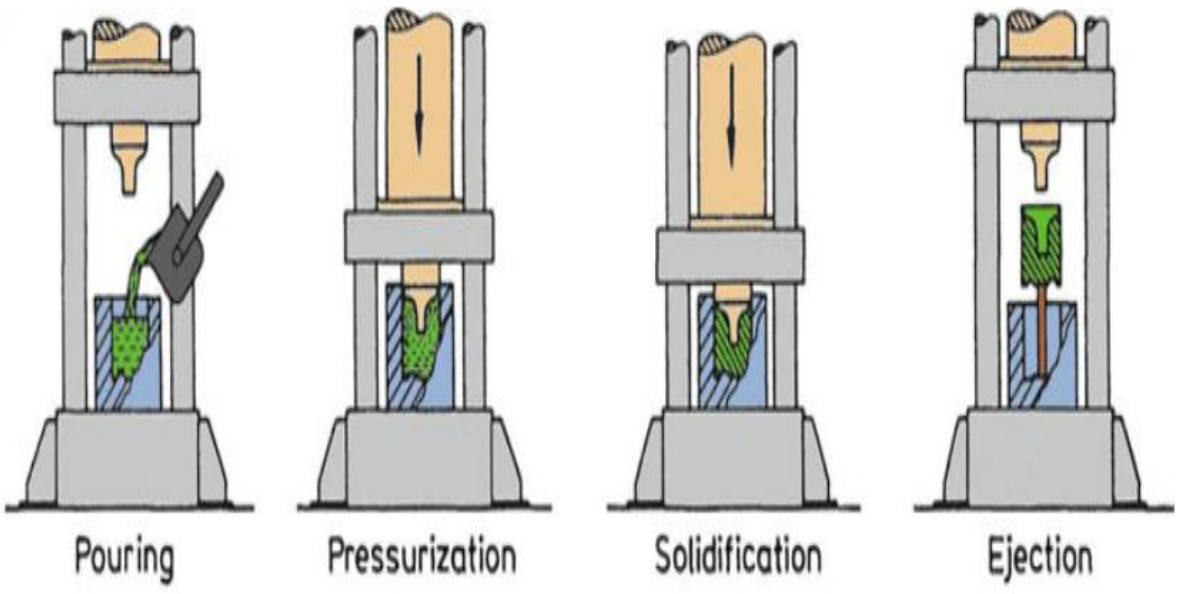

Figure 1.6: Squeeze casting process

[Courtesy of G. Eggeler]

1.4.2.3 Spray forming Technique

The Spray forming technique is very fast and totally computer-controlled method. In this technique, spray gun is utilized to atomize the molten aluminum alloy matrix. Ceramic particulates like silicon carbide are injected into this stream. Figure 1.7 shows a schematic of spray forming process.

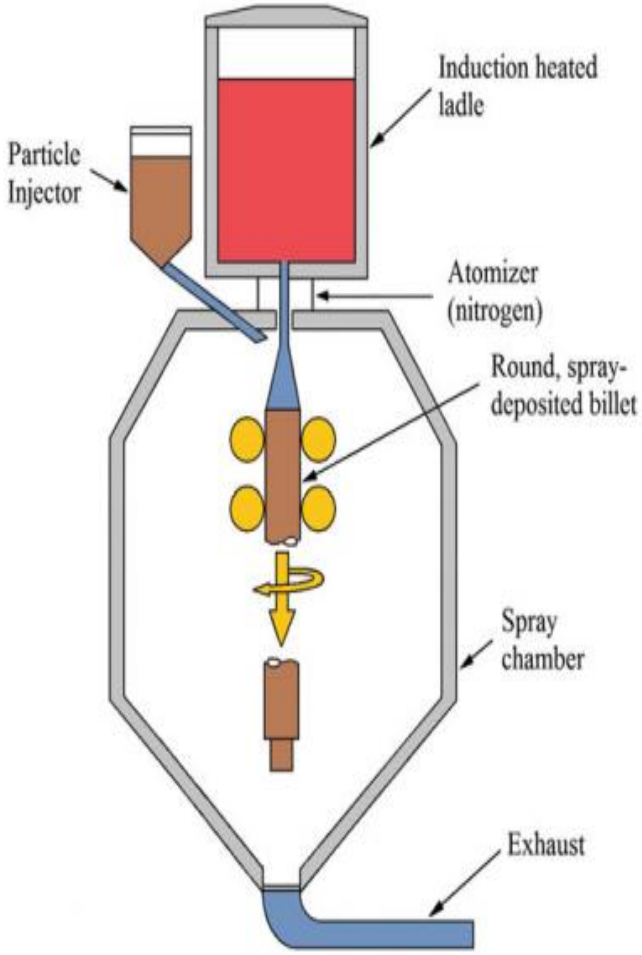

Figure 1.7: Spray forming process

[Courtesy of Krishan. K.Chawla]

1.4.2.4 Compocasting

Compocasting is one of the most economical methods of fabricating a composite with discontinuous fibers. It can be performed at temperatures lower than those conventionally employed in foundry practice during pouring, resulting in reduced thermochemical degradation of the reinforced surface. When a liquid metal is vigorously stirred during solidification, it forms slurry of fine, spheroidal solids floating in the liquid. Stirring at high speeds creates a high shear rate, which tends to reduce the viscosity of the slurry even at solid fractions as high as 50 to 60% volume. The process of casting such slurry is called rheocasting [56]. The slurry can be blended with short fibers or whiskers, particulates prior to casting. The new developed method of rheocasting is to produce metal matrix composite parts known as Compocasting. Compocasting owns a homogeneous distribution of reinforced material in the matrix. Continuous mixing of the slurry creates good contact between reinforcement material and matrix. Better bonding is obtained by decreasing the slurry viscosity as well as improving the mixing time. [9].

1.4.2.5 Stir casting

Stir-casting technique is used for producing metal matrix composites. In this technique, the reinforced particulates and matrix material are mixed in crucible and then it is poured into desired mould shape before the complete solidification [62 and 65-66]. In this process, wettability between reinforced material and matrix material is difficult without proper stirring. In the Figure 1.8 a) stir casting equipment and Figure 1.8 b) the crucible inside the stir casting furnace are shown.

Figure 1.8: a) Stir casting equipment b) Crucible inside the stir casting furnace

In this present work, powder metallurgy route has been adopted for preparing the hybrid metal matrix composites out of all manufacturing methods. Powder metallurgy process has efficient material utilization. Powder metallurgy is used for better material characteristics. Their improved material characteristics make them potentially suitable for several applications in aerospace like airframe structures, wings, fuselage, light structures, engine components and other structural applications. Light weight machine components, drive belt pulleys, hubs, caps and connection collars are manufactured through powder metallurgy route in marine industry. The automobile components such as shock absorber, oil transmission gears, piston, cam shaft, pulleys, rod guides, anti-lock breaking system and push rods etc., are prepared through powder metallurgy. Powder metallurgy process has the capability of manufacturing complex shapes and parts. It is suitable for medium to high volume range component production. Furthermore, parts that require very close dimensional tolerances (e.g., gears and bushings) may be economically produced using powder metallurgy technique.

1.5 ORGANIZATION OF THE THESIS

The entire thesis has been divided into seven chapters and its details are given below.

1. Chapter - 1 presents the comprehensive overview of aluminium composites, aluminium hybrid composites, and manufacturing methods. The significance of engineering materials and their applications are discussed.
2. Chapter – 2 provides a review of literature relevant to the current investigation. The main objective of the critical review of the literature was to carefully examine any research works done previously related to the present work and identified the gaps from literature. It reports the motivation, objectives, aim and overall research plan of the thesis.
3. Chapter - 3 gives the selection of materials, experimental details on high energy ball milling, X-Ray Diffraction (XRD) analysis for nano red mud, the experimental setup for conventional sintering through powder metallurgy for sample preparation.
4. Chapter - 4 presents mechanical characterization of pure aluminium with red mud and pure aluminium with red mud and tungsten carbide such as hardness at normal and heat treatment conditions, mathematical modeling using regression analysis for hardness values at normal and heat treatment conditions, compression test and validation of compression test results with Deform -2D software and microstructural observations such as SEM and EDX used in the current work.
5. Chapter - 5 provides a tribological characterization of pure aluminium with red mud at normal and heat treatment conditions and mathematical modeling using regression analysis for various testing conditions.
6. Chapter - 6 presents results and discussions of the investigations in which the experimental results of the tribological characterization of pure aluminium with red mud and tungsten carbide at normal and heat treatment conditions are analyzed. The mathematical modeling using regression analysis for various testing conditions are discussed.

7. Chapter - 7 contains the conclusions drawn from the current research work, limitation of work and the scope for future research work.

1.6 SUMMARY

The present chapter gives the introduction to the engineering materials and their applications are discussed. The importance of aluminium composites and aluminium hybrid composites are provided in this chapter. The present chapter also provides the various manufacturing methods and organization of the thesis.

CHAPTER-2

LITERATURE REVIEW

2.1 INTRODUCTION

The review of the literature was carried out on various engineering materials and their applications, metal matrix composites, aluminium composites and aluminium hybrid metal matrix composites. Many researchers have investigated on desirable properties of alloys, composites, metal matrix composites and hybrid composites. Aluminium composites have become more considerable, because of light weight, good strength, better toughness and resistance to wear and corrosion. Recent advancements in material characterization with composite materials were improved using metal matrix composites and hybrid composites.

2.2 ENGINEERING MATERIALS AND THEIR APPLICATIONS

The role of nano-size reinforcement and milling on the synthesis of nano-crystalline aluminium alloy composites by mechanical alloying and their applications were studied. A wide variety of reinforcement particulates such as Al_2O_3, SiC, B_4C, Si_3N_4 TiC, TiO_2, TiB_2 and graphite have been reinforced into aluminium composites. High-energy wet ball milling was successfully employed to synthesize nano crystalline Al 6063 alloy powders reinforced with 1.3 vol.%Al_2O_3, 1.3 vol.%Y_2O_3 and 0.65 vol.%Al_2O_3/0.65 vol.%Y_2O_3 at nano-size level [1].

The various innovative methodologies for the utilisation of wastes from metallurgical and allied industries were investigated. The main limitations of stir cast Al-SiC MMC are improper distribution of SiC reinforcement in matrix and less wettability of SiC reinforcement particle with molten Al. Literature survey indicate that various properties of stir cast Al-SiC MMC depends upon fabrication method, volume fraction, shape, size of particles and distribution and properties of constituents [32, 74, 89]. The utilisation of red mud in different industrial applications and structural investigation relating to the cement activity of bauxite residue which is also known as red mud was studied.

The aluminum alloy (A356.1) matrix composites reinforced with 1.5, 2.5 and 5 vol% nano-particle MgO were fabricated via stir casting method. Optimum amount of reinforcement and

casting temperature were determined by evaluating the density, microstructure and mechanical properties of composites [75]. The annotated equilibrium diagrams of some aluminium alloy systems were reported. Yong Liu et.al, red mud derived from a combined Bayer Process and bauxite calcination method was characterized. The results show that pH of the red mud decreased with increasing duration of storage time. Na dominated among the soluble cations, but the concentration of soluble Na decreased with increasing duration of storage time as a result of leaching [76].

The aluminium alloys through liquid phase sintering were studied and impact of lubricants and aids for sintering were also described [55]. Sintering under pure nitrogen resulted in higher sintered densities as compared with vacuum sintering for this grade of Al alloy. Tensile properties of the degassed and vacuum sintered (and T6 tempered) prealloyed powder compacts were higher than those of the equivalent alloy prepared by elemental mixing and comparable with those of the commercial (wrought) 6061 Al alloys.

The reasonable utilisation of red mud in the cement industry was carried out [79]. It was found that the cement manufactured by red mud having capabilities of reduction in energy consumption and increases the strength of cement which resist from sulphate problem [80]. The development and growth of aluminum P/M as a viable component of the industry is chronicled. This historical profile identifies primary drivers and early pioneers of the technology. Some key advances in monolithic alloy powders and composite powders are reviewed in relation to the fabrication of parts by pressing and sintering.

The usage of red mud for different applications such as the removal of harmful pollutants from water was studied [12]. The development and growth of aluminum P/M as a viable component of the industry is chronicled. This historical profile identifies primary drivers and early pioneers of the technology. Some key advances in monolithic alloy powders and composite powders are reviewed in relation to the fabrication of parts by pressing and sintering [15-17]. The corrosion resistance of various metal matrix composites with aluminium and its automotive applications were investigated.

Red mud (an aluminium industry waste) has received wide attention as an effective adsorbent for water pollution control, showing significant adsorption potential for the removal of various aquatic pollutants. Red mud has been found to be efficient for the removal of various aquatic pollutants, especially arsenic and phosphate. However, there is still a need to investigate the practical utility of these adsorbents on a commercial scale [11-12].

The utilisation of a treated bauxite waste i.e. red mud for environmental sustainability and cement industry applications were reported [51, 60]. The average automobile currently produced in North America contains about 90 kg of aluminum. That figure is expected to grow, driven by environmental needs, the Partnership for a New Generation of Vehicles, safety mandates, consumer preferences, and an increasingly global marketplace. This paper examines those issues, along with current automotive applications for aluminum, the technology being developed to meet future demand, and the forces driving changes in technology [63].

2.3 ALUMINIUM COMPOSITES

The various processing and different properties of discontinuously reinforced aluminium composites were analysed in addition to magnesium metal matrix composites [65]. The effect of fibre reinforcement of aluminium, magnesium and Mg-9Al-1Zn on the wear properties has been investigated [92]. Dry sliding, two- and three-body abrasion and solid particle erosion testing were performed [64, 87]. The results show that the tribological behaviour of metal matrix composites (MMCs) depends very much on the type of MMC and the type of contact situation, *i.e.* tribosystem. In erosion, aluminium and magnesium displayed decreasing wear resistance with higher fibre content whereas the magnesium alloy was hardly affected. The relations between wear rate, wear mechanisms and matrix parameters are discussed [61, 97-103].

Discontinuously-reinforced aluminum (DRA) SiC whisker or particle-reinforced Al-alloy matrix composites produced by P/M methods have progressed toward commercial applications, supported by growing data bases and large-scale production facilities. Attention is presently given to the elastic modulus, plastic, ductile, and toughness characteristics of representative DRA formulations, as well as to the DRAs commercially available in the forms of sheets, extrusions, and optical and instrument grade structures able to supplant beryllium [3].

The high strength and highly-uniform composites produced by compocasting and cold rolling processes were investigated. Silicon carbide reinforced aluminum alloy composite materials produced by casting methods are increasingly used in many engineering fields. Composites fabricated by compocasting method were rolled at five different reductions of 30, 60, 75, 85 and 95%. The rolled specimens exhibited reduced porosity as well as a more uniform particle distribution when compared with the as-cast samples. Microscopic investigations of the composites after 95% reduction showed an excellent uniform distribution of silicon carbide particles in the matrix. During cold rolling process it was observed that the tensile strength and ductility of the samples increased by increasing the reduction content [7].

Many researchers have studied the importance of metal matrix composites for aerospace propulsion systems, the usage of aluminium composites in automotive applications, the wear behaviour of aluminium and various mechanical properties of liquid-phase sintered seeded silicon carbide. The effect of seeding on the microstructure of these liquid-phase sintered materials was investigated. So the adding of seeds did not seem to control the matrix microstructure. The image analysis of microstructures allowed to show that the growth of equiaxed grains was continuous, whereas that of elongated grains occurred in two steps. The influence of microstructure on mechanical properties was also examined. The hardness of materials was inversely proportional to the square root of mean grain diameter and their fracture toughness was proportional to this square root. Such results suggested that the mechanical properties could be controlled by the microstructure [8-9].

The red mud as pulverised fuel and utilisation of iron ore for developing ceramic tiles were investigated. Environmental compatibility of a treated red mud was studied in order to evaluate its

possible recycling in environmental compartments [41]. Moreover, in order to better evaluate the environmental compatibility, three different types of eco-toxicological tests were applied (Microtox™ test, ASTM microalgae toxicity test and sea urchin embryo toxicity test). These chemical and eco-toxicological tests gave encouraging results. The possibility to use this material for treating contaminated waters and soils was evaluated, again with particular attention to the Italian regulatory system, through experiments on the treated red mud metal trapping ability and on the subsequent release of trapped metals, at low pH conditions. The treated red mud showed a general high metal trapping capacity and the release at low pH was generally low [14, 15, 49].

The processing of metal matrix composites using powder metallurgy and strengthening mechanisms were described. The processing methods utilized to manufacture particulate reinforced MMCs can be grouped depending on the temperature of the metallic matrix during processing. Accordingly, the processes can be classified into three categories: (a) liquid phase processes, (b) solid state processes, and (c) two phase (solid-liquid) processes. Regarding physical properties, strengthening in metal matrix composites has been related to dislocations of a very high density in the matrix originating from differential thermal contraction, geometrical constraints and plastic deformation during processing [16-19].

A new development in managing these tailings by converting them into value added products such as ceramic floor and wall tiles for building application. These tiles have high strength and hardness compared to conventional tiles and confirms to most of the EN standards. Energy economy and lower production costs are some other benefits [21, 59]. The wear behaviour of aluminium alloys and preparation of metal matrix composites through the sintering process and Al–Mg–Cu-based composites were studied [21, 24-26, 31, 77].

Al_2O_3/SiC ceramic preforms are processed and liquid aluminium infiltrations were discussed [52]. The Al 356/SiC composites have fabricated and investigated by casting technique for moderate mechanical properties. Heavy-duty operation, especially under tribological conditions, frequently in corrosive environment, requires knowledge on their corrosion resistance. This paper presents the initial results of the research on susceptibility of aluminium alloy matrix composite material reinforced by SiC particles to corrosion. The purpose of the research was to

determine the influence of reinforcing phases, their type and shape on corrosion behaviour in a typical corrosion environment, with low NaCl concentration, in relation to the matrix alloy [53].

The challenges of current and future demands of metal matrix composites and its applications were reported for helping automotive and aerospace engineers. Metal-matrix composites (MMCs) offer a number of potential benefits to the aerospace industry, and these have led to important applications on systems such as the Space Shuttle Orbiter, the Hubble Space Telescope, and communications satellites. However, even after decades of development, MMCs have not seen widespread use. Several technical and non-technical challenges remain to their successful insertion into a variety of space applications. This article attempts to provide an overview of these challenges and potential pathways to resolving them [33, 68, 71].

Aluminium-based metal-matrix composites (MMCs) containing hard particles offer superior operating performance and resistance to wear [57-58]. The Microstructure and different material properties for aluminium metal matrix composites with various conditions were described [65-68]. The synthesis of metal matrix composites in particulate form and wear properties for different metal matrix composites were described. The improvement of the wear properties was substantial, decreasing the wear rate in two orders of magnitude, result that is independent of volume fraction and nature of the reinforcement [57, 64]. The metal matrix composites were developed using red mud which is an industrial waste through stir casting process at micron level only was studied [17, 50]. They found that improved hardness and wear resistance at micron level only done through stir casting.

The processing of metal matrix composites using powder metallurgy was discussed in a comprehensive manner [24, 34-37]. The wear studies of aluminium alloys under dry sliding conditions are described. The sliding wear response of several wrought aluminium alloys (2124, 3004, 5056 and 6092) against a high purity alumina (99.9%) counterface was investigated, at a fixed sliding speed of 1 m/s and a load range of 23–140 N. The counterface was chosen so as to minimise the chemically driven aspects of adhesive wear. Severe wear was observed at all loads, with specific wear rates ranging from 0.37×10^{-4} to 2.37×10^{-4} $mm^3/N\,m$. In all cases a

mechanically mixed layer (MML) was formed, principally from severely work hardened aluminium alloy, but also including fine alumina particles [26-27, 96].

The important factors and parameters were developed to produce metal matrix composites for aerospace challenges [38]. The various advanced applications of aluminium composites were discussed by many researchers. The results of experimental investigation on the characterization and analysis of mechanical properties of composites formed. Three aluminum metal matrix composites reinforced with 10 wt% of B_4C, SiC and Al_2O_3 particles were processed. The stir casting method followed by hot rolling was used for fabrications of aluminium 7075 metal matrix composites, being one of the cost effective industrial methods. [57-58, 70].

2.4 ALUMINIUM HYBRID COMPOSITES

The trends in red mud utilisation in which red mud is mixed with fly ash, lime and water in a ratio of 2:1:0.5:2.43, and then pumped the mixture into the mine to prevent ground subsidence during bauxite mining [94]. The rheological behaviour on hardened state behaviour of cement mortars with the addition of red mud are studied. The cementitious behavior of red mud derived from Bauxite-Calcination method was investigated in this research. Red mud were calcinated in the interval 400–900^{0}C to enhance their pozzolanic activity and then characterized in depth through XRD technique with the aim to correlate phase transitions and structural features with the cementitious activity. The cementitious activity of calcinated red mud was evaluated through testing the compressive strength of blended cement mortars. The results indicate that red mud calcinated at 600^{0}C has good cementitious activity due to the formation of poorly-crystallized Ca_2SiO_4 [90].

Reduction of radioactive levels of red mud based ceramic materials was also studied. Self-glazing red mud based ceramic materials (RMCM) were produced by normal pressure sintering process using the main raw materials of red mud. The properties of the RMCM samples were investigated by the measurements of mechanical properties, radiation measurement, X-ray diffraction (XRD) and scanning electron microscopy (SEM) [73].

The hybrid composites reinforced by short fibres and nano-particulates were investigated. A new method for an inexpensive fabrication of bulk lightweight metal matrix nano composites (MMNCs) with reproducible microstructures and superior properties by use of ultrasonic nonlinear effects, namely transient cavitation and acoustic streaming, to achieve uniform dispersion of nano-sized SiC particles in molten aluminum alloy A356 [88].

The researchers were made an attempt to propose that the hardness of the alloy increases with the addition of hybrid reinforcements and the increase in hardness may be due to the presence of relatively hard ceramic particles in the composite. The effects of warm compaction on the green density and sintering behaviour of aluminium alloys were investigated [74-75]. Aluminium-MMCs by powder metallurgy using ceramic particles as reinforcements were investigated [43-44, 46-48, 94].

The characteristics were correlated with different aluminium metal matrix composites. The tensile deformation and fracture behaviour of aluminium alloy 2014 discontinuously-reinforced with particulates of Al_2O_3 was studied with the primary objective of understanding the influence of reinforcement content on composite microstructure, tensile properties and quasi-static fracture behaviour. The injection of powders in the form of MMCs leads to considerable improvement in incorporation and distribution of Al_2O_3 particulates in the Aluminium matrix alloy leading to the improvement in tensile properties. Improvement in tensile properties is attributed to the better wetting of Al_2O_3 by melt as well as removing micro channels and roughness on alumina particles as a consequence of ball milling process [81-82].

The impact of nano size particles on metal matrix composites was studied [90]. The hybrid composites offer more flexibility and reliability in the design of possible components depending upon the reinforcement's combination and compositions were studied. The feasibility and viability of developing low cost-high performance hybrid composites are used for automotive and aerospace applications. Further, the fabrication characteristics and mechanical behavior of Hybrid aluminum matrix composites (HAMCs) fabricated by stir casting route have also been reviewed [75].

Red mud (RM) is a hazardous waste produced vastly by aluminum industry worldwide. Because of its rich metal oxide content, it has potential to be utilized in various applications, such

as ceramics production, construction, and catalysis. The structural modification of red mud by simple acid treatments using HCl and H_2SO_4 at different molarities, and at different digestion temperatures followed by calcinations at various temperatures were performed [78]. The removed red mud and soil mixture (RMSM) was transferred into the reservoirs for storage. In this paper the application of RMSM is evaluated in a field study aiming at re-utilizing waste, decreasing cost of waste disposal and providing a value-added product [28].

Structures before and after these treatments were characterized in deep detail by combining electron microscopy, diffraction, and spectroscopy complemented by thermal analysis and mass spectrometry to elucidate any changes in morphology, structure, and chemical composition introduced by these treatments. Many studies have proved that the presence of particulate reinforcements can tremendously influence the mechanical and wear behaviour of aluminium metal matrix composites. Red mud of micro level particulates reinforced aluminium metal matrix composites have demandable attention in recent years, due to their excellent mechanical and tribological capabilities using stir casting process [50].

The tribological behaviour of a commercial low-metallic friction material during dry sliding against a pearlitic cast iron has been investigated and the evolution of pin and disc temperature was recorded. The temperature distributions in the pin and the disc were modelled using a finite element analysis with three different approaches, i.e. considering a perfect contact, the separated bodies concept, and the presence of a third body between the sliding surfaces. The results were then discussed by considering the damaging phenomena occurring at the sliding contact. Wear was found to be nearly mild in nature in agreement with the contact temperatures that were determined to be lower than 100 °C.

In addition, literature studies also tell that most of the published work has recommended aluminium-based composites with their attractions of low density, heat treatment capability and processing flexibility [48]. Al matrix composites reinforced with Ti_3AlC_2 and Cu coated Ti_3AlC_2 were prepared by hot-press sintering approach. It was confirmed that Ti_3AlC_2 displayed poor wettability with Al, resulting in the poor interfacial bonding strength between Ti_3AlC_2 and Al matrix. However, Al_2Cu layer could be formed due to the reaction between Cu and Al during the

sintering process, when Cu coated Ti_3AlC_2 was incorporated in Al matrix. Because of the formation of enhanced Al_2Cu interface, the mechanical and tribological properties were significantly improved.

Even though large numbers of researchers have worked on the experimental investigation of metal matrix composites, only a few researchers have attempted metal matrix hybrid composites at micro and nano level. The present work is focussed on the mechanical and wear behaviour of red mud at micro and nano level with tungsten carbide particle reinforced in aluminium through conventional sintering.

2.5 GAP ANALYSIS

After thoroughly going through the literature, aluminium with red mud of micro level only reinforced metal matrix composites with stir casting process is available. Some of the major limitations in the existing literature on metal matrix hybrid composites with micro and nano level are given as below:

i. There is no attempt made to investigate on nano level red mud reinforced in aluminium metal matrix composites through powder metallurgy route.
ii. There is no attempt made to study on red mud and tungsten carbide reinforced in aluminium metal matrix hybrid composites.
iii. There is no studies are made for evaluation of experimental compression stress values with Deform-2D simulation software on aluminium-red mud and aluminium-red mud-tungsten carbide metal matrix hybrid micro as well as nano composites.
iv. Mathematical relations to predict the hardness and wear behaviour of aluminium with micro and nano red mud has not presented.
v. The impact of heat treatment conditions on aluminium-red mud and aluminium-red mud-tungsten carbide metal matrix hybrid micro as well as nano composites at normal condition and heat treatment conditions have not been reported.
vi. To predict the hardness and wear behaviour of aluminium with micro and nano red mud with tungsten carbide after heat treatment using regression analysis, mathematical modeling has not been presented.

2.6 MOTIVATION OF THE WORK

Presently it has been difficult for the industries to dispose of their wastage and utilisation of by-products. The huge amount of industrial byproducts/wastes is becoming clients for increasing environmental pollution and generation of a huge amount of unutilized resources. The present research work is aimed at finding out the solution of utilising the industrial byproducts for value-added applications and also makes easier to solve the environmental problems. Aluminium is the second most widely used metal in the world, after the iron. Red mud is one of the wastages produced during manufacturing of alumina. For every 2.5 tonnes of alumina production, 1.5 tonnes of red mud is produced [42, 54, 76, 79]. The application of red mud as a basic catalyst for bio-diesel production and manufacturing of ceramic tiles are studied [59, 95]. The evolution of red mud is shown in Figure 2.1.

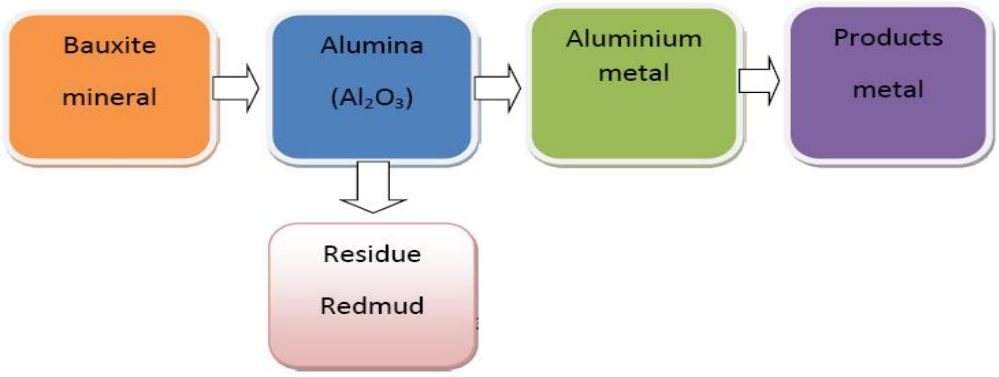

Figure 2.1: Evolution of red mud

More than 4 million tonnes of red mud is generated annually only in India. Presently, it is stored or dumped on land, or in the oceans near alumina refineries. It is a potential pollution problem to threat water, land and air due to its high alkalinity nature [45, 91]. While high costs are associated with the large area of land required for storage of the residue [93]. India is amongst the major producers of alumina in the world. The effects of red mud on the environment are shown in Figure 2.2 and 2.3. There are some differences in mineralogical composition between the residues from India and other countries due to the difference in the ore type in its production processes.

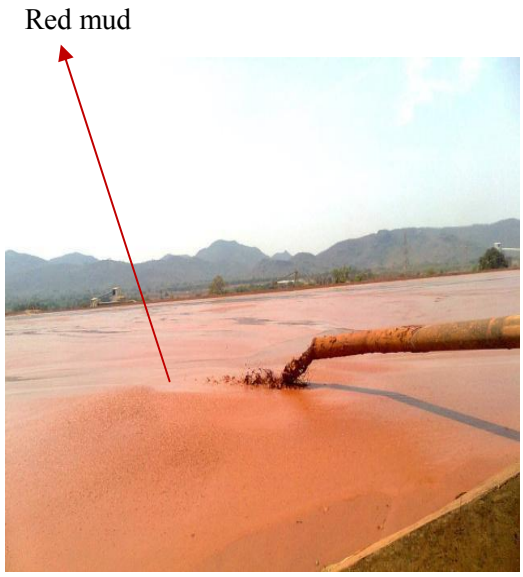

Figure 2.2: Water polluted by red mud **Figure 2.3: Sun flower plants destroyed by red mud**

2.7 OBJECTIVES AND SCOPE OF RESEARCH WORK

Depend on the limitations of the available information in literature review concerning aluminium metal matrix composites, the current investigation is formulated to study the mechanical characterization, micro structural observations and tribological behaviour of red mud and tungsten carbide particle reinforced in aluminium metal matrix nano composites.

In general, the objectives of the current investigation are as follows: To investigate the use of red mud (bauxite residue) as a reinforcing material as a low-cost option.

1) To investigate the best weight fraction of red mud as reinforcing material required in the aluminium metal matrix composites for optimum properties.
2) To evaluate the merits of nano red mud reinforcement over micro red mud reinforcement.
3) To explore mechanical behaviour and determine the hardness at normal and heat treatment conditions validate with mathematical modeling using Regression Analysis, compression test and validation of compression test with Deform -2D software.
4) To evaluate the effect of tribological behaviour of micro and nano red mud reinforced in aluminium metal matrix composites.

5) To investigate the heat treatment effect on micro and nano red mud and tungsten carbide reinforced in aluminium metal matrix hybrid composites.
6) To develop mathematical equations that predict the hardness, wear rate of micro and nano red mud and tungsten carbide reinforced in aluminium metal matrix hybrid composites at normal and heat treatment temperatures.

2.8 PROBLEM FORMULATION / METHODOLOGY

The present research work is aimed at determining the utilisation of industrial byproducts for value-added applications and also makes easier to solve the environmental problems. The continuous demand for reinforcement materials improved the interest towards utilization of bauxite residue (red mud) which contains major elements like iron oxide (Fe_2O_3), Al_2O_3, Na_2O and TiO_2 etc., to aluminium and tungsten carbide for making the metal matrix hybrid composites especially for wear resistant applications. An attempt has been made in the current work, red mud is mixed with other metals mainly aluminium and tungsten carbide to form hybrid metal matrix composites synthesised by powder metallurgy.

1) Preparation of the nano red mud using high energy ball milling and X-Ray Diffraction (XRD) analysis is to be carried out.
2) Mixing and compacting the pure aluminium powder with micro and nano level red mud and tungsten carbide.
3) Evaluation of conventional sintering process for the samples of pure aluminium, red mud and tungsten carbide metal matrix hybrid micro as well as nano composites.
4) Conducting hardness tests at normal and heat treatment conditions and compression tests validated by Deform-2D software with compressive stress at 10%, 20% and 30% reduction.
5) Adopting micro structural observations based on Scanning Electron Microscope (SEM) and Energy Dispersive X-Ray spectroscopy (EDX).
6) Conducting wear tests on pin-on-disc wear testing equipment for evaluating wear behaviour before and after heat treatment conditions.
7) Employing regression analysis approach with for various processing conditions of the hardness, wear rate of micro and nano red mud and tungsten carbide reinforced in aluminium metal matrix hybrid composites at normal and heat treatment temperatures.

2.9 OVERALL RESEARCH PLAN

The overall research plan is shown in Figure 2.4.

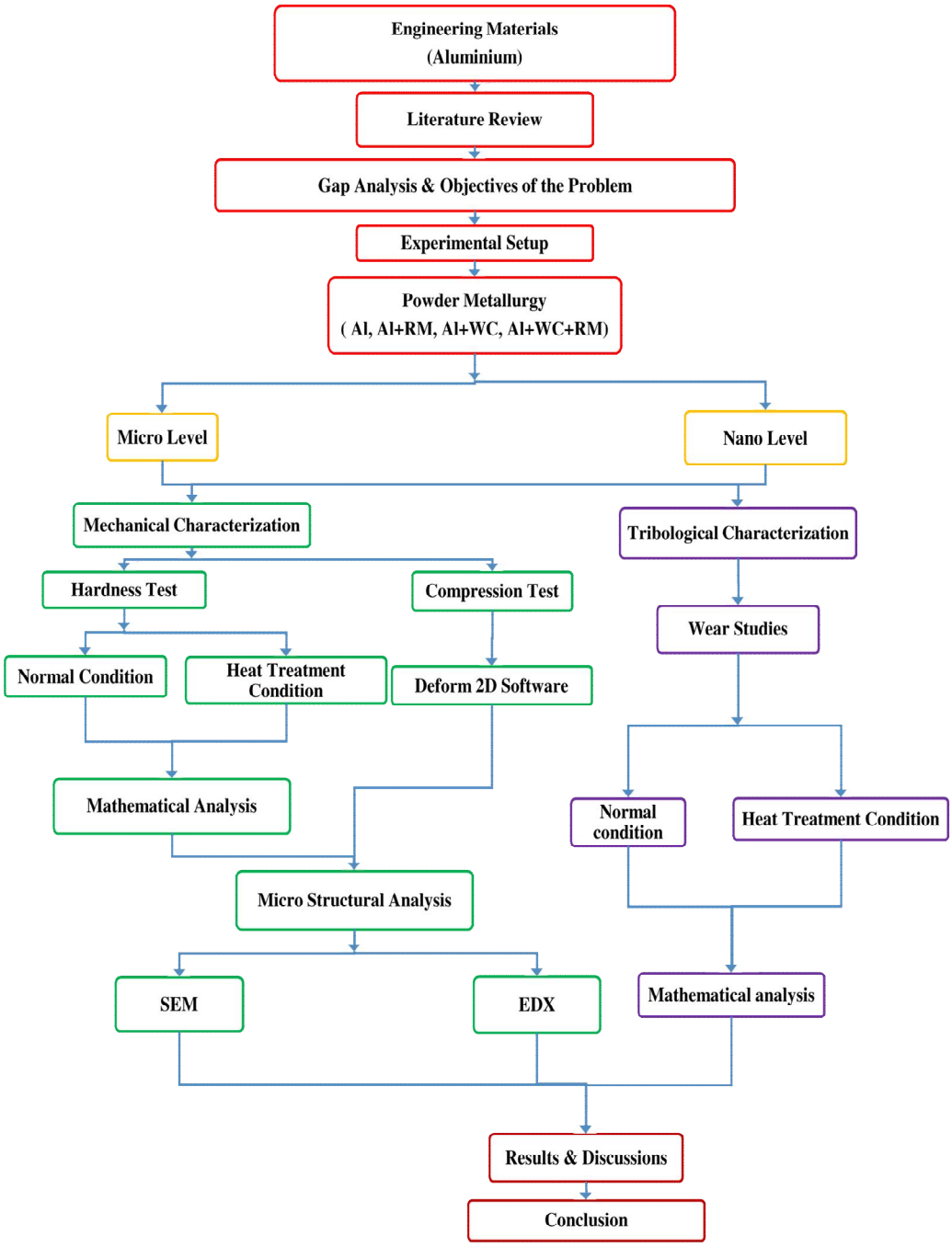

Figure 2.4: Overall research plan

2.10 SUMMARY

In this chapter, earlier works related to aluminium composites and aluminium hybrid composites are briefly presented. The significance of engineering materials and their applications are also discussed. From the literature review, most of the work has completed on aluminium metal matrix composites and very few of researches have studied on aluminium hybrid metal matrix composites. This chapter gives the information about gap analysis, the motivation of the work, objectives and scope of the research work, problem formulation and methodology of the current research work. The overall research plan of the thesis is also presented.

CHAPTER-3

EXPERIMENTAL SET UP

3.1 INTRODUCTION

The present chapter is describing the selection of raw materials, preparation of nano level red mud, aluminium-red mud metal matrix composites and aluminium- red mud- tungsten carbide metal matrix hybrid composites used in this experimental work. Pure aluminum is taken as matrix material. Red mud and tungsten carbide are used as reinforcements. The Red mud material is subjected to high energy ball milling and converted into nano structured powder. The nano structured red mud has been characterized for its structure by X-ray diffraction studies [29]. The high-energy ball mill is typically used to produce particles in the nano scale size range. The standard mill for conducting mechanical attrition experiments is Pulverisette which is referred to as the planetary ball mill [30, 82-86].

3.2 SELECTION OF MATERIALS

The material used in this experimental work is finely pulverized, pure aluminum powder of 99.72% purity. The aluminum powder is used to prepare aluminium-red mud and aluminium-red mud-tungsten carbide sintered compacts of aspect ratio i.e. height to diameter ratio 0.5 with a die size of 15 mm diameter and 30 mm height.

3.2.1 Sieve analysis

Sieve analysis (or gradation test) is a procedure used to assess the particle size distribution of a granular material. The red mud used for the present investigation is collected from the National Aluminum Company Limited (NALCO) Damanjodi, Odisha, India. The chemical compositions of pure aluminum powder, red mud and tungsten carbide are shown in Table 3.1, 3.2 and 3.3 respectively.

Table 3.1: Chemical composition of pure aluminum

Element	Fe	Si	Mg	Cu	Zn	Mn	Al
Wt%	0.17	0.07	0.001	0.005	0.003	0.0008	0.75

Table 3.2: Chemical composition of red mud

Element	Fe_2O_3	Al_2O_3	SiO_2	Na_2O	TiO_2	Sc	MnO	CaO	K_2O	Sr	MgO	V_2O_5
Wt%	53.8	14.3	8.34	4.3	3.9	3.2	2.95	2.5	2.25	2.45	1.63	0.38

Table 3.3: Chemical composition of tungsten carbide

Element	W	Cr	Si	B	C	Mg
Wt%	4.5	2.42	1.71	0.8	0.5	0.07

The received red mud is subjected to sieve analysis using mechanical sieve shaker for collecting particles of uniform sizes of 100, 150, and 200 microns for preparing the micro sized red mud powder.

3.3 HIGH ENERGY BALL MILLING

Nano particles are formed in a mechanical device known as high energy ball mill referred to as pulverisette for conducting mechanical attrition experiments which are shown in Figure 3.1. The planetary high energy ball mill has its name which implies the planet-like rotation of its vials. These vials are arranged on a rotating support disk, and drive mechanism causes them to rotate around their own axes. The centrifugal force produced by these vials rotating around their own axes and that produced by the rotating support disk both act on the vial contents, consisting of material to be ground and the grinding balls. Since the vials and the supporting disk rotate in opposite directions, the centrifugal forces alternately act in like and opposite directions. The reduction in particle size of red mud from micron level to the nano level is carried out using a high-energy planetary ball mill in a stainless steel chamber using tungsten carbide of 10 mm Φ balls size. The balls of 10 mm diameter tungsten carbide are used to crush the micro-size red mud powder into nano-size red mud powder in ball milling. The micron-sized red mud powder is milled for 30 hours by maintaining the rotation speed of the planet carrier at 200 rpm. The ball mill is loaded with the ball to powder weight ratio (BPR) of 10:1. Toluene is used as the medium

with an anionic surface active agent to avoid agglomeration. The preparation of nano red mud is shown in Figure 3.2.

Figure 3.1 Pulverisette - High energy ball mill

Figure 3.2 Preparation of nano red mud

3.4 X-RAY DIFFRACTION (XRD) ANALYSIS

The milled sample red mud powder is taken out after 6 hours, 13 hours, 24 hours and 30 hours of high energy ball milling and dried with mechanical drier. The X-Ray Diffraction (XRD) testing machine was carried out at IIT, Madras (Figure 3.3).

Figure 3.3: X-Ray Diffraction (XRD) testing machine

The X-Ray Diffraction (XRD) Patterns for 0 hours, 6 hours, 13 hours, 24 hours and 30 hours are shown in Figures 3.4 to 3.8. It is clearly observed that the intensity of the peaks in the XRD pattern got reduced and the peak broadening increased as the duration of milling increases. Fe_2O_3 was observed in XRD given for 6 hours milled red mud. The peak labels are strongly placed in Figures 3.4-3.8. Due to high energy ball milling, the elements of $NaTiO_2$ which were combined with other elements in the red mud powder after 24 hours of milling. The fine nano red mud powder is obtained after 30 hours.

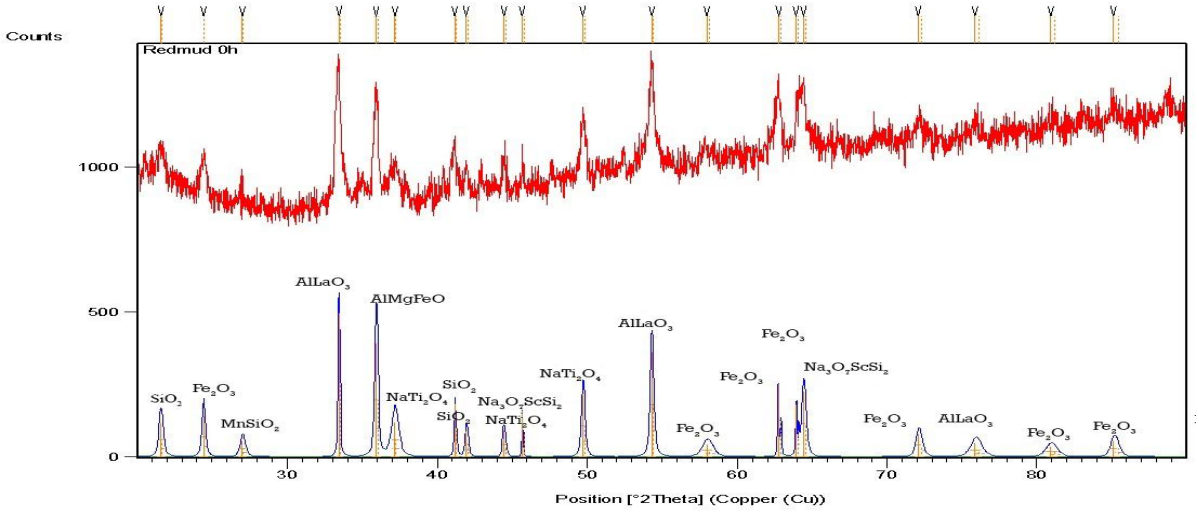

Figure 3.4: XRD Pattern for 0 hours milled red mud

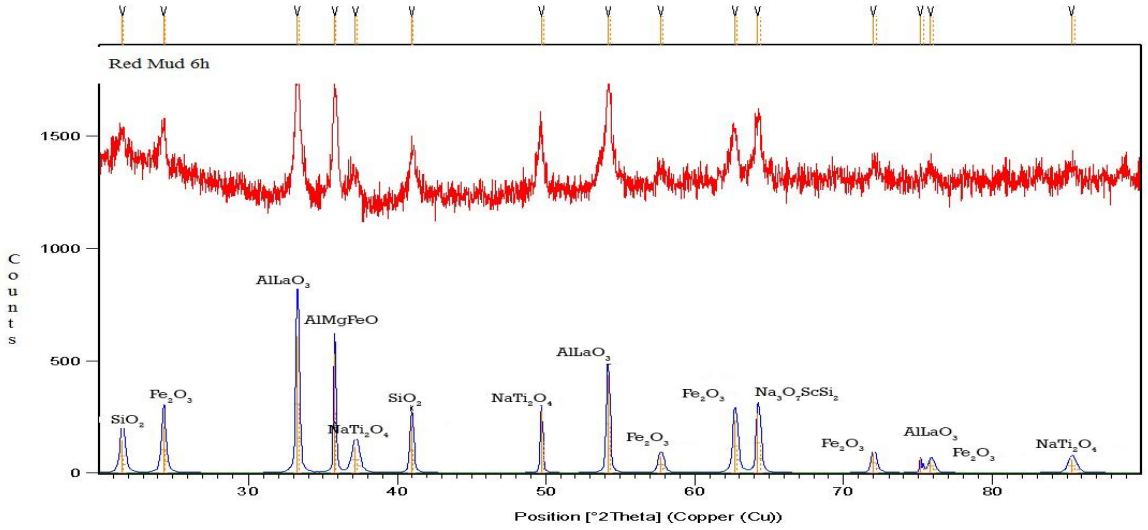

Figure 3.5: XRD Pattern for 6 hours milled red mud

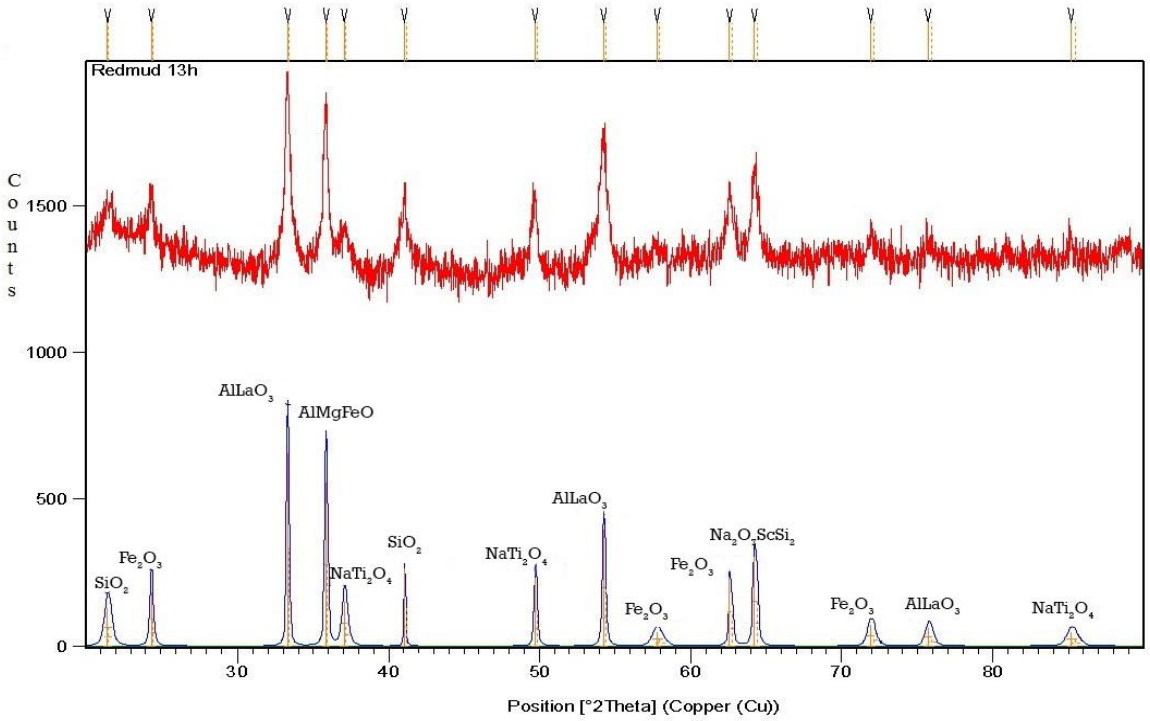

Figure 3.6: XRD Pattern for 13 hours milled red mud

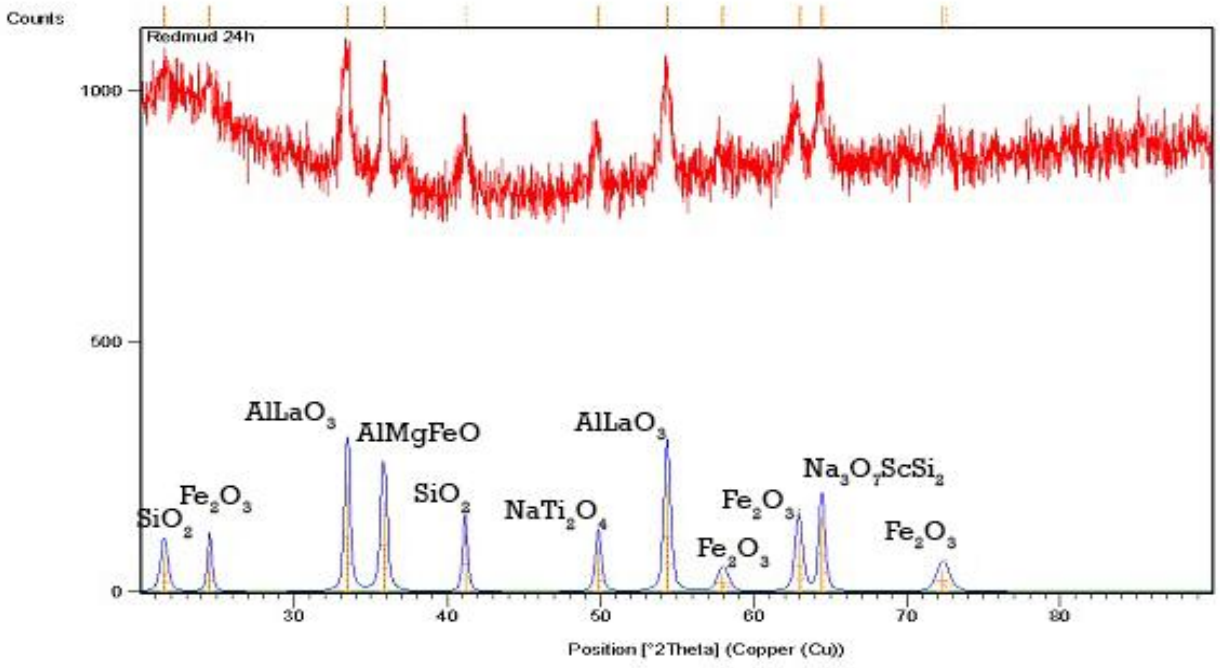

Figure 3.7: XRD Pattern for 24 hours milled red mud

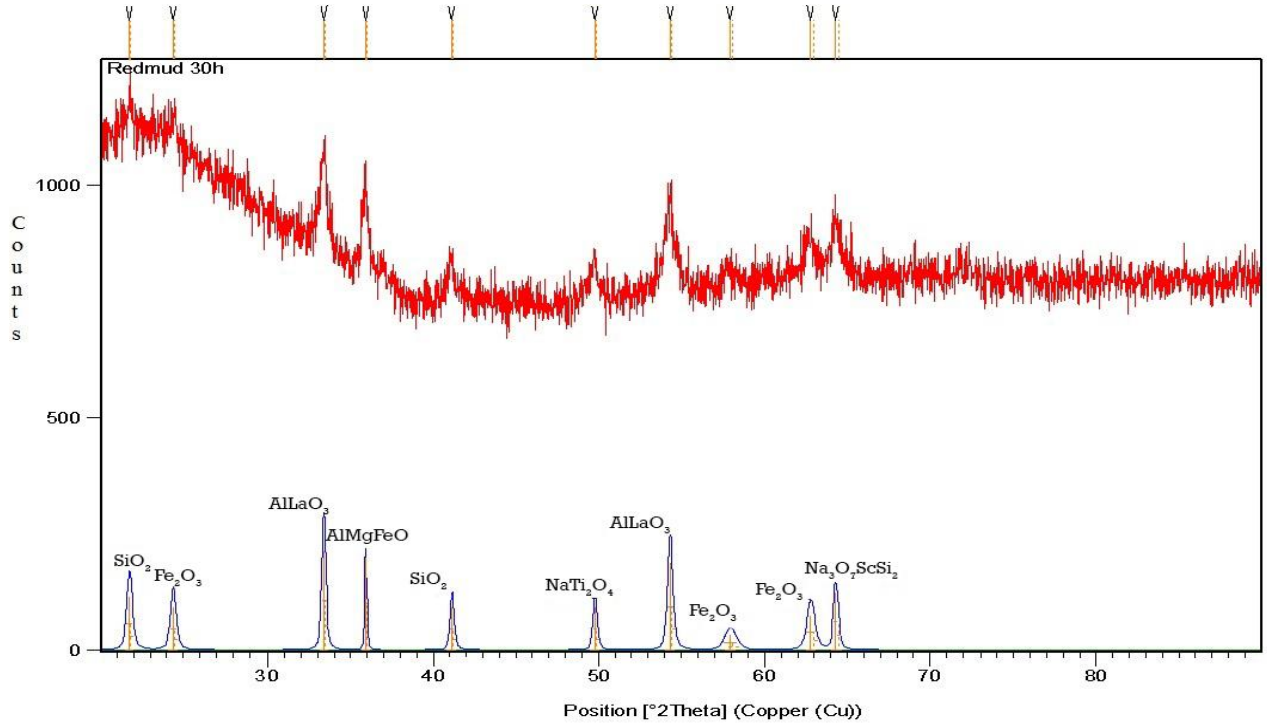

Figure 3.8: XRD Pattern for 30 hours milled red mud

The most widely used equation to determine grain size from XRD data is the Scherrer equation as

$L_0 = k\lambda /(\beta Cos\theta)$ ……. 3.1

where K is a constant of order 1 dependent on particle shape,

λ is the wavelength of the X-ray radiation,

θ is the diffraction angle and

β is the peak full width at half-maximum (FWHM),

The evaluation of nano particle size for XRD Pattern at 30 hours milled red mud powder is shown in Figure 3.9. The XPert HighScore Plus software is used to analyse the particle size of red mud after 30 hours of high energy ball milling. The particle size of 42 nm (418 A^0= 41.8 nm) is obtained after 30 hours of high energy ball milling using Scherrer Calculator which is shown in Figure 3.9.

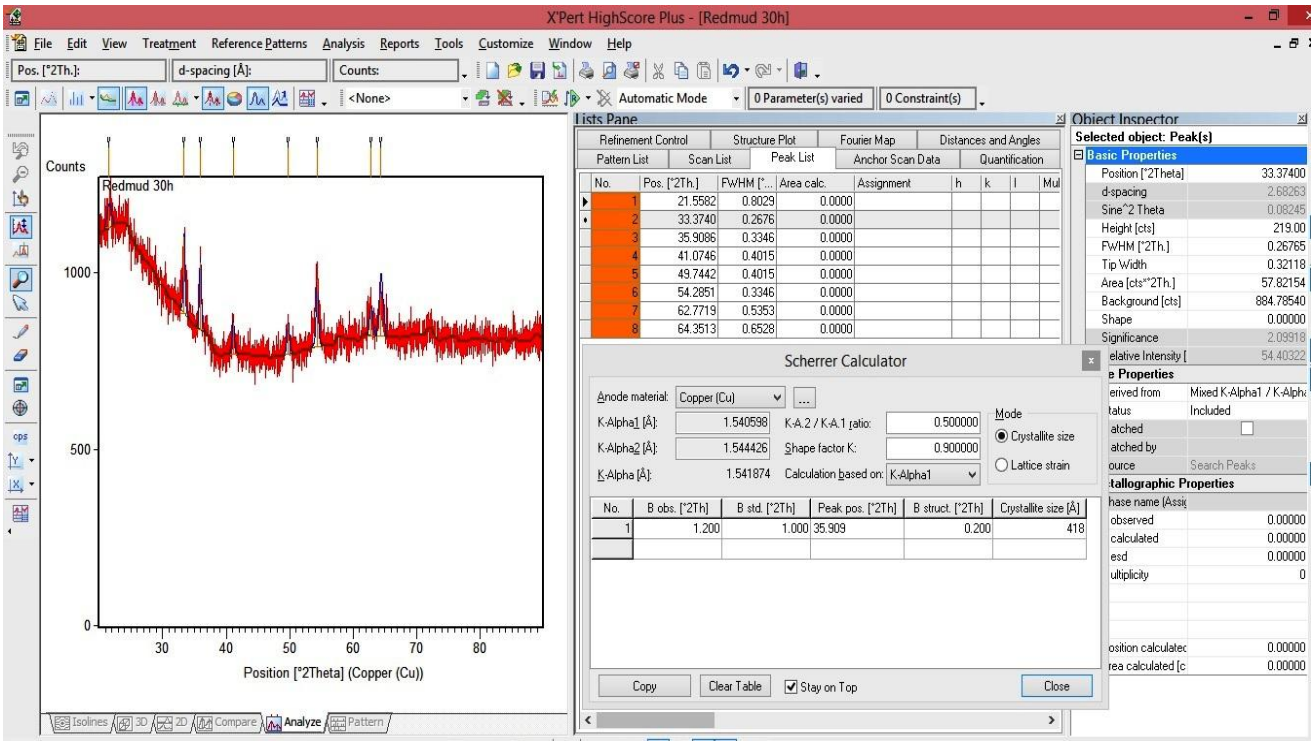

Figure 3.9: Evaluation of nano particle size for XRD Pattern at 30 hours milled red mud

The mean or average size of the crystallite sizes should be displayed by the Scherrer Calculator as 418 A^0 in XRD –analysis software of X'Pert High Score Plus for 30 hours milled red mud powder shown in the above Figure 3.9.

3.5 CONVENTIONAL SINTERING THROUGH POWDER METALLURGY

3.5.1 Mixing and Compacting

The micro level red mud powders of 100 µm, 150 µm and 200 µm and nano level red mud powder of 42 nm are used at 2%, 4% and 6% of weight fractions with pure aluminium powder. These mixtures are blended in a double cone mixer which is shown in Figure 3.10 for 10 hours in order to obtain proper mixing of particles with each other [28].

The different proportions of aluminium-red mud sample materials are compacted in a hydraulic press of 100 ton load capacity which is shown in Figure 3.11. During compacting, the applied pressure and compact pressing time were 40 bar and 10 seconds respectively. The pure aluminum powder at 2%, 4%, and 6% weight fractions of red mud at 100 microns size as well as 42 nano meters along with 4% weight fraction of tungsten carbide powder of 5 microns size are also prepared.

Figure 3.10: Double cone mixer

Figure 3.11: Hydraulic press

3.5.2 Sintering and manufacturing of composite preparation

Sintering is a thermal treatment process, which transforms a metallic or ceramic powder (or a powder compact) into a bulk material below the melting temperature of the main constituent material. The Vacuum sinter furnace is manufactured by ACME (Advanced Corporation for Materials and Equipments), China. The Model No ZSJ-25x25x50 with a loaded weight of 50 kg and loaded vacuum of $4x10^{-3}$ Pa. The temperature of the sintering furnace is raised up to 1550^{0}C with a heating power capacity of 50kW. In the Figure 3.12, the sintering machine is shown and sintering is performed in a vacuum chamber. The compacted pure aluminum and red mud

samples in the sintering furnace are shown in Figure 3.13. The aluminium-red mud and aluminium-red mud-tungsten carbide hybrid metal matrix micro level and nano level sintered samples are prepared.

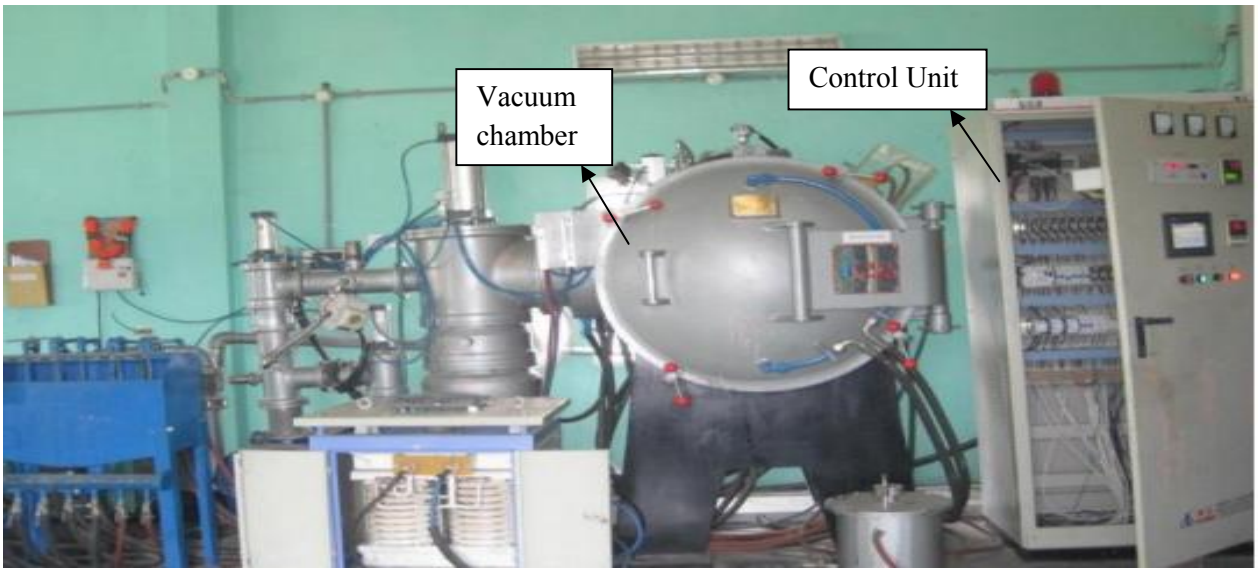

Figure 3.12: Sintering Machine

The vacuum maintained during sintering is 250 Pa (using a compressor of 1.5 H.P) and the temperature is raised to 300^0C in 30 minutes and soaked at 300^0C for 30 minutes. To avoid oxidation and maintain vacuum, Argon gas medium is used to evacuate the air in the sintering chamber. Adhesive bonding is obtained inside the sintering samples. The temperature is further raised to 500^0C in 35 minutes and again soaked at 500^0C for 30 minutes. Then cooling is done to room temperature in 3 hours. Hence the total sintering cycle time was 5 hours 5 minutes. The XRD pattern for pure aluminium and 6% nano red mud sintered sample which has Al-Al_3Fe, $AlFe_2Mn$ and $Fe_4Mn_{72}Si_{19}CuO$ phases are shown in Figure 3.14.

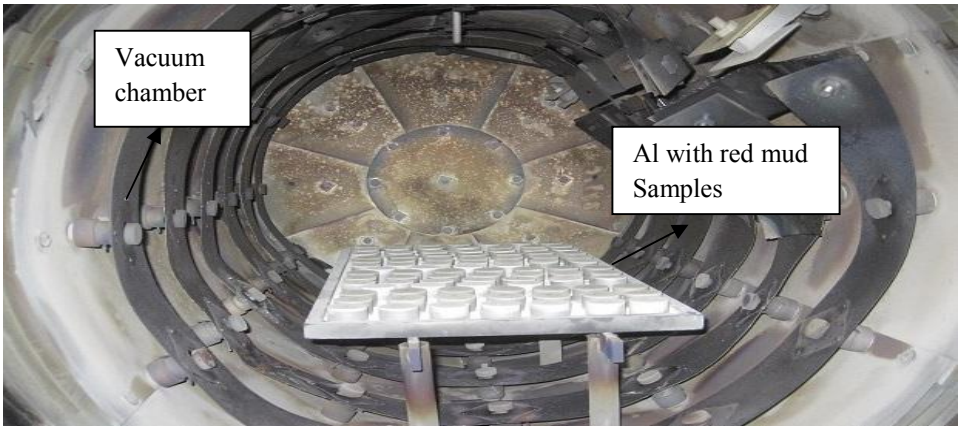

Figure 3.13: Compacted Pure Aluminium and Red mud samples in Sintering Furnace

The XRD pattern for pure aluminium with 4% tungsten carbide and 6% nano red mud sintered sample which has $AlFe_3V_2O_5W_2C$, $AlFe_2Mn$, W_2C , $AlFe_2O_3TiO_2W_2C$ and $Fe_2O_3MnSiO_2$ phases are shown in Figure 3.15.

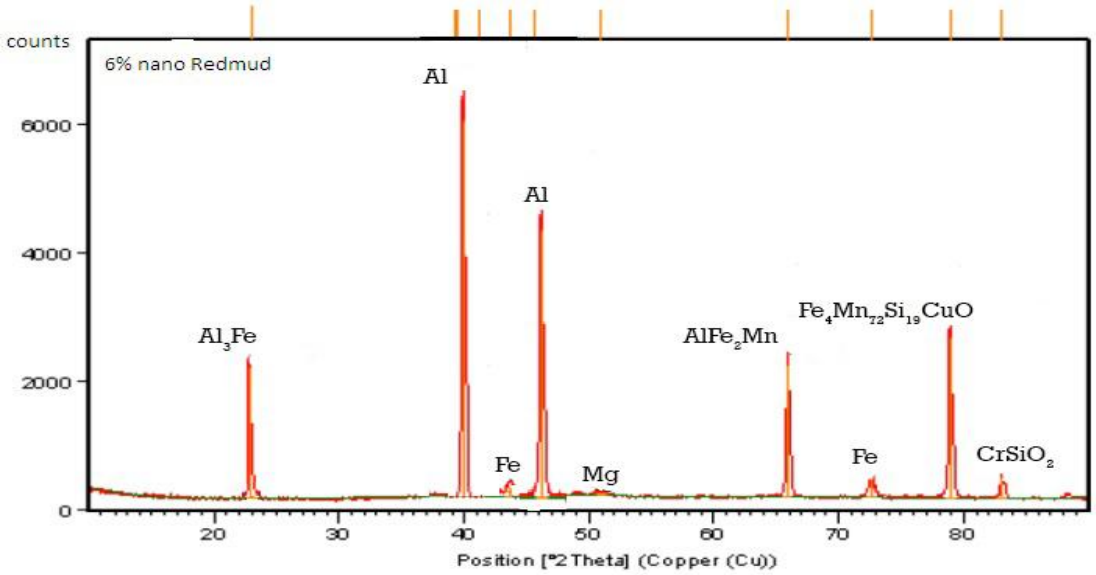

Figure 3.14: XRD pattern for pure aluminium and 6% nano red mud sample after Sintering

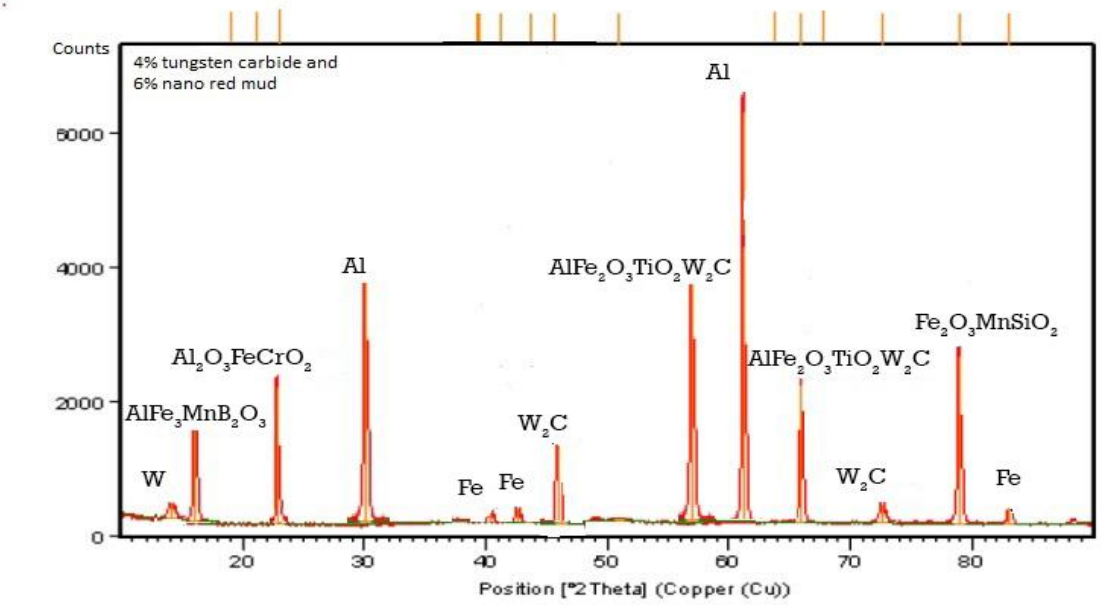

Figure 3.15: XRD pattern for pure aluminium with 4% tungsten carbide and 6% nano red mud sample after Sintering

3.6 RESULTS

The red mud powder with particle size of 100, 150 and 200 at micron level and 42 at nano level are prepared. The aluminium with the red mud of 2%, 4% and 6% weight fractions with 100 μm, 150 μm, 200 μm and 42 nm and aluminium with red mud and tungsten carbide of 2%, 4% and 6% weight fractions with 100 μm and 42 nm samples are prepared through conventional sintering.

The fresh red mud powder particles after 30 hours of high energy ball milling at 42 nm are in irregular shapes and the surface morphology is rough. The relative lattice strain is increasing with increasing the duration of milling time. The XPert- HighScore Plus software is used for analysing the X-Ray Diffraction (XRD) data which shows the lattice strain increases whenever milling time increases from 0 hours to 30 hours. This lattice strain is increased from 0.12 to 0.28 after 30 hours of high energy ball milling. The particle size of 42 nm is obtained after 30 hours of high energy ball milling.

3.7 SUMMARY

This chapter gives the information about the selection of materials, sieve analysis, high energy ball milling and X-Ray Diffraction (XRD) analysis at 0 hours, after 6 hours, 13 hours, 24 hours and 30 hours of high energy ball milling. It provides the details about conventional sintering through powder metallurgy for sample preparation. It also gives the information about mixing, compacting and sintering machine.

CHAPTER-4

MECHANICAL CHARACTERIZATION

4.1 INTRODUCTION

The present chapter is describing mechanical characterization of pure aluminium with red mud, pure aluminium with red mud and tungsten carbide. The mechanical properties such as hardness and compression strength are evaluated using Micro Vickers hardness testing machine and compression testing machine respectively. The mathematical prediction is done for hardness values using regression analysis.

4.2 HARDNESS TEST AT NORMAL CONDITION

Hardness values are measured using Micro Vickers Hardness tester according to ASTM E-32. The Vickers Hardness Number (VHN) is given by $1.854L/d^2$ where L is known as the applied load in kgf and d is known as diagonal length of a square impression in mm. The hardness results for aluminium- red mud metal matrix composites at normal condition are shown in Table 4.1. The graph between hardness and percentage (%) weight fraction of red mud with pure aluminium at normal condition is shown in Figure 4.1.

Table 4.1: Hardness results for aluminium-red mud metal matrix composites at normal condition

Aluminium with % weight fraction of Red mud(RM)	Particle size	Hardness (VHN)
Pure Al	45 µm	47.4
Al+2% RM	100 µm	60.2
Al+4% RM	100 µm	67.6
Al+6% RM	100 µm	74.5
Al+2% RM	150 µm	58.3
Al+4% RM	150 µm	62.4
Al+6% RM	150 µm	69.2
Al+2% RM	200 µm	56.7
Al+4% RM	200 µm	59.3
Al+6% RM	200 µm	63.5
Al+2% RM	42 nm	73.6
Al+4% RM	42 nm	77.4
Al+6% RM	42 nm	83.9

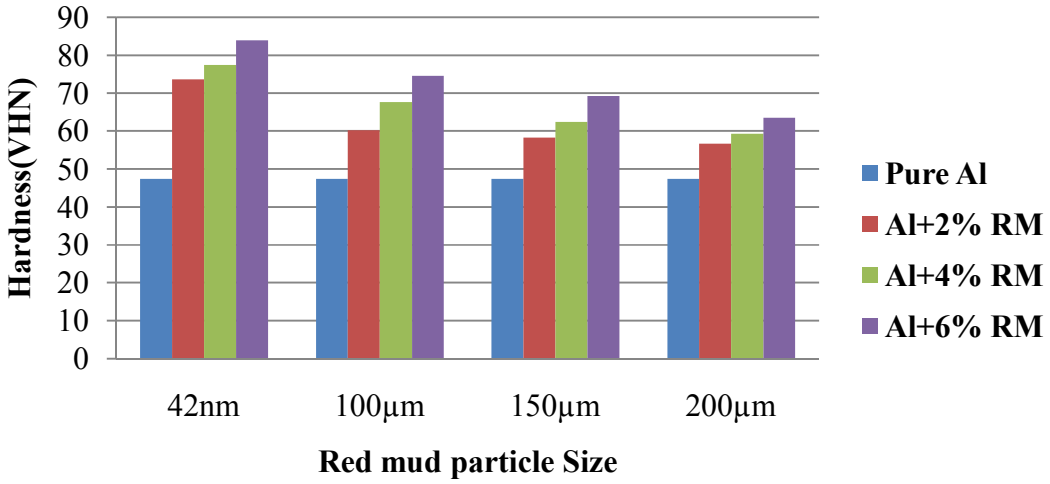

Figure 4.1: Hardness Vs % weight fraction of red mud with pure aluminium at normal condition

It is observed that, for the same percentage weight fraction of red mud, the hardness is higher for the nano level reinforcement than micro level reinforcement. The hardness results for aluminium- red mud-tungsten carbide metal matrix composites at normal condition are shown in Table 4.2. The graph between hardness and % weight fraction of red mud and 4% tungsten carbide with pure aluminium at normal condition is shown in Figure 4.2.

Table 4.2: Hardness results for aluminium-red mud-tungsten carbide metal matrix composites at normal condition

Aluminium and 4% WC with % weight fraction of Red mud(RM)	Particle size	Hardness (VHN)
Al+4% WC	45 µm	47.70
Al+4% WC +2% RM	100 µm	62.35
Al+4% WC + 4% RM	100 µm	68.74
Al+4% WC +6% RM	100 µm	75.23
Al+4% WC +2% RM	42 nm	75.43
Al+4% WC +4% RM	42 nm	79.21
Al+4% WC +6% RM	42 nm	84.90

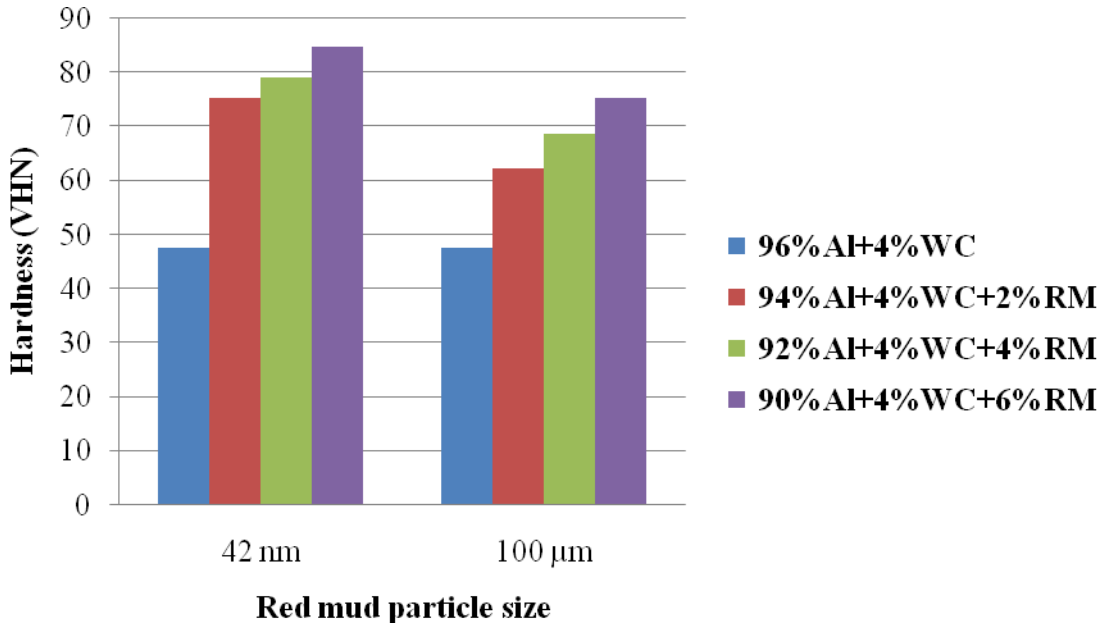

Figure 4.2: Hardness Vs % weight fraction of red mud and 4% tungsten carbide with pure aluminium at normal condition

Porosity analysis is conducted and obtained as 87% and 89% of Al+Red mud and Al+Red mud+WC metal matrix composites respectively. It is observed that the 6% nano level red mud with pure aluminium and 4% tungsten carbide has better hardness value of 84.9 VHN compared to remaining proporions. Aluminium, red mud and tungsten carbide hybrid metal matrix composites have shown better hardness compared to aluminium with red mud metal matrix composites. As percentage weight fraction composition of red mud increases, hardness values are also increases. Since the red mud consists of ferrous oxide as its major constituent about 53.8%. and harder in nature. Finer particles are strongly bonded to each other in nano-sized red mud powder and improved the surface hardness compared with the micro-sized red mud powder.

4.3 HARDNESS TEST FOR HEAT TREATMENT CONDITIONS

The effects of heat treatment on mechanical properties of aluminium cast alloys are studied [22]. In the present work, heat treatment is carried out for the hardness results of pure aluminium and aluminium-red mud metal matrix composites at heat treatment conditions of 350^0C, 400^0C, 450^0C and 500^0C are conducted and shown in Table 4.3. The graphs between

hardness and percentage (%) weight fraction of red mud with pure aluminium at heat treatment conditions of 350^0C, 400^0C, 450^0C and 500^0C are shown from Figure 4.3-4.6.

Table 4.3: Hardness results for aluminium-red mud metal matrix composites at heat treatment conditions

Aluminium with % weight fraction of Red mud(RM)	Particle size	Temperature (^{0}C)	Hardness (VHN)
Pure Al	45 µm	350	48.6
Al+2% RM	100 µm	350	62.7
Al+2% RM	42 nm	350	74.3
Al+4% RM	100 µm	350	68.7
Al+4% RM	42 nm	350	81.8
Al+6% RM	100 µm	350	77.1
Al+6% RM	42 nm	350	85.4
Pure Al	45 µm	400	50.4
Al+2% RM	100 µm	400	64.3
Al+2% RM	42 nm	400	76.8
Al+4% RM	100 µm	400	69.7
Al+4% RM	42 nm	400	83.6
Al+6% RM	100 µm	400	79.3
Al+6% RM	42 nm	400	88.9
Pure Al	45 µm	450	51.2
Al+2% RM	100 µm	450	66.8
Al+2% RM	42 nm	450	79.6
Al+4% RM	100 µm	450	73.1
Al+4% RM	42 nm	450	87.5
Al+6% RM	100 µm	450	82.4
Al+6% RM	42 nm	450	95.7
Pure Al	45 µm	500	50.7
Al+2% RM	100 µm	500	65.7
Al+2% RM	42 nm	500	77.4
Al+4% RM	100 µm	500	71.9
Al+4% RM	42 nm	500	85.2
Al+6% RM	100 µm	500	80.8
Al+6% RM	42 nm	500	88.5

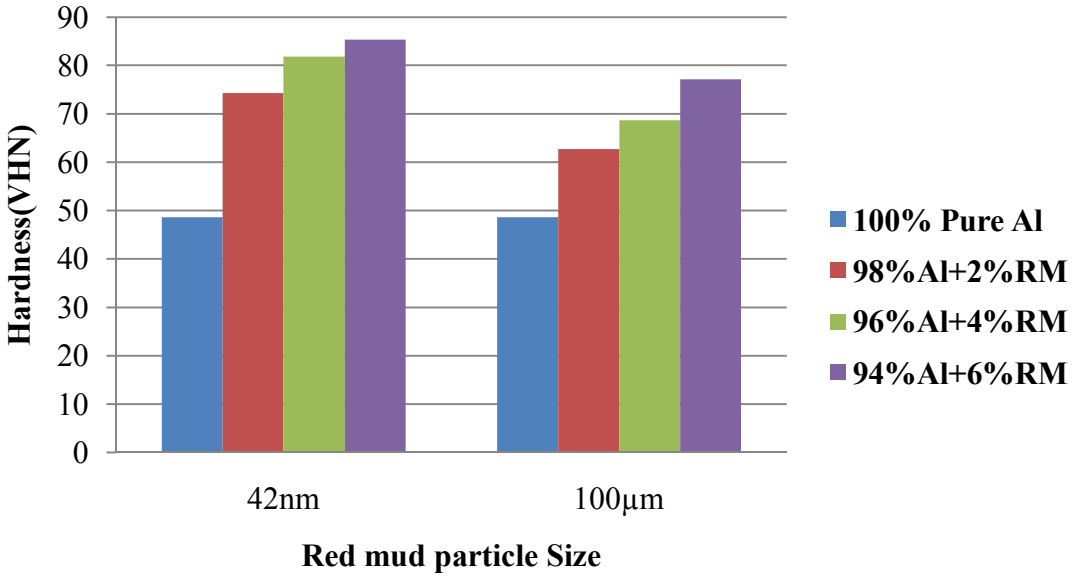

Figure 4.3: Hardness and % weight fraction of red mud with pure aluminium at 350^0C

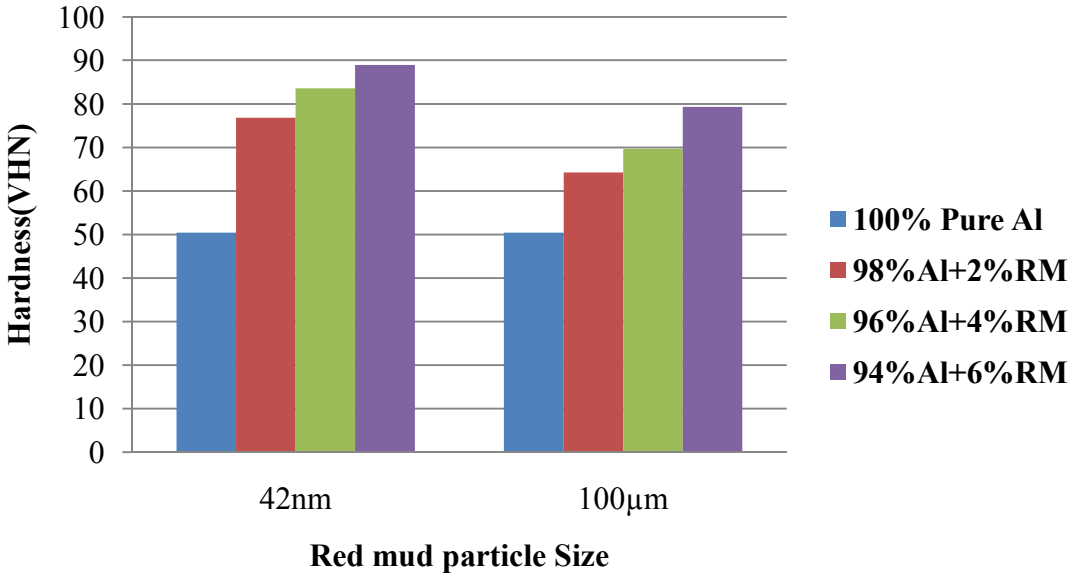

Figure 4.4: Hardness and % weight fraction of red mud with pure aluminium at 400^0C

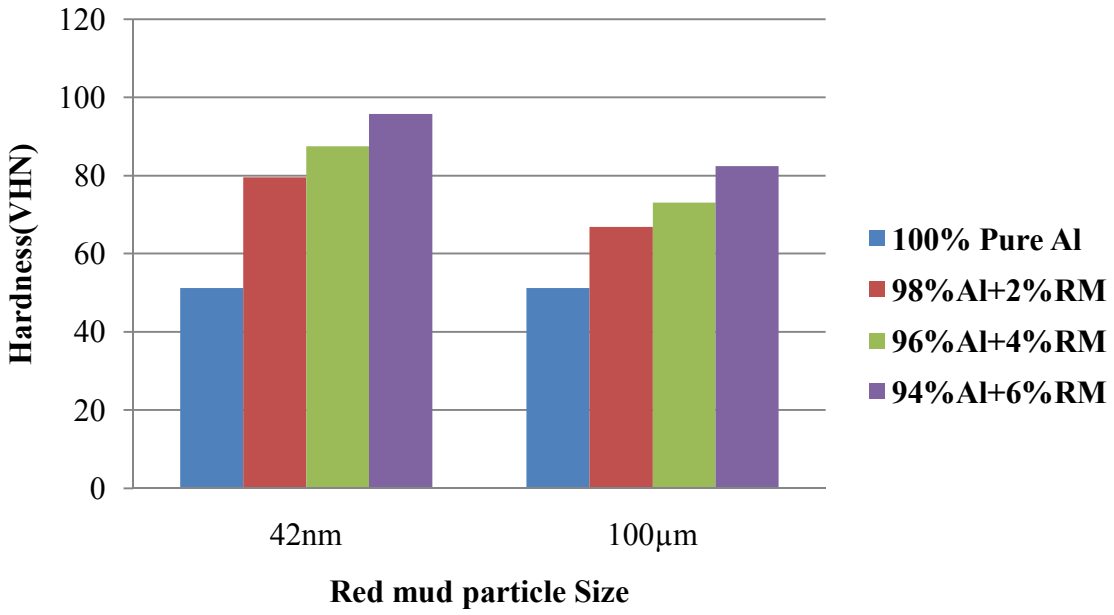

Figure 4.5: Hardness and % Weight fraction of red mud with pure aluminium at 450^{0}C

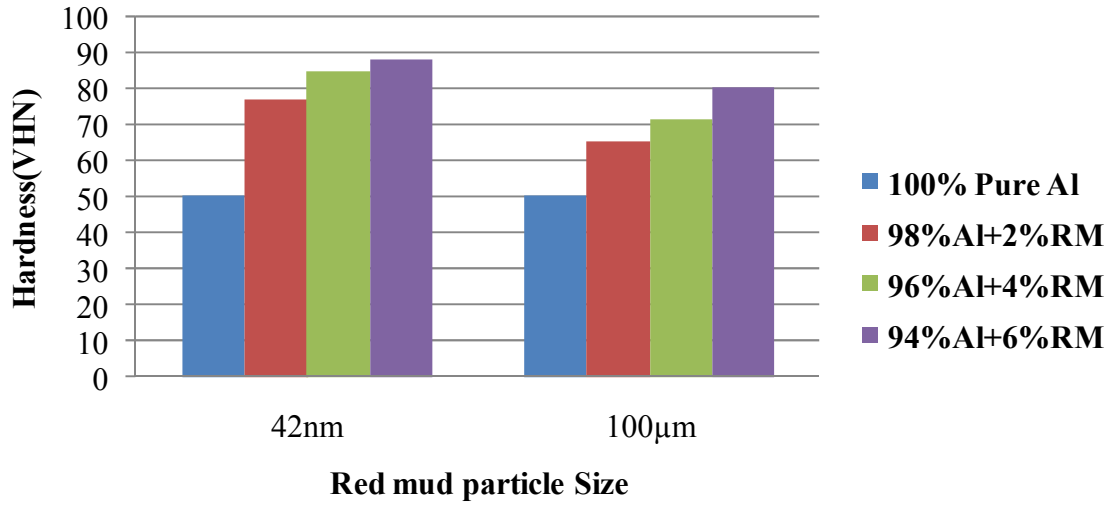

Figure 4.6: Hardness and % Weight fraction of red mud with pure aluminium at 500^{0}C

It is observed that nano level (42nm) red mud possessed better hardness compared to micro level (100µm) red mud with aluminium metal matrix composites at heat treatment conditions as shown in Figure 4.3- 4.6. It is observed that the hardness is more with increase in the amount of percentage weight fraction from 2% to 6% of red mud. The hardness results for aluminium-red mud-4% tungsten carbide metal matrix hybrid composites at heat treatment

conditions of 350^0C, 400^0C, 450^0C and 500^0C are conducted and shown in Table 4.4. The plots between hardness and percentage (%) weight fraction of red mud with pure aluminium and 4% tungsten carbide at heat treatment conditions of 350^0C, 400^0C, 450^0C and 500^0C are shown from Figure 4.7-4.10.

Table 4.4: Hardness Results for Aluminium-Red mud-Tungsten Carbide metal matrix composites at heat treatment conditions

Aluminium and 4% Tungsten Carbide with % weight fraction of Red mud(RM)	Particle size	Temperature (^{0}C)	Hardness (VHN)
Al+4% WC	45 µm	350	48.90
Al+4% WC +2%RM	100 µm	350	67.21
Al+4% WC +2%RM	42 nm	350	74.33
Al+4% WC +4%RM	100 µm	350	71.32
Al+4% WC +4%RM	42 nm	350	83.74
Al+4% WC +6%RM	100 µm	350	79.20
Al+4% WC +6%RM	42 nm	350	87.24
Al+4% WC	45 µm	400	50.40
Al+4% WC +2%RM	100 µm	400	66.81
Al+4% WC +2%RM	42 nm	400	79.57
Al+4% WC +4%RM	100 µm	400	73.21
Al+4% WC +4%RM	42 nm	400	84.78
Al+4% WC +6%RM	100 µm	400	81.42
Al+4% WC +6%RM	42 nm	400	87.98
Al+4% WC	45 µm	450	51.20
Al+4% WC +2%RM	100 µm	450	67.92
Al+4% WC +2%RM	42 nm	450	81.45
Al+4% WC +4%RM	100 µm	450	74.54
Al+4% WC +4%RM	42 nm	450	88.63
Al+4% WC +6%RM	100 µm	450	75.10
Al+4% WC +6%RM	42 nm	450	96.82
Al+4% WC	45 µm	500	50.70
Al+4% WC +2%RM	100 µm	500	66.21
Al+4% WC +2%RM	42 nm	500	79.38
Al+4% WC +4%RM	100 µm	500	70.28
Al+4% WC +4%RM	42 nm	500	87.23
Al+4% WC +6%RM	100 µm	500	82.46
Al+4% WC +6%RM	42 nm	500	90.90

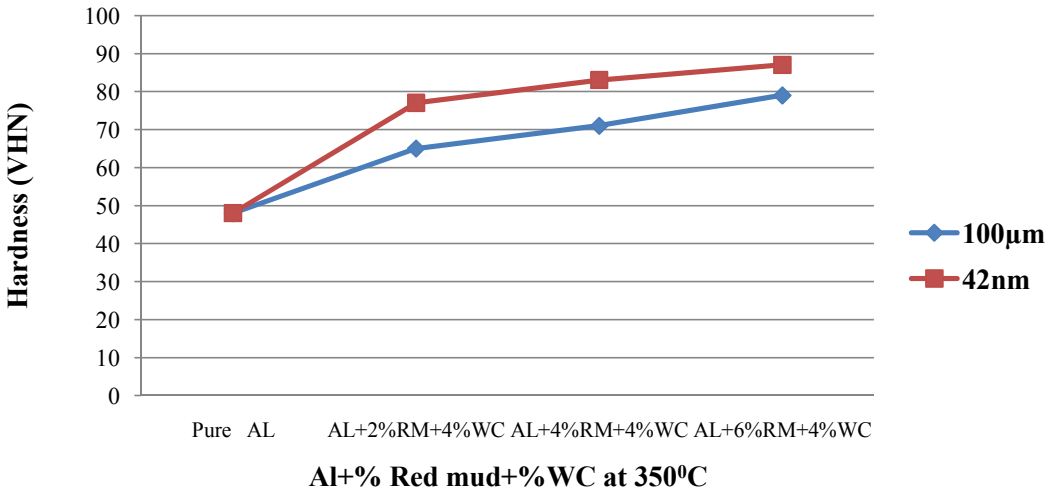

Figure 4.7: Hardness Vs % weight fraction of red mud and 4% tungsten carbide with pure aluminium at 350^{0}C

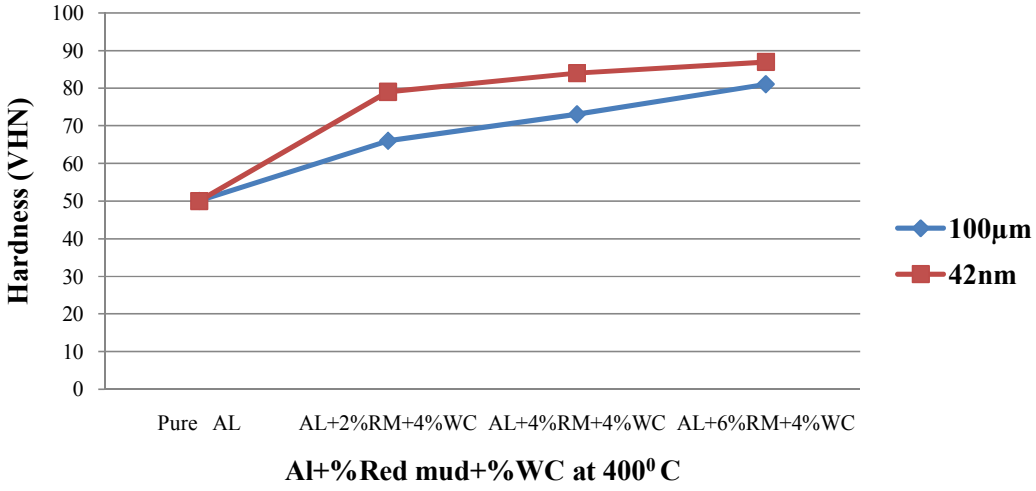

Figure 4.8: Hardness Vs % weight fraction of red mud and 4% tungsten carbide with pure aluminium at 400^{0}C

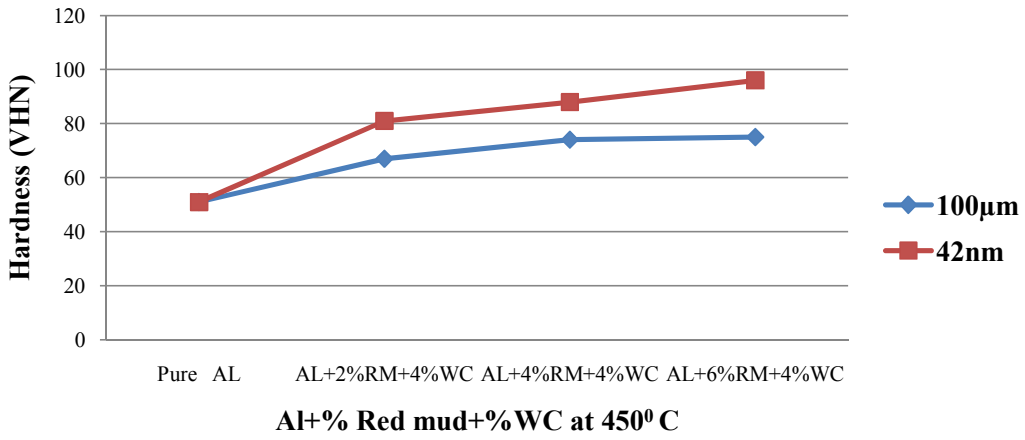

Figure 4.9: Hardness Vs % weight fraction of red mud and 4% tungsten carbide with pure aluminium at 450^{0}C

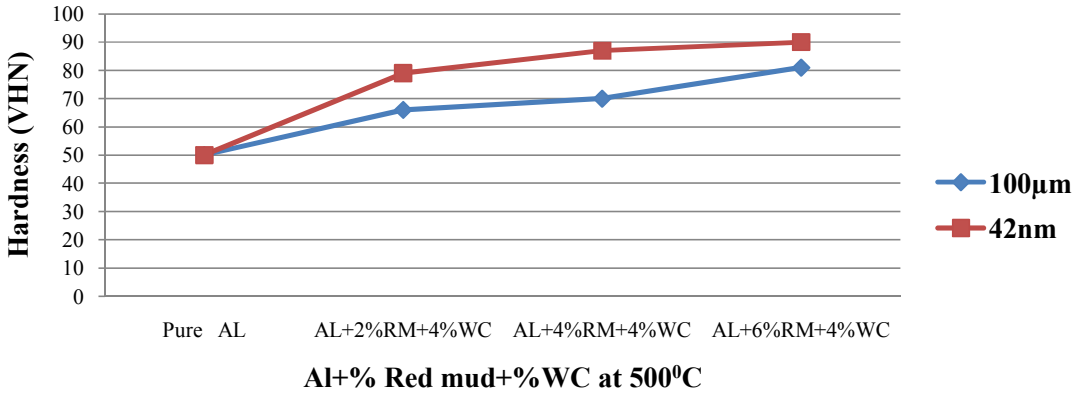

Figure 4.10: Hardness Vs % weight fraction of red mud and 4% tungsten carbide with pure aluminium at 500^{0}C

It has been observed that the hardness values are improved up to 450^{0}C, after that there is a decrement in hardness values. In heat treatment conditions, hardness values are higher for the nano level reinforcement than micro level reinforcement compared to normal condition. This is resulted because of the increase in surface area of contact and higher bond strengths. The excessive heat generated at the disc-pin interface may cause thermal stresses. Under the highest load applied, the mating material raised the specimen temperature could cause oxidation of contact surfaces. The oxide films were brittle and easily smashed in the wear process. These

oxide debris were embedded in the specimen surface by the contact load which enhanced its bond strength, hardness and increased its wear resistance. This is so called glazed hardening.

4.4 MATHEMATICAL MODELING BY REGRESSION ANALYSIS

A mathematical model is developed using regression analysis for the hardness values of aluminium and red mud. The overall equations at normal condition and heat treatment conditions (350^0C, 400^0C, 450^0C and 500^0C) are shown in equations 4.1 and 4.2 respectively. Here particle size, percentage weight fraction of red mud and temperature are taken as random variables for evaluating the linear relationship between hardness and these parameters.

Hardness = 67.149 + [(2.64375) x particle size] - [(0.00339) x percentage weight fraction of red mud] ---------- (4.1)

Hardness = 47.9363 + [(5.5625) x percentage weight fraction of red mud] - [(0.09041)x particle size] + [(0.0256) x temperature] ---------- (4.2)

It has been observed that the R-square values for equations 1 and 2 are 0.9717 and 0.8849 from regression statistics as shown in Figure 4.11.

SUMMARY OUTPUT

Regression Statistics	
Multiple R	0.94069942
R Square	0.8849154
Adjusted R Square	0.87258491
Standard Error	5.13161246
Observations	32

	Coefficients	*Standard Error*	*t Stat*	*P-value*	*Lower 95%*	*Upper 95%*	*Lower 95.0%*	*Upper 95.0%*
Intercept	47.9362973	7.119920508	6.732701	2.61E-07	33.351802	62.52079	33.3518015	62.52079317
X Variable 1	5.5625	0.405689586	13.71122	6.03E-14	4.7314826	6.393517	4.73148257	6.393517434
X Variable 2	-0.090413	0.018150613	-4.98126	2.92E-05	-0.1275928	-0.05323	-0.12759282	-0.05323313
X Variable 3	0.0256	0.016227583	1.577561	0.125899	-0.0076407	0.058841	-0.0076407	0.058840697

Figure 4.11: Regression statistics of Hardness results for pure aluminium and red mud at heat treatment condition

Regression analysis in the context of sensitivity analysis invoves fitting a linear regression to the model response and using standardized regression coefficients as direct measures of sensitivity. The regression is required to be linear with respect to the data (i.e., hyperplane hence with no quadratic terms etc as regressors). Therefore, this method is most suitable when the model response is linear. The regression analysis has the advantage of simple and low computational cost.

A mathematical model is developed using regression analysis for the hardness values of aluminium, red mud and tungsten carbide. The overall equations at normal condition and heat treatment conditions (350^0C, 400^0C, 450^0C and 500^0C) are shown in equations 4.3 and 4.4 respectively.

Hardness = 59.9167 - [(0.08311) x particle size] + [(4.37475) x percentage weight fraction of red mud] ---------- (4.3)

Hardness = 55.9024 - [(0.08422) x particle size] + [(4.5149) x percentage weight fraction of red mud] + [(0.02113) x temperature] ---------- (4.4)

It has been observed that the R-square values for equations 3 and 4 are 0.8861 and 0.8883 from regression statistics as shown in Figure 4.12.

SUMMARY OUTPUT

Regression Statistics	
Multiple R	0.942503897
R Square	0.888313596
Adjusted R Square	0.876347196
Standard Error	4.170312542
Observations	32

	Coefficients	*Standard Error*	*t Stat*	*P-value*	*Lower 95%*	*Upper 95%*	*Lower 95.0%*	*Upper 95.0%*
Intercept	55.9024121	5.786152799	9.661413039	2.04746E-10	44.05001554	67.75480866	44.05001554	67.75480866
X Variable 1	-0.084216621	0.014750477	-5.709416944	4.01119E-06	-0.114431602	-0.05400164	-0.114431602	-0.05400164
X Variable 2	4.5149375	0.329692155	13.69440381	6.21556E-14	3.839593745	5.190281255	3.839593745	5.190281255
X Variable 3	0.0211325	0.013187686	1.602441831	0.120280858	-0.00588125	0.04814625	-0.00588125	0.04814625

Figure 4.12: Regression statistics of Hardness results for pure aluminium, red mud and tungsten carbide at heat treatment condition

In statistical modeling, regression analysis is a statistical analysis for estimating the relationships among variables. It includes many techniques for modeling and analyzing several variables when the focus is on the relationship between a dependent variable and one or more independent variables (or predictors). More specifically, regression analysis illustrates that how the typical value of dependent variable or criterion variable changes when any one of the independent variables is varied, while the other independent variables are held fixed.

Most commonly, regression analysis estimates the conditional expectation of the dependent variable given the impact of independent variables. Regression analysis is used to measure the "Goodness of Fit" that how well the calculated co-efficient which tells the calculated linear regression equation fits the input data. In the Figure 4.12, Multiple R is 0.9425, the correlation coefficient tells that strongness of the linear relationship. R-squared is the coeffiecient of determination. It tells that how many points fall on the regression line. For example 80% means that 80% of the variation of y-values around the mean are explained by the x-values. In otherwords, 80% of the values fit the model. In the Figure 4.12, R square is 0.88 i.e., 88% of the values fit the regression model. The Adjusted R square is 0.8763, which adjusts more than one x-variable for the regression model.

An estimate of the standard deviation of the error 'μ'. The standard error of the regression is the precision that the regression co-efficient is measured. If the co-efficient is large compared to the standard error, then the co-efficient is probably different from 0. In the Figure 4.12, the standard deviation of the error is 4.17. Therefore the regression model exhibits results with 1-4% error difference. In the Figure 4.12, the number of observations in the sample are 32. After 450^0C, aluminium was started to reach the melting temperature of 660^0C and reduced the adhesive bonding between matrix and reinforcement materials.

4.5 COMPRESSION TEST

Compression strength values were calculated experimentally at 10, 20, and 30 percent reduction using compression testing machine as shown in Figure 4.13 and validated using Deform-2D software. The compressive stress for pure aluminium and pure aluminium with 2%, 4% and 6% weight fractions of 100μm, 150μm and 200μm red mud particle size at 10%, 20%

and 30% reduction using Deform-2D software are shown in Appendix-I. The compressive stress for pure aluminium with 2% and 4% weight fraction of red mud (42 nm) at 10%, 20% and 30% reduction using Deform-2D software are also shown in Appendix-I. In this present chapter, the compressive stress for pure aluminium with 6% weight fraction of red mud (42 nm) at 10%, 20% and 30% reduction using Deform-2D software are shown from Figure 4.14 to 4.16.

Figure 4.13: Compression testing machine

4.6 VALIDATION OF COMPRESSION TEST WITH DEFORM -2D SOFTWARE

The compressive stress for pure aluminium with 6% weight fraction of red mud (42 nm) at 10% reduction using Deform-2D software is shown in Figure 4.14. The effective stress value is 58.2 MPa.

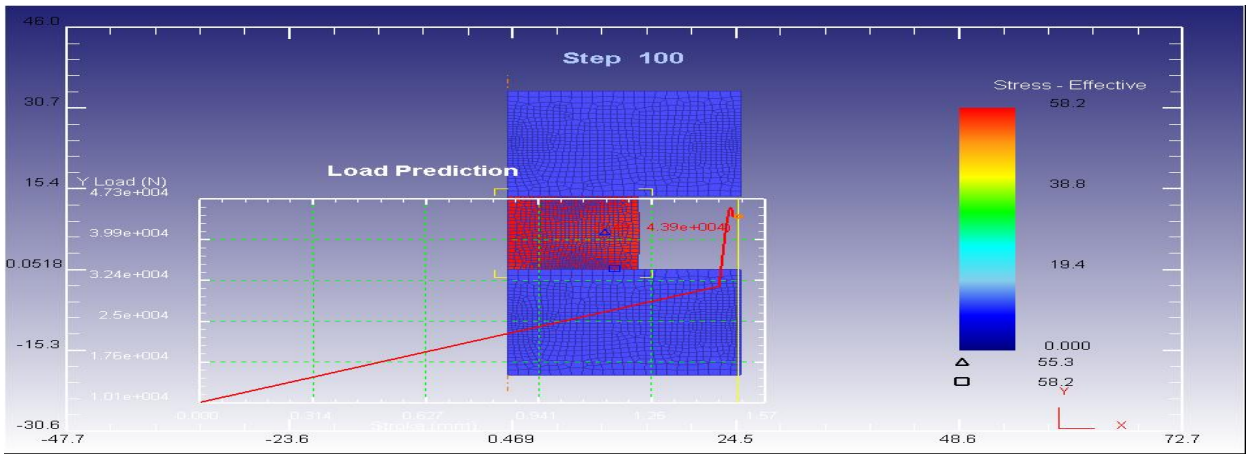

Figure 4.14: Compressive Stress for aluminium with 6% weight fraction of red mud (42 nm) at 10% reduction using Deform-2D software

The compressive stress at 20% and 30% reduction for pure aluminium with 6% weight fraction of red mud (42 nm) using Deform-2D software are shown in Figure 4.15 and 4.16 respectively and the effective stress values are 92.1 MPa and 98.4 MPa.

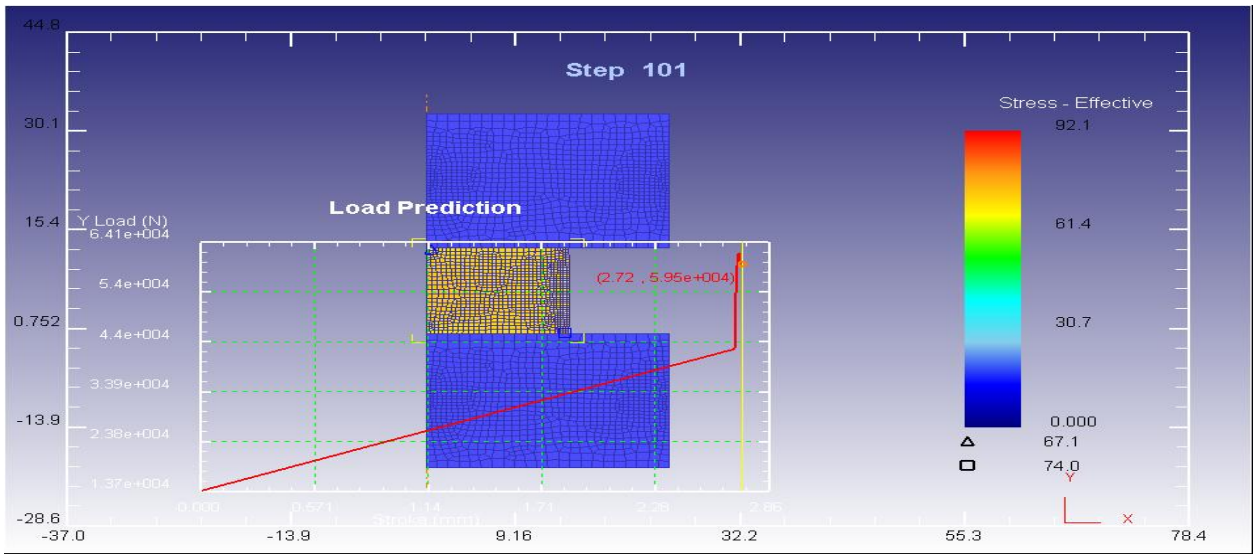

Figure 4.15: Compressive Stress for aluminium with 6% weight fraction of red mud (42 nm) at 20% reduction using Deform-2D software

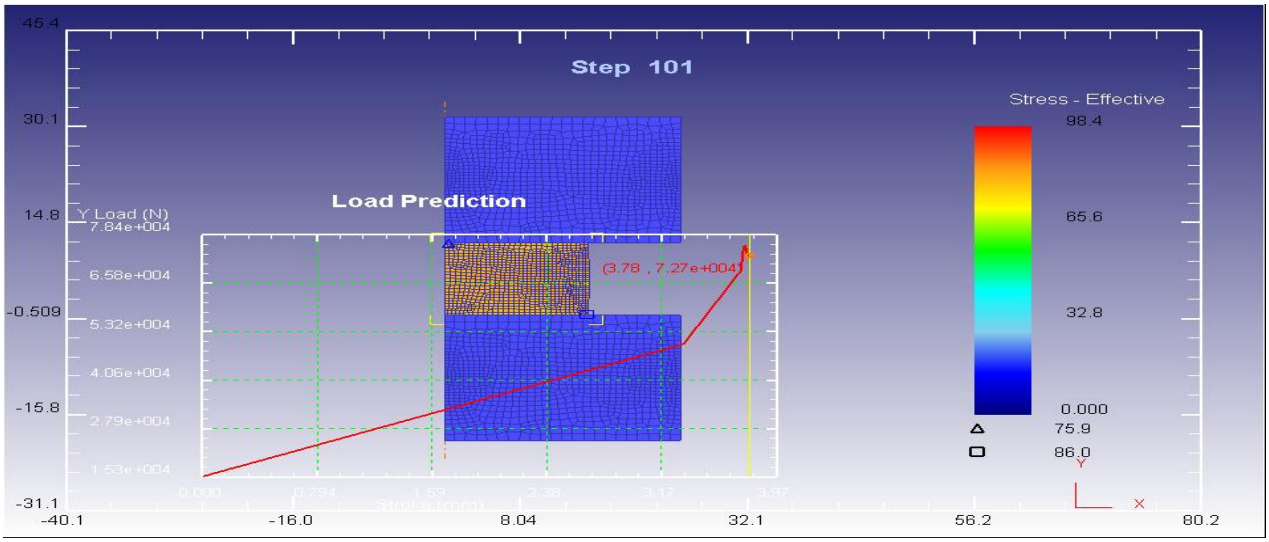

Figure 4.16: Compressive stress for aluminium with 6% weight fraction of red mud (42 nm) at 30% reduction using Deform-2D software

4.6.1 Overall Compression test results with Deform -2D Software

Both experimental and Deform-2D simulated compressive stress values are shown in Table 4.5.

Table 4.5: Experimental and Deform-2D simulated compressive stress results

s.no	%Wt. of RM		Particle size of RM	Stress at 10% reduction			Stress at 20% reduction			Speed at 30% reduction		
				Experimental Result (MPa)	Simulation Result (MPa)	Error(%)=(Experimental-simulated)x100(experimental	Experimental Result (MPa)	Simulation Result (MPa)	Error (%)	Experimental Result (MPa)	Simulation Result (MPa)	Error (%)
1	2		100 µm	52.6	48.9	7.03	76.8	75.2	2.08	84.5	81.5	3.55
2	2		150 µm	52.1	48.3	7.29	75.2	74.1	1.46	83.9	81	3.46
3	2		200 µm	51.4	47.3	7.98	74.6	72.8	2.41	82.6	80.3	2.78
4	2		42 nm	50.1	49.9	0.40	78.2	77	1.53	86.1	82.4	4.30
5	4		100 µm	54.8	51.4	6.20	81.4	80.8	0.74	88.5	87.8	0.79
6	4		150 µm	60.2	57.7	4.15	80.7	78.1	3.22	86.7	84.8	2.19
7	4		200 µm	59.2	57.7	2.53	79.8	77	3.51	85.5	83.3	2.57
8	4		42 nm	62.9	62.3	0.95	82.3	76.4	7.17	90.9	89.6	1.43
9	6		100 µm	71.5	70.3	1.68	91.4	89.7	1.86	97.3	96.4	0.92
10	6		150 µm	58.3	56.2	3.60	89.7	85.9	4.24	95.1	93.2	2.00
11	6		200 µm	57.3	54.5	4.89	86.6	84.7	2.19	94	91.7	2.45
12	6		42 nm	63.1	58.2	7.77	92.9	92.1	0.86	98.8	98.4	0.40

From the Figure 4.14 – 4.16, Appendix-I and Table 4.5, it has been observed that the compression strength values are higher for the 42nm particle size of red mud than 100 µm, 150 µm and 200 µm particle size of red mud with aluminium metal matrix composites. This is due to the better surface area of contact and higher bond strengths of nano particles.

4.7 MICRO STRUCTURAL OBSERVATIONS

4.7.1. Scanning Electron Microscope (SEM) Analysis

The micro structural observation for pure aluminium with 6% red mud and 4% tungsten carbide metal matrix composite of better hardness and compression strength sample is performed. The Scanning Electron Microscope (SEM) analysis for pure aluminium with 6% red mud and 4% tungsten carbide is analysed by JEOL, JSM-6610LV made in Japan having the particle dispersion of the given hybrid metal matrix composite. The SEM images of sintered pure aluminium with 6% red mud of 42 nm and pure aluminium with 6% red mud of 42 nm and 4% tungsten carbide are shown in Figure 4.17 and 4.18 respectively.

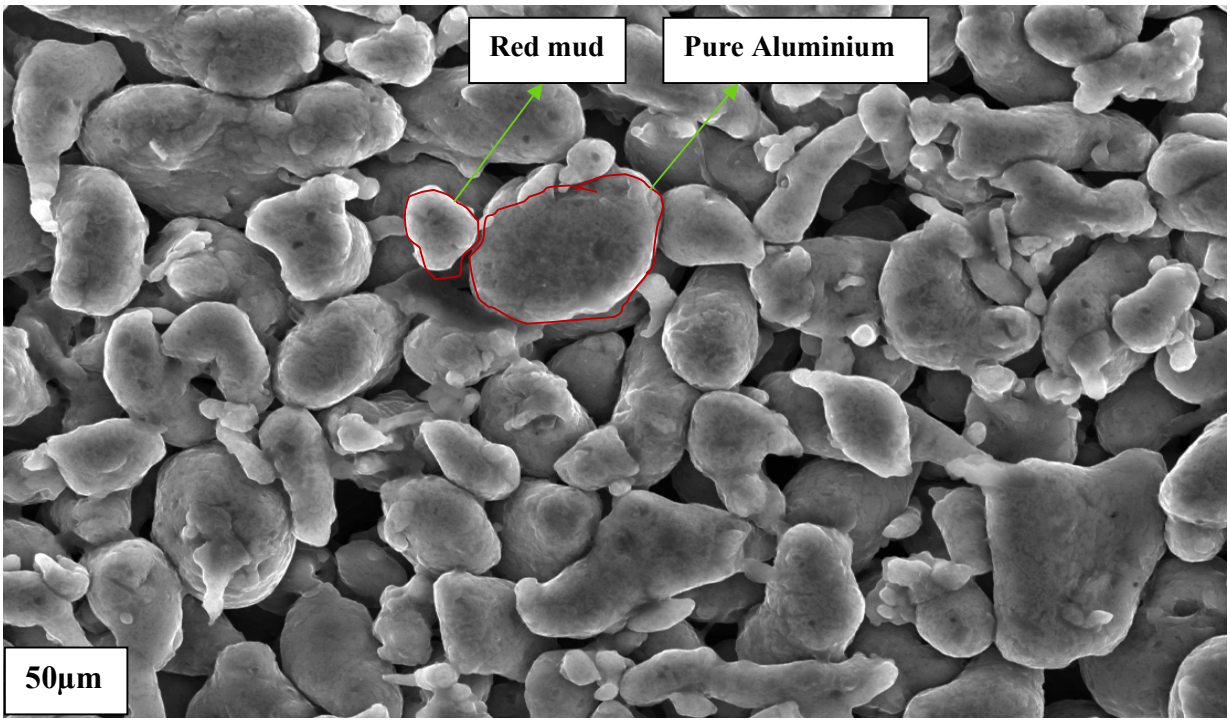

Figure 4.17: SEM analysis for sintered pure aluminium with 6% red mud (42 nm)

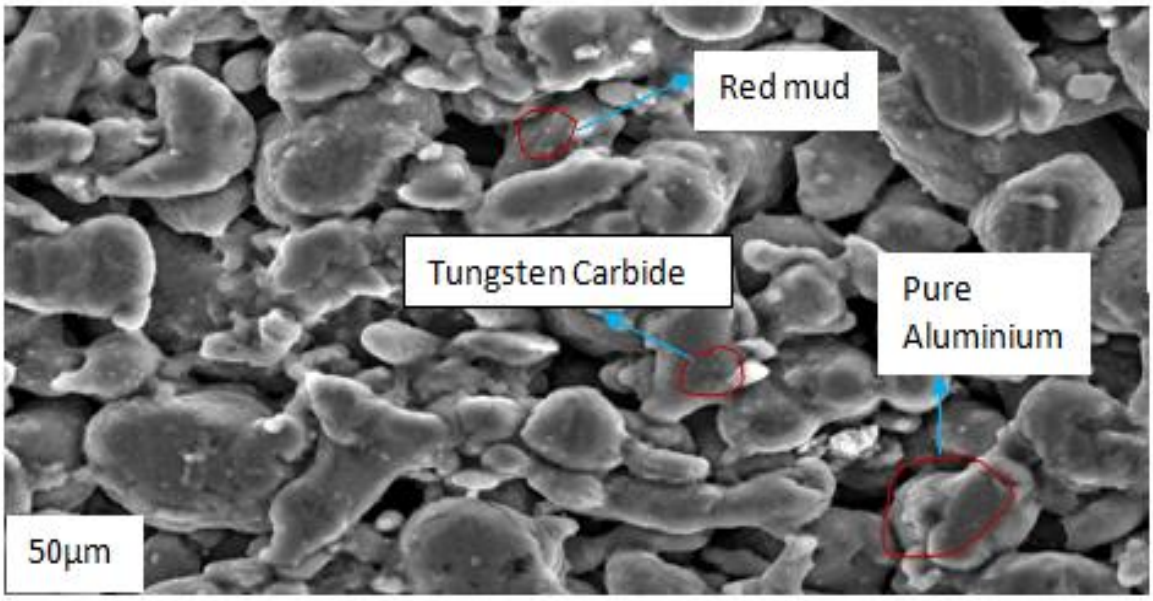

Figure 4.18: SEM analysis for sintered pure aluminium with 6% red mud (42 nm) and 4%tungsten Carbide

4.7.2. Energy Dispersive X-Ray Spectroscopy (EDX)

The Energy dispersive X-ray spectroscopy (EDX) analysis for pure aluminium with red mud and pure aluminium with 6% red mud and 4% tungsten carbide are shown in Figure 4.19 and 4.20 respectively by Inca Penta FET X3 of model no:7573 and resolution 129eV which is made by Oxford instruments.

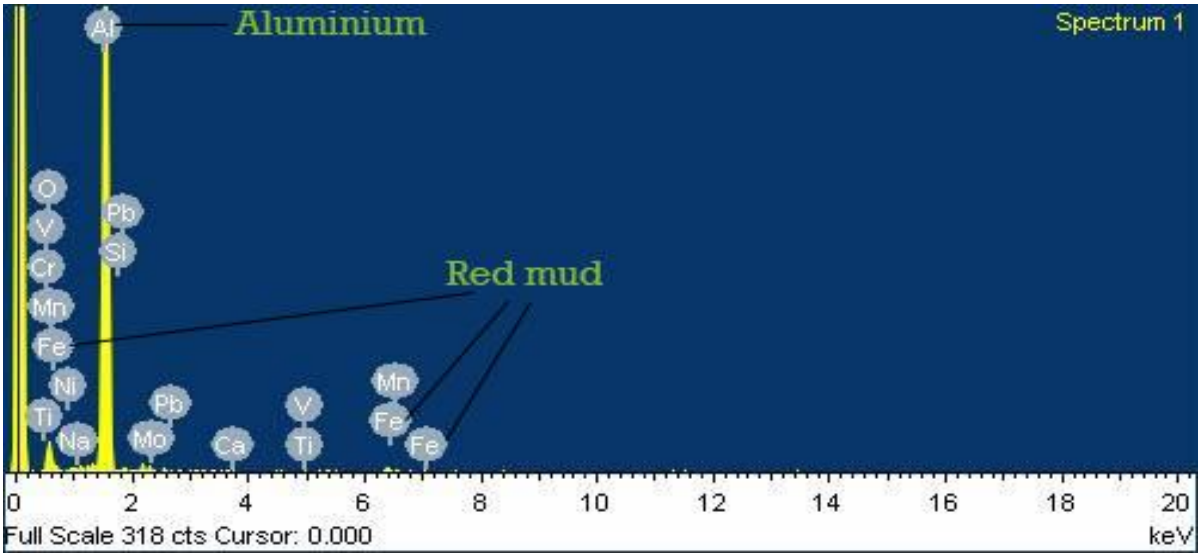

Figure 4.19: EDX analysis for pure aluminium with red mud

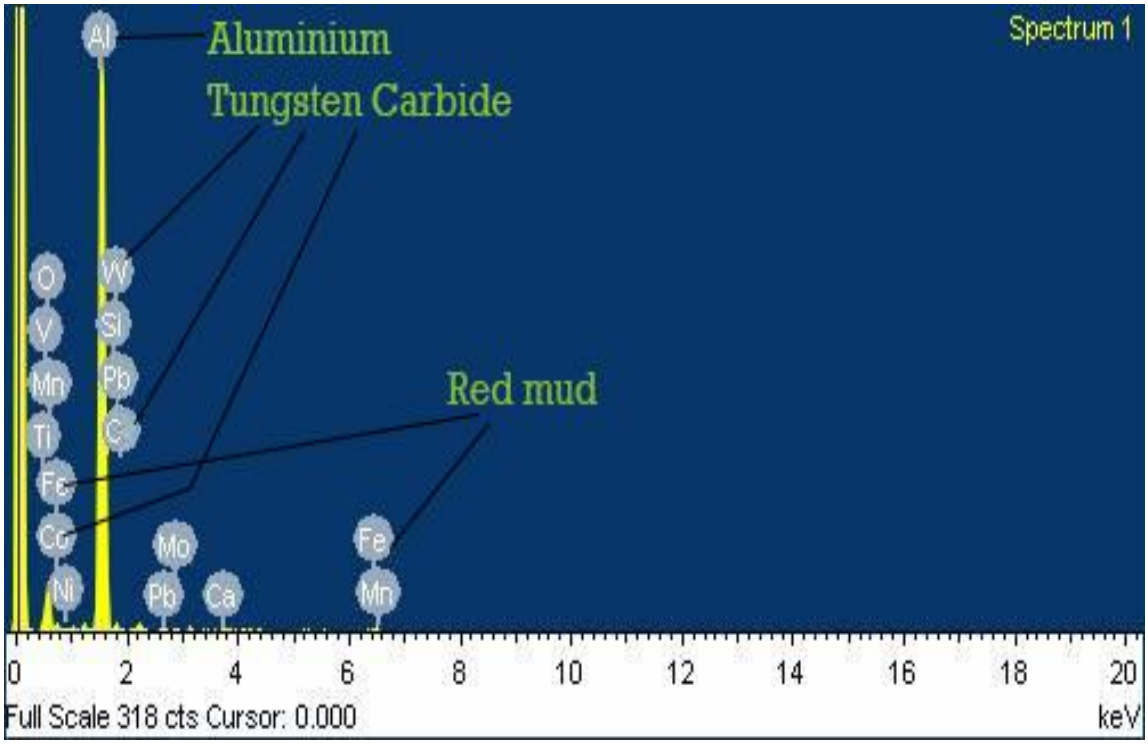

Figure 4.20: EDX analysis for pure aluminium with 6% red mud and 4%tungsten Carbide

4.8 RESULTS

- It has been observed that the hardness values variation depicts the information that nano red mud specimens have more hardness when compared with micro nature specimens. An increase in hardness and compression strength is observed for 6% weight fraction of nano level red mud.
- Since finer particles are strongly bonded to each other in a composite, the hardness and compression strength values of the nano composites are higher when compared to the micro level.
- It is also observed that for the same percentage weight fraction of red mud, the hardness and compression strength are higher for the nano structured reinforcement than micro structured reinforcement. This is owing to the increase in surface area of contact and higher bond strengths. Hardness and compression strength properties are improved for nano level aluminium-red mud test specimen with 42 nm size and 6% weight fraction of red mud.

- Initially, hardness increased with the addition of the tungsten carbide and then it is improved with an increment of the red mud. The simulated results of compression strength using Deform-2D software and experimental values are within the limits of 1-8% difference i.e., the % error is varied from 0.24 - 7.51 as shown in Table 4.5. Energy Dispersive X-ray spectroscopy (EDX) and Scanning Electron Microscope (SEM) structures are analysed to study the particle dispersion.
- A mathematical model is developed using regression analysis for the hardness values of aluminium with red mud and aluminium, red mud with tungsten carbide at normal and heat treatment conditions. The predicted equations are significant in nature with near unity R-square values.

4.9 SUMMARY

The present chapter gives the information regarding hardness test at normal condition and heat treatment conditions of pure aluminium, aluminium-red mud and aluminium-tungsten carbide-red mud of different weight fractions. The mathematical modeling is done by regression analysis. Compression test experimental results are validated using simulated Deform-2D software results and it has been observed that % error of both experimental and simulated values are close to each other. The micro structural observation such as Scanning Electron Microscope (SEM) analysis and Energy Dispersive X-Ray Spectroscopy (EDX) analysis are carried out.

CHAPTER-5

TRIBOLOGICAL CHARACTERIZATION OF PURE ALUMINIUM WITH RED MUD

5.1 INTRODUCTION

The present chapter is describing the tribological characterization of aluminium with red mud at normal and heat treatment conditions. The wear characteristics are investigated with an optimal combination of aluminium and 2%, 4% and 6% weight fractions of micro and nano level red mud metal matrix composites. Using regression analysis, the mathematical prediction is carried out for both normal and heat treatment conditions.

5.2 WEAR CHARACTERISTICS ANALYSIS AT NORMAL CONDITIONS

Experiments have been conducted in the pin-on-disc wear testing machine monitor with data acquisition system, which is used to evaluate the wear behaviour of the composite, against hardened ground steel disc (EN-32) having surface roughness (Ra) 0.5µm. Sliding generally occurs between a stationary pin and a rotating disc. The disc rotates with the help of a D.C. motor having speed range 0-1000 rpm with wear track diameter 50 mm-80 mm, which could yield sliding speed 0 to 10 m/sec. The pin-on-disc wear testing machine is shown in Figure 5.1. The load is to be applied on the pin (specimen) by dead weight through pulley string arrangement. The wear tests are performed as per standards of ASTM G-99 with the unlubricated condition in a normal laboratory atmosphere at 55% relative humidity and a temperature of 27-31ºC. Each aluminium-red mud composite samples are conducted wear tests for 6 hours. The samples are cleaned with the solution of tetra chloro ethylene before and after the wear test.

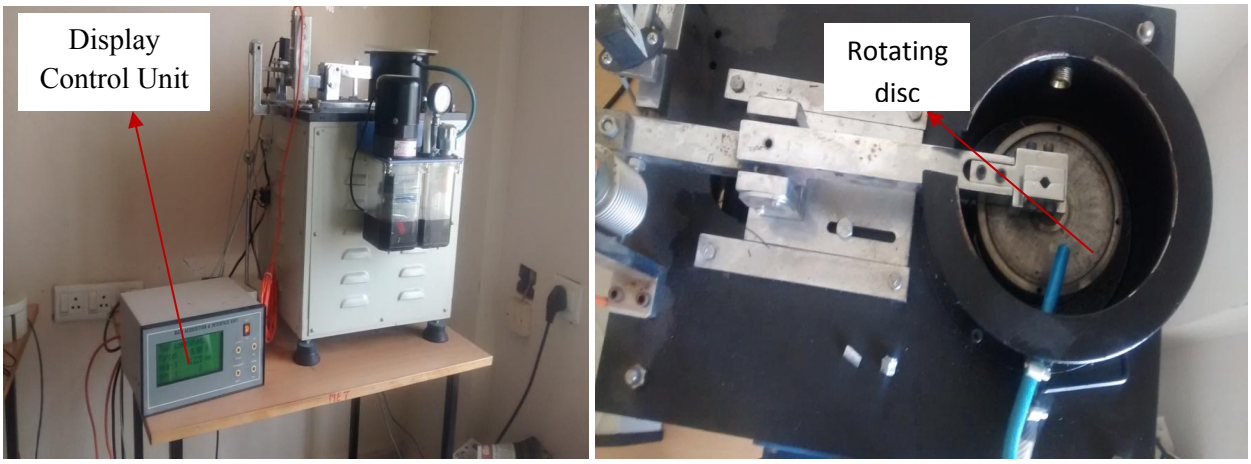

Figure 5.1: Pin-on-disc wear testing machine

The wear rate tables for pure aluminium with 2%, 4% and 6% weight fractions of red mud with 200 rpm, 400 rpm and 600 rpm pin-on-disc speed at normal condition are placed in Appendix-II-A (i, ii, and iii). The experimental wear test results of aluminium-red mud metal matrix composites at normal condition are placed in Table 5.1. It has been observed that the better wear resistance is obtained for pure aluminium with 6% red mud of 42 nm particle size at 600 rpm. The higher percentage of nano particles provided with greater iron oxide (Fe_2O_3), SiO_2 and TiO_2.

Table 5.1: Experimental wear test results of aluminum-red mud metal matrix composites at normal condition

S. No	Weight of red mud (%)	Particle size	Speed (RPM)	Wear rate x10^{-6} N/m		
				At 10N load	At 20N load	At 30N load
1	0	45µm	200	0.691	1.012	1.331
2	0	45µm	400	0.685	1.004	1.322
3	0	45µm	600	0.569	0.887	1.205
4	2	100 µm	200	0.415	0.742	1.069
5	2	100 µm	400	0.385	0.695	1.005
6	2	100 µm	600	0.350	0.632	0.914
7	2	150 µm	200	0.524	0.943	1.362
8	2	150 µm	400	0.495	0.895	1.315
9	2	150 µm	600	0.450	0.854	1.258
10	2	200 µm	200	0.582	1.021	1.512
11	2	200 µm	400	0.550	1.070	1.500
12	2	200 µm	600	0.510	0.918	1.326
13	2	42 nm	200	0.281	0.506	0.731
14	2	42 nm	400	0.243	0.439	0.635
15	2	42 nm	600	0.223	0.412	0.601
16	4	100 µm	200	0.246	0.443	0.640
17	4	100 µm	400	0.225	0.415	0.608
18	4	100 µm	600	0.207	0.374	0.541
19	4	150 µm	200	0.317	0.571	0.825

20	4	150 µm	400	0.295	0.537	0.779
21	4	150 µm	600	0.240	0.435	0.630
22	4	200 µm	200	0.384	0.691	0.998
23	4	200 µm	400	0.360	0.653	0.946
24	4	200 µm	600	0.342	0.627	0.912
25	4	42 nm	200	0.156	0.280	0.404
26	4	42 nm	400	0.143	0.260	0.377
27	4	42 nm	600	0.152	0.254	0.369
28	6	100 µm	200	0.182	0.328	0.474
29	6	100 µm	400	0.162	0.291	0.420
30	6	100 µm	600	0.154	0.278	0.402
31	6	150 µm	200	0.262	0.472	0.682
32	6	150 µm	400	0.245	0.447	0.649
33	6	150 µm	600	0.192	0.346	0.492
34	6	200 µm	200	0.317	0.571	0.825
35	6	200 µm	400	0.319	0.575	0.821
36	6	200 µm	600	0.283	0.513	0.744
37	6	42 nm	200	0.145	0.262	0.379
38	6	42 nm	400	0.132	0.235	0.334
39	6	42 nm	600	0.122	0.229	0.332

The plot between wear rate and 2%, 4% and 6% weight fractions of red mud, for the particle size of 100µm at 10N load is shown in Figure 5.2.

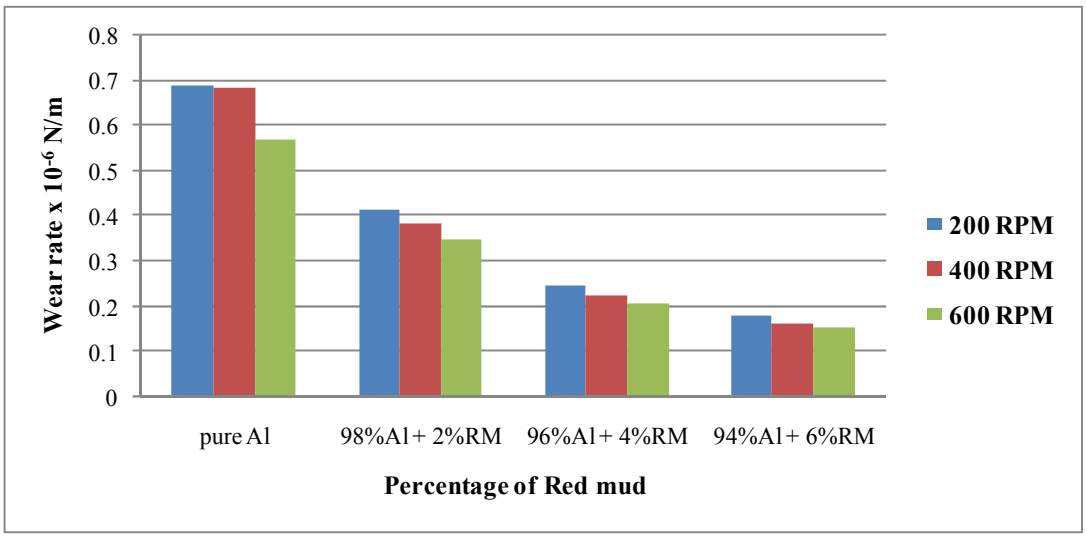

Figure 5.2: Plot between wear rate and percentage of red mud, for particle size of 100µm of 10N load

The plot between wear rate and 2%, 4% and 6% weight fractions of red mud, for the particle size of 150µm at 10N load is shown in Figure 5.3.

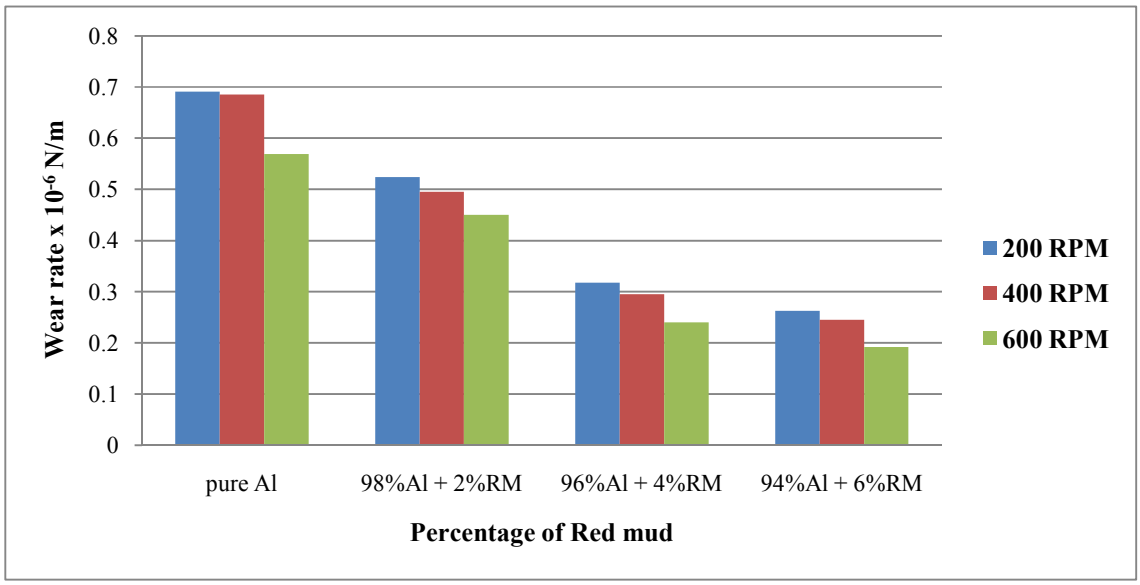

Figure 5.3: Plot between wear rate and percentage of red mud, for particle size of 150µm of 10N load

The plot between wear rate and 2%, 4% and 6% weight fractions of red mud, for the particle size of 200µm at 10N load is shown in Figure 5.4.

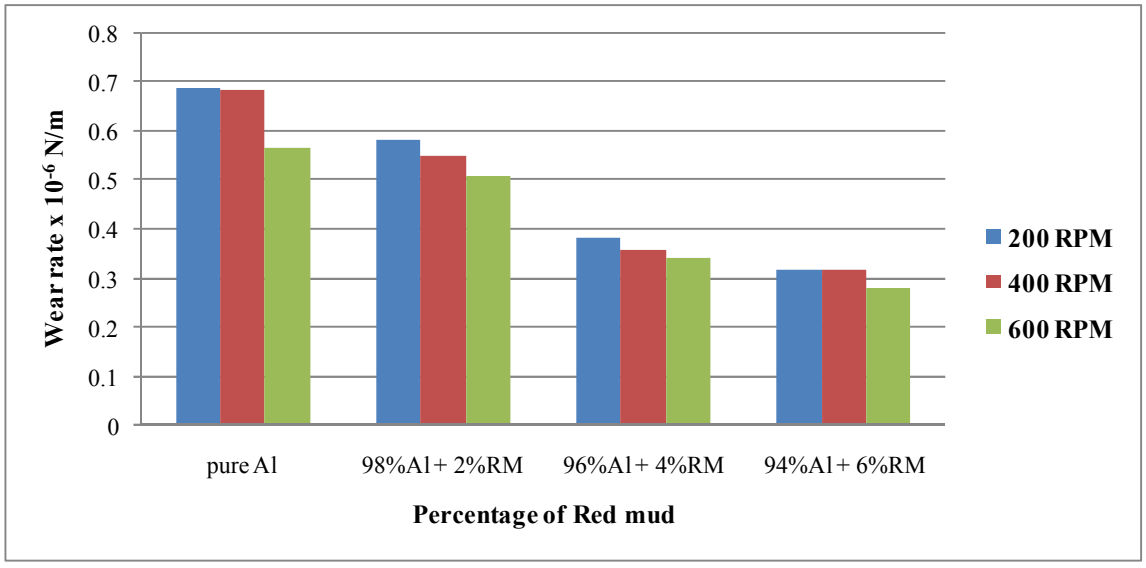

Figure 5.4: Plot between wear rate and percentage of red mud, for particle size of 200µm of 10N load

The plot between wear rate and 2%, 4% and 6% weight fractions of red mud, for the particle size of 42 nm at 10N load is shown in Figure 5.5.

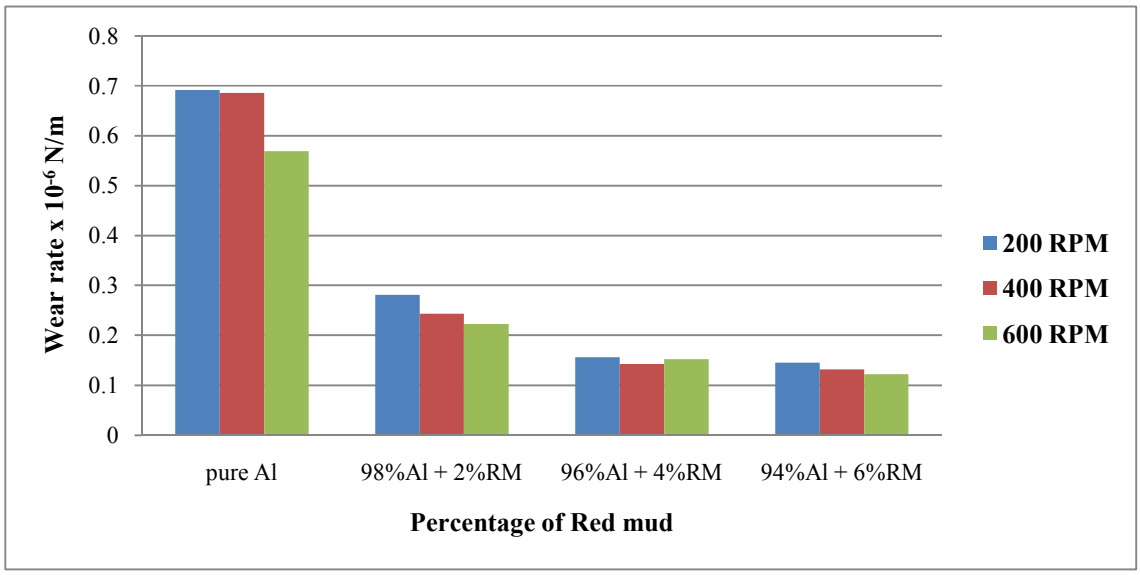

Figure 5.5: Plot between wear rate and percentage of red mud, for particle size of 42nm of 10N load

The plot between wear rate and 2%, 4% and 6% weight fractions of red mud, for the particle size of 100µm at 20N load is shown in Figure 5.6.

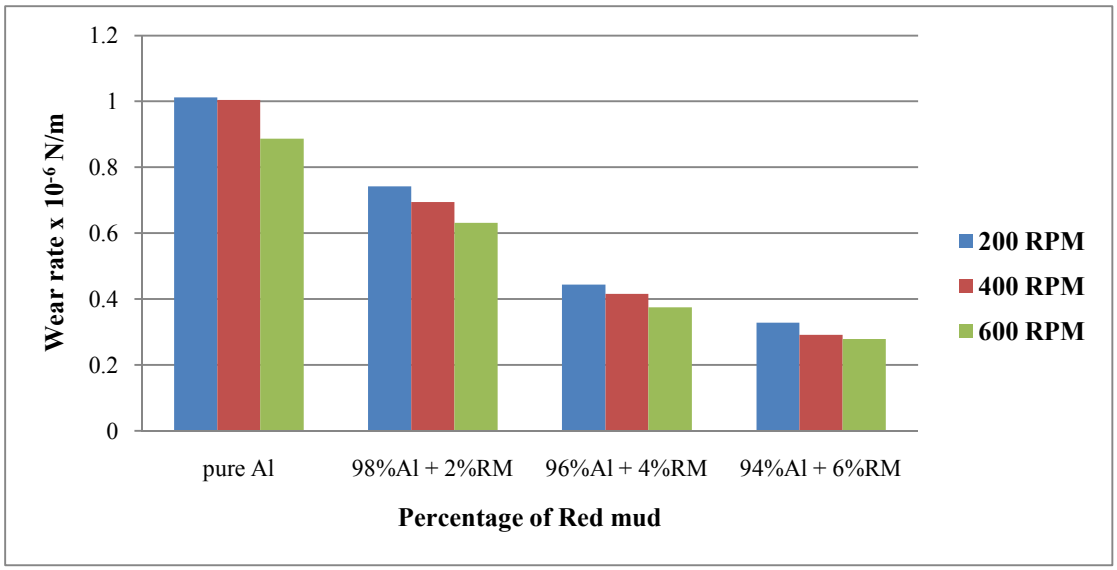

Figure 5.6: Plot between wear rate and percentage of red mud, for particle size of 100µm of 20N load

The plot between wear rate and 2%, 4% and 6% weight fractions of red mud, for the particle size of 150µm at 20N load is shown in Figure 5.7.

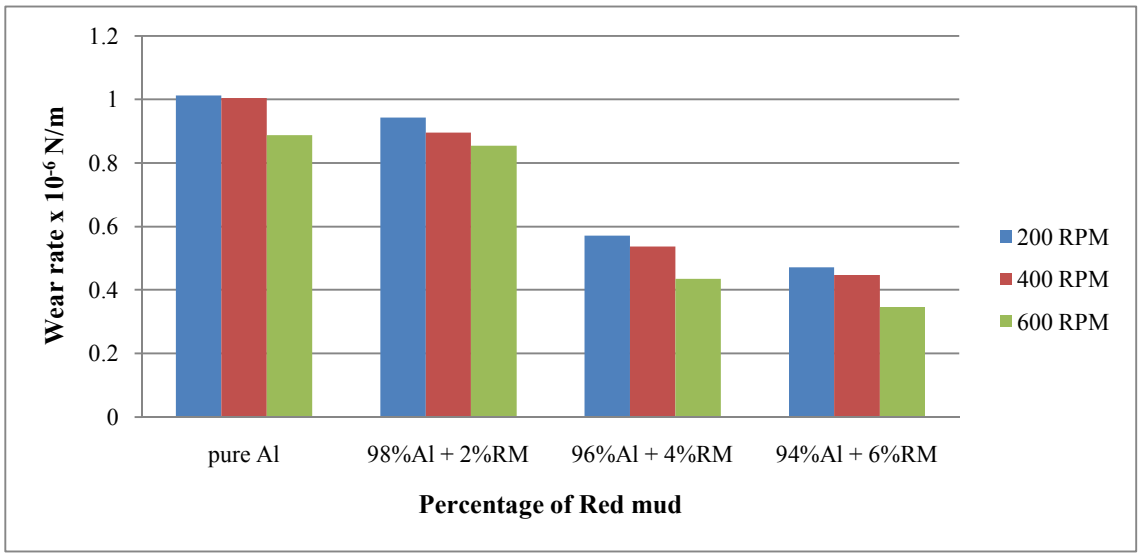

Figure 5.7: Plot between wear rate and percentage of red mud, for particle size of 150µm of 20N load

The plot between wear rate and 2%, 4% and 6% weight fractions of red mud, for the particle size of 200µm at 20N load is shown in Figure 5.8.

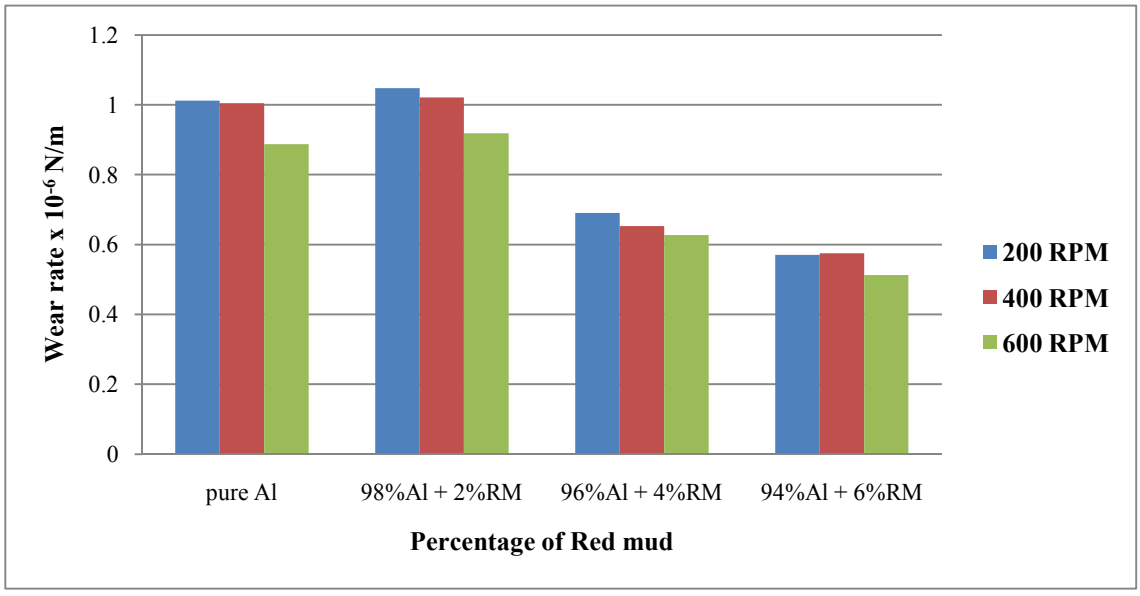

Figure 5.8: Plot between wear rate and percentage of red mud, for particle size of 200µm of 20N load

The plot between wear rate and 2%, 4% and 6% weight fractions of red mud, for the particle size of 42nm at 20N load is shown in Figure 5.9.

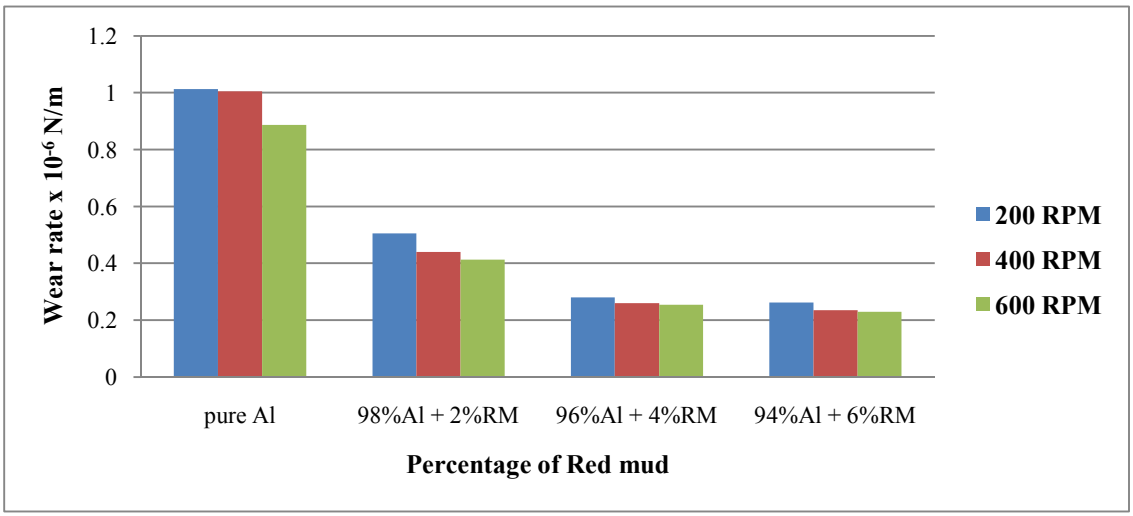

Figure 5.9: Plot between wear rate and percentage of red mud, for particle size of 42nm of 20N load

The plot between wear rate and 2%, 4% and 6% weight fractions of red mud, for the particle size of 100µm at 30N load is shown in Figure 5.10.

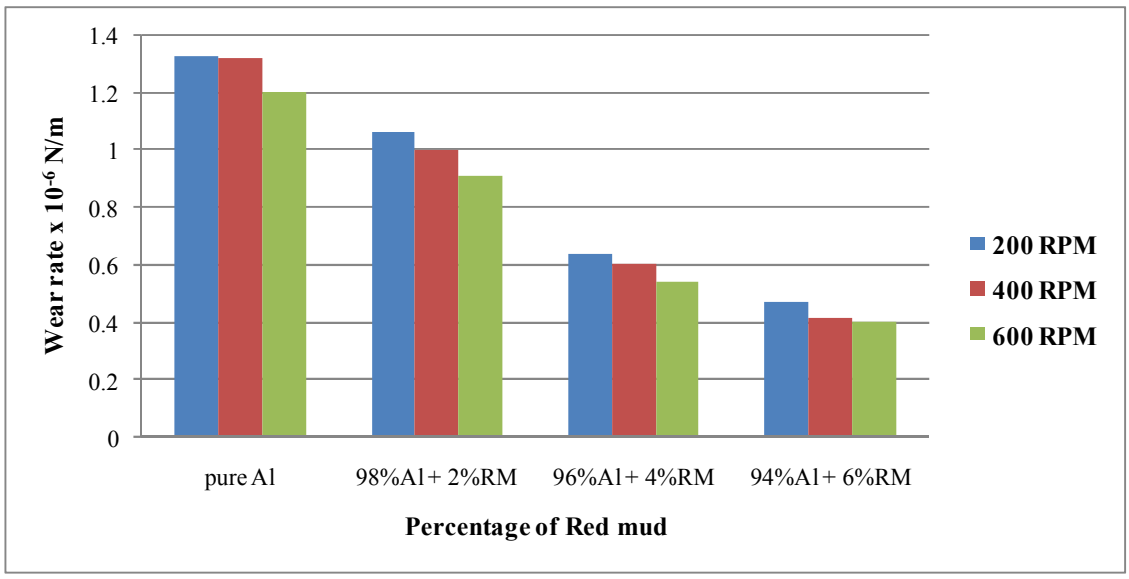

Figure 5.10: Plot between wear rate and percentage of red mud, for particle size of 100µm of 30N load

The plot between wear rate and 2%, 4% and 6% weight fractions of red mud, for the particle size of 150µm at 30N load is shown in Figure 5.11.

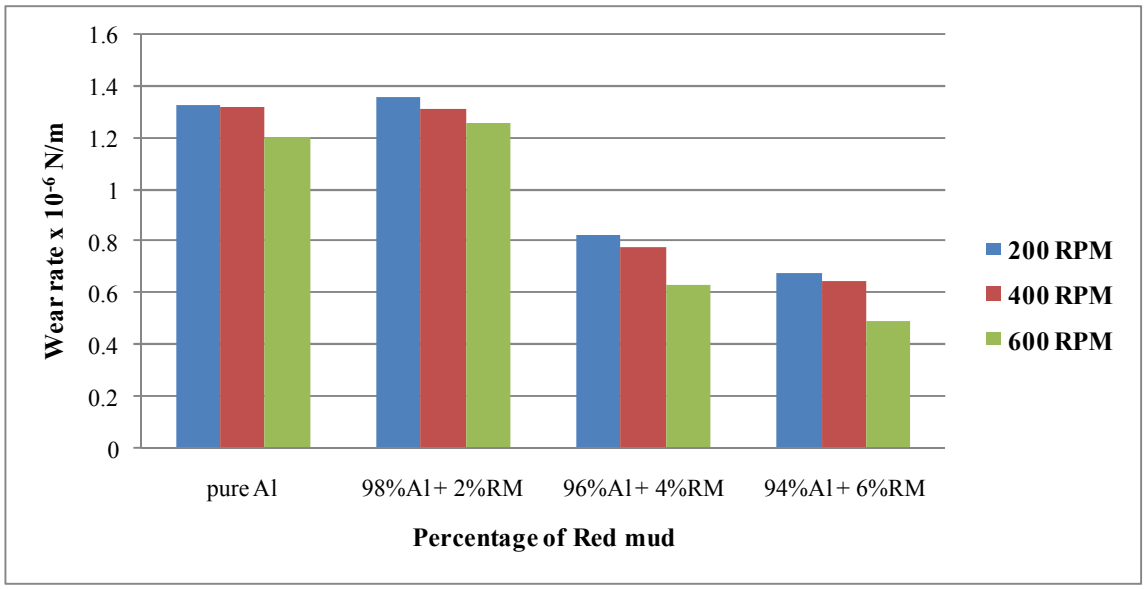

Figure 5.11: Plot between wear rate and percentage of red mud, for particle size of 150µm of 30N load

The plot between wear rate and 2%, 4% and 6% weight fractions of red mud, for the particle size of 200µm at 30N load is shown in Figure 5.12.

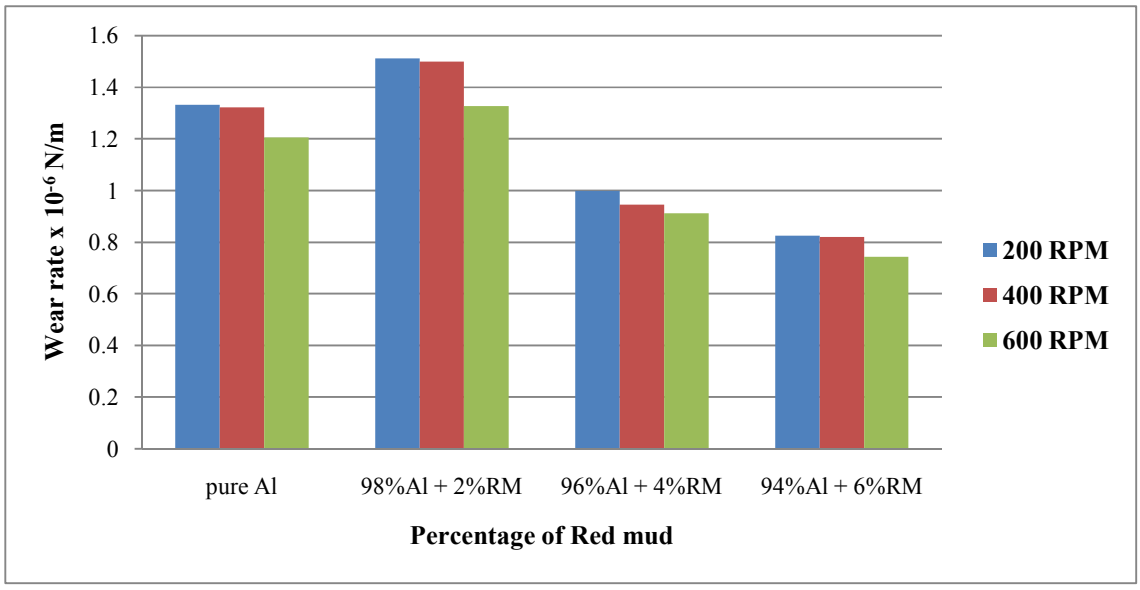

Figure 5.12: Plot between wear rate and percentage of red mud, for particle size of 200µm of 30N load

The plot between wear rate and 2%, 4% and 6% weight fractions of red mud, for the particle size of 42 nm at 30N load is shown in Figure 5.13.

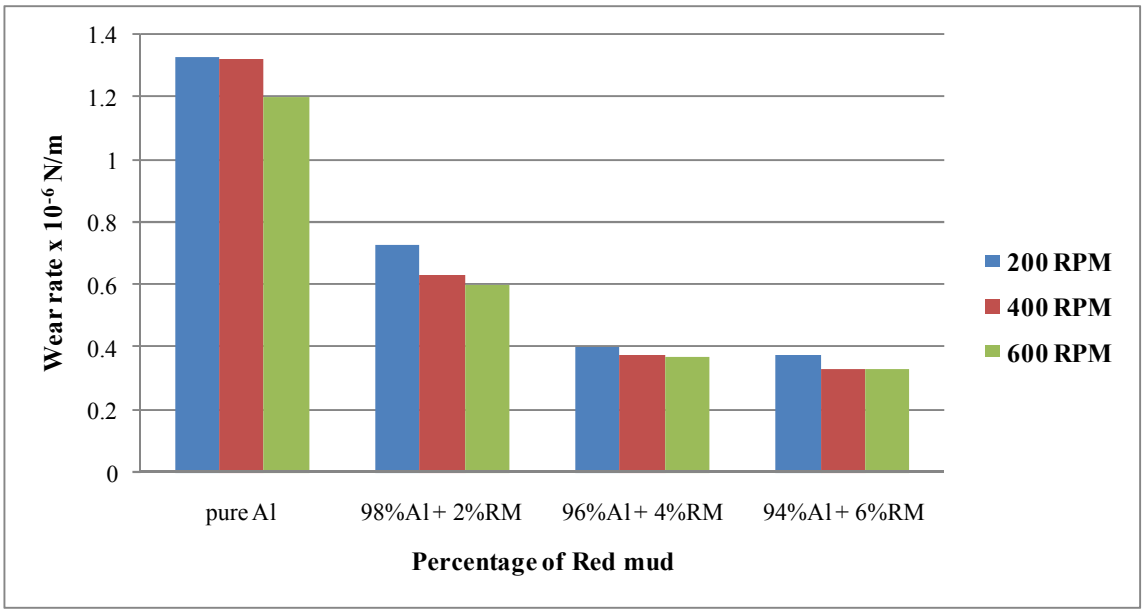

Figure 5.13: Plot between wear rate and percentage of red mud, for particle size of 42nm of 30N load

From Figure 5.2 to 5.13, it has been observed that the wear resistance is higher at 600 rpm speed compared to 400 rpm and 200 rpm speed. The 6% weight fraction of red mud with aluminium has better wear resistance because of the more iron oxide percentage value about 53.8% as a constituent element in red mud. As the increase in speed of rotation of the specimen, higher is the wear resistance. The Wear rate tables of 2%, 4% and 6% weight fractions of red mud, for the particle size of 100µm, 150µm, 200µm and 42 nm at 10N, 20N and 30N load are shown in Appendix-II-A (i, ii and iii).

5.3 WEAR CHARACTERISTICS ANALYSIS AT HEAT TREATMENT CONDITIONS

From Appendix-II-A (i, ii and iii), it is observed that red mud particle size of 100 µm has better wear resistance among 100 µm, 150 µm and 200 µm particle size of red mud with pure aluminium at normal condition. So, heat treatment is done for the particle size of 100 µm (micron level) and 42 nm (nano level) red mud of 6% weight composition with pure aluminium at 350^0C, 400^0C, 450^0C and 500^0C (Air Cooling) conditions. The wear rate tests are performed at 200 rpm,

400 rpm, and 600 rpm for both micro and nano level red mud with pure aluminium metal matrix composites. The wear rate tables for pure aluminium with 2%, 4% and 6% weight fractions of red mud with 200 rpm, 400 rpm and 600 rpm pin-on-disc speed at heat treatment conditions are placed in Appendix-II-B (i, ii and iii).

5.3.1 Micro Level (100 µm)

The wear rate values for pure aluminium with 6% red mud of 100 µm particle size at 600 rpm and 450^0C temperature is shown in Table 5.2. The remaining 100 µm, 150 µm and 200 µm (2%, 4% and 6% weight fraction of red mud) at 200 rpm, 400 rpm and 600 rpm are shown in Appendix II:B.

It has been observed that the better wear resistance is obtained for pure aluminium with 6% red mud of 100 µm particle size (micro level) at 600 rpm speed. In the case of 100 µm, the wear resistance is improved up to 450^0C only and then wear resistance starts declining in nature.

5.3.2 Nano Level (42 nm)

The wear rate values for pure aluminium with 6% red mud of 42 nm particle size at 600 rpm and 450^0C temperature is shown in Table 5.2. The 42 nm particle size of 2%, 4% and 6% weight fraction of red mud at 200 rpm, 400 rpm and 600 rpm are shown in Appendix II:B. The wear rate values for pure aluminium with 6% red mud of 42 nm particle size at 600 rpm, at 450^0C temperature is shown in Table 5.2.

It has been observed that the better wear resistance is obtained for pure aluminium with 6% red mud of 42 nm particle size (nano level) at 600 rpm speed. In the case of 42 nm, the wear resistance is improved up to 450^0C only and then wear resistance starts declining in nature.

In Table 5.2, the experimental wear test results of heat treated aluminium-red mud metal matrix composite samples are shown at 10N, 20N and 30N load.

Table 5.2: Experimental wear test results of heat treated aluminum-red mud metal matrix composites

S.No.	Wt of Red mud (%)	Temperature (^{0} C)	Particle Size	Speed (rpm)	Wear Rate x10^{-6}N/m		
					at 10 N load	at 20 N load	at 30 N load
1	6	350	100 µm	200	0.169	0.179	0.182
2	6	400	100 µm	200	0.162	0.171	0.176
3	6	450	100 µm	200	0.149	0.158	0.169
4	6	500	100 µm	200	0.156	0.165	0.174
5	6	350	100 µm	400	0.138	0.146	0.153
6	6	400	100 µm	400	0.132	0.140	0.148
7	6	450	100 µm	400	0.122	0.129	0.135
8	6	500	100 µm	400	0.125	0.132	0.139
9	6	350	100 µm	600	0.127	0.134	0.141
10	6	400	100 µm	600	0.120	0.127	0.136
11	6	450	100 µm	600	0.112	0.118	0.120
12	6	500	100 µm	600	0.118	0.125	0.128
13	6	350	42 nm	200	0.123	0.131	0.137
14	6	400	42 nm	200	0.118	0.125	0.132
15	6	450	42 nm	200	0.107	0.113	0.119
16	6	500	42 nm	200	0.115	0.122	0.126
17	6	350	42 nm	400	0.102	0.108	0.114
18	6	400	42 nm	400	0.095	0.101	0.105
19	6	450	42 nm	400	0.089	0.094	0.101
20	6	500	42 nm	400	0.091	0.096	0.105
21	6	350	42 nm	600	0.094	0.099	0.103
22	6	400	42 nm	600	0.085	0.090	0.095
23	6	450	42 nm	600	0.081	0.086	0.089
24	6	500	42 nm	600	0.083	0.088	0.092

The plot between wear rate, speed and temperature at 6% red mud of 100 µm particle size with pure aluminium at 10N, 20N and 30N load are shown in Figure 5.14, 5.15 and 5.16 respectively.

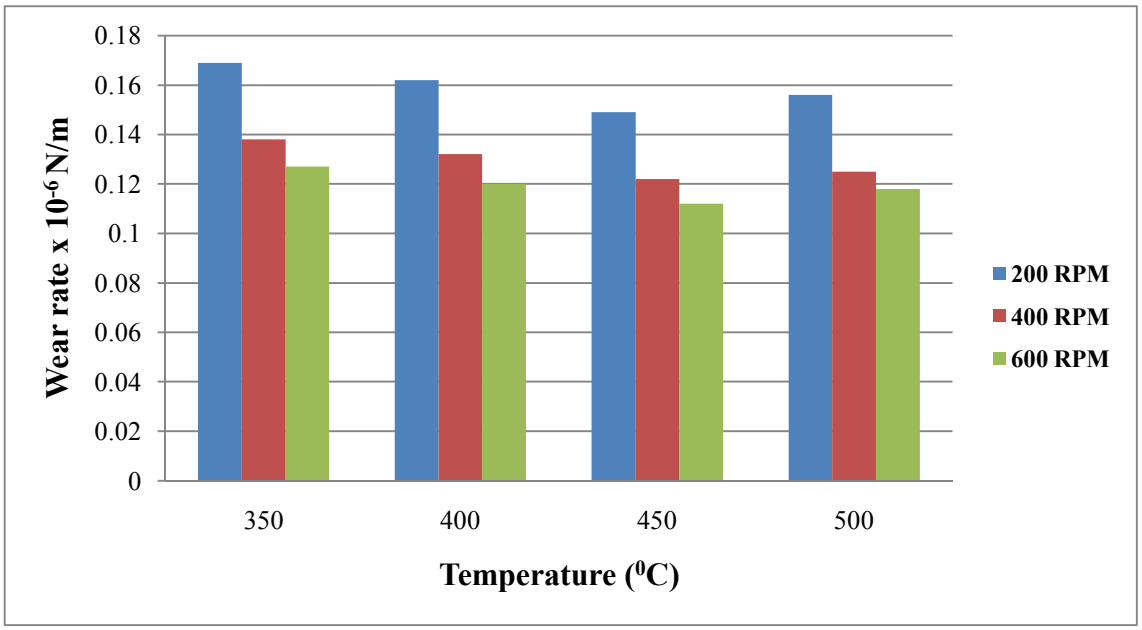

Figure 5.14: Wear rate, speed Vs temperature at 6% red mud (100 µm) with pure aluminium at 10N load

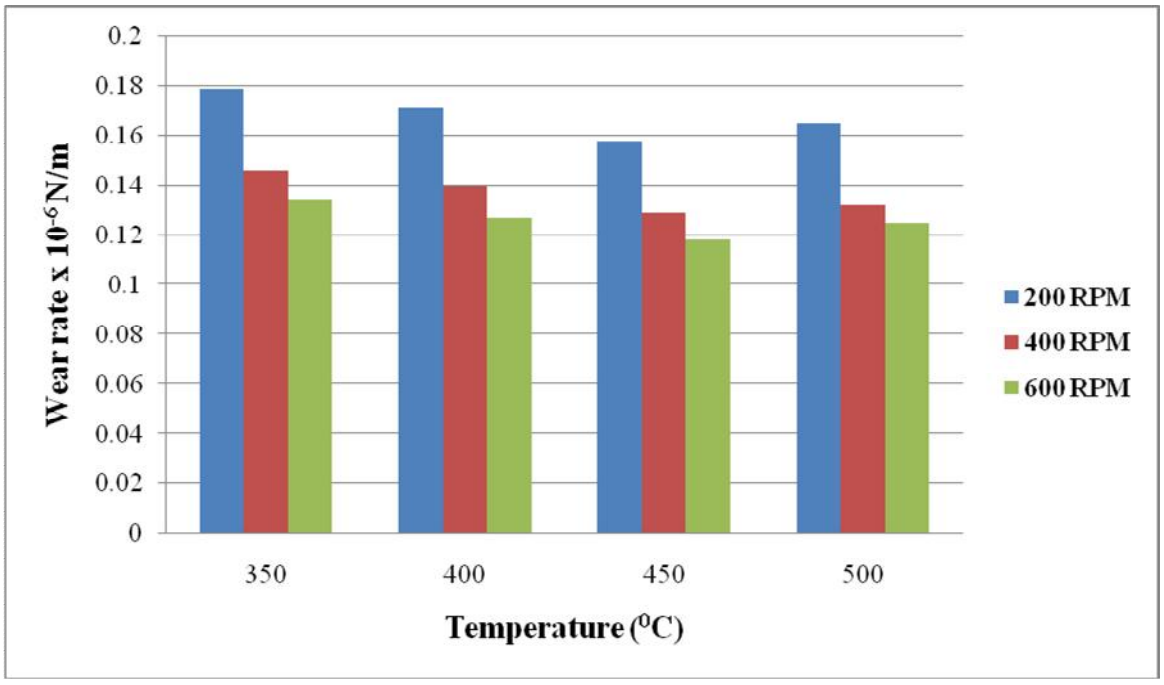

Figure 5.15: Wear rate, speed Vs temperature at 6% red mud (100 µm) with pure aluminium at 20N load

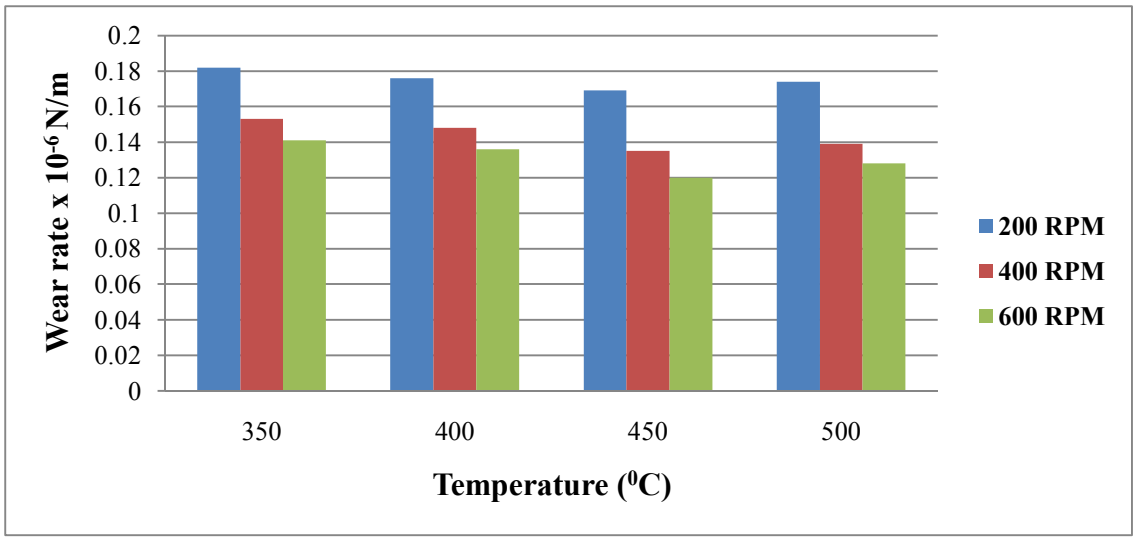

Figure 5.16: Wear rate, speed Vs temperature at 6% red mud (100 µm) with pure aluminium at 30N load

From Figure 5.14 -5.16, it has been observed that the specific wear rate decreases with increase in percentage weight fraction of red mud for 100 µm particle size at higher loads. Therefore, wear resistance is improved as co-efficient of friction decreases at higher loads.

The plot between wear rate, speed and temperature at 6% red mud of 42 nm particle size with pure aluminium at 10N, 20N and 30N load are shown in Figure 5.17, 5.18 and 5.19 respectively.

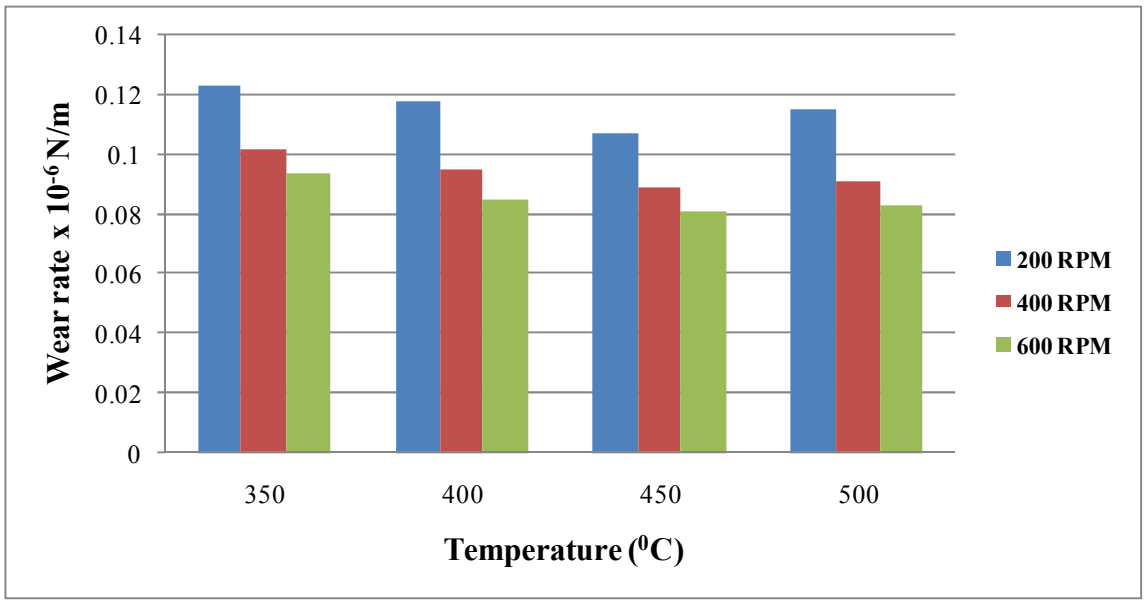

Figure 5.17: Wear rate, speed Vs temperature at 6% red mud (42 nm) with pure aluminium at 10N load

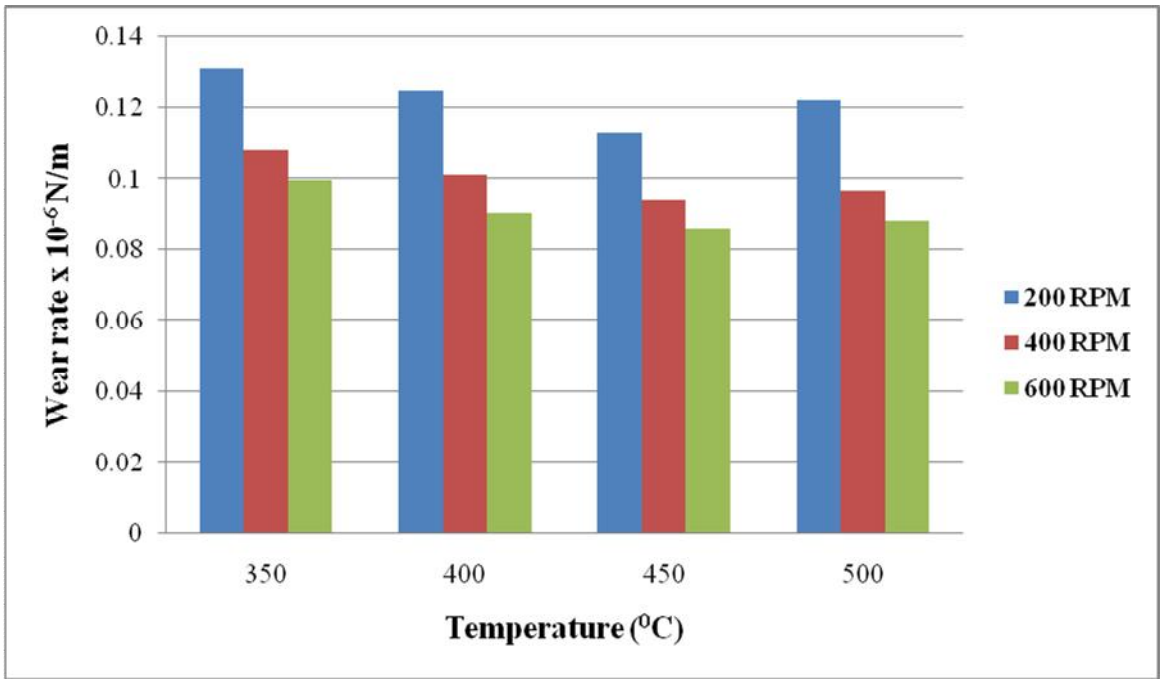

Figure 5.18: Wear rate, speed Vs temperature at 6% red mud (42 nm) with pure aluminium at 20N load

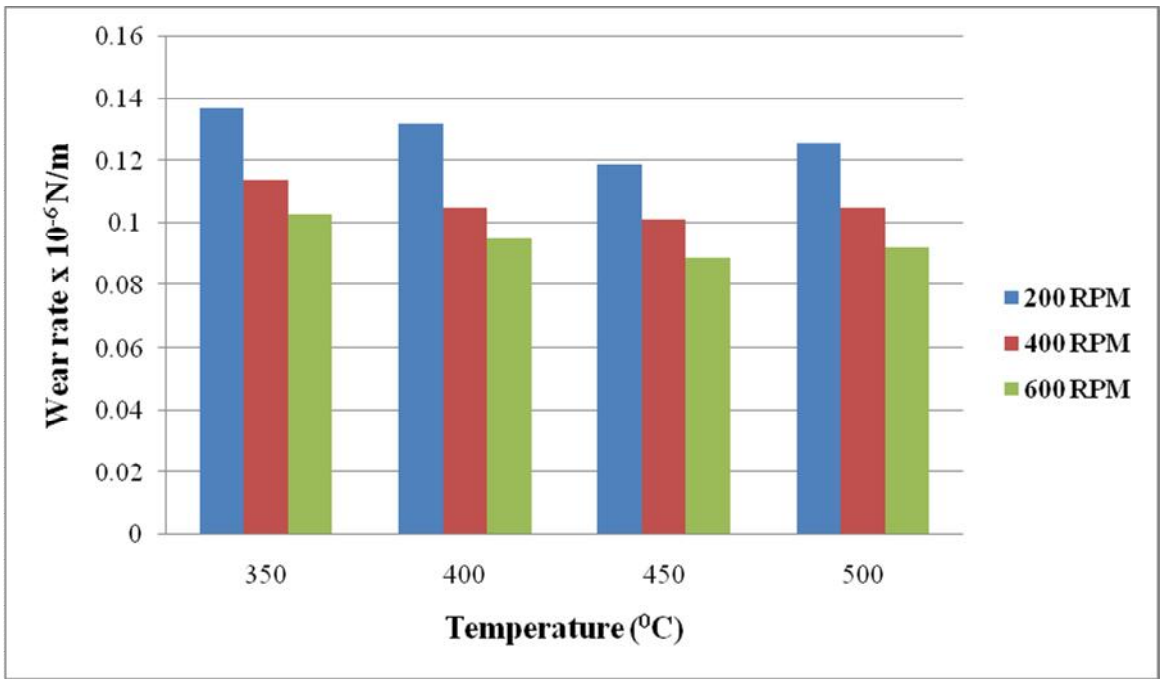

Figure 5.19: Wear rate, speed Vs temperature at 6% red mud (42 nm) with pure aluminium at 30N load

From Figure 5.17 -5.19, it has been observed that the specific wear rate decreases with increase in percentage weight fraction of red mud for 42 nm particle size at higher loads. Therefore, wear resistance is improved as co-efficient of friction decreases at higher loads.

5.4 MATHEMATICAL MODELING BY REGRESSION ANALYSIS

A mathematical model is developed for pure aluminium and red mud at normal condition and the overall equation is obtained using Regression analysis which is shown in equation 5.1.

Wear rate = 0.434552+ [(0.001107) x particle size] - [(0.0519) x percentage Weight fraction of red mud] - [(0.00013) x speed] ---------- (5.1)

As per the developed regression statistics, the R square value is 0.912814 and obtained standard error is 0.03928.

A ma $^{100\ \mu m}$ model is developed for pure aluminium and red mud at heat treatment condition and the overall equation is obtained using Regression analysis which is shown in equation 5.2.

Wear rate = $0.168434 - [(8.2 \times 10^{-5}) \times \text{Temperature}] + [(0.000373) \times \text{particle size}] - [(8.7 \times 10^{-5}) \times (\text{speed})]$ ---------- (5.2)

SUMMARY OUTPUT								
Regression Statistics								
Multiple R	0.97272108							
R Square	0.9461863							
Adjusted R Square	0.93811425							
Standard Error	0.00624144							
Observations	24							
	Coefficients	*Standard Error*	*t Stat*	*P-value*	*Lower 95%*	*Upper 95%*	*Lower 95.0%*	*Upper 95.0%*
Intercept	0.16843435	0.010334702	16.2979394	5.1601E-13	0.146876538	0.18999216	0.14687654	0.18999216
X Variable 1	-8.233E-05	2.27905E-05	-3.6126113	0.00173671	-0.000129874	-3.479E-05	-0.00012987	-3.479E-05
X Variable 2	0.00037266	2.54913E-05	14.6189713	3.864E-12	0.000319483	0.00042583	0.00031948	0.00042583
X Variable 3	-8.719E-05	7.80181E-06	-11.175298	4.733E-10	-0.000103462	-7.091E-05	-0.00010346	-7.091E-05

Figure 5.20: Regression statistics of Wear rate results for pure aluminium and red mud at heat treatment condition

The regression statistics for pure aluminium and red mud metal matrix composites at heat treatment condition is shown in Figure 5.20. It is observed that the R-square value is 0.9461 and adjusted R-square value is 0.9381. As per the regression statistics, the influence of red mud particle size has much higher than temperature and speed properties.

5.5 RESULTS

- The red mud constituents (Ferrous oxide) are harder in nature, as the percentage weight fraction of the red mud increases, the wear resistance of the whole composite also increases. The maximum wear resistance is obtained for 42 nm level of 6% weight fraction of red mud with pure aluminium compared to 100 μm level of red mud reinforced aluminium metal matrix composites.
- The dispersion of oxide phases like Fe_2O_3, Al_2O_3 and TiO_2 etc., might have uniformly presented throughout the pure aluminium matrix which strengthened the metal matrix composite material.
- As the increase in speed of rotation of the specimen, the wear rate is decreased which means that wear resistance is higher. Highest wear resistance is observed for the test specimen with 42 nm size and 6% weight fraction of red mud with pure aluminium at 600 RPM speed.
- As particle size decreases, there is a significant improvement in wear resistance. As compared to micro level, nano level has achieved the highest wear resistance also due to the interfacial area between the matrix material aluminium and reinforced material red mud. In both the cases of 100 μm and 42 nm, up to 450^0C only the wear resistances is improved and then wear resistance starts declining in nature.

5.6 SUMMARY

The present chapter gives the results of tribological characterization such as wear rate at normal condition and heat treatment conditions of pure aluminium with red mud metal matrix composites. The graphs are plotted for micro and nano level combinations of red mud with pure aluminium metal matrix composites. The chapter also presents mathematical modeling using regression analysis.

CHAPTER-6

TRIBOLOGICAL CHARACTERIZATION OF PURE ALUMINIUM WITH RED MUD AND TUNGSTEN CARBIDE

6.1 INTRODUCTION

The present chapter is describing the tribological characterization of aluminium with red mud and tungsten carbide metal matrix hybrid composites at normal and heat treatment conditions. The wear characteristics are investigated with an optimal combination of aluminium with 4% tungsten carbide and 2%, 4% and 6% weight fractions of micro and nano level red mud metal matrix composites. Using regression analysis, the mathematical prediction is carried out for both normal and heat treatment conditions.

6.2 WEAR CHARACTERISTICS ANALYSIS AT NORMAL CONDITION

The pin-on-disc wear testing machine conditions are specified in section 5.2 in chapter 5. All the wear tests were carried out as per ASTM G-99 standard under unlubricated condition in a normal laboratory atmosphere at 50-60% relative humidity and a temperature of 28-32ºC. The mass loss in the specimen after each test was estimated by measuring the weight of the specimen before and after each test using an electronic weighing machine having accuracy up to 0.01mg. Care has been taken so that the specimens under test are continuously cleaned with a woolen cloth to avoid the entrapment of wear debris and to achieve uniformity in the experimental procedure. The test pieces are cleaned with a tetra-chloro-ethylene solution prior and after each test.

The wear rate results for aluminium- red mud-tungsten carbide metal matrix composites at normal condition are shown in Table 6.1. The graph between wear rate and % weight fraction of red mud and 4% tungsten carbide with pure aluminium at normal condition is shown in Figure 6.1.

Table 6.1: Wear rate results for aluminium-red mud-tungsten carbide metal matrix composites at normal condition

Aluminium and 4% WC with % weight fraction of Red mud(RM)	Particle size	Wear rate x 10^{-6} (N/m)		
		at 10 N	at 20 N	at 30 N
Al+4% WC +2% RM	100 µm	0.346	0.618	0.887
Al+4% WC + 4% RM	100 µm	0.201	0.355	0.507
Al+4% WC +6% RM	100 µm	0.151	0.298	0.443
Al+4% WC +2% RM	42 nm	0.216	0.391	0.565
Al+4% WC +4% RM	42 nm	0.151	0.323	0.494
Al+4% WC +6% RM	42 nm	0.119	0.227	0.334

The plots between wear rate and percentage weight fractions of red mud, for the particle size of 100µm, 150µm, 200µm and 42 nm at 10N, 20N and 30N load are shown in Figure 6.1 to 6.3.

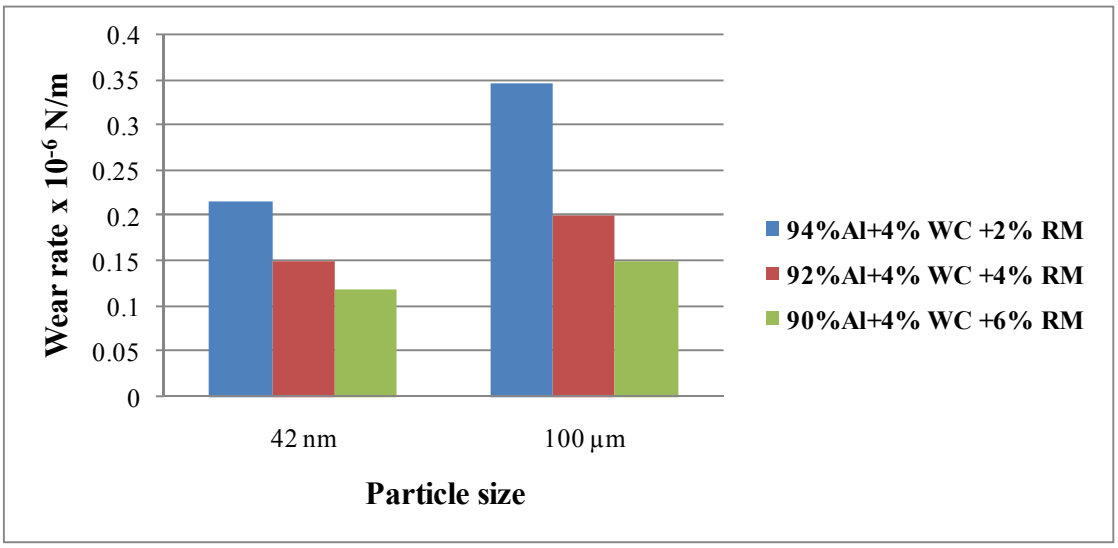

Figure 6.1: Plot between wear rate and particle size of Al+%WC+%RM for 10N load at normal condition

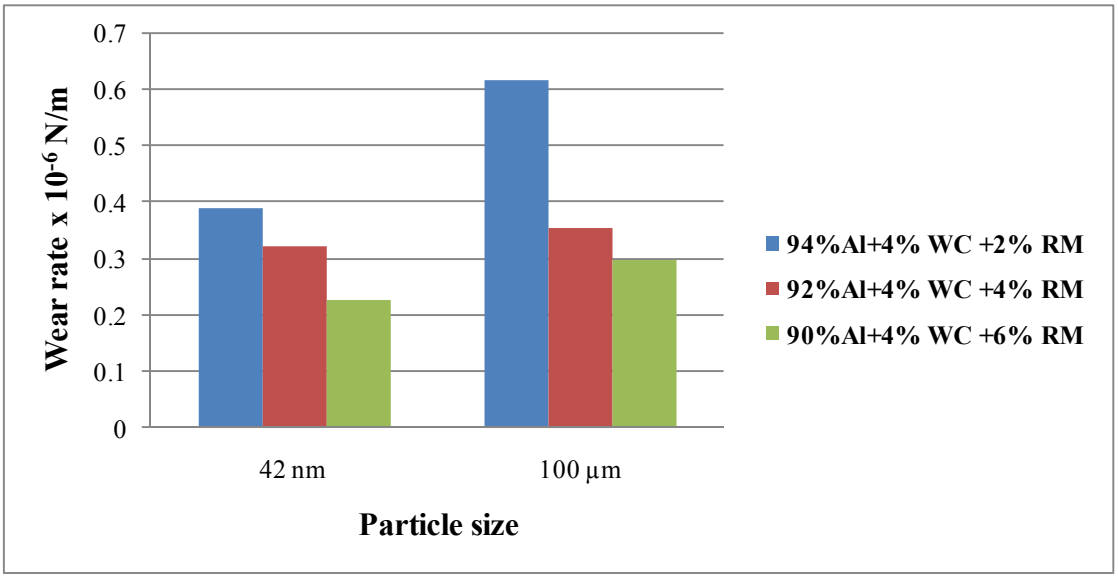

Figure 6.2: Plot between wear rate and particle size of Al+%WC+%RM for 20N load at normal condition

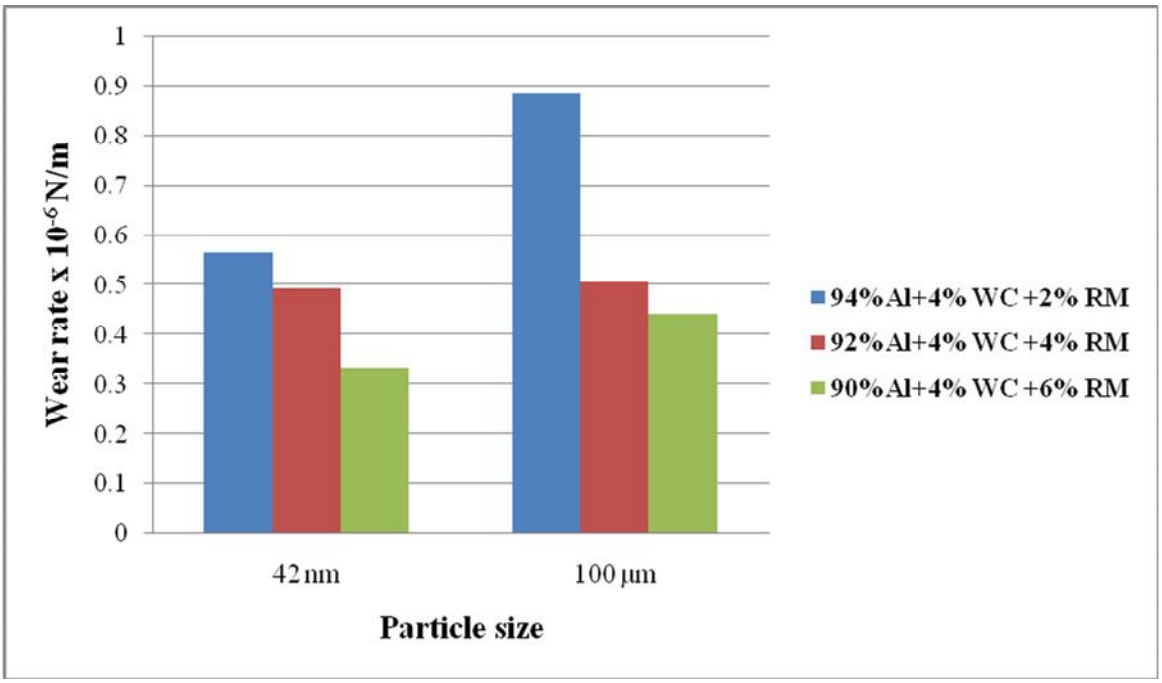

Figure 6.3: Plot between wear rate and particle size of Al+%WC+%RM for 30N load at normal condition

It is observed that for the same percentage weight fraction of red mud, the wear rate is higher for the micro level reinforcement than nano level reinforcement from Figure 6.1 - 6.3. Therefore, wear resistance is more for nano level 6% weight fraction of red mud with 90% aluminium and 4% tungsten carbide metal matrix hybrid composite. The wear rate tables for pure aluminium with red mud and tungsten carbide at normal condition are placed in Appendix III: A (i, ii, and iii).

6.3 WEAR CHARACTERISTICS ANALYSIS AT HEAT TREATMENT CONDITIONS

In Table 6.2, the experimental wear test results of heat treated aluminium-red mud-tungsten carbide metal matrix hybrid composites are shown at 10N, 20N and 30N load. The plot between wear rate, % weight fraction of red mud and temperature of 100 µm particle size with pure aluminium and 4% tungsten carbide at 10N, 20N and 30N loads are shown in Figure 6.4, 6.5 and 6.6 respectively. The wear rate tables for pure aluminium with red mud and tungsten carbide at heat treatment conditions are placed in Appendix III: B (i, ii, and iii).

Table 6.2: Experimental wear test results of heat treated aluminium - red mud – tungsten carbide metal matrix hybrid composites

S.No	Weight of red mud (%)	Weight of Tungsten Carbide (%)	Particle size (Microns)	Heat treatment Temperature (^{0}C)	Wear rate x10^{-6}N/m		
					At 10N load	At 20N load	At 30N load
1	2	4	100 µm	350	0.318	0.334	0.362
2	4	4	100 µm	350	0.182	0.191	0.207
3	6	4	100 µm	350	0.121	0.127	0.137
4	2	4	100 µm	400	0.312	0.328	0.355
5	4	4	100 µm	400	0.179	0.188	0.204
6	6	4	100 µm	400	0.117	0.123	0.133
7	2	4	100 µm	450	0.301	0.316	0.343
8	4	4	100 µm	450	0.173	0.182	0.197
9	6	4	100 µm	450	0.108	0.113	0.123
10	2	4	100 µm	500	0.312	0.328	0.355
11	4	4	100 µm	500	0.177	0.186	0.199
12	6	4	100 µm	500	0.113	0.118	0.128
13	2	4	42 nm	350	0.195	0.205	0.222
14	4	4	42 nm	350	0.112	0.118	0.127
15	6	4	42 nm	350	0.093	0.097	0.106
16	2	4	42 nm	400	0.184	0.193	0.209
17	4	4	42 nm	400	0.108	0.113	0.121
18	6	4	42 nm	400	0.082	0.086	0.093
19	2	4	42 nm	450	0.177	0.186	0.201
20	4	4	42 nm	450	0.104	0.109	0.118
21	6	4	42 nm	450	0.078	0.082	0.088
22	2	4	42 nm	500	0.182	0.191	0.207
23	4	4	42 nm	500	0.106	0.111	0.120
24	6	4	42 nm	500	0.080	0.084	0.091

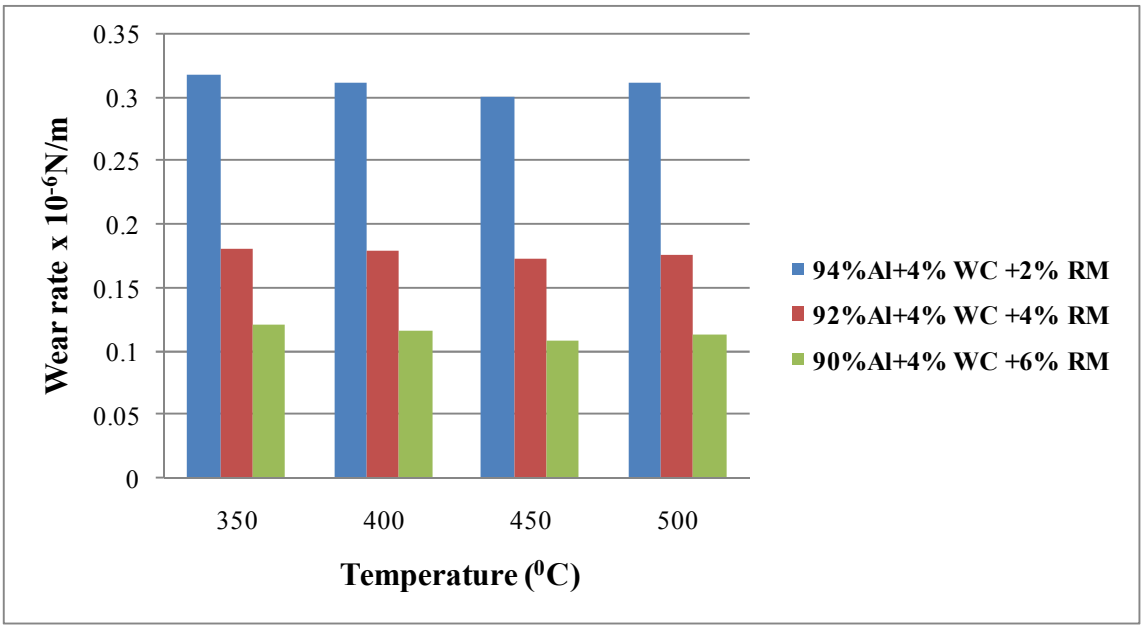

Figure 6.4: Wear rate, % weight fraction of red mud (100 µm) with aluminium and tungsten carbide and temperature at 10N load

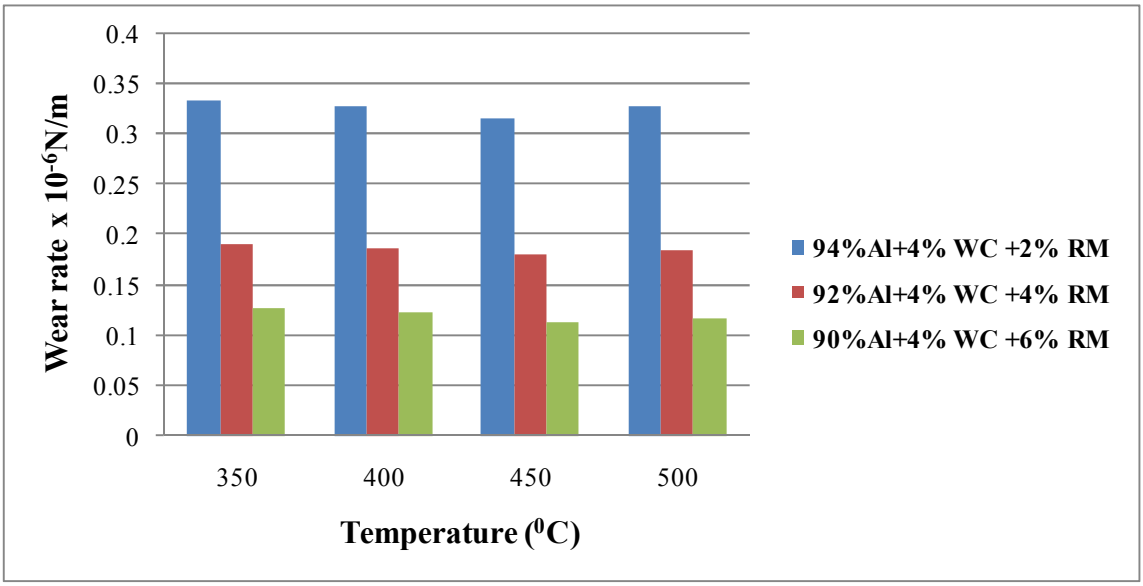

Figure 6.5: Wear rate and % weight fraction of red mud (100 µm) with aluminium and tungsten carbide and temperature at 20N load

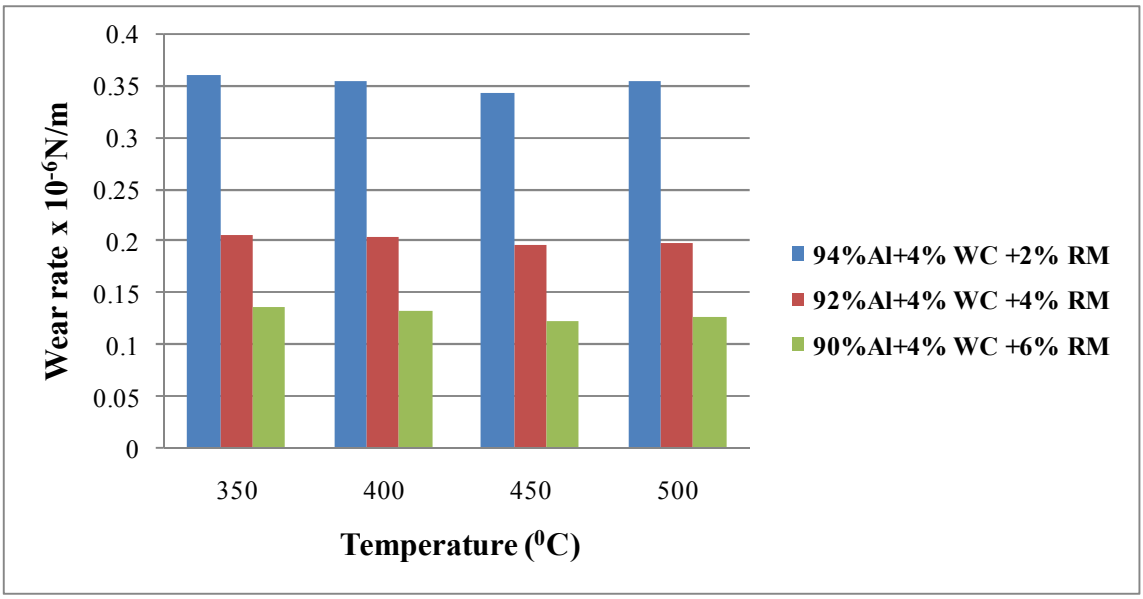

Figure 6.6: Wear rate and % weight fraction of red mud (100 µm) with aluminium and tungsten carbide and temperature at 30N load

The plot between wear rate, % weight fraction of red mud and temperature of 42 nm particle size with pure aluminium and 4% tungsten carbide at 10N, 20N and 30N loads are shown in Figure 6.7, 6.8 and 6.9 respectively.

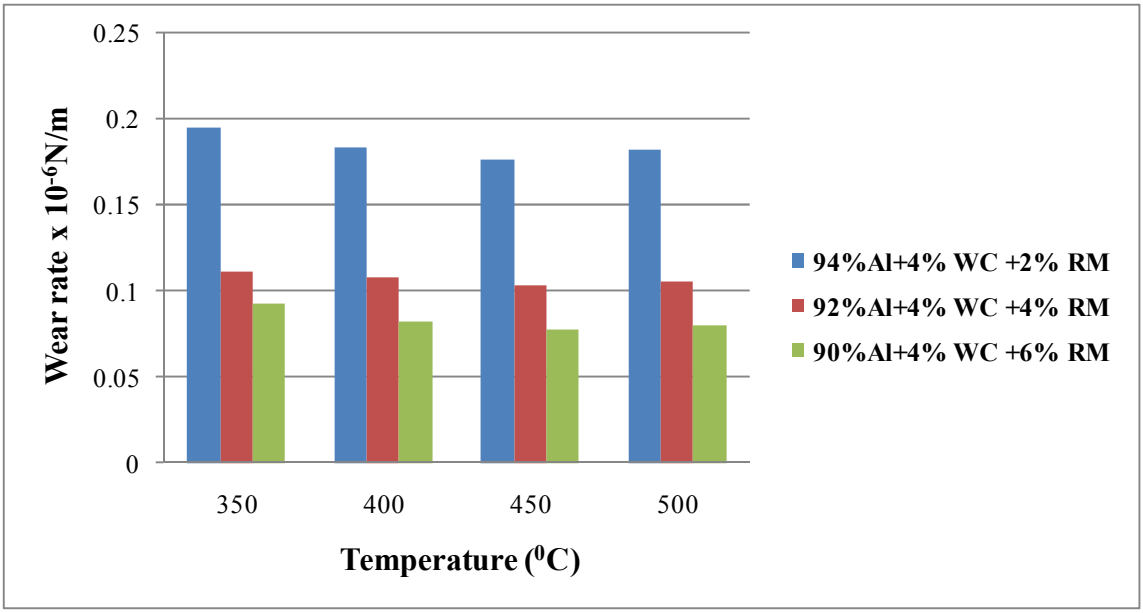

Figure 6.7: Wear rate, % weight fraction of red mud (42 nm) with aluminium and tungsten carbide and temperature at 10N load

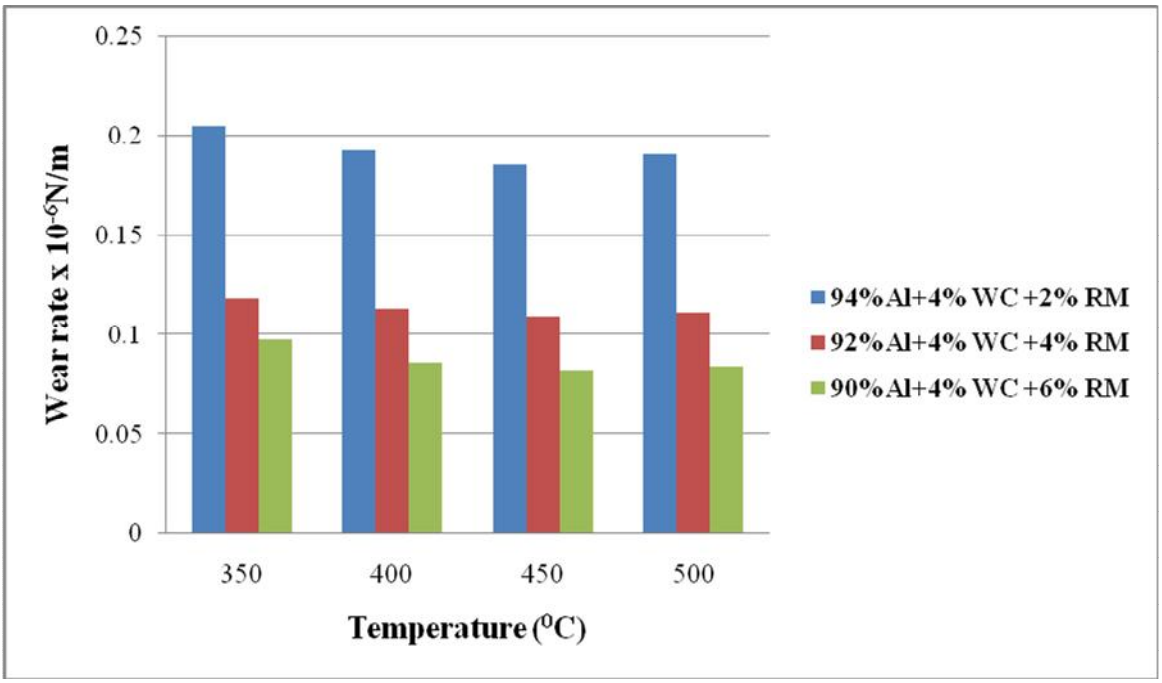

Figure 6.8: Wear rate and % weight fraction of red mud (42 nm) with aluminium and tungsten carbide and temperature at 20N load

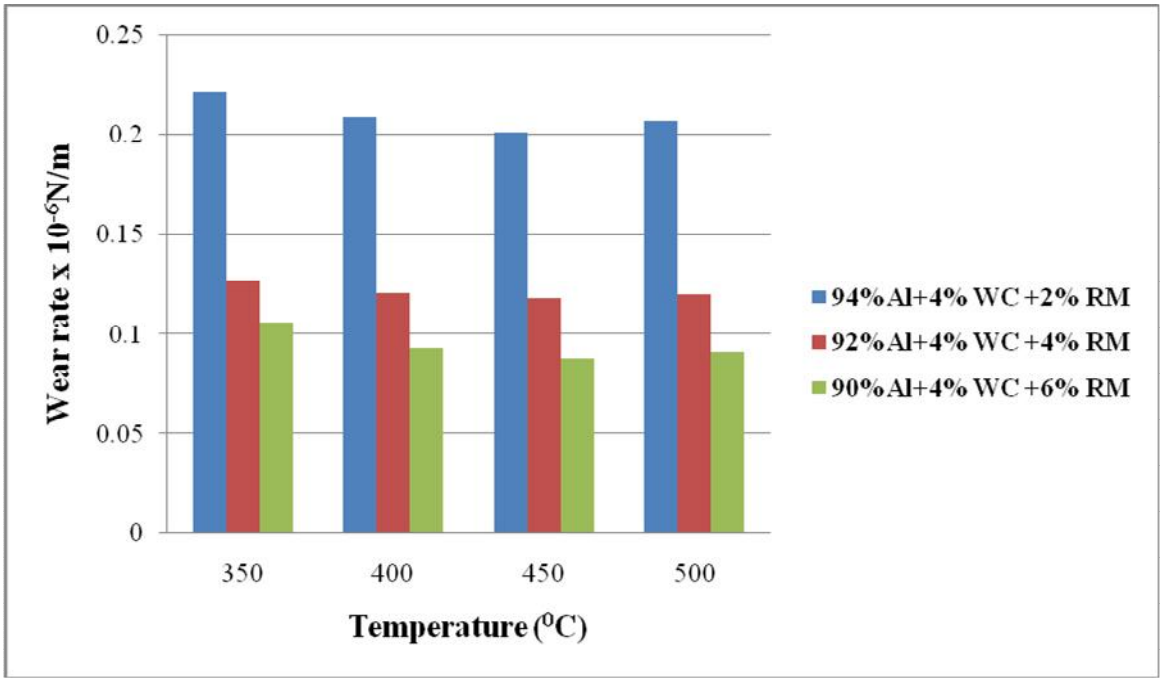

Figure 6.9: Wear rate and % weight fraction of red mud (42 nm) with aluminium and tungsten carbide and temperature at 30N load

The wear rate tables for pure aluminium with red mud and tungsten carbide at heat treatment conditions are placed in Appendix III: B. From Figure 6.7 – 6.9, it is observed that the wear resistance values are improved up to 450^0C, after that there is a decrement in wear resistance values. In heat treatment conditions, wear resistance values are higher for the nano level reinforcement than micro level reinforcement compared to normal condition. This is owing to the increase in surface area of contact and higher bond strengths.

6.4 MATHEMATICAL MODELING BY REGRESSION ANALYSIS

A mathematical model is developed for aluminium, red mud and tungsten carbide at normal condition and the overall equation is obtained using Regression analysis which is shown in equation 6.1. The R-square value 0.8757 is obtained from regression statistics.

Wear Rate = 0.3079739 -Wt% Red mud (0.0365) +Particle size (0.00070693)……..... (6.1)

A mathematical model is developed for aluminium, red mud and tungsten carbide at heat treatment condition and the overall equation is obtained using Regression analysis which is shown in equation 6.2.

Wear Rate = 0.3278566 – [Temperature in ^{0}C x (0.000153666)] + [Particle size x (0.00083451)]

– [% weight composition of red mud x (0.034)]……..…….…… (6.2)

The regression statistics for pure aluminium and red mud metal matrix composites at heat treatment condition is shown in Figure 6.10. It is observed that the R-square value is 0.8643 and adjusted R-square value is 0.7940. As per the regression statistics in Figure 6.10, the influence of red mud particle size has much higher than temperature and speed properties.

SUMMARY OUTPUT

Regression Statistics	
Multiple R	0.929713436
R Square	0.864367073
Adjusted R Square	0.794022133
Standard Error	0.030574424
Observations	24

	Coefficients	*Standard Error*	*t Stat*	*P-value*	*Lower 95%*	*Upper 95%*	*Lower 95.0%*	*Upper 95.0%*
Intercept	0.327856617	0.050625714	6.476088743	2.584E-06	0.222253228	0.43346001	0.22225323	0.433460006
X Variable 2	-0.034375	0.003821803	-8.99444575	1.8222E-08	-0.042347141	-0.0264029	-0.04234714	-0.026402859
X Variable 3	-0.000153667	0.000111642	-1.3764233	0.18390658	-0.000386548	7.9214E-05	-0.00038655	7.92145E-05
X Variable 4	0.000834517	0.000124872	6.682980123	1.666E-06	0.000574039	0.001095	0.00057404	0.001094996

Figure 6.10: Regression statistics for pure aluminium, red mud and tungsten carbide at heat treatment condition

6.5 RESULTS

- As % weight composition of red mud with pure aluminium and tungsten carbide increases, there is an improvement in wear resistance.
- The maximum wear resistance is obtained for 42 nm or 0.042 microns level of 6% weight fraction of red mud with pure aluminium and tungsten carbide.
- It is also observed that, for the same weight fraction of red mud compacted with pure aluminium and tungsten carbide, the wear resistance is higher for the nano structured reinforcement than micro structured reinforcement. This is owing to the increase in surface area of contact and higher bond strengths.
- As the increase in speed of rotation of the specimen, the wear resistance is increased. The highest wear resistance is observed for the test specimen with 42 nm size and 6% weight fraction of red mud powder at 600 RPM speed.
- A decrease in wear rate is observed with increase in the amount of temperature up to 450^0C and then it is started for declining in nature.

6.6 SUMMARY

The present chapter gives the results of tribological characterization such as wear rate at normal condition and heat treatment conditions of pure aluminium with red mud and tungsten carbide metal matrix hybrid composites. The graphs are plotted for micro and nano level combinations of red mud and tungsten carbide with pure aluminium metal matrix hybrid composites. The chapter also presents mathematical modeling using regression analysis.

CHAPTER-7

CONCLUSIONS

7.1 CONCLUSIONS

The present work is focussed on the mechanical and wear behaviour of aluminium metal matrix composite reinforced with micro and nano red mud and tungsten carbide particles fabricated through powder metallurgy route. The influence of heat treatment on aluminium-red mud and aluminium-red mud-tungsten carbide metal matrix hybrid micro as well as nano composites at normal condition and heat treatment conditions have been reported. The prediction of hardness and wear behaviour of aluminium with micro and nano particulates of red mud and tungsten carbide at normal and heat treatment conditions using regression analysis.

The investigation is mainly to find the best weight fraction of red mud and tungsten carbide particulates as reinforced the aluminium metal matrix hybrid composites for optimum properties. Red mud is abundantly available in India. Such materials at micro/nano particulates can be used to develop aluminium hybrid composites at lower price, which are strong, hard and high wear resistance compared to base aluminium and such hybrid metal matrix composites can be used in place of aluminium.

The maximum hardness values at normal condition and heat treatment condition of 450^0C at 6% weight fraction of red mud are shown in Table 7.1 and 7.2 respectively. Aluminium metal matrix composite of (94%Al+6%RM) with 100 micron particulates has 74.50 VHN where as with 42 nano particulates has 75.23 VHN at normal condition. Aluminium metal matrix hybrid composite of (90%Al+4%WC+6%RM) with 100 micron particulates has 83.90 VHN where as with 42 nano particulates has 84.91 VHN at normal condition.

Table 7.1: Maximum hardness values at normal condition

Particle Size	Hardness (VHN) for 94%Al+6%RM	Hardness (VHN) for 90%Al+4%WC+6%RM
100 μm	74.50	83.90
42 nm	75.23	84.91

Aluminium metal matrix composite of (94%Al+6%RM) with 100 micron particulates has 82.4 VHN where as with 42 nano particulates has 84.2 VHN at heat treatment condition. Aluminium metal matrix hybrid composite of (90%Al+4%WC+6%RM) with 100 micron particulates has 95.7 VHN where as with 42 nano particulates has 96.8 VHN at heat treatment condition.

Table 7.2: Maximum hardness values at heat treatment condition of 450^0C

Particle Size	Hardness (VHN) for 94%Al+6%RM	Hardness (VHN) for 90%Al+4%WC+6%RM
100 μm	82.4	95.7
42 nm	84.2	96.8

The following conclusions have been observed and drawn from this work.

- The particulate size of red mud is reduced from 400 nm to 42 nm after 30 hours of ball milling. Decreasing size of reinforced particle increases its surface to volume ratio tremendously. This is further exploited in the preparation of nano composites.
- The author has observed that the properties of aluminium based nano composites prepared by powder metallurgy route are better than the composites prepared by stir casting method. Naresh Prasad et al, 2013 presented the hardness of aluminium-red mud with 10% weight fraction of red mud is 52.78 VHN by stir casting method, where as the author developed same composite i.e aluminium-red mud with 6% weight fraction of red mud is 74.5 VHN. An improvement of 22% in hardness is achieved by composites prepared by powder metallurgy route compared to stir casting method.
- It is also observed that for the 6% weight fraction of red mud, the hardness and compression strength are higher for the nano structured reinforcement than micro structured reinforcement. The hardness is higher for 94%Al+6%RM of about 75.23 VHN at the nano level.

- Aluminium, red mud and tungsten carbide hybrid metal matrix composite is having more hardness compared to aluminium with red mud metal matrix composite. The hardness for 90%Al+4%WC+6%RM metal matrix hybrid composite is 95.7 VHN at micro level and 96.8 VHN at nano level of red mud. This is due to the presence of iron oxide in red mud and tungsten carbide.
- Hardness and compression strength properties are improved for nano level aluminium-red mud test specimen with 42 nm size and 6% weight fraction of Red mud. The simulated results of compression strength using Deform-2D software and experimental values are within the limits of 1-8% difference i.e., the % error is varied from 0.40 - 7.98.
- In heat treatment conditions, hardness values are higher for the nano structured reinforcement than micro structured reinforcement compared to normal condition. This is owing to the increase in surface area of contact and higher bond strengths. Under the highest load applied, the mating material raised the specimen temperature could cause oxidation of contact surfaces. The oxide films were brittle and easily smashed in the wear process. These oxide debris were embedded in the specimen surface by the contact load which enhanced its bond strength, hardness and increased its wear resistance. This is so called glazed hardening.
- As percentage weight fraction of red mud increases from 2%, 4% and 6%, better wear resistance is obtained at 6% red mud with 30N load on pin-on-disc wear testing machine.
- Highest wear resistance is observed for the test specimen with 42 nm particle size and 6% weight fraction of red mud with pure aluminium at 600 rpm speed and 30N load. The 6% weight fraction of nano red mud possessed more Fe_2O_3. So, the test coupons exhibited a reduced wear rate at 600rpm because of iron oxide compared with 200 and 400 rpm. The higher percentage of nano particles provided with greater iron oxide (Fe_2O_3), SiO_2 and TiO_2.
- The increase in bulk temperatures of the rubbing bodies decreases the flow stresses of the rubbing materials to a certain extent, which results in an increased in plastic zone size in the sub surfaces of the rubbing bodies, consequently the friction co-efficient as well as wear rate increases as the load on pin-on-disc wear testing machine increases.

- The predicted mathematical modeling results of wear rate using regression analysis and experimental values are within the limits of 1-4% error difference of pure aluminium-red mud metal matrix composites and pure aluminium-red mud-tungsten carbide hybrid metal matrix composites.
- Highest wear resistance is observed for the test specimen with 42 nm particle size and 6% weight fraction of red mud with pure aluminium and 4% tungsten carbide at 600 rpm speed.
- The chemical compatibility is excellent between pure aluminium, red mud and tungsten carbide Brunori, C et.al, [15]. The results are shown that the addition of tungsten carbide particles to the pure aluminium with micro level and nano level red mud tremendously increased the wear resistance of hybrid metal matrix composite.

7.2 LIMITATION OF THIS WORK

- The current study is limited to the compacting pressure of 40 bar, it can be further be increased.

7.3 SCOPE FOR THE FUTURE WORK

- In this study, the tribological characterization of heat treatment samples with air cooling is done. The work can be further extended to other quenching media like water, oil quenching, brine solution etc at different soaking times for good wear resistant properties.
- The present investigation is limited to conventional sintering through powder metallurgy only. However, other available advanced techniques like Spark Plasma Sintering etc could be tried.
- The present investigation is limited to sintering with vacuum as medium. However, other inert gases will also be used for preparation of powder metallurgy samples.
- The present work can also be extended to study various sintering parameters.

APPENDIX - I

INTRODUCTION

The Appendix-I consists of compressive stresses for pure aluminium, pure aluminium with 2% and 4% weight fractions of 100 µm, 150 µm, 200 µm and 42 nm particle size red mud at 10%, 20% and 30% reduction using Deform-2D software. This Appendix-I also consists of compressive stresses for pure aluminium with 6% weight fractions of 100 µm, 150 µm and 200 µm particle size red mud at 10%, 20% and 30% reduction using Deform-2D software. The compressive stress for pure aluminium with 6% weight fraction of 42 nm red mud at 10%, 20%, and 30% reduction using Deform-2D software are shown in Chapter-4 (Figure 4.14-4.16).

The compressive stress for pure aluminium at 10% reduction and 20% reduction using Deform-2D software are shown in Figure 1 and 2 respectively.

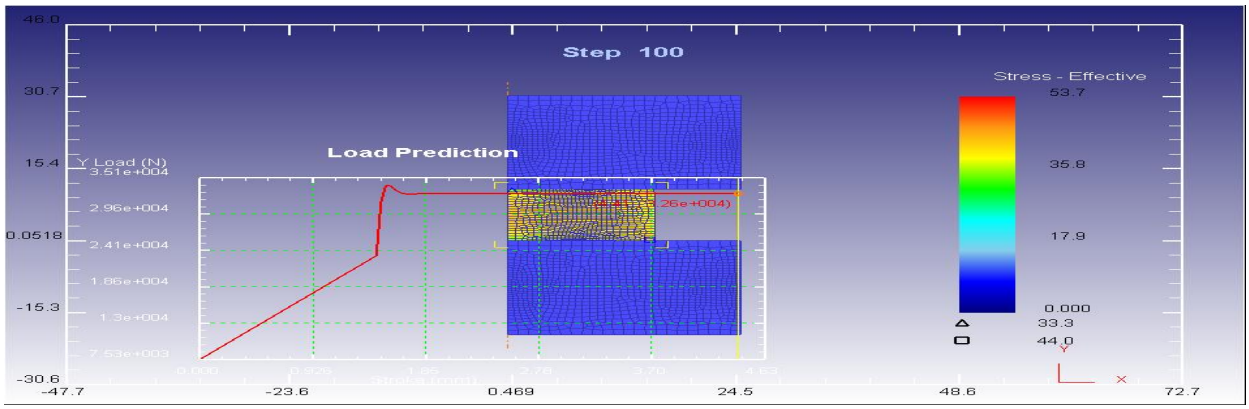

Figure 1: Compressive Stress for pure aluminium at 10% reduction using Deform-2D software

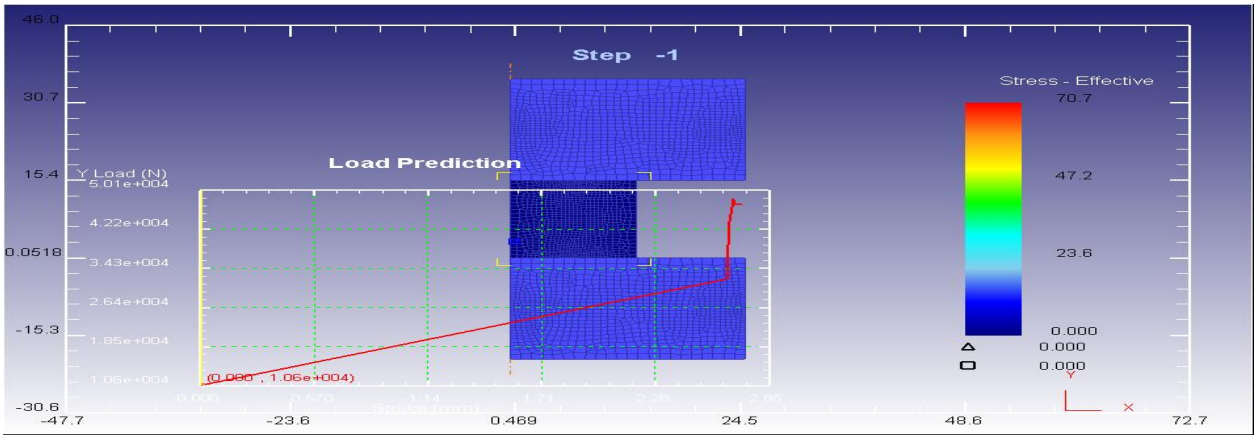

Figure 2: Compressive Stress for pure aluminium at 20% reduction using Deform-2D software

The compressive stress for pure aluminium at 30% reduction using Deform-2D software is shown in Figure 3.

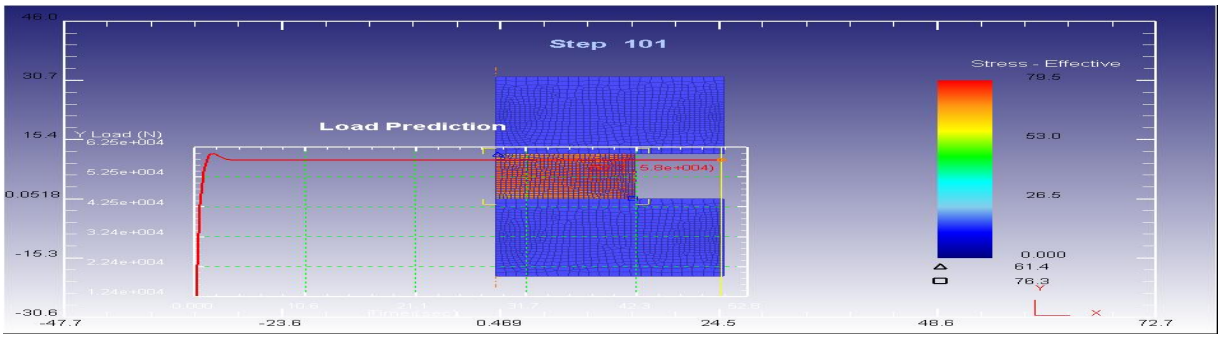

Figure 3: Compressive Stress for pure aluminium at 30% reduction using Deform-2D software

The compressive stress for pure aluminium with 2% weight fraction of red mud (100 µm) at 10% reduction and 20% reduction using Deform-2D software are shown in Figure 4 and 5 respectively.

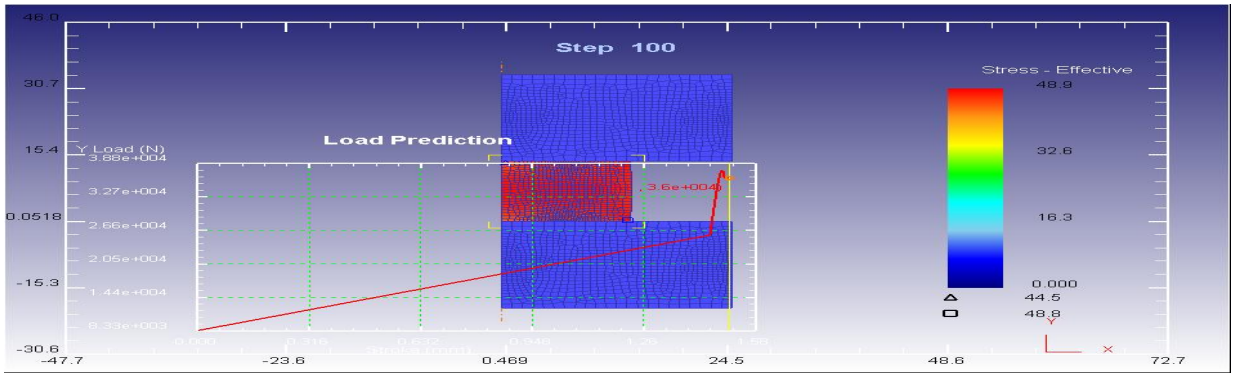

Figure 4: Compressive Stress for aluminium with 2% weight fraction of red mud (100 µm) at 10% reduction using Deform-2D software

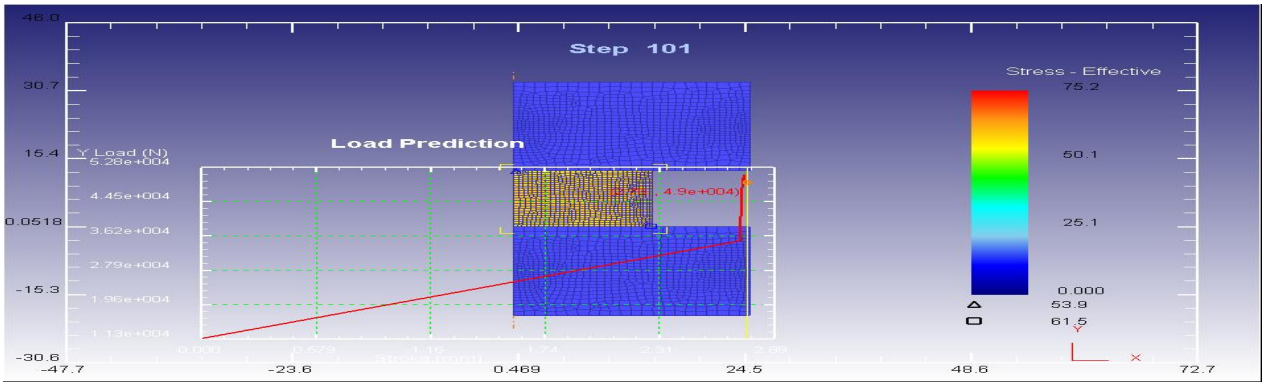

Figure 5: Compressive Stress for aluminium with 2% weight fraction of red mud (100 µm) at 20% reduction using Deform-2D software

The compressive stress for pure aluminium with 2% weight fraction of red mud (100 µm) at 30% reduction using Deform-2D software is shown in Figure 6.

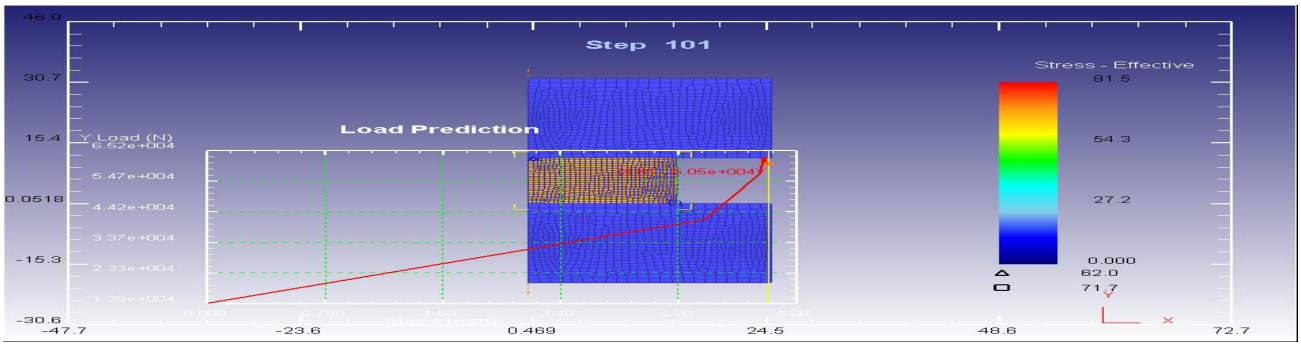

Figure 6: Compressive Stress for aluminium with 2% weight fraction of red mud (100 µm) at 30% reduction using Deform-2D software

The compressive stress for pure aluminium with 2% weight fraction of red mud (150 µm) at 10% reduction and 20% reduction using Deform-2D software are shown in Figure 7 and 8 respectively.

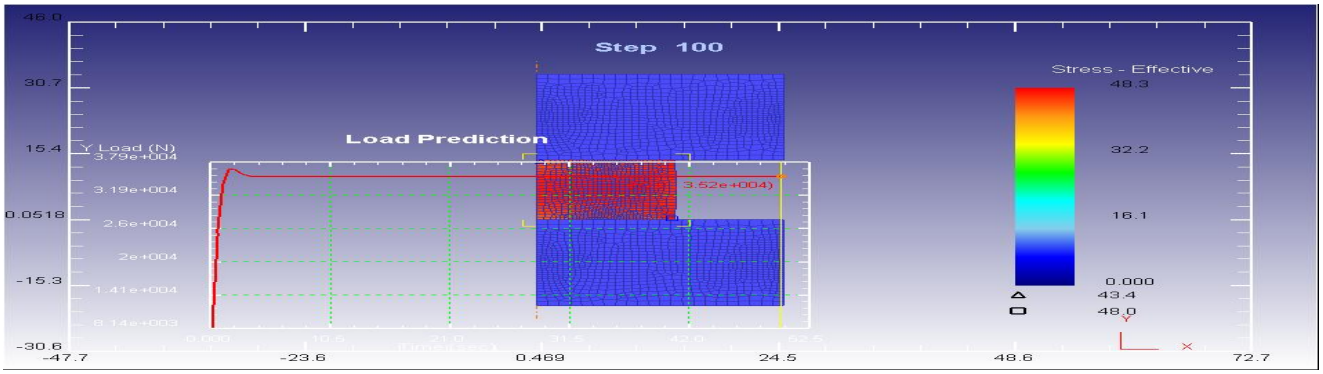

Figure 7: Compressive Stress for aluminium with 2% weight fraction of red mud (150 µm) at 10% reduction using Deform-2D software

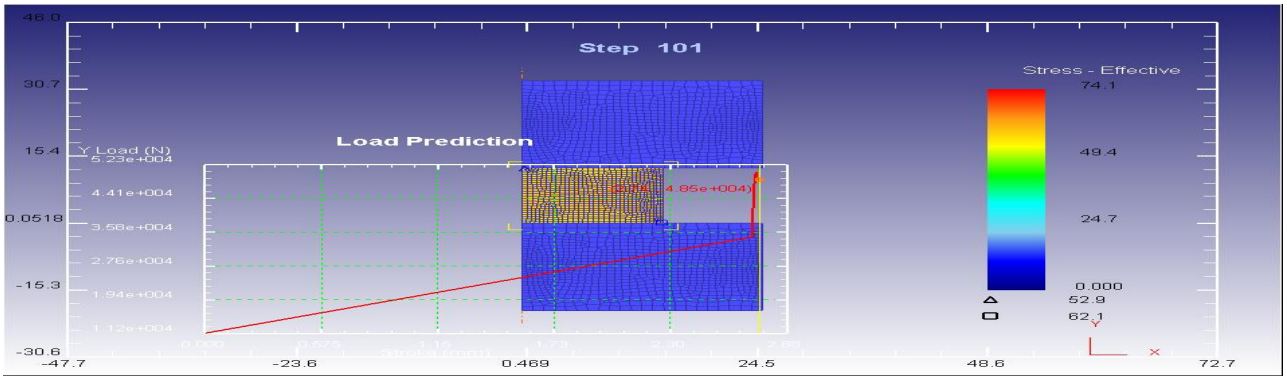

Figure 8: Compressive Stress for aluminium with 2% weight fraction of red mud (150 µm) at 20% reduction using Deform-2D software

The compressive stress for pure aluminium with 2% weight fraction of red mud (150 µm) at 30% reduction using Deform-2D software is shown in Figure 9.

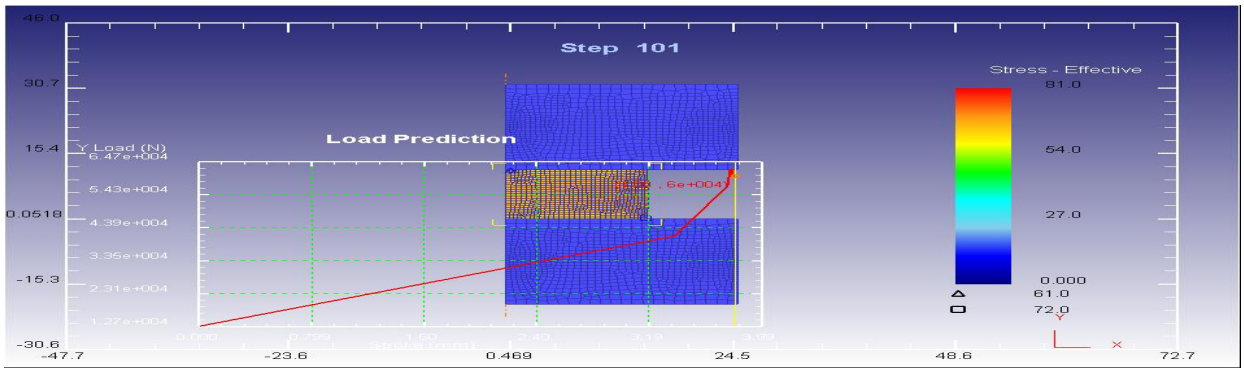

Figure 9: Compressive Stress for aluminium with 2% weight fraction of red mud (150 µm) at 30% reduction using Deform-2D software

The compressive stress for pure aluminium with 2% weight fraction of red mud (200 µm) at 10% reduction and 20% reduction using Deform-2D software are shown in Figure 10 and 11 respectively.

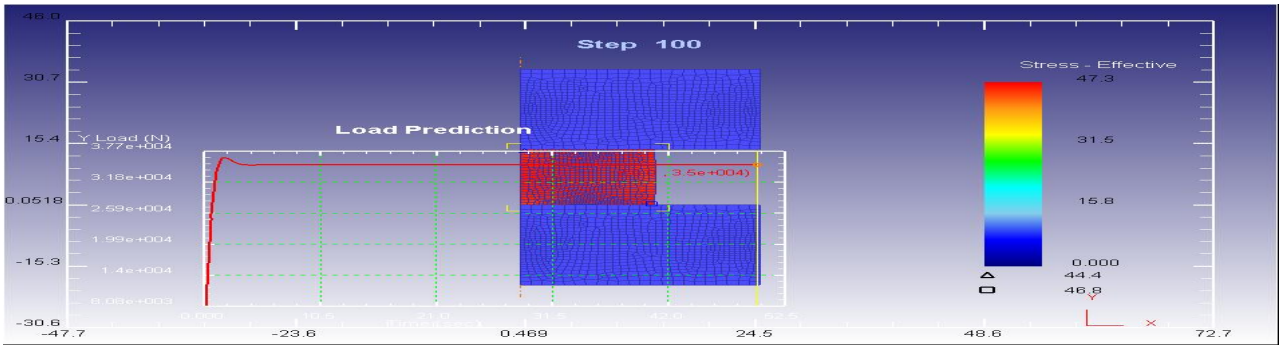

Figure 10: Compressive Stress for aluminium with 2% weight fraction of red mud (200 µm) at 10% reduction using Deform-2D software

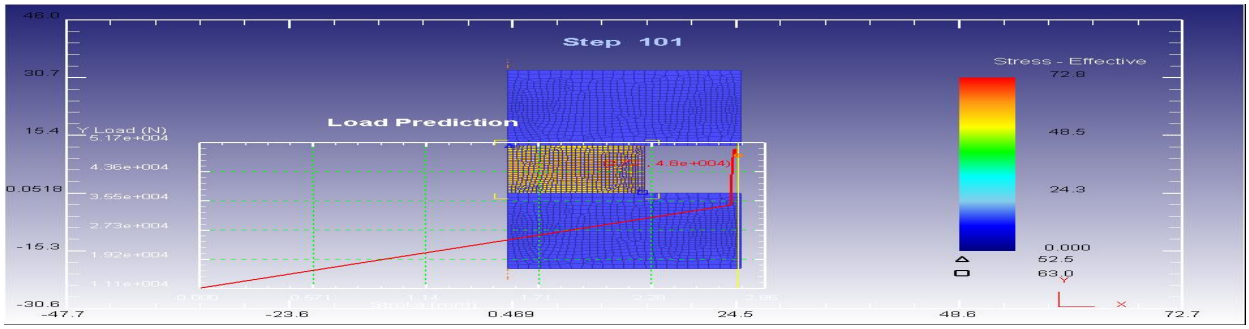

Figure 11: Compressive Stress for aluminium with 2% weight fraction of red mud (200 µm) at 20% reduction using Deform-2D software

The compressive stress for pure aluminium with 2% weight fraction of red mud (200 µm) at 30% reduction using Deform-2D software is shown in Figure 12.

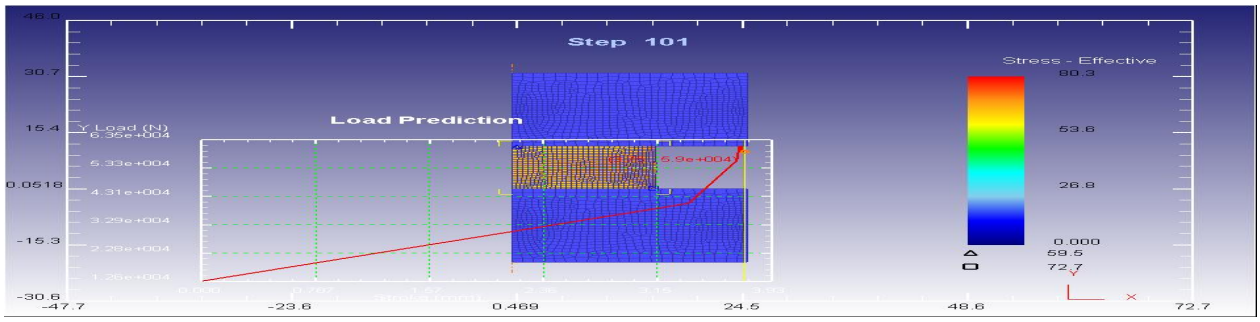

Figure 12: Compressive Stress for aluminium with 2% weight fraction of red mud (200 µm) at 30% reduction using Deform-2D software

The compressive stress for pure aluminium with 2% weight fraction of red mud (42 nm) at 10% reduction and 20% reduction using Deform-2D software are shown in Figure 13 and 14 respectively.

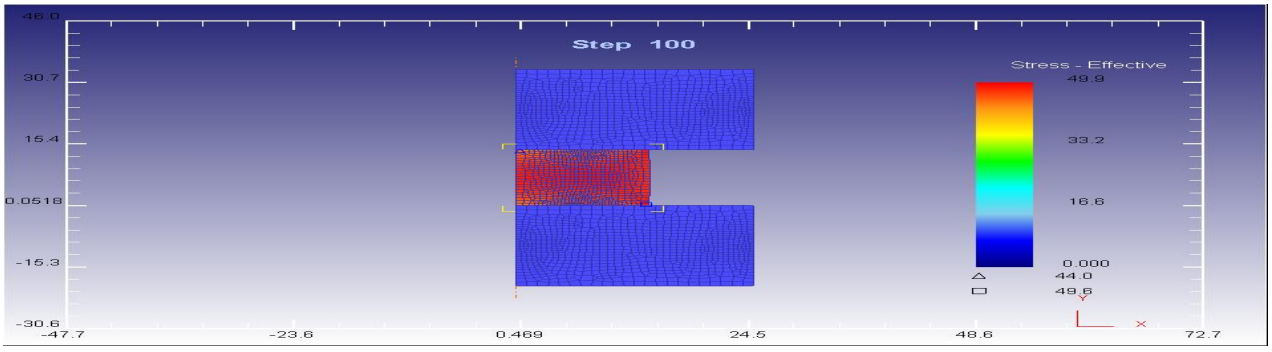

Figure 13: Compressive Stress for aluminium with 2% weight fraction of red mud (42 nm) at 10% reduction using Deform-2D software

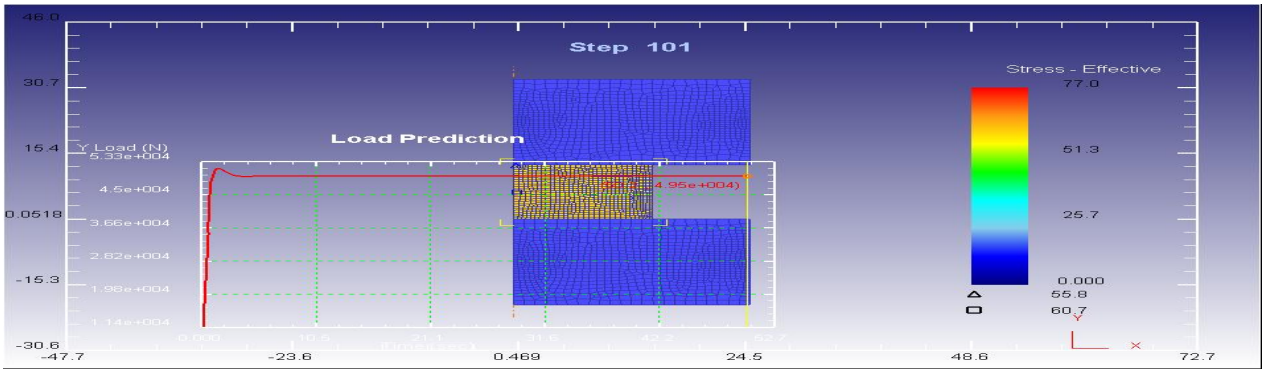

Figure 14: Compressive Stress for aluminium with 2% weight fraction of red mud (42 nm) at 20% reduction using Deform-2D software

The compressive stress for pure aluminium with 2% weight fraction of red mud (42 nm) at 30% reduction using Deform-2D software is shown in Figure 15.

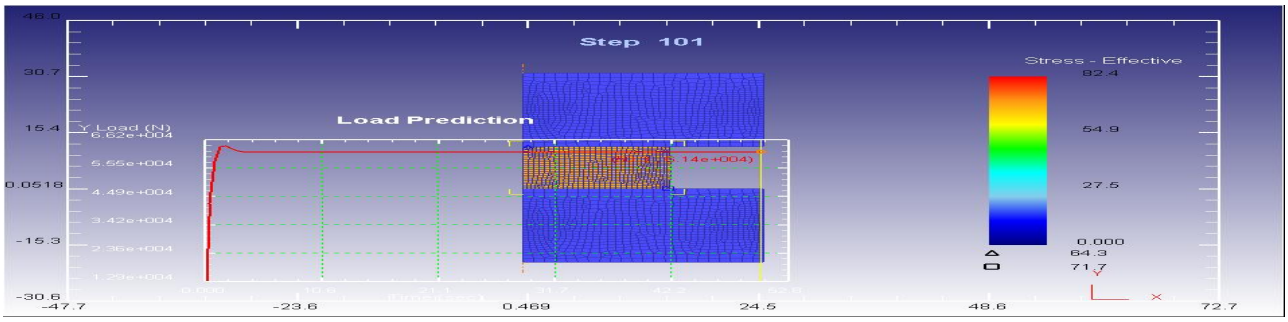

Figure 15: Compressive Stress for aluminium with 2% weight fraction of red mud (42 nm) at 30% reduction using Deform-2D software

The compressive stress for pure aluminium with 4% weight fraction of red mud (100 µm) at 10% reduction and 20% reduction using Deform-2D software are shown in Figure 16 and 17 respectively.

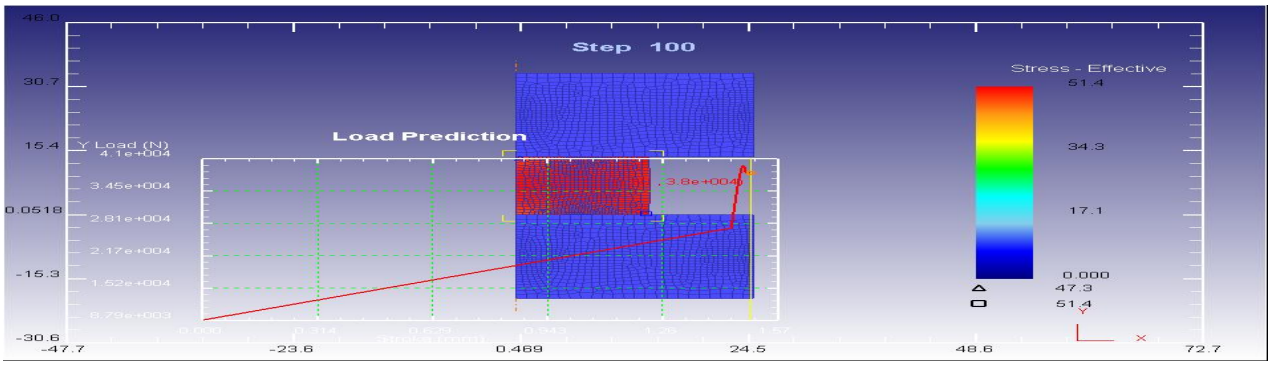

Figure 16: Compressive Stress for aluminium with 4% weight fraction of red mud (100 µm) at 10% reduction using Deform-2D software

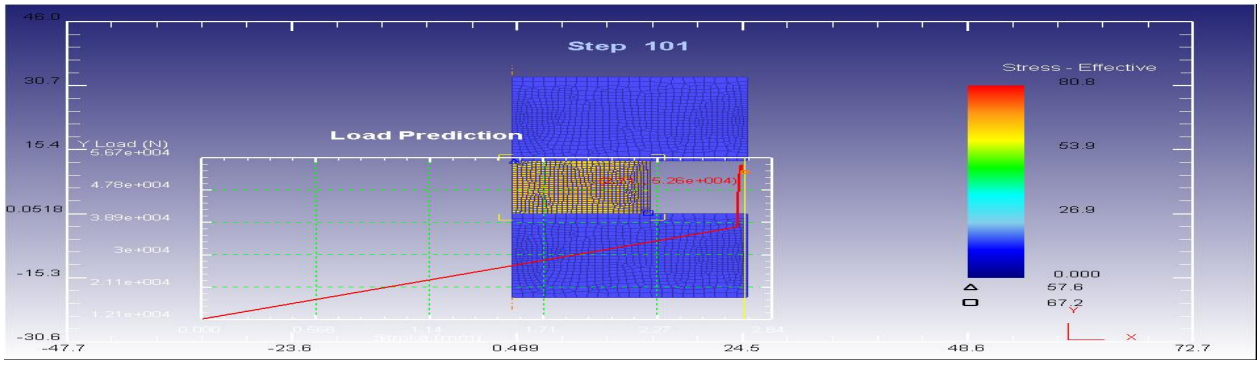

Figure 17: Compressive Stress for aluminium with 4% weight fraction of red mud (100 µm) at 20% reduction using Deform-2D software

The compressive stress for pure aluminium with 4% weight fraction of red mud (100 µm) at 30% reduction using Deform-2D software is shown in Figure 18 respectively.

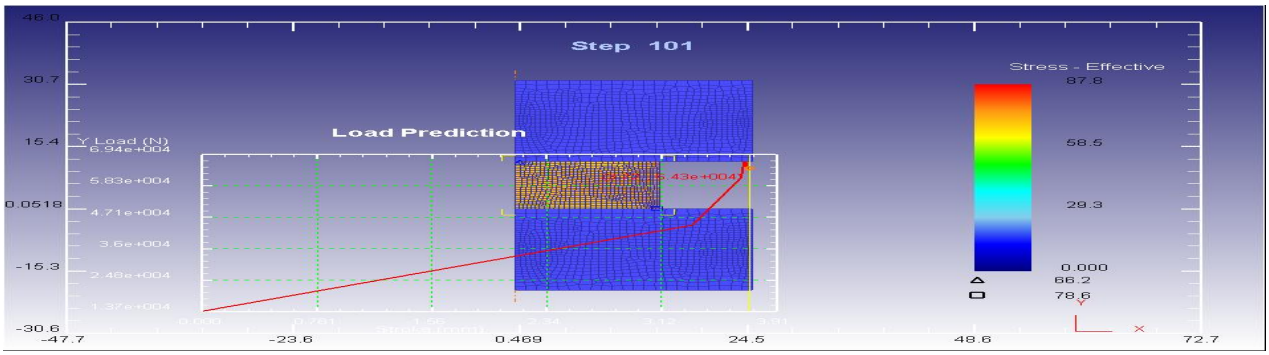

Figure 18: Compressive Stress for aluminium with 4% weight fraction of red mud (100 µm) at 30% reduction using Deform-2D software

The compressive stress for pure aluminium with 4% weight fraction of red mud (150 µm) at 10% reduction and 20% reduction using Deform-2D software are shown in Figure 19 and 20 respectively

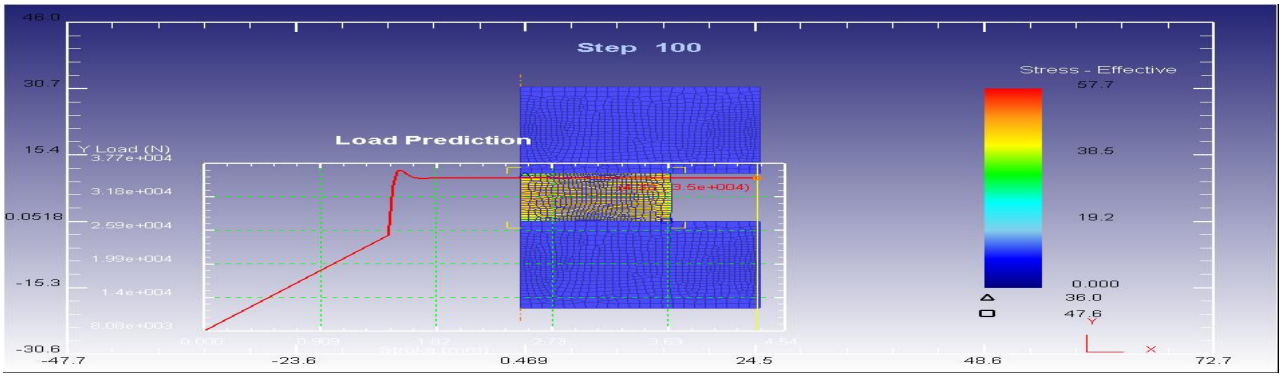

Figure 19: Compressive Stress for aluminium with 4% weight fraction of red mud (150 µm) at 10% reduction using Deform-2D software

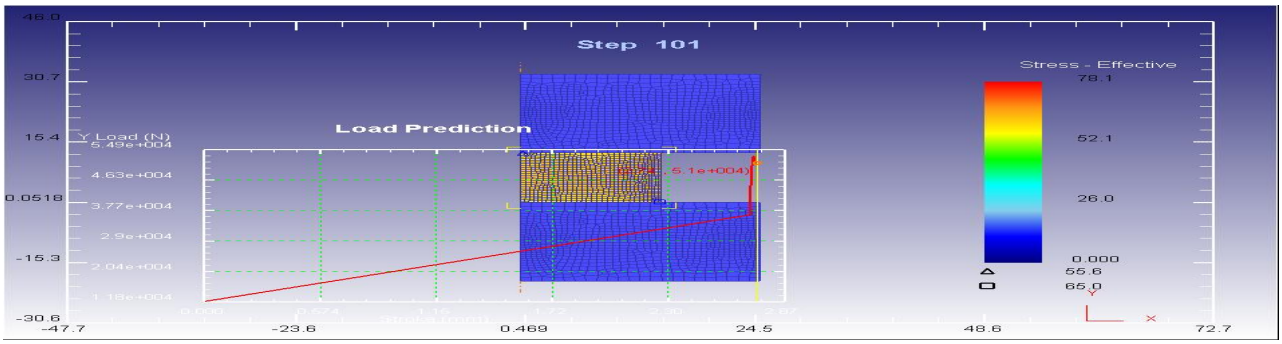

Figure 20: Compressive Stress for aluminium with 4% weight fraction of red mud (150 µm) at 20% reduction using Deform-2D software

The compressive stress for pure aluminium with 4% weight fraction of red mud (150 µm) at 30% reduction using Deform-2D software is shown in Figure 21.

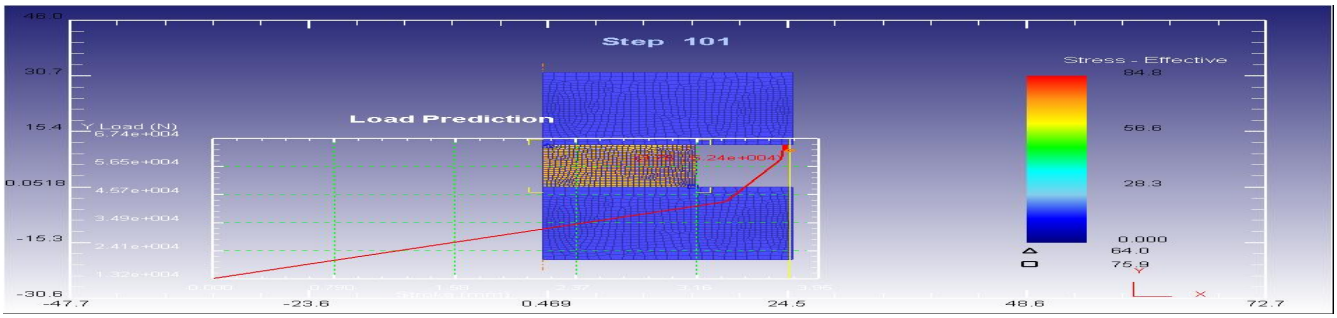

Figure 21: Compressive Stress for aluminium with 4% weight fraction of red mud (150 µm) at 30% reduction using Deform-2D software

The compressive stress for pure aluminium with 4% weight fraction of red mud (200 µm) at 10% reduction and 20% reduction using Deform-2D software are shown in Figure 22 and 23 respectively.

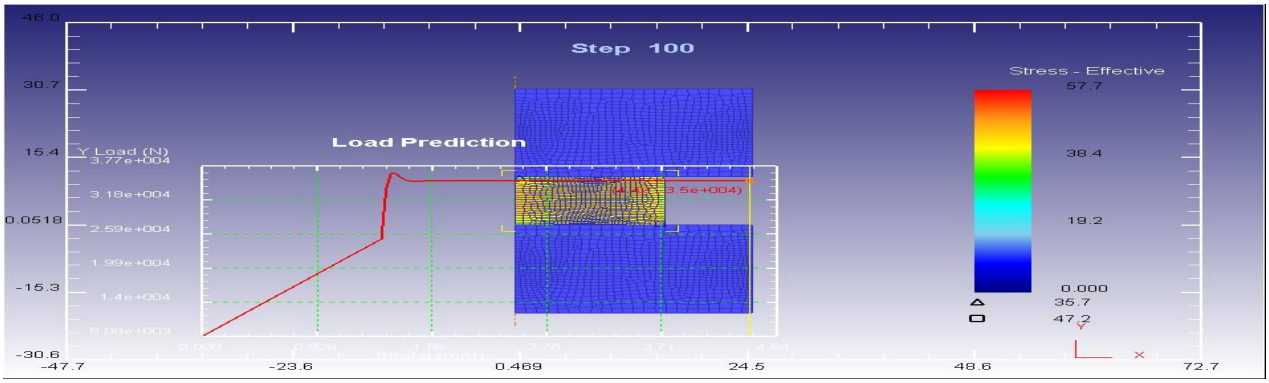

Figure 22: Compressive Stress for aluminium with 4% weight fraction of red mud (200 µm) at 10% reduction using Deform-2D software

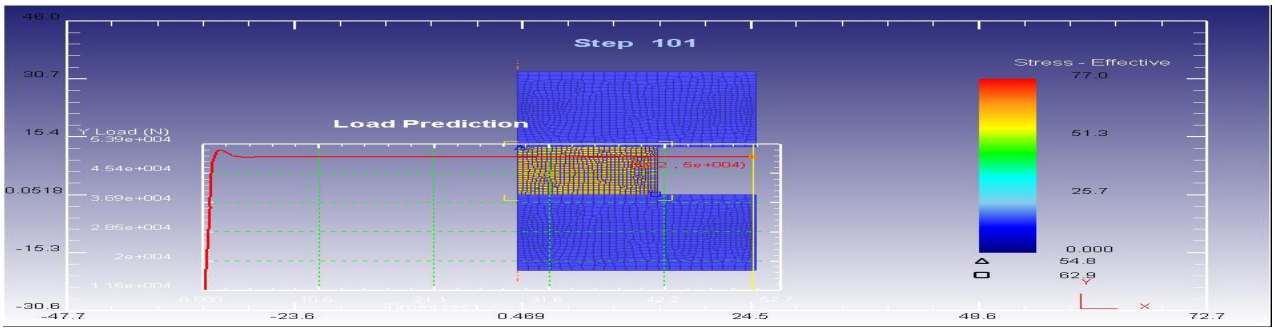

Figure 23: Compressive Stress for aluminium with 4% weight fraction of red mud (200 µm) at 20% reduction using Deform-2D software

The compressive stress for pure aluminium with 4% weight fraction of red mud (200 µm) at 30% reduction using Deform-2D software is shown in Figure 24.

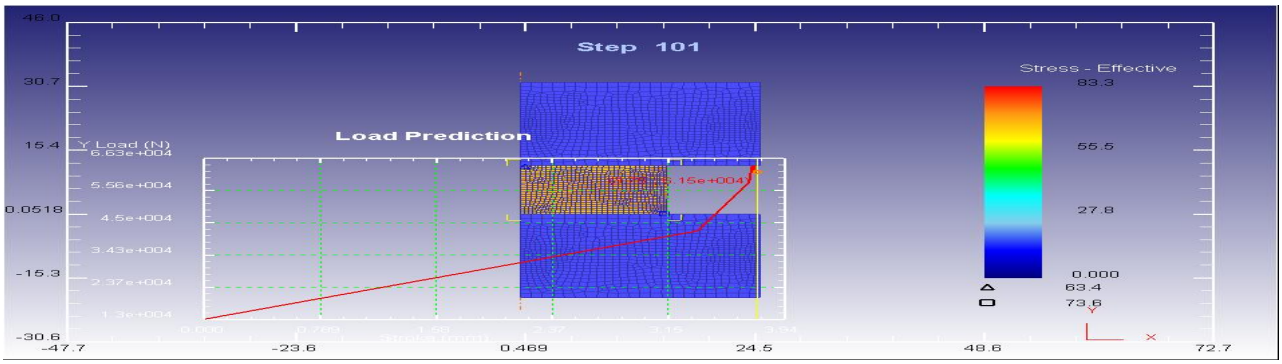

Figure 24: Compressive Stress for aluminium with 4% weight fraction of red mud (200 µm) at 30% reduction using Deform-2D software

The compressive stress for pure aluminium with 4% weight fraction of red mud (42 nm) at 10% reduction and 20% reduction using Deform-2D software are shown in Figure 25 and 26 respectively.

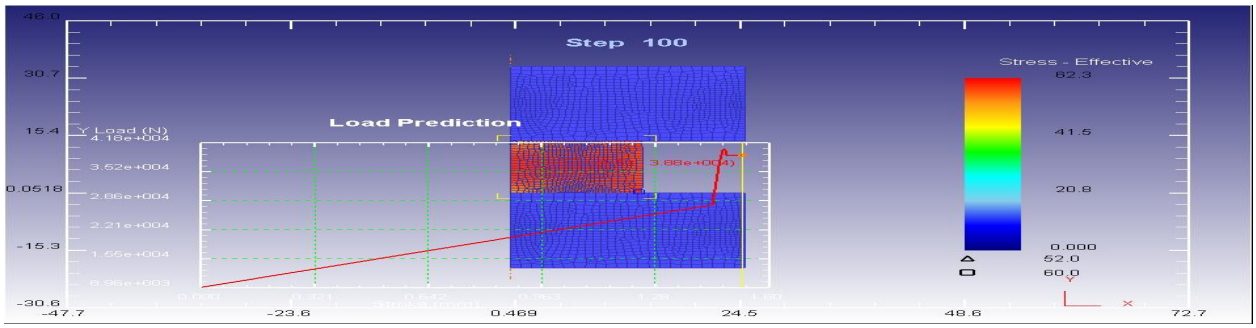

Figure 25: Compressive Stress for aluminium with 4% weight fraction of red mud (42 nm) at 10% reduction using Deform-2D software

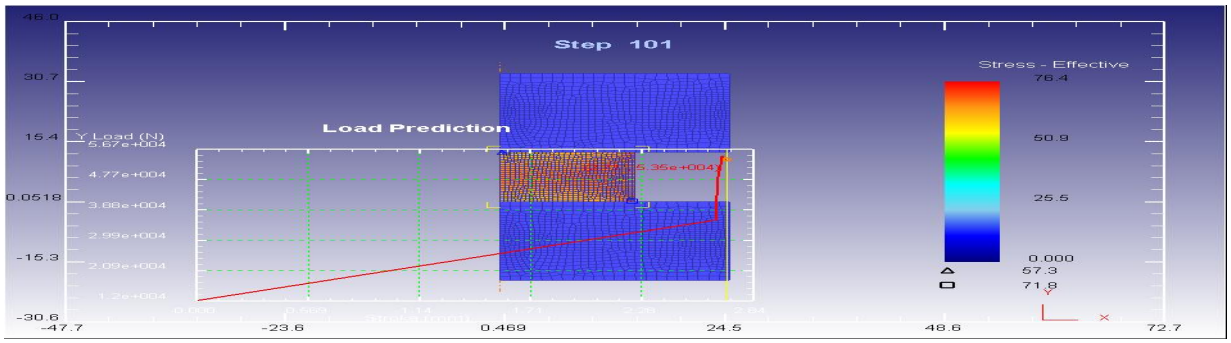

Figure 26: Compressive Stress for aluminium with 4% weight fraction of red mud (42 nm) at 20% reduction using Deform-2D software

The compressive stress for pure aluminium with 4% weight fraction of red mud (42 nm) at 30% reduction using Deform-2D software is shown in Figure 27.

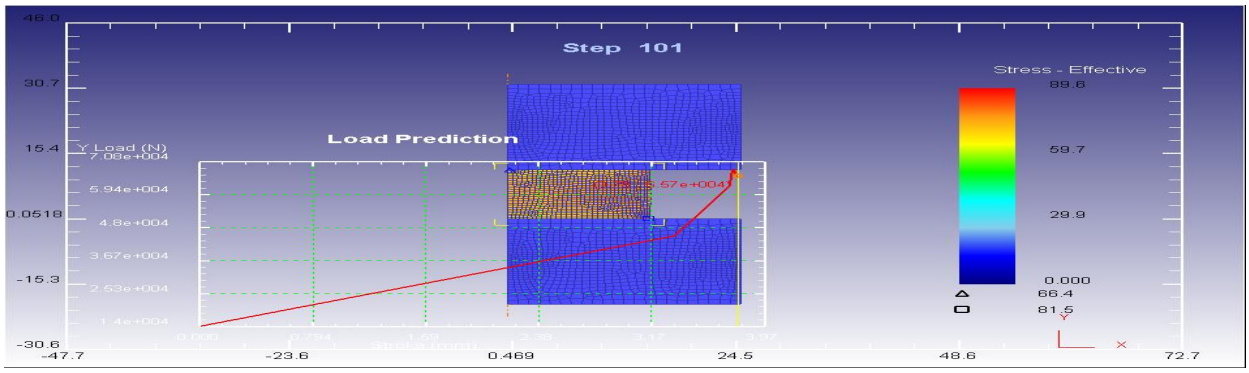

Figure 27: Compressive Stress for aluminium with 4% weight fraction of red mud (42 nm) at 30% reduction using Deform-2D software

The compressive stress for pure aluminium with 6% weight fraction of red mud (100 µm) at 10%, 20% reduction and 30% reduction using Deform-2D software are shown in Figure 28, 29 and 30 respectively.

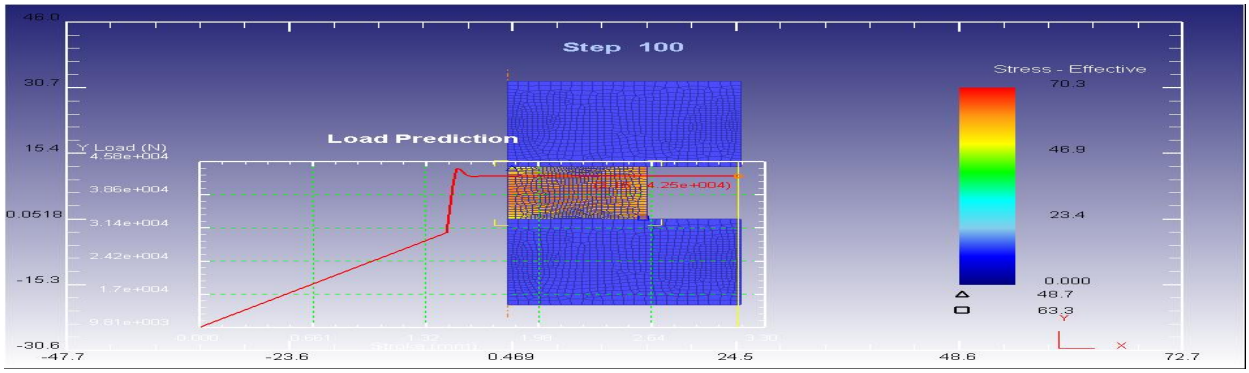

Figure 28: Compressive stress for aluminium with 6% weight fraction of red mud (100µm) at 10% reduction using Deform-2D software

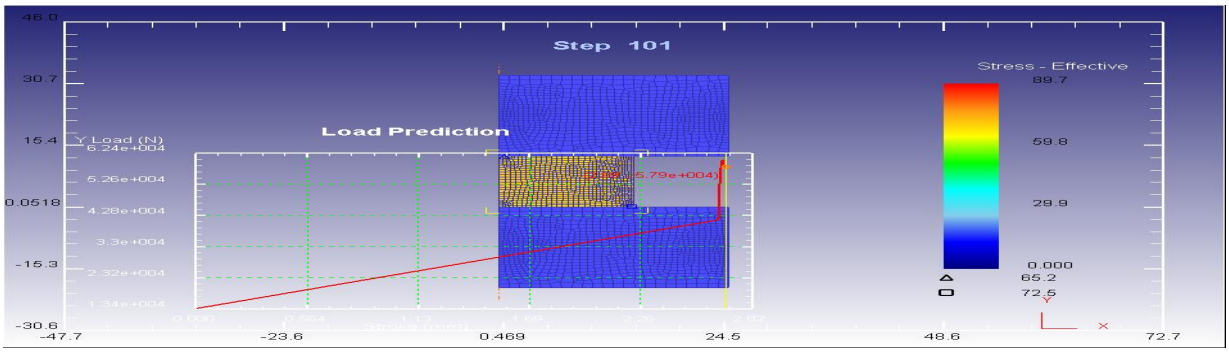

Figure 29: Compressive Stress for aluminium with 6% weight fraction of red mud (100µm) at 20% reduction using Deform-2D software

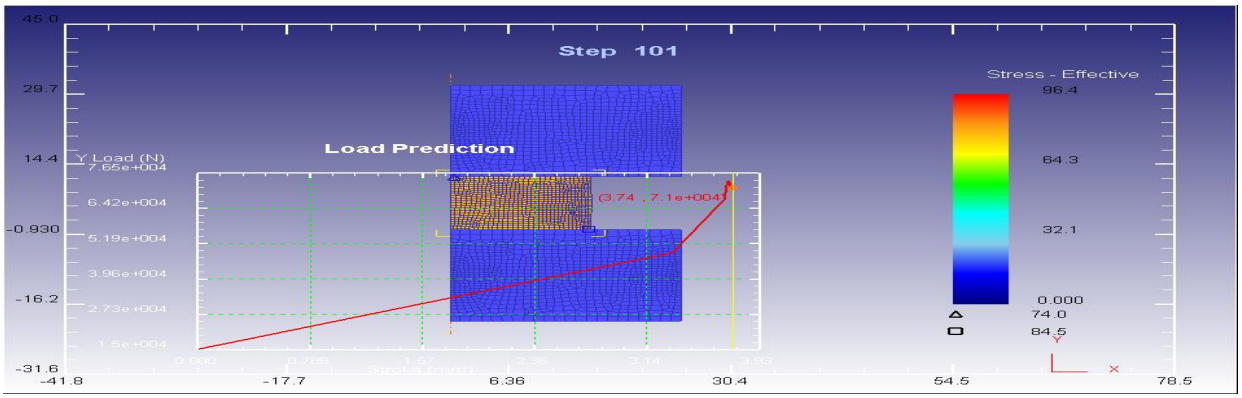

Figure 30: Compressive Stress for aluminium with 6% weight fraction of red mud (100µm) at 30% reduction using Deform-2D software

CONCLUSION

The present Appendix-I gives the Deform-2D Compressive stress simulation results for pure aluminium, pure aluminium with 2 % and 4 % weight fractions of 100 µm, 150 µm, 200 µm and 42 nm particle size red mud at 10%, 20% and 30% reduction. The compressive stress for pure aluminium with 6% weight fraction of 42 nm red mud at 10%, 20%, and 30% reduction using Deform-2D software are shown in Chapter-4 (Figure 4.14-4.16). The compressive stresses for pure aluminium with 6% weight fractions of 150 µm and 200 µm particle size red mud at 10%, 20% and 30% reduction figures using Deform-2D software are removed due to lengthy appendix. This Appendix-I also consists of compressive stresses for pure aluminium with 6% weight fractions of 100 µm particle size red mud at 10%, 20% and 30% reduction using Deform-2D software.

APPENDIX - II

INTRODUCTION

The Appendix-II consists of Appendix-II-A and Appendix-II-B parts. The Appendix-II-A consists of wear rate tables for pure aluminium with red mud of 10 N, 20 N and 30 N loads at normal condition. The Appendix-II-B consists of wear rate tables for pure aluminium with red mud of 10 N, 20 N and 30 N loads at heat treatment conditions. The various graphs between wear rate, percentage weight fraction of red mud, particle size of red mud at normal and heat treatment conditions are shown in Chapter-5 (Figure 5.2- 5.19)

APPENDIX II-A

i) Wear rate tables for pure aluminium with red mud at normal condition at 10 N load

The Wear rate values for pure aluminium at 200 rpm and 400 rpm are shown in Tables 1 and 2 respectively.

Table 1: Wear Rate values for Pure Aluminium at 200 rpm

V_s = 3.93 X 10^{-1} m/sec **ρ = 2.58 x 1000 kg/m³**

m_1 (gm)	m_2 (gm)	Δm (gm)	T (sec)	F_f kgf	μ	R.Dx10^{-3} m	W_r×10^{-6} (N/m)	W_v×10^{-12} (m³/sec)	W_s ×10^{-13} (m³/N-m)
6.45	6.35	0.1	3600	0.29	0.29	1.418	0.691	11.394	28.926
6.45	6.25	0.2	7200	0.3	0.3	2.836	0.691	11.394	28.926
6.45	6.16	0.29	10800	0.28	0.28	4.254	0.668	11.014	27.961
6.45	6.07	0.38	14400	0.27	0.27	5.672	0.657	10.824	27.479
6.45	5.98	0.47	18000	0.27	0.27	7.09	0.650	10.71	27.190
6.45	5.88	0.57	21600	0.25	0.25	8.508	0.657	10.824	27.479

Where V_S = Sliding velocity (pin-on-disc wear testing machine), m/sec; ρ=density, kg/m³;

m_1 = Initial mass, gm; m_2 = Final mass, gm; Δm = Initial mass – Final mass, gm;

t = Time, sec; F_f = Average frictional force, kgf;

μ = Co-efficient of friction;

R.D = Rolling / Sliding distance, m;

Wr = Wear rate, N/m;

W_v = Volumetric Wear rate, m³/sec; W_s= Specific Wear rate, m³/N-m

Table 2: Wear Rate values for Pure Aluminium at 400 rpm

V_S =8.35 X 10^{-1} m/sec **ρ=2.58 x 1000 kg/m³**

m_1	m_2	Δm	T	F_f	μ	R.Dx10^{-3}	W_r×10^{-6}	W_v×10^{-12}	W_s ×10^{-13}
(gm)	(gm)	(gm)	(sec)	kgf		m	(N/m)	(m³/sec)	(m³/N-m)
6.52	6.31	0.21	3600	0.33	0.33	3.006	0.6853	23.927	28.654
6.52	6.1	0.42	7200	0.34	0.34	6.012	0.6852	23.927	28.654
6.52	5.9	0.62	10800	0.33	0.33	9.018	0.6745	23.547	28.199
6.52	5.7	0.82	14400	0.32	0.32	12.024	0.669	23.357	27.972
6.52	5.51	1.01	18000	0.3	0.3	15.03	0.6592	23.015	27.563
6.52	5.31	1.21	21600	0.31	0.31	18.036	0.6581	22.977	27.517

The Wear rate values for pure aluminium at 600 rpm and pure aluminium with 2% red mud of 100 μm particle size at 200 rpm and 400 rpm are shown in Tables 3, 4 and 5 respectively.

Table 3: Wear Rate values for Pure Aluminium at 600 rpm

V_S =1.244 m/sec **ρ=2.58 x 1000 kg/m³**

m_1	m_2	Δm	T	F_f	μ	R.Dx10^{-3}	W_r×10^{-6}	W_v×10^{-12}	W_s ×10^{-13}
(gm)	(gm)	(gm)	(sec)	kgf		m	(N/m)	(m³/sec)	(m³/N-m)
6.54	6.28	0.26	3600	0.35	0.35	4.48	0.569	29.624	23.804
6.54	6.03	0.51	7200	0.34	0.34	8.96	0.558	29.054	23.346
6.54	5.78	0.76	10800	0.33	0.33	13.44	0.554	28.864	23.194
6.54	5.53	1.01	14400	0.31	0.31	17.92	0.552	28.769	23.117
6.54	5.28	1.26	18000	0.33	0.33	22.4	0.551	28.712	23.072
6.54	5.03	1.51	21600	0.34	0.34	26.88	0.551	28.674	23.041

Table 4: Wear Rate values for Pure Aluminium with 2% Red mud of 100 μm particle size at 200 rpm

V_S =3.93 X 10^{-1} m/sec **ρ=2.4380 x 1000 kg/m³**

m_1	m_2	Δm	T	F_f	μ	R.Dx10^{-3}	W_r×10^{-6}	W_v×10^{-12}	W_s ×10^{-13}
(gm)	(gm)	(gm)	(sec)	kgf		m	(N/m)	(m³/sec)	(m³/N-m)
6.45	6.39	0.06	3600	0.29	0.29	1.418	0.415	6.836	17.355
6.45	6.33	0.12	7200	0.28	0.28	2.836	0.415	6.836	17.355
6.45	6.27	0.18	10800	0.26	0.26	4.254	0.415	6.836	17.355
6.45	6.22	0.23	14400	0.28	0.28	5.672	0.397	6.551	16.632
6.45	6.16	0.29	18000	0.25	0.25	7.09	0.401	6.608	16.777
6.45	6.1	0.35	21600	0.26	0.26	8.508	0.403	6.646	16.873

Table 5: Wear Rate values for Pure Aluminium with 2% Red mud of 100 µm particle size at 400 rpm

V_S =8.35 X 10^{-1} m/sec **ρ=2.4380 x 1000 kg/m³**

m_1	m_2	Δm	T	F_f	µ	R.Dx10^{-3}	$W_r \times 10^{-6}$	$W_v \times 10^{-12}$	$W_s \times 10^{-13}$
(gm)	(gm)	(gm)	(sec)	kgf		m	(N/m)	(m³/sec)	(m³/N-m)
6.520	6.402	0.118	3600	0.310	0.310	3.006	0.385	13.441	16.097
6.520	6.282	0.238	7200	0.290	0.290	6.012	0.388	13.557	16.236
6.520	6.172	0.348	10800	0.300	0.300	9.018	0.379	13.216	15.827
6.520	6.062	0.458	14400	0.310	0.310	12.024	0.374	13.045	15.623
6.520	5.942	0.578	18000	0.280	0.280	15.030	0.377	13.170	15.773
6.520	5.842	0.678	21600	0.300	0.300	18.036	0.369	12.874	15.418

The Wear rate values for pure aluminium with 2% red mud of 100 µm particle size at 600 rpm and pure aluminium with 2% red mud of 150 µm particle size at 200 rpm and 400 rpm are shown in Tables 6, 7 and 8 respectively.

Table 6: Wear Rate values for Pure Aluminium with 2% Red mud of 100 µm particle size at 600 rpm

V_S =12.44 m/sec **ρ=2.4380 x 1000 kg/m³**

m_1	m_2	Δm	T	F_f	µ	R.Dx10^{-3}	$W_r \times 10^{-6}$	$W_v \times 10^{-12}$	$W_s \times 10^{-13}$
(gm)	(gm)	(gm)	(sec)	kgf		m	(N/m)	(m³/sec)	(m³/N-m)
6.54	6.38	0.16	3600	0.32	0.32	4.48	0.350	18.229	14.649
6.54	6.22	0.32	7200	0.31	0.31	8.96	0.350	18.229	14.649
6.54	6.07	0.47	10800	0.3	0.3	13.44	0.343	17.850	14.343
6.54	5.91	0.63	14400	0.28	0.28	17.92	0.344	17.945	14.420
6.54	5.75	0.79	18000	0.3	0.3	22.4	0.345	18.002	14.465
6.54	5.6	0.94	21600	0.29	0.29	26.88	0.343	17.850	14.343

Table 7: Wear Rate values for Pure Aluminium with 2% Red mud of 150 µm particle size at 200 rpm

V_S =3.93 X 10^{-1}m/sec **ρ=2.4380 x 1000 kg/m³**

m_1	m_2	Δm	T	F_f	µ	R.Dx10^{-3}	$W_r \times 10^{-6}$	$W_v \times 10^{-12}$	$W_s \times 10^{-13}$
(gm)	(gm)	(gm)	(sec)	kgf		m	(N/m)	(m³/sec)	(m³/N-m)
6.52	6.44	0.08	3600	0.33	0.33	1.497	0.524	9.114	21.919
6.52	6.36	0.16	7200	0.32	0.32	2.994	0.524	9.114	21.919
6.52	6.29	0.23	10800	0.29	0.29	4.491	0.502	8.735	21.006
6.52	6.22	0.3	14400	0.28	0.3	5.988	0.491	8.545	20.549
6.52	6.14	0.38	18000	0.3	0.3	7.485	0.498	8.659	20.823
6.52	6.07	0.45	21600	0.29	0.29	8.982	0.491	8.545	20.549

Table 8: Wear Rate values for Pure Aluminium with 2% Red mud of 150 µm particle size at 400 rpm

V_S =8.35 X 10^{-1} m/sec **ρ=2.4380 x 1000 kg/m³**

m_1	m_2	Δm	T	F_f	µ	R.Dx10^{-3}	$W_r \times 10^{-6}$	$W_v \times 10^{-12}$	$W_s \times 10^{-13}$
(gm)	(gm)	(gm)	(sec)	kgf		m	(N/m)	(m³/sec)	(m³/N-m)
6.490	6.338	0.152	3600	0.320	0.320	3.012	0.495	17.316	20.738
6.490	6.198	0.292	7200	0.310	0.310	6.024	0.475	16.634	19.921
6.490	6.058	0.432	10800	0.290	0.290	9.036	0.469	16.406	19.648
6.490	5.918	0.572	14400	0.270	0.270	12.049	0.466	16.292	19.512
6.490	5.778	0.712	18000	0.310	0.310	15.061	0.464	16.224	19.430
6.490	5.648	0.842	21600	0.280	0.280	18.073	0.457	15.989	19.148

The Wear rate values for pure aluminium with 2% red mud of 150 µm particle size at 600 rpm and the wear rate values for pure aluminium with 2% red mud of 200 µm particle size at 200 rpm and 400 rpm are shown in Tables 9, 10 and 11 respectively.

Table 9: Wear Rate values for Pure Aluminium with 2% Red mud of 150 µm particle size at 600 rpm

V_S =1.27166 m/sec **ρ=2.4380 x 1000 kg/m³**

m_1	m_2	Δm	T	F_f	µ	R.Dx10^{-3}	$W_r \times 10^{-6}$	$W_v \times 10^{-12}$	$W_s \times 10^{-13}$
(gm)	(gm)	(gm)	(sec)	kgf		m	(N/m)	(m³/sec)	(m³/N-m)
6.53	6.32	0.21	3600	0.55	0.55	4.578	0.45	23.926	18.815
6.53	6.11	0.42	7200	0.54	0.54	9.156	0.45	23.926	18.815
6.53	5.91	0.62	10800	0.52	0.52	13.734	0.442	23.546	18.516
6.53	5.71	0.82	14400	0.49	0.49	18.312	0.439	23.357	18.367
6.53	5.51	1.02	18000	0.47	0.47	22.89	0.437	23.243	18.277
6.53	5.32	1.21	21600	0.5	0.5	27.468	0.432	22.977	18.068

Table 10: Wear Rate values for Pure Aluminium with 2% Red mud of 200 µm particle size at 200 rpm

V_S =4.213 X 10^{-1} m/sec **ρ=2.4380 x 1000 kg/m³**

m_1	m_2	Δm	T	F_f	µ	R.Dx10^{-3}	$W_r \times 10^{-6}$	$W_v \times 10^{-12}$	$W_s \times 10^{-13}$
(gm)	(gm)	(gm)	(sec)	kgf		m	(N/m)	(m³/sec)	(m³/N-m)
6.66	6.57	0.09	3600	0.39	0.39	1.517	0.582	10.254	24.334
6.66	6.48	0.18	7200	0.38	0.38	3.034	0.582	10.254	24.334
6.66	6.39	0.27	10800	0.35	0.35	4.551	0.582	10.254	24.334
6.66	6.31	0.35	14400	0.36	0.36	6.068	0.565	9.969	23.658
6.66	6.23	0.43	18000	0.35	0.35	7.585	0.556	9.798	23.253
6.66	6.15	0.51	21600	0.33	0.33	9.102	0.549	9.684	22.982

Table 11: Wear Rate values for Pure Aluminium with 2% Red mud of 200 µm particle size at 400 rpm

V_S =8.3537X 10^{-1} m/sec **ρ=2.4380 x 1000 kg/m³**

m_1	m_2	Δm	T	F_f	µ	R.Dx10^{-3}	$W_r \times 10^{-6}$	$W_v \times 10^{-12}$	$W_s \times 10^{-13}$
(gm)	(gm)	(gm)	(sec)	kgf		m	(N/m)	(m³/sec)	(m³/N-m)
6.57	6.4	0.17	3600	0.37	0.37	3.014	0.553	19.369	23.135
6.57	6.23	0.34	7200	0.36	0.36	6.028	0.553	19.369	23.135
6.57	6.06	0.51	10800	0.35	0.35	9.042	0.553	19.369	23.135
6.57	5.9	0.67	14400	0.34	0.34	12.056	0.545	19.084	22.794
6.57	5.74	0.83	18000	0.35	0.35	15.07	0.540	18.913	22.590
6.57	5.58	0.99	21600	0.37	0.37	18.084	0.537	18.799	22.454

The Wear rate values for pure aluminium with 2% red mud of 200 µm particle size at 600 rpm and Wear rate values for pure aluminium with 2% red mud of 42 nm particle size at 200 rpm and 400 rpm are shown in Tables 12, 13 and 14 respectively.

Table 12: Wear Rate values for Pure Aluminium with 2% Red mud of 200 µm particle size at 600 rpm

V_S =12.27 m/sec **ρ=2.4380 x 1000 kg/m³**

m_1	m_2	Δm	T	F_f	µ	R.Dx10^{-3}	$W_r \times 10^{-6}$	$W_v \times 10^{-12}$	$W_s \times 10^{-13}$
(gm)	(gm)	(gm)	(sec)	kgf		m	(N/m)	(m³/sec)	(m³/N-m)
6.71	6.48	0.23	3600	0.35	0.35	4.424	0.510	26.205	21.324
6.71	6.25	0.46	7200	0.35	0.35	8.848	0.510	26.205	21.324
6.71	6.03	0.68	10800	0.34	0.34	13.272	0.502	25.825	21.015
6.71	5.81	0.9	14400	0.3	0.3	17.696	0.498	25.635	20.860
6.71	5.59	1.12	18000	0.33	0.33	22.12	0.496	25.521	20.768
6.71	5.37	1.34	21600	0.32	0.32	26.544	0.495	25.445	20.706

Table 13: Wear Rate values for Pure Aluminium with 2% Red mud of 42 nm particle size at 200 rpm

V_S =3.93 X 10^{-1} m/sec **ρ=2.4380 x 1000 kg/m³**

m_1	m_2	Δm	T	F_f	µ	R.Dx10^{-3}	$W_r \times 10^{-6}$	$W_v \times 10^{-12}$	$W_s \times 10^{-13}$
(gm)	(gm)	(gm)	(sec)	kgf		m	(N/m)	(m³/sec)	(m³/N-m)
6.530	6.489	0.041	3600	0.220	0.220	1.418	0.281	4.628	11.776
6.530	6.449	0.081	7200	0.210	0.210	2.836	0.279	4.593	11.686
6.530	6.409	0.121	10800	0.190	0.190	4.254	0.278	4.581	11.656
6.530	6.369	0.161	14400	0.200	0.200	5.672	0.278	4.575	11.641
6.530	6.339	0.191	18000	0.180	0.180	7.090	0.264	4.344	11.053
6.530	6.299	0.231	21600	0.190	0.190	8.508	0.266	4.379	11.143

Table 14: Wear Rate values for Pure Aluminium with 2% Red mud of 42 nm particle size at 400 rpm

V_S =8.408 X 10^{-1} m/sec **ρ=2.4380 x 1000 kg/m³**

m_1	m_2	Δm	T	F_f	μ	R.Dx10^{-3}	W_r×10^{-6}	W_v×10^{-12}	W_s×10^{-13}
(gm)	(gm)	(gm)	(sec)	kgf		m	(N/m)	(m³/sec)	(m³/N-m)
6.580	6.505	0.075	3600	0.240	0.240	3.027	0.243	8.543	10.231
6.580	6.425	0.155	7200	0.230	0.230	6.054	0.251	8.829	10.574
6.580	6.355	0.225	10800	0.210	0.210	9.081	0.243	8.545	10.233
6.580	6.285	0.295	14400	0.220	0.220	12.108	0.239	8.402	10.063
6.580	6.215	0.365	18000	0.190	0.190	15.135	0.237	8.317	9.960
6.580	6.145	0.435	21600	0.210	0.210	18.162	0.235	8.260	9.892

The Wear rate values for pure aluminium with 2% red mud of 42 nm particle size at 600 rpm and the wear rate values for pure aluminium with 4% red mud of 100 μm particle size at 200 rpm and 400 rpm are shown in Tables 15, 16 and 17 respectively.

Table 15: Wear Rate values for Pure Aluminium with 2% Red mud of 42 nm particle size at 600 rpm

V_S =1.243 m/sec **ρ=2.4380 x 1000 kg/m³**

m_1	m_2	Δm	T	F_f	μ	R.Dx10^{-3}	W_r×10^{-6}	W_v×10^{-12}	W_s ×10^{-13}
(gm)	(gm)	(gm)	(sec)	kgf		m	(N/m)	(m³/sec)	(m³/N-m)
6.54	6.44	0.1	3600	0.26	0.26	4.399	0.223	11.393	9.324
6.54	6.34	0.2	7200	0.26	0.26	8.798	0.223	11.393	9.324
6.54	6.25	0.29	10800	0.25	0.25	13.197	0.215	11.013	9.013
6.54	6.16	0.38	14400	0.23	0.23	17.596	0.211	10.823	8.858
6.54	6.07	0.47	18000	0.22	0.22	21.995	0.209	10.710	8.764
6.54	5.98	0.56	21600	0.23	0.23	26.394	0.208	10.634	8.702

Table 16: Wear Rate values for Pure Aluminium with 4% Red mud of 100 μm particle size at 200 rpm

V_S =4.212 X 10^{-1} m/sec **ρ=2.44 x 1000 kg/m³**

m_1	m_2	Δm	T	F_f	μ	R.Dx10^{-3}	W_r×10^{-6}	W_v×10^{-12}	W_s×10^{-13}
(gm)	(gm)	(gm)	(sec)	kgf		m	(N/m)	(m³/sec)	(m³/N-m)
7.100	7.062	0.038	3600	0.270	0.270	1.515	0.246	4.325	11.005
7.100	7.022	0.078	7200	0.260	0.260	3.030	0.253	4.439	11.296
7.100	6.992	0.108	10800	0.250	0.250	4.545	0.233	4.098	10.428
7.100	6.962	0.138	14400	0.270	0.270	6.060	0.223	3.927	9.993
7.100	6.932	0.168	18000	0.240	0.240	7.575	0.218	3.825	9.733
7.100	6.902	0.198	21600	0.250	0.250	9.090	0.214	3.757	9.559

Table 17: Wear Rate values for Pure Aluminium with 4% Red mud of 100 µm particle size at 400 rpm

V_S =8.35 X 10^{-1} m/sec **ρ=2.44 x 1000 kg/m³**

m_1	m_2	Δm	T	F_f	µ	R.Dx10^{-3}	$W_r \times 10^{-6}$	$W_v \times 10^{-12}$	$W_s \times 10^{-13}$
(gm)	(gm)	(gm)	(sec)	kgf		m	(N/m)	(m³/sec)	(m³/N-m)
7.120	7.051	0.069	3600	0.290	0.290	3.010	0.225	7.859	9.412
7.120	6.990	0.130	7200	0.280	0.280	6.020	0.212	7.402	8.865
7.120	6.930	0.190	10800	0.260	0.260	9.030	0.206	7.211	8.636
7.120	6.870	0.250	14400	0.240	0.240	12.040	0.204	7.116	8.522
7.120	6.810	0.310	18000	0.250	0.250	15.050	0.202	7.059	8.454
7.120	6.750	0.370	21600	0.240	0.240	18.060	0.201	7.021	8.408

The Wear rate values for pure aluminium with 4% red mud of 100 µm particle size and 600 rpm and wear rate values for pure aluminium with 4% red mud of 150 µm particle size at 200 rpm and 400 rpm are shown in Tables 18, 19 and 20 respectively.

Table 18: Wear Rate values for Pure Aluminium with 4% Red mud of 100 µm particle size at 600 rpm

V_S =1.184m/sec **ρ=2.44 x 1000 kg/m³**

m_1	m_2	Δm	T	F_f	µ	R.Dx10^{-3}	$W_r \times 10^{-6}$	$W_v \times 10^{-12}$	$W_s \times 10^{-13}$
(gm)	(gm)	(gm)	(sec)	kgf		m	(N/m)	(m³/sec)	(m³/N-m)
6.83	6.74	0.09	3600	0.3	0.3	4.265	0.207	10.254	8.655
6.83	6.65	0.18	7200	0.29	0.29	8.53	0.207	10.254	8.655
6.83	6.57	0.26	10800	0.3	0.3	12.795	0.199	9.874	8.334
6.83	6.49	0.34	14400	0.28	0.28	17.06	0.195	9.684	8.174
6.83	6.41	0.42	18000	0.27	0.27	21.325	0.193	9.570	8.078
6.83	6.33	0.5	21600	0.29	0.29	25.59	0.191	9.494	8.014

Table 19: Wear Rate values for Pure Aluminium with 4% Red mud of 150 µm particle size at 200 rpm

V_S =4.213 X 10^{-1} m/sec **ρ=2.44 x 1000 kg/m³**

m_1	m_2	Δm	T	F_f	µ	R.Dx10^{-3}	$W_r \times 10^{-6}$	$W_v \times 10^{-12}$	$W_s \times 10^{-13}$
(gm)	(gm)	(gm)	(sec)	kgf		m	(N/m)	(m³/sec)	(m³/N-m)
7.2	7.151	0.049	3600	0.33	0.33	1.516	0.317	5.582	13.257
7.2	7.11	0.09	7200	0.32	0.32	3.032	0.291	5.127	12.175
7.2	7.07	0.13	10800	0.34	0.34	4.548	0.280	4.937	11.724
7.2	7.03	0.17	14400	0.31	0.31	6.064	0.275	4.842	11.498
7.2	6.99	0.21	18000	0.32	0.32	7.58	0.271	4.785	11.363
7.2	6.95	0.25	21600	0.3	0.3	9.096	0.269	4.747	11.273

Table 20: Wear Rate values for Pure Aluminium with 4% Red mud of 150 µm particle size at 400 rpm

V_S =8.305 X 10^{-1} m/sec **ρ=2.44 x 1000 kg/m³**

m_1	m_2	Δm	T	F_f	µ	R.Dx10^{-3}	W_r×10^{-6}	W_v×10^{-12}	W_s ×10^{-13}
(gm)	(gm)	(gm)	(sec)	kgf		m	(N/m)	(m³/sec)	(m³/N-m)
6.98	6.89	0.09	3600	0.35	0.35	2.99	0.295	10.254	12.346
6.98	6.8	0.18	7200	0.36	0.36	5.98	0.295	10.254	12.346
6.98	6.72	0.26	10800	0.33	0.33	8.97	0.284	9.874	11.889
6.98	6.64	0.34	14400	0.34	0.34	11.96	0.278	9.684	11.660
6.98	6.56	0.42	18000	0.33	0.33	14.95	0.275	9.570	11.523
6.98	6.48	0.5	21600	0.32	0.32	17.94	0.273	9.494	11.431

The Wear rate values for pure aluminium with 4% red mud of 150 µm particle size at 600 rpm and the wear rate values for pure aluminium with 4% red mud of 200 µm particle size at 200 rpm and 400 rpm are shown in Tables 21, 22 and 23 respectively.

Table 21: Wear Rate values for Pure Aluminium with 4% Red mud of 150 µm particle size at 600 rpm

V_S =1.243m/sec **ρ=2.44 x 1000 kg/m³**

m_1	m_2	Δm	T	F_f	µ	R.Dx10^{-3}	W_r×10^{-6}	W_v×10^{-12}	W_s×10^{-13}
(gm)	(gm)	(gm)	(sec)	kgf		m	(N/m)	(m³/sec)	(m³/N-m)
6.850	6.740	0.110	3600	0.370	0.370	4.496	0.240	12.522	10.066
6.850	6.620	0.230	7200	0.320	0.320	8.992	0.251	13.092	10.524
6.850	6.510	0.340	10800	0.360	0.360	13.488	0.247	12.902	10.371
6.850	6.400	0.450	14400	0.350	0.350	17.984	0.245	12.807	10.295
6.850	6.280	0.570	18000	0.340	0.340	22.480	0.249	12.978	10.432
6.850	6.170	0.680	21600	0.360	0.360	26.976	0.247	12.902	10.371

Table 22: Wear Rate values for Pure Aluminium with 4% Red mud of 200 µm particle size at 200 rpm

V_S =4.187 X 10^{-1} m/sec **ρ=2.44 x 1000 kg/m³**

m_1	m_2	Δm	T	F_f	µ	R.Dx10^{-3}	W_r×10^{-6}	W_v×10^{-12}	W_s×10^{-13}
(gm)	(gm)	(gm)	(sec)	kgf		m	(N/m)	(m³/sec)	(m³/N-m)
6.760	6.701	0.059	3600	0.380	0.380	1.507	0.384	6.717	17.093
6.760	6.641	0.119	7200	0.370	0.370	3.015	0.387	6.774	17.237
6.760	6.591	0.169	10800	0.350	0.350	4.522	0.367	6.413	16.319
6.760	6.541	0.219	14400	0.360	0.360	6.030	0.356	6.233	15.860
6.760	6.491	0.269	18000	0.330	0.330	7.537	0.350	6.125	15.585
6.760	6.441	0.319	21600	0.350	0.350	9.044	0.346	6.053	15.401

Table 23: Wear Rate values for Pure Aluminium with 4% Red mud of 200 µm particle size at 400 rpm

V_S =8.35 X 10^{-1} m/sec **ρ=2.44 x 1000 kg/m³**

m_1	m_2	Δm	T	F_f	µ	R.Dx10^{-3}	$W_r \times 10^{-6}$	$W_v \times 10^{-12}$	$W_s \times 10^{-13}$
(gm)	(gm)	(gm)	(sec)	kgf		m	(N/m)	(m³/sec)	(m³/N-m)
6.86	6.75	0.11	3600	0.4	0.4	2.99	0.360	12.533	15.089
6.86	6.64	0.22	7200	0.39	0.39	5.98	0.360	12.533	15.089
6.86	6.54	0.32	10800	0.37	0.37	8.97	0.349	12.153	14.632
6.86	6.44	0.42	14400	0.36	0.36	11.96	0.344	11.963	14.404
6.86	6.34	0.52	18000	0.32	0.32	14.95	0.341	11.849	14.266
6.86	6.24	0.62	21600	0.35	0.35	17.94	0.339	11.773	14.175

The Wear rate values for pure aluminium with 4% red mud of 200 µm particle size at 600 rpm Wear rate values for pure aluminium with 4% red mud of 42 nm particle size at 200 rpm and 400 rpm and 600 rpm are shown in Tables 24, 25 and 26 respectively.

Table 24: Wear Rate values for Pure Aluminium with 4% Red mud of 200 µm particle size at 600 rpm

V_S =1.2716 m/sec **ρ=2.44 x 1000 kg/m³**

m_1	m_2	Δm	T	F_f	µ	R.Dx10^{-3}	$W_r \times 10^{-6}$	$W_v \times 10^{-12}$	$W_s \times 10^{-13}$
(gm)	(gm)	(gm)	(sec)	kgf		m	(N/m)	(m³/sec)	(m³/N-m)
6.85	6.69	0.16	3600	0.43	0.43	4.589	0.342	18.229	14.301
6.85	6.53	0.32	7200	0.41	0.41	9.178	0.342	18.229	14.301
6.85	6.38	0.47	10800	0.39	0.39	13.767	0.334	17.850	14.003
6.85	6.23	0.62	14400	0.42	0.42	18.356	0.331	17.660	13.854
6.85	6.08	0.77	18000	0.37	0.37	22.945	0.329	17.546	13.764
6.85	5.93	0.92	21600	0.39	0.39	27.534	0.327	17.470	13.705

Table 25: Wear Rate values for Pure Aluminium with 4% Red mud of 42 nm particle size at 200 rpm

V_S =4.189 X 10^{-1} m/sec **ρ=2.44 x 1000 kg/m³**

m_1	m_2	Δm	T	F_f	µ	R.Dx10^{-3}	$W_r \times 10^{-6}$	$W_v \times 10^{-12}$	$W_s \times 10^{-13}$
(gm)	(gm)	(gm)	(sec)	kgf		m	(N/m)	(m³/sec)	(m³/N-m)
6.530	6.506	0.024	3600	0.190	0.190	1.509	0.156	2.732	6.951
6.530	6.476	0.054	7200	0.180	0.180	3.018	0.176	3.074	7.821
6.530	6.446	0.084	10800	0.190	0.190	4.527	0.182	3.187	8.111
6.530	6.416	0.114	14400	0.170	0.170	6.036	0.185	3.244	8.256
6.530	6.396	0.134	18000	0.150	0.150	7.545	0.174	3.051	7.763
6.530	6.376	0.154	21600	0.170	0.170	9.054	0.167	2.922	7.435

Table 26: Wear Rate values for Pure Aluminium with 4% Red mud of 42 nm particle size at 400 rpm

V_S =8.39 X 10^{-1} m/sec **ρ=2.44 x 1000 kg/m³**

m_1	m_2	Δm	T	F_f	μ	R.Dx10^{-3}	W_r×10^{-6}	W_v×10^{-12}	W_s×10^{-13}
(gm)	(gm)	(gm)	(sec)	kgf		m	(N/m)	(m³/sec)	(m³/N-m)
6.870	6.826	0.044	3600	0.210	0.210	3.020	0.143	5.012	6.002
6.870	6.776	0.094	7200	0.200	0.200	6.040	0.153	5.352	6.409
6.870	6.726	0.144	10800	0.180	0.180	9.060	0.156	5.465	6.545
6.870	6.686	0.184	14400	0.170	0.170	12.080	0.149	5.237	6.272
6.870	6.636	0.234	18000	0.220	0.220	15.100	0.152	5.328	6.381
6.870	6.596	0.274	21600	0.190	0.190	18.120	0.148	5.199	6.227

The Wear rate values for pure aluminium with 4% red mud of 42 nm particle size at 600 rpm and the wear rate values for pure aluminium with 6% red mud of 100 μm particle size at 200 rpm and 400 rpm are shown in Tables 27, 28 and 29 respectively.

Table 27: Wear Rate values for Pure Aluminium with 4% Red mud of 42 nm particle size at 600 rpm

V_S =1.244 m/sec **ρ=2.44 x 1000 kg/m³**

m_1	m_2	Δm	T	F_f	μ	R.Dx10^{-3}	W_r×10^{-6}	W_v×10^{-12}	W_s×10^{-13}
(gm)	(gm)	(gm)	(sec)	kgf		m	(N/m)	(m³/sec)	(m³/N-m)
6.720	6.650	0.070	3600	0.220	0.220	4.518	0.152	7.969	6.406
6.720	6.580	0.140	7200	0.200	0.200	9.036	0.152	7.969	6.406
6.720	6.520	0.200	10800	0.170	0.170	13.554	0.145	7.590	6.101
6.720	6.460	0.260	14400	0.190	0.190	18.072	0.141	7.400	5.948
6.720	6.400	0.320	18000	0.180	0.180	22.590	0.139	7.286	5.857
6.720	6.350	0.370	21600	0.190	0.190	27.108	0.134	7.020	5.643

Table 28: Wear Rate values for Pure Aluminium with 6% Red mud of 100 μm particle size at 200 rpm

V_S =4.189 X 10^{-1} m/sec **ρ=2.45 x 1000 kg/m³**

m_1	m_2	Δm	T	F_f	μ	R.Dx10^{-3}	W_r×10^{-6}	W_v×10^{-12}	W_s×10^{-13}
(gm)	(gm)	(gm)	(sec)	kgf		m	(N/m)	(m³/sec)	(m³/N-m)
7.100	7.072	0.028	3600	0.250	0.250	1.509	0.182	3.174	8.077
7.100	7.042	0.058	7200	0.240	0.240	3.018	0.189	3.288	8.366
7.100	7.012	0.088	10800	0.260	0.260	4.527	0.191	3.326	8.462
7.100	6.982	0.118	14400	0.230	0.230	6.036	0.192	3.345	8.510
7.100	6.962	0.138	18000	0.250	0.250	7.545	0.179	3.129	7.962
7.100	6.932	0.168	21600	0.220	0.220	9.054	0.182	3.175	8.078

Table 29: Wear Rate values for Pure Aluminium with 6% Red mud of 100 µm particle size at 400 rpm

V_S =8.301 X 10^{-1} m/sec **ρ=2.45 x 1000 kg/m³**

m_1	m_2	Δm	T	F_f	µ	R.Dx10^{-3}	$W_r \times 10^{-6}$	$W_v \times 10^{-12}$	$W_s \times 10^{-13}$
(gm)	(gm)	(gm)	(sec)	kgf		m	(N/m)	(m³/sec)	(m³/N-m)
7.120	7.071	0.049	3600	0.260	0.260	2.967	0.162	5.555	6.653
7.120	7.021	0.099	7200	0.240	0.240	5.934	0.164	5.612	6.721
7.120	6.981	0.139	10800	0.230	0.230	8.901	0.153	5.253	6.291
7.120	6.941	0.179	14400	0.260	0.260	11.868	0.148	5.074	6.076
7.120	6.901	0.219	18000	0.230	0.230	14.835	0.145	4.966	5.947
7.120	6.861	0.259	21600	0.250	0.250	17.802	0.143	4.894	5.861

The Wear rate values for pure aluminium with 6% red mud of 100 µm particle size and 600 rpm and Wear rate values for pure aluminium with 6% red mud of 150 µm particle size at 200 rpm and 400 rpm are shown in Tables 30, 31 and 32 respectively.

Table 30: Wear Rate values for Pure Aluminium with 6% Red mud of 100 µm particle size at 600 rpm

V_S =1.227 m/sec **ρ=2.45 x 1000 kg/m³**

m_1	m_2	Δm	T	F_f	µ	R.Dx10^{-3}	$W_r \times 10^{-6}$	$W_v \times 10^{-12}$	$W_s \times 10^{-13}$
(gm)	(gm)	(gm)	(sec)	kgf		m	(N/m)	(m³/sec)	(m³/N-m)
6.830	6.760	0.070	3600	0.280	0.280	4.460	0.154	7.938	6.381
6.830	6.690	0.140	7200	0.270	0.270	8.920	0.154	7.937	6.380
6.830	6.630	0.200	10800	0.280	0.280	13.380	0.147	7.559	6.076
6.830	6.570	0.260	14400	0.250	0.250	17.840	0.143	7.370	5.924
6.830	6.510	0.320	18000	0.260	0.260	22.300	0.141	7.257	5.833
6.830	6.450	0.380	21600	0.270	0.270	26.760	0.139	7.181	5.772

Table 31: Wear Rate values for Pure Aluminium with 6% Red mud of 150 µm particle size at 200 rpm

V_S =4.158 m/sec **ρ=2.45 x 1000 kg/m³**

m_1	m_2	Δm	T	F_f	µ	R.Dx10^{-3}	$W_r \times 10^{-6}$	$W_v \times 10^{-12}$	$W_s \times 10^{-13}$
(gm)	(gm)	(gm)	(sec)	kgf		m	(N/m)	(m³/sec)	(m³/N-m)
7.200	7.160	0.040	3600	0.300	0.300	1.498	0.262	4.536	11.542
7.200	7.120	0.080	7200	0.290	0.290	2.996	0.262	4.536	11.541
7.200	7.090	0.110	10800	0.310	0.310	4.494	0.240	4.158	10.579
7.200	7.060	0.140	14400	0.320	0.320	5.992	0.229	3.968	10.098
7.200	7.030	0.170	18000	0.280	0.280	7.490	0.223	3.855	9.809
7.200	7.000	0.200	21600	0.320	0.320	8.988	0.218	3.779	9.617

Table 32: Wear Rate values for Pure Aluminium with 6% Red mud of 150 µm particle size at 400 rpm

V_S =8.36X 10^{-1} m/sec **ρ=2.45 x 1000 kg/m³**

m_1	m_2	Δm	T	F_f	µ	R.Dx10^{-3}	W_r×10^{-6}	W_v×10^{-12}	W_s ×10^{-13}
(gm)	(gm)	(gm)	(sec)	kgf		m	(N/m)	(m³/sec)	(m³/N-m)
6.980	6.905	0.075	3600	0.320	0.320	3.010	0.245	8.523	10.207
6.980	6.835	0.145	7200	0.310	0.310	6.020	0.237	8.230	9.856
6.980	6.775	0.205	10800	0.300	0.300	9.030	0.223	7.754	9.286
6.980	6.715	0.265	14400	0.280	0.280	12.040	0.216	7.516	9.001
6.980	6.645	0.335	18000	0.310	0.310	15.050	0.218	7.600	9.102
6.980	6.585	0.395	21600	0.310	0.310	18.060	0.215	7.467	8.943

The Wear rate values for pure aluminium with 6% red mud of 150 µm particle size at 600 rpm and the wear rate values for pure aluminium with 6% red mud of 200 µm particle size at 200 rpm and 400 rpm are shown in Tables 33, 34 and 35 respectively.

Table 33: Wear Rate values for Pure Aluminium with 6% Red mud of 150 µm particle size at 600 rpm

V_S =1.271 m/sec **ρ=2.45 x 1000 kg/m³**

m_1	m_2	Δm	T	F_f	µ	R.Dx10^{-3}	W_r×10^{-6}	W_v×10^{-12}	W_s ×10^{-13}
(gm)	(gm)	(gm)	(sec)	kgf		m	(N/m)	(m³/sec)	(m³/N-m)
6.85	6.76	0.09	3600	0.33	0.33	4.59	0.192	10.254	8.042
6.85	6.67	0.18	7200	0.34	0.34	9.18	0.192	10.254	8.042
6.85	6.59	0.26	10800	0.32	0.32	13.77	0.185	9.874	7.744
6.85	6.51	0.34	14400	0.33	0.33	18.36	0.181	9.684	7.595
6.85	6.43	0.42	18000	0.29	0.29	22.95	0.179	9.570	7.506
6.85	6.35	0.5	21600	0.28	0.28	27.54	0.178	9.494	7.446

Table 34: Wear Rate values for Pure Aluminium with 6% Red mud of 200 µm particle size at 200 rpm

V_S =4.128 X 10^{-1} m/sec **ρ=2.45 x 1000 kg/m³**

m_1	m_2	Δm	T	F_f	µ	R.Dx10^{-3}	W_r×10^{-6}	W_v×10^{-12}	W_s×10^{-13}
(gm)	(gm)	(gm)	(sec)	kgf		m	(N/m)	(m³/sec)	(m³/N-m)
6.760	6.712	0.048	3600	0.350	0.350	1.485	0.317	5.441	13.844
6.760	6.662	0.098	7200	0.340	0.340	2.970	0.324	5.555	14.134
6.760	6.612	0.148	10800	0.360	0.360	4.455	0.326	5.593	14.231
6.760	6.572	0.188	14400	0.340	0.340	5.940	0.310	5.328	13.558
6.760	6.522	0.238	18000	0.330	0.330	7.425	0.314	5.397	13.732
6.760	6.482	0.278	21600	0.320	0.320	8.910	0.306	5.253	13.366

Table 35: Wear Rate values for Pure Aluminium with 6% Red mud of 200 µm particle size at 400 rpm

V_S =8.401 X 10^{-1} m/sec **ρ=2.45 x 1000 kg/m³**

m_1	m_2	Δm	T	F_f	µ	R.Dx10^{-3}	$W_r \times 10^{-6}$	$W_v \times 10^{-12}$	$W_s \times 10^{-13}$
(gm)	(gm)	(gm)	(sec)	kgf		m	(N/m)	(m³/sec)	(m³/N-m)
6.860	6.762	0.098	3600	0.370	0.370	3.013	0.319	11.108	13.303
6.860	6.662	0.198	7200	0.380	0.380	6.026	0.322	11.223	13.441
6.860	6.572	0.288	10800	0.360	0.360	9.039	0.313	10.883	13.034
6.860	6.482	0.378	14400	0.350	0.350	12.052	0.308	10.714	12.831
6.860	6.392	0.468	18000	0.350	0.350	15.065	0.305	10.612	12.709
6.860	6.302	0.558	21600	0.340	0.340	18.078	0.303	10.544	12.627

The Wear rate values for pure aluminium with 6% red mud of 200 µm particle size at 600 rpm and wear rate values for pure aluminium with 6% red mud of 42 nm particle size at 200 rpm and 400 rpm are shown in 36, 37 and 38 respectively.

Table 36: Wear Rate values for Pure Aluminium with 6% Red mud of 200 µm particle size at 600 rpm

V_S =1.2516m/sec **ρ=2.45 x 1000 kg/m³**

m_1	m_2	Δm	T	F_f	µ	R.Dx10^{-3}	$W_r \times 10^{-6}$	$W_v \times 10^{-12}$	$W_s \times 10^{-13}$
(gm)	(gm)	(gm)	(sec)	kgf		m	(N/m)	(m³/sec)	(m³/N-m)
6.850	6.720	0.130	3600	0.390	0.390	4.510	0.283	14.751	11.858
6.850	6.590	0.260	7200	0.380	0.380	9.020	0.283	14.745	11.853
6.850	6.470	0.380	10800	0.370	0.370	13.530	0.276	14.365	11.548
6.850	6.350	0.500	14400	0.350	0.350	18.040	0.272	14.175	11.395
6.850	6.230	0.620	18000	0.350	0.350	22.550	0.270	14.061	11.303
6.850	6.110	0.740	21600	0.360	0.360	27.060	0.268	13.985	11.242

Table 37: Wear Rate values for Pure Aluminium with 6% Red mud of 42 nm particle size at 200 rpm

V_S =3.758 X 10^{-1} m/sec **ρ=2.45 x 1000 kg/m³**

m_1	m_2	Δm	T	F_f	µ	R.Dx10^{-3}	$W_r \times 10^{-6}$	$W_v \times 10^{-12}$	$W_s \times 10^{-13}$
(gm)	(gm)	(gm)	(sec)	kgf		m	(N/m)	(m³/sec)	(m³/N-m)
6.53	6.51	0.02	3600	0.118	0.118	1.353	0.145	2.278	6.063
6.53	6.49	0.04	7200	0.112	0.112	2.706	0.145	2.278	6.063
6.53	6.47	0.06	10800	0.11	0.11	4.059	0.145	2.278	6.063
6.53	6.46	0.07	14400	0.119	0.119	5.412	0.126	1.993	5.305
6.53	6.45	0.08	18000	0.114	0.114	6.765	0.116	1.822	4.850
6.53	6.44	0.09	21600	0.12	0.12	8.118	0.108	1.709	4.547

Table 38: Wear Rate values for Pure Aluminium with 6% Red mud of 42 nm particle size at 400 rpm

V_S =8.305 X 10^{-1} m/sec **ρ=2.45 x 1000 kg/m³**

m_1	m_2	Δm	T	F_f	μ	R.Dx10^{-3}	$W_r \times 10^{-6}$	$W_v \times 10^{-12}$	$W_s \times 10^{-13}$
(gm)	(gm)	(gm)	(sec)	kgf		m	(N/m)	(m³/sec)	(m³/N-m)
6.870	6.830	0.040	3600	0.152	0.152	2.973	0.132	4.536	5.432
6.870	6.790	0.080	7200	0.152	0.152	5.946	0.132	4.535	5.432
6.870	6.760	0.110	10800	0.149	0.149	8.919	0.121	4.157	4.979
6.870	6.720	0.150	14400	0.131	0.131	11.892	0.124	4.252	5.092
6.870	6.690	0.180	18000	0.143	0.143	14.865	0.119	4.082	4.888
6.870	6.660	0.210	21600	0.132	0.132	17.838	0.115	3.968	4.752

The Wear rate values for pure aluminium with 6% red mud of 42 nm particle size at 600 rpm is shown in 39 respectively.

Table 39: Wear Rate values for Pure Aluminium with 6% Red mud of 42 nm particle size at 600 rpm

V_S =1.338m/sec **ρ=2.45 x 1000 kg/m³**

m_1	m_2	Δm	t	F_f	μ	R.Dx10^{-3}	$W_r \times 10^{-6}$	$W_v \times 10^{-12}$	$W_s \times 10^{-13}$
(gm)	(gm)	(gm)	(sec)	kgf		m	(N/m)	(m³/sec)	(m³/N-m)
6.72	6.66	0.06	3600	0.161	0.161	4.82	0.122	6.836	5.105
6.72	6.6	0.12	7200	0.168	0.168	9.64	0.122	6.836	5.105
6.72	6.54	0.18	10800	0.167	0.167	14.46	0.122	6.836	5.105
6.72	6.49	0.23	14400	0.159	0.159	19.28	0.117	6.551	4.893
6.72	6.43	0.29	18000	0.162	0.162	24.1	0.118	6.608	4.935
6.72	6.37	0.35	21600	0.158	0.158	28.92	0.118	6.646	4.964

ii) Wear rate tables for pure aluminium with red mud at normal condition at 20 N load

The Wear rate values for pure aluminium of 45 μm particle size at 200 rpm, 400 rpm and 600 rpm is shown in tables 1, 2 and 3 respectively.

Table 1: Wear Rate values for Pure Aluminium at 200 rpm

V_S =3.93 X 10^{-1} m/sec **ρ=2.58 x 1000 kg/m³**

m_1	m_2	Δm	T	F_f	μ	R.Dx10^{-3}	$W_r \times 10^{-6}$	$W_v \times 10^{-12}$	$W_s \times 10^{-13}$
(gm)	(gm)	(gm)	(sec)	kgf		m	(N/m)	(m³/sec)	(m³/N-m)
6.450	6.304	0.146	3600	0.290	0.145	1.418	1.012	15.749	20.037
6.450	6.204	0.246	7200	0.300	0.150	2.836	0.852	13.258	16.868
6.450	6.114	0.336	10800	0.280	0.140	4.254	0.775	12.069	15.355
6.450	6.024	0.426	14400	0.270	0.135	5.672	0.737	11.474	14.598
6.450	5.934	0.516	18000	0.270	0.135	7.090	0.714	11.117	14.144
6.450	5.834	0.616	21600	0.250	0.125	8.508	0.711	11.059	14.070

Table 2: Wear Rate values for Pure Aluminium at 400 rpm

V_S =8.35 X 10^{-1} m/sec **ρ=2.58 x 1000 kg/m³**

m_1	m_2	Δm	T	F_f	μ	R.Dx10^{-3}	$W_r \times 10^{-6}$	$W_v \times 10^{-12}$	$W_s \times 10^{-13}$
(gm)	(gm)	(gm)	(sec)	kgf		m	(N/m)	(m³/sec)	(m³/N-m)
6.520	6.212	0.308	3600	0.330	0.165	3.006	1.004	33.123	19.834
6.520	6.002	0.518	7200	0.340	0.170	6.012	0.845	27.866	16.687
6.520	5.802	0.718	10800	0.330	0.165	9.018	0.781	25.755	15.422
6.520	5.602	0.918	14400	0.320	0.160	12.024	0.749	24.700	14.790
6.520	5.412	1.108	18000	0.300	0.150	15.030	0.723	23.851	14.282
6.520	5.212	1.308	21600	0.310	0.155	18.036	0.711	23.465	14.051

Table 3: Wear Rate values for Pure Aluminium at 600 rpm

V_S =1.244 m/sec **ρ=2.58 x 1000 kg/m³**

m_1	m_2	Δm	T	F_f	μ	R.Dx10^{-3}	$W_r \times 10^{-6}$	$W_v \times 10^{-12}$	$W_s \times 10^{-13}$
(gm)	(gm)	(gm)	(sec)	kgf		m	(N/m)	(m³/sec)	(m³/N-m)
6.540	6.135	0.405	3600	0.350	0.175	4.480	0.887	43.612	17.529
6.540	5.885	0.655	7200	0.340	0.170	8.960	0.717	35.264	14.174
6.540	5.635	0.905	10800	0.330	0.165	13.440	0.661	32.482	13.055
6.540	5.385	1.155	14400	0.310	0.155	17.920	0.632	31.090	12.496
6.540	5.135	1.405	18000	0.330	0.165	22.400	0.615	30.256	12.161
6.540	4.885	1.655	21600	0.340	0.170	26.880	0.604	29.699	11.937

The Wear rate values for pure aluminium with 2% red mud of 100 µm particle size at 200rpm,400 rpm and 600 rpm is shown in tables 4, 5 and 6 respectively.

Table 4: Wear Rate values for Pure Aluminium with 2% Red mud of 100 µm particle size at 200 rpm

V_S =3.93 X 10^{-1} m/sec **ρ=2.4380 x 1000 kg/m³**

m_1	m_2	Δm	T	F_f	µ	R.Dx10^{-3}	$W_r \times 10^{-6}$	$W_v \times 10^{-12}$	$W_s \times 10^{-13}$
(gm)	(gm)	(gm)	(sec)	kgf		m	(N/m)	(m³/sec)	(m³/N-m)
6.450	6.343	0.107	3600	0.290	0.145	1.418	0.742	12.220	15.547
6.450	6.283	0.167	7200	0.280	0.140	2.836	0.579	9.528	12.122
6.450	6.223	0.227	10800	0.260	0.130	4.254	0.524	8.631	10.981
6.450	6.173	0.277	14400	0.280	0.140	5.672	0.480	7.897	10.048
6.450	6.113	0.337	18000	0.250	0.125	7.090	0.467	7.685	9.777
6.450	6.053	0.397	21600	0.260	0.130	8.508	0.458	7.544	9.597

Table 5: Wear Rate values for Pure Aluminium with 2% Red mud of 100 µm particle size at 400 rpm

V_S =8.35 X 10^{-1} m/sec **ρ=2.4380 x 1000 kg/m³**

m_1	m_2	Δm	T	F_f	µ	R.Dx10^{-3}	$W_r \times 10^{-6}$	$W_v \times 10^{-12}$	$W_s \times 10^{-13}$
(gm)	(gm)	(gm)	(sec)	kgf		m	(N/m)	(m³/sec)	(m³/N-m)
6.520	6.307	0.213	3600	0.310	0.155	3.006	0.695	24.264	14.530
6.520	6.187	0.333	7200	0.290	0.145	6.012	0.543	18.968	11.358
6.520	6.077	0.443	10800	0.300	0.150	9.018	0.482	16.823	10.074
6.520	5.967	0.553	14400	0.310	0.155	12.024	0.451	15.751	9.432
6.520	5.847	0.673	18000	0.280	0.140	15.030	0.439	15.335	9.183
6.520	5.747	0.773	21600	0.300	0.150	18.036	0.420	14.678	8.789

Table 6: Wear Rate values for Pure Aluminium with 2% Red mud of 100 µm particle size at 600 rpm

V_S =1.244 m/sec **ρ=2.4380 x 1000 kg/m³**

m_1	m_2	Δm	T	F_f	µ	R.Dx10^{-3}	$W_r \times 10^{-6}$	$W_v \times 10^{-12}$	$W_s \times 10^{-13}$
(gm)	(gm)	(gm)	(sec)	kgf		m	(N/m)	(m³/sec)	(m³/N-m)
6.540	6.251	0.289	3600	0.320	0.160	4.480	0.632	32.884	13.217
6.540	6.091	0.449	7200	0.310	0.155	8.960	0.491	25.557	10.272
6.540	5.941	0.599	10800	0.300	0.150	13.440	0.437	22.735	9.138
6.540	5.781	0.759	14400	0.280	0.140	17.920	0.415	21.609	8.685
6.540	5.621	0.919	18000	0.300	0.150	22.400	0.402	20.933	8.414
6.540	5.471	1.069	21600	0.290	0.145	26.880	0.390	20.293	8.156

The Wear rate values for pure aluminium with 2% red mud of 150 µm particle size at 200rpm,400 rpm and 600 rpm is shown in tables 7, 8 and 9 respectively.

Table 7: Wear Rate values for Pure Aluminium with 2% Red mud of 150 µm particle size at 200 rpm

V_S =3.93 X 10^{-1} m/sec **ρ=2.4380 x 1000 kg/m³**

m_1	m_2	Δm	T	F_f	µ	R.Dx10^{-3}	$W_r \times 10^{-6}$	$W_v \times 10^{-12}$	$W_s \times 10^{-13}$
(gm)	(gm)	(gm)	(sec)	kgf		m	(N/m)	(m³/sec)	(m³/N-m)
6.520	6.376	0.144	3600	0.330	0.165	1.497	0.943	16.396	20.860
6.520	6.296	0.224	7200	0.320	0.160	2.994	0.734	12.755	16.228
6.520	6.226	0.294	10800	0.290	0.145	4.491	0.642	11.162	14.201
6.520	6.156	0.364	14400	0.280	0.140	5.988	0.596	10.365	13.188
6.520	6.076	0.444	18000	0.300	0.150	7.485	0.582	10.115	12.869
6.520	6.006	0.514	21600	0.290	0.145	8.982	0.561	9.759	12.416

Table 8: Wear Rate values for Pure Aluminium with 2% Red mud of 150 µm particle size at 400 rpm

V_S =8.35 X 10^{-1} m/sec **ρ=2.4380 x 1000 kg/m³**

m_1	m_2	Δm	T	F_f	µ	R.Dx10^{-3}	$W_r \times 10^{-6}$	$W_v \times 10^{-12}$	$W_s \times 10^{-13}$
(gm)	(gm)	(gm)	(sec)	kgf		m	(N/m)	(m³/sec)	(m³/N-m)
6.490	6.215	0.275	3600	0.320	0.160	3.012	0.895	31.309	18.748
6.490	6.075	0.415	7200	0.310	0.155	6.024	0.675	23.630	14.150
6.490	5.935	0.555	10800	0.290	0.145	9.036	0.602	21.071	12.617
6.490	5.795	0.695	14400	0.270	0.135	12.049	0.566	19.791	11.851
6.490	5.655	0.835	18000	0.310	0.155	15.061	0.544	19.023	11.391
6.490	5.525	0.965	21600	0.280	0.140	18.073	0.524	18.321	10.971

Table 9: Wear Rate values for Pure Aluminium with 2% Red mud of 150 µm particle size at 600 rpm

V_S =1.244 m/sec **ρ=2.4380 x 1000 kg/m³**

m_1	m_2	Δm	T	F_f	µ	R.Dx10^{-3}	$W_r \times 10^{-6}$	$W_v \times 10^{-12}$	$W_s \times 10^{-13}$
(gm)	(gm)	(gm)	(sec)	kgf		m	(N/m)	(m³/sec)	(m³/N-m)
6.530	6.131	0.399	3600	0.550	0.275	4.578	0.854	45.408	18.251
6.530	5.921	0.609	7200	0.540	0.270	9.156	0.652	34.667	13.934
6.530	5.721	0.809	10800	0.520	0.260	13.734	0.578	30.707	12.342
6.530	5.521	1.009	14400	0.490	0.245	18.312	0.540	28.727	11.546
6.530	5.321	1.209	18000	0.470	0.235	22.890	0.518	27.539	11.069
6.530	5.131	1.399	21600	0.500	0.250	27.468	0.499	26.557	10.674

The Wear rate values for pure aluminium with 2% red mud of 200 µm particle size at 200rpm,400 rpm and 600 rpm is shown in tables 10, 11 and 12 respectively.

Table 10: Wear Rate values for Pure Aluminium with 2% Red mud of 200 µm particle size at 200 rpm

V_S =3.93 X 10^{-1} m/sec **ρ=2.4380 x 1000 kg/m³**

m_1	m_2	Δm	T	F_f	µ	R.Dx10^{-3}	W_r×10^{-6}	W_v×10^{-12}	W_s×10^{-13}
(gm)	(gm)	(gm)	(sec)	kgf		m	(N/m)	(m³/sec)	(m³/N-m)
6.660	6.502	0.158	3600	0.390	0.195	1.517	1.021	17.989	22.887
6.660	6.412	0.248	7200	0.380	0.190	3.034	0.802	14.122	17.966
6.660	6.322	0.338	10800	0.350	0.175	4.551	0.728	12.833	16.326
6.660	6.242	0.418	14400	0.360	0.180	6.068	0.676	11.903	15.144
6.660	6.162	0.498	18000	0.350	0.175	7.585	0.644	11.345	14.434
6.660	6.082	0.578	21600	0.330	0.165	9.102	0.623	10.974	13.961

Table 11: Wear Rate values for Pure Aluminium with 2% Red mud of 200 µm particle size at 400 rpm

V_S =8.35 X 10^{-1} m/sec **ρ=2.4380 x 1000 kg/m³**

m_1	m_2	Δm	T	F_f	µ	R.Dx10^{-3}	W_r×10^{-6}	W_v×10^{-12}	W_s×10^{-13}
(gm)	(gm)	(gm)	(sec)	kgf		m	(N/m)	(m³/sec)	(m³/N-m)
6.570	6.241	0.329	3600	0.370	0.185	3.014	1.070	37.456	22.429
6.570	6.071	0.499	7200	0.360	0.180	6.028	0.812	28.413	17.014
6.570	5.901	0.669	10800	0.350	0.175	9.042	0.726	25.398	15.208
6.570	5.741	0.829	14400	0.340	0.170	12.056	0.674	23.606	14.135
6.570	5.581	0.989	18000	0.350	0.175	15.070	0.644	22.531	13.492
6.570	5.421	1.149	21600	0.370	0.185	18.084	0.623	21.814	13.062

Table 12: Wear Rate values for Pure Aluminium with 2% Red mud of 200 µm particle size at 600 rpm

V_S =1.244 m/sec **ρ=2.4380 x 1000 kg/m³**

m_1	m_2	Δm	T	F_f	µ	R.Dx10^{-3}	W_r×10^{-6}	W_v×10^{-12}	W_s×10^{-13}
(gm)	(gm)	(gm)	(sec)	kgf		m	(N/m)	(m³/sec)	(m³/N-m)
6.710	6.296	0.414	3600	0.350	0.175	4.424	0.918	47.169	18.958
6.710	6.066	0.644	7200	0.350	0.175	8.848	0.714	36.687	14.746
6.710	5.846	0.864	10800	0.340	0.170	13.272	0.639	32.813	13.189
6.710	5.626	1.084	14400	0.300	0.150	17.696	0.601	30.877	12.410
6.710	5.406	1.304	18000	0.330	0.165	22.120	0.578	29.714	11.943
6.710	5.186	1.524	21600	0.320	0.160	26.544	0.563	28.940	11.632

The Wear rate values for pure aluminium with 2% red mud of 42 nm particle size at 200rpm, 400 rpm and 600 rpm is shown in tables 13, 14 and 15 respectively

Table 13: Wear Rate values for Pure Aluminium with 2% Red mud of 42 nm particle size at 200 rpm

V_S =3.93 X 10^{-1} m/sec **ρ=2.4380 x 1000 kg/m³**

m_1	m_2	Δm	T	F_f	μ	R.Dx10^{-3}	W_r×10^{-6}	W_v×10^{-12}	W_s×10^{-13}
(gm)	(gm)	(gm)	(sec)	kgf		m	(N/m)	(m³/sec)	(m³/N-m)
6.530	6.457	0.073	3600	0.220	0.110	1.418	0.506	8.333	10.602
6.530	6.417	0.113	7200	0.210	0.105	2.836	0.391	6.445	8.200
6.530	6.377	0.153	10800	0.190	0.095	4.254	0.353	5.816	7.400
6.530	6.337	0.193	14400	0.200	0.100	5.672	0.334	5.501	6.999
6.530	6.307	0.223	18000	0.180	0.090	7.090	0.309	5.085	6.469
6.530	6.267	0.263	21600	0.190	0.095	8.508	0.303	4.997	6.357

Table 14: Wear Rate values for Pure Aluminium with 2% Red mud of 42 nm particle size at 400 rpm

V_S =8.35 X 10^{-1} m/sec **ρ=2.4380 x 1000 kg/m³**

m_1	m_2	Δm	T	F_f	μ	R.Dx10^{-3}	W_r×10^{-6}	W_v×10^{-12}	W_s×10^{-13}
(gm)	(gm)	(gm)	(sec)	kgf		m	(N/m)	(m³/sec)	(m³/N-m)
6.580	6.445	0.135	3600	0.240	0.120	3.027	0.439	15.434	9.242
6.580	6.365	0.215	7200	0.230	0.115	6.054	0.349	12.274	7.350
6.580	6.295	0.285	10800	0.210	0.105	9.081	0.308	10.841	6.492
6.580	6.225	0.355	14400	0.220	0.110	12.108	0.288	10.125	6.063
6.580	6.155	0.425	18000	0.190	0.095	15.135	0.276	9.695	5.805
6.580	6.085	0.495	21600	0.210	0.105	18.162	0.268	9.408	5.634

Table 15: Wear Rate values for Pure Aluminium with 2% Red mud of 42 nm particle size at 600 rpm

V_S =1.244 m/sec **ρ=2.4380 x 1000 kg/m³**

m_1	m_2	Δm	T	F_f	μ	R.Dx10^{-3}	W_r×10^{-6}	W_v×10^{-12}	W_s×10^{-13}
(gm)	(gm)	(gm)	(sec)	kgf		m	(N/m)	(m³/sec)	(m³/N-m)
6.540	6.355	0.185	3600	0.260	0.130	4.399	0.412	21.050	8.460
6.540	6.255	0.285	7200	0.260	0.130	8.798	0.318	16.222	6.520
6.540	6.165	0.375	10800	0.250	0.125	13.197	0.279	14.233	5.720
6.540	6.075	0.465	14400	0.230	0.115	17.596	0.259	13.238	5.321
6.540	5.985	0.555	18000	0.220	0.110	21.995	0.247	12.641	5.081
6.540	5.895	0.645	21600	0.230	0.115	26.394	0.240	12.243	4.921

The Wear rate values for pure aluminium with 4% red mud of 100 µm particle size at 200rpm,400 rpm and 600 rpm is shown in tables 16, 17 and 18 respectively.

Table 16: Wear Rate values for Pure Aluminium with 4% Red mud of 100 µm particle size at 200 rpm

V_S =3.93 X 10^{-1} m/sec **ρ=2.44 x 1000 kg/m³**

m_1	m_2	Δm	T	F_f	µ	R.Dx10^{-3}	W_r×10^{-6}	W_v×10^{-12}	W_s×10^{-13}
(gm)	(gm)	(gm)	(sec)	kgf		m	(N/m)	(m³/sec)	(m³/N-m)
7.100	7.032	0.068	3600	0.270	0.135	1.515	0.443	7.789	9.909
7.100	6.992	0.108	7200	0.260	0.130	3.030	0.351	6.171	7.851
7.100	6.962	0.138	10800	0.250	0.125	4.545	0.299	5.253	6.683
7.100	6.932	0.168	14400	0.270	0.135	6.060	0.273	4.793	6.098
7.100	6.902	0.198	18000	0.240	0.120	7.575	0.257	4.518	5.748
7.100	6.872	0.228	21600	0.250	0.125	9.090	0.247	4.334	5.514

Table 17: Wear Rate values for Pure Aluminium with 4% Red mud of 100 µm particle size at 400 rpm

V_S =8.35 X 10^{-1} m/sec **ρ=2.44 x 1000 kg/m³**

m_1	m_2	Δm	T	F_f	µ	R.Dx10^{-3}	W_r×10^{-6}	W_v×10^{-12}	W_s×10^{-13}
(gm)	(gm)	(gm)	(sec)	kgf		m	(N/m)	(m³/sec)	(m³/N-m)
7.120	6.993	0.127	3600	0.290	0.145	3.010	0.415	14.496	8.680
7.120	6.932	0.188	7200	0.280	0.140	6.020	0.307	10.720	6.419
7.120	6.872	0.248	10800	0.260	0.130	9.030	0.270	9.424	5.643
7.120	6.812	0.308	14400	0.240	0.120	12.040	0.251	8.775	5.255
7.120	6.752	0.368	18000	0.250	0.125	15.050	0.240	8.386	5.022
7.120	6.692	0.428	21600	0.240	0.120	18.060	0.233	8.127	4.867

Table 18: Wear Rate values for Pure Aluminium with 4% Red mud of 100 µm particle size at 600 rpm

V_S =1.244 m/sec **ρ=2.44 x 1000 kg/m³**

m_1	m_2	Δm	T	F_f	µ	R.Dx10^{-3}	W_r×10^{-6}	W_v×10^{-12}	W_s×10^{-13}
(gm)	(gm)	(gm)	(sec)	kgf		m	(N/m)	(m³/sec)	(m³/N-m)
6.830	6.667	0.163	3600	0.300	0.150	4.265	0.374	18.511	7.440
6.830	6.577	0.253	7200	0.290	0.145	8.530	0.291	14.378	5.779
6.830	6.497	0.333	10800	0.300	0.150	12.795	0.255	12.621	5.073
6.830	6.417	0.413	14400	0.280	0.140	17.060	0.237	11.743	4.720
6.830	6.337	0.493	18000	0.270	0.135	21.325	0.227	11.216	4.508
6.830	6.257	0.573	21600	0.290	0.145	25.590	0.220	10.864	4.367

The Wear rate values for pure aluminium with 4% red mud of 150 µm particle size at 200rpm,400 rpm and 600 rpm is shown in tables 19, 20 and 21 respectively.

Table 19: Wear Rate values for Pure Aluminium with 4% Red mud of 150 µm particle size at 200 rpm

V_S =3.93 X 10^{-1} m/sec **ρ=2.44 x 1000 kg/m³**

m_1	m_2	Δm	T	F_f	µ	R.Dx10^{-3}	W_r×10^{-6}	W_v×10^{-12}	W_s×10^{-13}
(gm)	(gm)	(gm)	(sec)	kgf		m	(N/m)	(m³/sec)	(m³/N-m)
7.200	7.112	0.088	3600	0.330	0.165	1.516	0.571	10.046	12.781
7.200	7.071	0.129	7200	0.320	0.160	3.032	0.418	7.357	9.359
7.200	7.031	0.169	10800	0.340	0.170	4.548	0.365	6.422	8.171
7.200	6.991	0.209	14400	0.310	0.155	6.064	0.338	5.955	7.577
7.200	6.951	0.249	18000	0.320	0.160	7.580	0.323	5.675	7.220
7.200	6.911	0.289	21600	0.300	0.150	9.096	0.312	5.488	6.982

Table 20: Wear Rate values for Pure Aluminium with 4% Red mud of 150 µm particle size at 400 rpm

V_S =8.35 X 10^{-1} m/sec **ρ=2.44 x 1000 kg/m³**

m_1	m_2	Δm	T	F_f	µ	R.Dx10^{-3}	W_r×10^{-6}	W_v×10^{-12}	W_s×10^{-13}
(gm)	(gm)	(gm)	(sec)	kgf		m	(N/m)	(m³/sec)	(m³/N-m)
6.980	6.816	0.164	3600	0.350	0.175	2.990	0.537	18.633	11.158
6.980	6.726	0.254	7200	0.360	0.180	5.980	0.416	14.439	8.646
6.980	6.646	0.334	10800	0.330	0.165	8.970	0.365	12.662	7.582
6.980	6.566	0.414	14400	0.340	0.170	11.960	0.339	11.773	7.050
6.980	6.486	0.494	18000	0.330	0.165	14.950	0.324	11.240	6.731
6.980	6.406	0.574	21600	0.320	0.160	17.940	0.314	10.885	6.518

Table 21: Wear Rate values for Pure Aluminium with 4% Red mud of 150 µm particle size at 600 rpm

V_S =1.244 m/sec **ρ=2.44 x 1000 kg/m³**

m_1	m_2	Δm	T	F_f	µ	R.Dx10^{-3}	W_r×10^{-6}	W_v×10^{-12}	W_s×10^{-13}
(gm)	(gm)	(gm)	(sec)	kgf		m	(N/m)	(m³/sec)	(m³/N-m)
6.850	6.651	0.199	3600	0.370	0.185	4.496	0.435	22.696	9.122
6.850	6.531	0.319	7200	0.320	0.160	8.992	0.348	18.179	7.307
6.850	6.421	0.429	10800	0.360	0.180	13.488	0.312	16.293	6.549
6.850	6.311	0.539	14400	0.350	0.175	17.984	0.294	15.351	6.170
6.850	6.191	0.659	18000	0.340	0.170	22.480	0.288	15.013	6.034
6.850	6.081	0.769	21600	0.360	0.180	26.976	0.280	14.598	5.867

The Wear rate values for pure aluminium with 4% red mud of 200 µm particle size at 200rpm,400 rpm and 600 rpm is shown in tables 22, 23 and 24 respectively.

Table 22: Wear Rate values for Pure Aluminium with 4% Red mud of 200 µm particle size at 200 rpm

V_S =3.93 X 10^{-1} m/sec **ρ=2.44 x 1000 kg/m³**

m_1	m_2	Δm	T	F_f	µ	R.Dx10^{-3}	$W_r \times 10^{-6}$	$W_v \times 10^{-12}$	$W_s \times 10^{-13}$
(gm)	(gm)	(gm)	(sec)	kgf		m	(N/m)	(m³/sec)	(m³/N-m)
6.760	6.654	0.106	3600	0.380	0.190	1.507	0.691	12.088	15.379
6.760	6.594	0.166	7200	0.370	0.185	3.015	0.541	9.459	12.035
6.760	6.544	0.216	10800	0.350	0.175	4.522	0.469	8.204	10.437
6.760	6.494	0.266	14400	0.360	0.180	6.030	0.433	7.576	9.638
6.760	6.444	0.316	18000	0.330	0.165	7.537	0.412	7.199	9.159
6.760	6.394	0.366	21600	0.350	0.175	9.044	0.397	6.948	8.839

Table 23: Wear Rate values for Pure Aluminium with 4% Red mud of 200 µm particle size at 400 rpm

V_s =8.35 X 10^{-1} m/sec **ρ=2.44 x 1000 kg/m³**

m_1	m_2	Δm	T	F_f	µ	R.Dx10^{-3}	$W_r \times 10^{-6}$	$W_v \times 10^{-12}$	$W_s \times 10^{-13}$
(gm)	(gm)	(gm)	(sec)	kgf		m	(N/m)	(m³/sec)	(m³/N-m)
6.860	6.661	0.199	3600	0.400	0.200	2.990	0.653	22.658	13.568
6.860	6.551	0.309	7200	0.390	0.195	5.980	0.507	17.590	10.533
6.860	6.451	0.409	10800	0.370	0.185	8.970	0.447	15.522	9.294
6.860	6.351	0.509	14400	0.360	0.180	11.960	0.418	14.487	8.675
6.860	6.251	0.609	18000	0.320	0.160	14.950	0.400	13.867	8.303
6.860	6.151	0.709	21600	0.350	0.175	17.940	0.388	13.453	8.056

Table 24: Wear Rate values for Pure Aluminium with 4% Red mud of 200 µm particle size at 600 rpm

V_s =1.244 m/sec **ρ=2.44 x 1000 kg/m³**

m_1	m_2	Δm	T	F_f	µ	R.Dx10^{-3}	$W_r \times 10^{-6}$	$W_v \times 10^{-12}$	$W_s \times 10^{-13}$
(gm)	(gm)	(gm)	(sec)	kgf		m	(N/m)	(m³/sec)	(m³/N-m)
6.850	6.557	0.293	3600	0.430	0.215	4.589	0.627	33.391	13.421
6.850	6.397	0.453	7200	0.410	0.205	9.178	0.485	25.803	10.371
6.850	6.247	0.603	10800	0.390	0.195	13.767	0.430	22.894	9.202
6.850	6.097	0.753	14400	0.420	0.210	18.356	0.403	21.440	8.617
6.850	5.947	0.903	18000	0.370	0.185	22.945	0.386	20.567	8.266
6.850	5.797	1.053	21600	0.390	0.195	27.534	0.375	19.985	8.033

The Wear rate values for pure aluminium with 4% red mud of 42 nm particle size at 200rpm, 400 rpm and 600 rpm is shown in tables 25, 26 and 27 respectively.

Table 25: Wear Rate values for Pure Aluminium with 4% Red mud of 42 nm particle size at 200 rpm

V_S =3.93 X 10^{-1} m/sec **ρ=2.44 x 1000 kg/m³**

m_1	m_2	Δm	T	F_f	μ	R.Dx10^{-3}	W_r×10^{-6}	W_v×10^{-12}	W_s×10^{-13}
(gm)	(gm)	(gm)	(sec)	kgf		m	(N/m)	(m³/sec)	(m³/N-m)
6.530	6.487	0.043	3600	0.190	0.095	1.509	0.280	4.903	6.238
6.530	6.457	0.073	7200	0.180	0.090	3.018	0.238	4.159	5.292
6.530	6.427	0.103	10800	0.190	0.095	4.527	0.223	3.911	4.976
6.530	6.397	0.133	14400	0.170	0.085	6.036	0.216	3.787	4.818
6.530	6.377	0.153	18000	0.150	0.075	7.545	0.199	3.485	4.434
6.530	6.357	0.173	21600	0.170	0.085	9.054	0.188	3.284	4.178

Table 26: Wear Rate values for Pure Aluminium with 4% Red mud of 42 nm particle size at 400 rpm

V_s =8.35 X 10^{-1} m/sec **ρ=2.44 x 1000 kg/m³**

m_1	m_2	Δm	T	F_f	μ	R.Dx10^{-3}	W_r×10^{-6}	W_v×10^{-12}	W_s×10^{-13}
(gm)	(gm)	(gm)	(sec)	kgf		m	(N/m)	(m³/sec)	(m³/N-m)
6.870	6.790	0.080	3600	0.210	0.105	3.020	0.260	9.112	5.456
6.870	6.740	0.130	7200	0.200	0.100	6.040	0.211	7.402	4.432
6.870	6.690	0.180	10800	0.180	0.090	9.060	0.195	6.832	4.091
6.870	6.650	0.220	14400	0.170	0.085	12.080	0.179	6.263	3.750
6.870	6.600	0.270	18000	0.220	0.110	15.100	0.175	6.148	3.682
6.870	6.560	0.310	21600	0.190	0.095	18.120	0.168	5.883	3.523

Table 27: Wear Rate values for Pure Aluminium with 4% Red mud of 42 nm particle size at 600 rpm

V_S =1.244 m/sec **ρ=2.44 x 1000 kg/m³**

m_1	m_2	Δm	T	F_f	μ	R.Dx10^{-3}	W_r×10^{-6}	W_v×10^{-12}	W_s×10^{-13}
(gm)	(gm)	(gm)	(sec)	kgf		m	(N/m)	(m³/sec)	(m³/N-m)
6.720	6.603	0.117	3600	0.220	0.110	4.518	0.254	13.317	5.353
6.720	6.533	0.187	7200	0.200	0.100	9.036	0.203	10.643	4.278
6.720	6.473	0.247	10800	0.170	0.085	13.554	0.179	9.372	3.767
6.720	6.413	0.307	14400	0.190	0.095	18.072	0.167	8.737	3.512
6.720	6.353	0.367	18000	0.180	0.090	22.590	0.159	8.356	3.358
6.720	6.303	0.417	21600	0.190	0.095	27.108	0.151	7.912	3.180

The Wear rate values for pure aluminium with 6% red mud of 100 µm particle size at 200rpm,400 rpm and 600 rpm is shown in tables 28, 29 and 30 respectively.

Table 28: Wear Rate values for Pure Aluminium with 6% Red mud of 100 µm particle size at 200 rpm

V_s =3.93 X 10^{-1} m/sec **ρ=2.45 x 1000 kg/m³**

m_1	m_2	Δm	T	F_f	µ	R.Dx10^{-3}	W_r×10^{-6}	W_v×10^{-12}	W_s×10^{-13}
(gm)	(gm)	(gm)	(sec)	kgf		m	(N/m)	(m³/sec)	(m³/N-m)
7.100	7.050	0.050	3600	0.250	0.125	1.509	0.328	5.720	7.278
7.100	7.020	0.080	7200	0.240	0.120	3.018	0.262	4.561	5.803
7.100	6.990	0.110	10800	0.260	0.130	4.527	0.239	4.174	5.311
7.100	6.960	0.140	14400	0.230	0.115	6.036	0.228	3.981	5.065
7.100	6.940	0.160	18000	0.250	0.125	7.545	0.209	3.638	4.629
7.100	6.910	0.190	21600	0.220	0.110	9.054	0.206	3.599	4.579

Table 29: Wear Rate values for Pure Aluminium with 6% Red mud of 100 µm particle size at 400 rpm

V_s =8.35 X 10^{-1} m/sec **ρ=2.45 x 1000 kg/m³**

m_1	m_2	Δm	T	F_f	µ	R.Dx10^{-3}	W_r×10^{-6}	W_v×10^{-12}	W_s×10^{-13}
(gm)	(gm)	(gm)	(sec)	kgf		m	(N/m)	(m³/sec)	(m³/N-m)
7.120	7.032	0.088	3600	0.260	0.130	2.967	0.291	9.979	5.975
7.120	6.982	0.138	7200	0.240	0.120	5.934	0.228	7.824	4.685
7.120	6.942	0.178	10800	0.230	0.115	8.901	0.196	6.728	4.028
7.120	6.902	0.218	14400	0.260	0.130	11.868	0.180	6.179	3.700
7.120	6.862	0.258	18000	0.230	0.115	14.835	0.171	5.851	3.503
7.120	6.822	0.298	21600	0.250	0.125	17.802	0.164	5.631	3.372

Table 30: Wear Rate values for Pure Aluminium with 6% Red mud of 100 µm particle size at 600 rpm

V_s =1.244 m/sec **ρ=2.45 x 1000 kg/m³**

m_1	m_2	Δm	T	F_f	µ	R.Dx10^{-3}	W_r×10^{-6}	W_v×10^{-12}	W_s×10^{-13}
(gm)	(gm)	(gm)	(sec)	kgf		m	(N/m)	(m³/sec)	(m³/N-m)
6.830	6.704	0.126	3600	0.280	0.140	4.460	0.278	14.330	5.760
6.830	6.634	0.196	7200	0.270	0.135	8.920	0.216	11.133	4.475
6.830	6.574	0.256	10800	0.280	0.140	13.380	0.188	9.690	3.895
6.830	6.514	0.316	14400	0.250	0.125	17.840	0.174	8.968	3.604
6.830	6.454	0.376	18000	0.260	0.130	22.300	0.166	8.535	3.430
6.830	6.394	0.436	21600	0.270	0.135	26.760	0.160	8.246	3.314

The Wear rate values for pure aluminium with 6% red mud of 150 µm particle size at 200rpm,400 rpm and 600 rpm is shown in tables 31, 32 and 33 respectively.

Table 31: Wear Rate values for Pure Aluminium with 6% Red mud of 150 µm particle size at 200 rpm

V_S =3.93 X 10^{-1} m/sec **ρ=2.45 x 1000 kg/m³**

m_1	m_2	Δm	T	F_f	µ	R.Dx10^{-3}	W_r×10^{-6}	W_v×10^{-12}	W_s×10^{-13}
(gm)	(gm)	(gm)	(sec)	kgf		m	(N/m)	(m³/sec)	(m³/N-m)
7.200	7.128	0.072	3600	0.300	0.150	1.498	0.472	8.172	10.397
7.200	7.088	0.112	7200	0.290	0.145	2.996	0.367	6.353	8.083
7.200	7.058	0.142	10800	0.310	0.155	4.494	0.310	5.369	6.831
7.200	7.028	0.172	14400	0.320	0.160	5.992	0.282	4.877	6.205
7.200	6.998	0.202	18000	0.280	0.140	7.490	0.265	4.582	5.830
7.200	6.968	0.232	21600	0.320	0.160	8.988	0.253	4.385	5.579

Table 32: Wear Rate values for Pure Aluminium with 6% Red mud of 150 µm particle size at 400 rpm

V_s =8.35 X 10^{-1} m/sec **ρ=2.45 x 1000 kg/m³**

m_1	m_2	Δm	T	F_f	µ	R.Dx10^{-3}	W_r×10^{-6}	W_v×10^{-12}	W_s×10^{-13}
(gm)	(gm)	(gm)	(sec)	kgf		m	(N/m)	(m³/sec)	(m³/N-m)
6.980	6.843	0.137	3600	0.320	0.160	3.010	0.447	15.550	9.312
6.980	6.773	0.207	7200	0.310	0.155	6.020	0.338	11.743	7.032
6.980	6.713	0.267	10800	0.300	0.150	9.030	0.290	10.096	6.046
6.980	6.653	0.327	14400	0.280	0.140	12.040	0.267	9.273	5.553
6.980	6.583	0.397	18000	0.310	0.155	15.050	0.259	9.006	5.393
6.980	6.523	0.457	21600	0.310	0.155	18.060	0.248	8.639	5.173

Table 33: Wear Rate values for Pure Aluminium with 6% Red mud of 150 µm particle size at 600 rpm

V_s =1.244 m/sec **ρ=2.45 x 1000 kg/m³**

m_1	m_2	Δm	T	F_f	µ	R.Dx10^{-3}	W_r×10^{-6}	W_v×10^{-12}	W_s×10^{-13}
(gm)	(gm)	(gm)	(sec)	kgf		m	(N/m)	(m³/sec)	(m³/N-m)
6.850	6.688	0.162	3600	0.330	0.165	4.590	0.346	18.355	7.377
6.850	6.598	0.252	7200	0.340	0.170	9.180	0.269	14.279	5.739
6.850	6.518	0.332	10800	0.320	0.160	13.770	0.236	12.543	5.041
6.850	6.438	0.412	14400	0.330	0.165	18.360	0.220	11.675	4.692
6.850	6.358	0.492	18000	0.290	0.145	22.950	0.210	11.154	4.483
6.850	6.278	0.572	21600	0.280	0.140	27.540	0.204	10.807	4.344

The Wear rate values for pure aluminium with 6% red mud of 200 µm particle size at 200rpm,400 rpm and 600 rpm is shown in tables 34, 35 and 36 respectively.

Table 34: Wear Rate values for Pure Aluminium with 6% Red mud of 200 µm particle size at 200 rpm

V_S =3.93 X 10^{-1} m/sec **ρ=2.45 x 1000 kg/m³**

m_1	m_2	Δm	T	F_f	µ	R.Dx10^{-3}	$W_r \times 10^{-6}$	$W_v \times 10^{-12}$	$W_s \times 10^{-13}$
(gm)	(gm)	(gm)	(sec)	kgf		m	(N/m)	(m³/sec)	(m³/N-m)
6.760	6.674	0.086	3600	0.350	0.175	1.485	0.571	9.800	12.468
6.760	6.624	0.136	7200	0.340	0.170	2.970	0.451	7.734	9.840
6.760	6.574	0.186	10800	0.360	0.180	4.455	0.411	7.046	8.964
6.760	6.534	0.226	14400	0.340	0.170	5.940	0.374	6.418	8.166
6.760	6.484	0.276	18000	0.330	0.165	7.425	0.365	6.268	7.975
6.760	6.444	0.316	21600	0.320	0.160	8.910	0.348	5.980	7.608

Table 35: Wear Rate values for Pure Aluminium with 6% Red mud of 200 µm particle size at 400 rpm

V_s =8.35 X 10^{-1} m/sec **ρ=2.45 x 1000 kg/m³**

m_1	m_2	Δm	T	F_f	µ	R.Dx10^{-3}	$W_r \times 10^{-6}$	$W_v \times 10^{-12}$	$W_s \times 10^{-13}$
(gm)	(gm)	(gm)	(sec)	kgf		m	(N/m)	(m³/sec)	(m³/N-m)
6.860	6.683	0.177	3600	0.370	0.185	3.013	0.575	20.023	11.990
6.860	6.583	0.277	7200	0.380	0.190	6.026	0.450	15.680	9.389
6.860	6.493	0.367	10800	0.360	0.180	9.039	0.398	13.855	8.296
6.860	6.403	0.457	14400	0.350	0.175	12.052	0.372	12.942	7.750
6.860	6.313	0.547	18000	0.350	0.175	15.065	0.356	12.395	7.422
6.860	6.223	0.637	21600	0.340	0.170	18.078	0.345	12.030	7.203

Table 36: Wear Rate values for Pure Aluminium with 6% Red mud of 200 µm particle size at 600 rpm

V_s =1.244 m/sec **ρ=2.45 x 1000 kg/m³**

m_1	m_2	Δm	T	F_f	µ	R.Dx10^{-3}	$W_r \times 10^{-6}$	$W_v \times 10^{-12}$	$W_s \times 10^{-13}$
(gm)	(gm)	(gm)	(sec)	kgf		m	(N/m)	(m³/sec)	(m³/N-m)
6.850	6.614	0.236	3600	0.390	0.195	4.510	0.513	26.740	10.747
6.850	6.484	0.366	7200	0.380	0.190	9.020	0.398	20.739	8.336
6.850	6.364	0.486	10800	0.370	0.185	13.530	0.352	18.361	7.380
6.850	6.244	0.606	14400	0.350	0.175	18.040	0.329	17.172	6.902
6.850	6.124	0.726	18000	0.350	0.175	22.550	0.316	16.459	6.615
6.850	6.004	0.846	21600	0.360	0.180	27.060	0.307	15.983	6.424

The Wear rate values for pure aluminium with 6% red mud of 42 nm particle size at 200rpm, 400 rpm and 600 rpm is shown in tables 37, 38 and 39 respectively.

Table 37: Wear Rate values for Pure Aluminium with 6% Red mud of 42 nm particle size at 200 rpm

V_S =3.93 X 10^{-1} m/sec **ρ=2.45 x 1000 kg/m³**

m_1	m_2	Δm	T	F_f	μ	R.Dx10^{-3}	W_r×10^{-6}	W_v×10^{-12}	W_s×10^{-13}
(gm)	(gm)	(gm)	(sec)	kgf		m	(N/m)	(m³/sec)	(m³/N-m)
6.530	6.494	0.036	3600	0.118	0.059	1.353	0.262	4.097	5.212
6.530	6.474	0.056	7200	0.112	0.056	2.706	0.204	3.182	4.049
6.530	6.454	0.076	10800	0.110	0.055	4.059	0.184	2.877	3.661
6.530	6.444	0.086	14400	0.119	0.060	5.412	0.156	2.441	3.106
6.530	6.434	0.096	18000	0.114	0.057	6.765	0.139	2.180	2.773
6.530	6.424	0.106	21600	0.120	0.060	8.118	0.128	2.006	2.552

Table 38: Wear Rate values for Pure Aluminium with 6% Red mud of 42 nm particle size at 400 rpm

V_s =8.35 X 10^{-1} m/sec **ρ=2.45 x 1000 kg/m³**

m_1	m_2	Δm	T	F_f	μ	R.Dx10^{-3}	W_r×10^{-6}	W_v×10^{-12}	W_s×10^{-13}
(gm)	(gm)	(gm)	(sec)	kgf		m	(N/m)	(m³/sec)	(m³/N-m)
6.870	6.799	0.071	3600	0.152	0.076	2.973	0.235	8.075	4.835
6.870	6.759	0.111	7200	0.152	0.076	5.946	0.183	6.305	3.775
6.870	6.729	0.141	10800	0.149	0.075	8.919	0.155	5.337	3.196
6.870	6.689	0.181	14400	0.131	0.066	11.892	0.149	5.137	3.076
6.870	6.659	0.211	18000	0.143	0.072	14.865	0.139	4.790	2.868
6.870	6.629	0.241	21600	0.132	0.066	17.838	0.133	4.558	2.729

Table 39: Wear Rate values for Pure Aluminium with 6% Red mud of 42 nm particle size at 600 rpm

V_s =1.244 m/sec **ρ=2.45 x 1000 kg/m³**

m_1	m_2	Δm	T	F_f	μ	R.Dx10^{-3}	W_r×10^{-6}	W_v×10^{-12}	W_s×10^{-13}
(gm)	(gm)	(gm)	(sec)	kgf		m	(N/m)	(m³/sec)	(m³/N-m)
6.720	6.607	0.113	3600	0.161	0.081	4.820	0.229	12.757	5.127
6.720	6.547	0.173	7200	0.168	0.084	9.640	0.176	9.780	3.931
6.720	6.487	0.233	10800	0.167	0.084	14.460	0.158	8.787	3.532
6.720	6.437	0.283	14400	0.159	0.080	19.280	0.144	8.008	3.219
6.720	6.377	0.343	18000	0.162	0.081	24.100	0.139	7.767	3.122
6.720	6.317	0.403	21600	0.158	0.079	28.920	0.137	7.606	3.057

iii) Wear rate tables for pure aluminium with red mud at normal condition at 30 N load

The Wear rate values for pure aluminium of 45 μm particle size at 200rpm, 400 rpm and 600 rpm is shown in tables 1, 2 and 3 respectively.

Table 1: Wear Rate values for Pure Aluminium at 200 rpm

V_S =3.93 X 10^{-1} m/sec **ρ=2.58 x 1000 kg/m³**

m_1	m_2	Δm	T	F_f	μ	R.Dx10^{-3}	W_r×10^{-6}	W_v×10^{-12}	W_s×10^{-13}
(gm)	(gm)	(gm)	(sec)	kgf		m	(N/m)	(m³/sec)	(m³/N-m)
6.450	6.258	0.192	3600	0.290	0.097	1.418	1.331	20.714	17.569
6.450	6.158	0.292	7200	0.300	0.100	2.836	1.011	15.740	13.351
6.450	6.068	0.382	10800	0.280	0.093	4.254	0.882	13.723	11.640
6.450	5.978	0.472	14400	0.270	0.090	5.672	0.817	12.715	10.785
6.450	5.888	0.562	18000	0.270	0.090	7.090	0.778	12.110	10.271
6.450	5.788	0.662	21600	0.250	0.083	8.508	0.764	11.886	10.082

Table 2: Wear Rate values for Pure Aluminium at 400 rpm

V_s =8.35 X 10^{-1} m/sec **ρ=2.58 x 1000 kg/m³**

m_1	m_2	Δm	T	F_f	μ	R.Dx10^{-3}	W_r×10^{-6}	W_v×10^{-12}	W_s×10^{-13}
(gm)	(gm)	(gm)	(sec)	kgf		m	(N/m)	(m³/sec)	(m³/N-m)
6.520	6.115	0.405	3600	0.330	0.110	3.006	1.322	43.614	17.411
6.520	5.905	0.615	7200	0.340	0.113	6.012	1.004	33.112	13.218
6.520	5.705	0.815	10800	0.330	0.110	9.018	0.887	29.252	11.678
6.520	5.505	1.015	14400	0.320	0.107	12.024	0.828	27.323	10.907
6.520	5.315	1.205	18000	0.300	0.100	15.030	0.787	25.949	10.359
6.520	5.115	1.405	21600	0.310	0.103	18.036	0.764	25.213	10.065

Table 3: Wear Rate values for Pure Aluminium at 600 rpm

V_s =1.244 m/sec **ρ=2.58 x 1000 kg/m³**

m_1	m_2	Δm	T	F_f	μ	R.Dx10^{-3}	W_r×10^{-6}	W_v×10^{-12}	W_s×10^{-13}
(gm)	(gm)	(gm)	(sec)	kgf		m	(N/m)	(m³/sec)	(m³/N-m)
6.540	5.990	0.550	3600	0.350	0.117	4.480	1.205	59.248	15.876
6.540	5.740	0.800	7200	0.340	0.113	8.960	0.876	43.082	11.544
6.540	5.490	1.050	10800	0.330	0.110	13.440	0.767	37.694	10.100
6.540	5.240	1.300	14400	0.310	0.103	17.920	0.712	34.999	9.378
6.540	4.990	1.550	18000	0.330	0.110	22.400	0.679	33.383	8.945
6.540	4.740	1.800	21600	0.340	0.113	26.880	0.657	32.305	8.656

The Wear rate values for pure aluminium with 2% red mud of 100 µm particle size at 200rpm,400 rpm and 600 rpm is shown in tables 4, 5 and 6respectively.

Table 4: Wear Rate values for Pure Aluminium with 2% Red mud of 100 µm particle size at 200 rpm

V_S =3.93 X 10^{-1} m/sec **ρ=2.4380 x 1000 kg/m^3**

m_1	m_2	Δm	T	F_f	µ	R.Dx10^{-3}	$W_r \times 10^{-6}$	$W_v \times 10^{-12}$	$W_s \times 10^{-13}$
(gm)	(gm)	(gm)	(sec)	kgf		m	(N/m)	(m^3/sec)	(m^3/N-m)
6.450	6.295	0.155	3600	0.290	0.097	1.418	1.069	17.606	14.933
6.450	6.235	0.215	7200	0.280	0.093	2.836	0.742	12.221	10.365
6.450	6.175	0.275	10800	0.260	0.087	4.254	0.633	10.426	8.843
6.450	6.125	0.325	14400	0.280	0.093	5.672	0.561	9.244	7.840
6.450	6.065	0.385	18000	0.250	0.083	7.090	0.532	8.762	7.432
6.450	6.005	0.445	21600	0.260	0.087	8.508	0.513	8.441	7.160

Table 5: Wear Rate values for Pure Aluminium with 2% Red mud of 100 µm particle size at 400 rpm

V_s =8.35 X 10^{-1} m/sec **ρ=2.4380 x 1000 kg/m^3**

m_1	m_2	Δm	T	F_f	µ	R.Dx10^{-3}	$W_r \times 10^{-6}$	$W_v \times 10^{-12}$	$W_s \times 10^{-13}$
(gm)	(gm)	(gm)	(sec)	kgf		m	(N/m)	(m^3/sec)	(m^3/N-m)
6.520	6.212	0.308	3600	0.310	0.103	3.006	1.005	35.087	14.007
6.520	6.092	0.428	7200	0.290	0.097	6.012	0.698	24.380	9.732
6.520	5.982	0.538	10800	0.300	0.100	9.018	0.585	20.431	8.156
6.520	5.872	0.648	14400	0.310	0.103	12.024	0.529	18.456	7.368
6.520	5.752	0.768	18000	0.280	0.093	15.030	0.501	17.500	6.986
6.520	5.652	0.868	21600	0.300	0.100	18.036	0.472	16.482	6.580

Table 6: Wear Rate values for Pure Aluminium with 2% Red mud of 100 µm particle size at 600 rpm

V_s =1.244 m/sec **ρ=2.4380 x 1000 kg/m^3**

m_1	m_2	Δm	T	F_f	µ	R.Dx10^{-3}	$W_r \times 10^{-6}$	$W_v \times 10^{-12}$	$W_s \times 10^{-13}$
(gm)	(gm)	(gm)	(sec)	kgf		m	(N/m)	(m^3/sec)	(m^3/N-m)
6.540	6.123	0.417	3600	0.320	0.107	4.480	0.914	47.557	12.743
6.540	5.963	0.577	7200	0.310	0.103	8.960	0.632	32.894	8.814
6.540	5.813	0.727	10800	0.300	0.100	13.440	0.531	27.626	7.402
6.540	5.653	0.887	14400	0.280	0.093	17.920	0.486	25.277	6.773
6.540	5.493	1.047	18000	0.300	0.100	22.400	0.459	23.868	6.395
6.540	5.343	1.197	21600	0.290	0.097	26.880	0.437	22.738	6.093

The Wear rate values for pure aluminium with 2% red mud of 150 µm particle size at 200rpm,400 rpm and 600 rpm is shown in tables 7, 8 and 9 respectively.

Table 7: Wear Rate values for Pure Aluminium with 2% Red mud of 150 µm particle size at 200 rpm

V_S =3.93 X 10^{-1} m/sec **ρ=2.4380 x 1000 kg/m^3**

m_1	m_2	Δm	T	F_f	µ	R.Dx10^{-3}	$W_r \times 10^{-6}$	$W_v \times 10^{-12}$	$W_s \times 10^{-13}$
(gm)	(gm)	(gm)	(sec)	kgf		m	(N/m)	(m^3/sec)	(m^3/N-m)
6.520	6.312	0.208	3600	0.330	0.110	1.497	1.362	23.681	20.085
6.520	6.232	0.288	7200	0.320	0.107	2.994	0.943	16.398	13.908
6.520	6.162	0.358	10800	0.290	0.097	4.491	0.782	13.590	11.527
6.520	6.092	0.428	14400	0.280	0.093	5.988	0.701	12.187	10.336
6.520	6.012	0.508	18000	0.300	0.100	7.485	0.666	11.572	9.815
6.520	5.942	0.578	21600	0.290	0.097	8.982	0.631	10.973	9.307

Table 8: Wear Rate values for Pure Aluminium with 2% Red mud of 150 µm particle size at 400 rpm

V_s =8.35 X 10^{-1} m/sec **ρ=2.4380 x 1000 kg/m^3**

m_1	m_2	Δm	T	F_f	µ	R.Dx10^{-3}	$W_r \times 10^{-6}$	$W_v \times 10^{-12}$	$W_s \times 10^{-13}$
(gm)	(gm)	(gm)	(sec)	kgf		m	(N/m)	(m^3/sec)	(m^3/N-m)
6.490	6.086	0.404	3600	0.320	0.107	3.012	1.315	46.002	18.364
6.490	5.946	0.544	7200	0.310	0.103	6.024	0.885	30.977	12.366
6.490	5.806	0.684	10800	0.290	0.097	9.036	0.742	25.968	10.366
6.490	5.666	0.824	14400	0.270	0.090	12.049	0.671	23.464	9.367
6.490	5.526	0.964	18000	0.310	0.103	15.061	0.628	21.961	8.767
6.490	5.396	1.094	21600	0.280	0.093	18.073	0.594	20.770	8.291

Table 9: Wear Rate values for Pure Aluminium with 2% Red mud of 150 µm particle size at 600 rpm

V_s =1.244 m/sec **ρ=2.4380 x 1000 kg/m^3**

vm_1	m_2	Δm	T	F_f	µ	R.Dx10^{-3}	$W_r \times 10^{-6}$	$W_v \times 10^{-12}$	$W_s \times 10^{-13}$
(gm)	(gm)	(gm)	(sec)	kgf		m	(N/m)	(m^3/sec)	(m^3/N-m)
6.530	5.943	0.587	3600	0.550	0.183	4.578	1.258	66.888	17.923
6.530	5.733	0.797	7200	0.540	0.180	9.156	0.854	45.408	12.167
6.530	5.533	0.997	10800	0.520	0.173	13.734	0.712	37.868	10.147
6.530	5.333	1.197	14400	0.490	0.163	18.312	0.641	34.097	9.137
6.530	5.133	1.397	18000	0.470	0.157	22.890	0.599	31.835	8.530
6.530	4.943	1.587	21600	0.500	0.167	27.468	0.567	30.138	8.075

The Wear rate values for pure aluminium with 2% red mud of 200 μm particle size at 200rpm, 400 rpm and 600 rpm is shown in tables 10, 11 and 12 respectively.

Table 10: Wear Rate values for Pure Aluminium with 2% Red mud of 200 μm particle size at 200 rpm

V_S =3.93 X 10^{-1} m/sec **ρ=2.4380 x 1000 kg/m³**

m_1	m_2	Δm	T	F_f	μ	R.Dx10^{-3}	W_r×10^{-6}	W_v×10^{-12}	W_s×10^{-13}
(gm)	(gm)	(gm)	(sec)	kgf		m	(N/m)	(m³/sec)	(m³/N-m)
6.660	6.426	0.234	3600	0.390	0.130	1.517	1.512	26.640	22.595
6.660	6.336	0.324	7200	0.380	0.127	3.034	1.047	18.447	15.646
6.660	6.246	0.414	10800	0.350	0.117	4.551	0.892	15.716	13.330
6.660	6.166	0.494	14400	0.360	0.120	6.068	0.798	14.066	11.930
6.660	6.086	0.574	18000	0.350	0.117	7.585	0.742	13.076	11.090
6.660	6.006	0.654	21600	0.330	0.110	9.102	0.705	12.416	10.531

Table 11: Wear Rate values for Pure Aluminium with 2% Red mud of 200 μm particle size at 400 rpm

V_s =8.35 X 10^{-1} m/sec **ρ=2.4380 x 1000 kg/m³**

m_1	m_2	Δm	T	F_f	μ	R.Dx10^{-3}	W_r×10^{-6}	W_v×10^{-12}	W_s×10^{-13}
(gm)	(gm)	(gm)	(sec)	kgf		m	(N/m)	(m³/sec)	(m³/N-m)
6.570	6.109	0.461	3600	0.370	0.123	3.014	1.500	52.508	20.961
6.570	5.939	0.631	7200	0.360	0.120	6.028	1.027	35.939	14.347
6.570	5.769	0.801	10800	0.350	0.117	9.042	0.869	30.416	12.142
6.570	5.609	0.961	14400	0.340	0.113	12.056	0.782	27.369	10.926
6.570	5.449	1.121	18000	0.350	0.117	15.070	0.730	25.541	10.196
6.570	5.289	1.281	21600	0.370	0.123	18.084	0.695	24.323	9.710

Table 12: Wear Rate values for Pure Aluminium with 2% Red mud of 200 μm particle size at 600 rpm

V_s =1.244 m/sec **ρ=2.4380 x 1000 kg/m³**

m_1	m_2	Δm	T	F_f	μ	R.Dx10^{-3}	W_r×10^{-6}	W_v×10^{-12}	W_s×10^{-13}
(gm)	(gm)	(gm)	(sec)	kgf		m	(N/m)	(m³/sec)	(m³/N-m)
6.710	6.112	0.598	3600	0.350	0.117	4.424	1.326	68.132	18.256
6.710	5.882	0.828	7200	0.350	0.117	8.848	0.918	47.169	12.639
6.710	5.662	1.048	10800	0.340	0.113	13.272	0.775	39.801	10.665
6.710	5.442	1.268	14400	0.300	0.100	17.696	0.703	36.117	9.678
6.710	5.222	1.488	18000	0.330	0.110	22.120	0.660	33.907	9.086
6.710	5.002	1.708	21600	0.320	0.107	26.544	0.631	32.434	8.691

The Wear rate values for pure aluminium with 2% red mud of 42 nm particle size at 200rpm, 400 rpm and 600 rpm is shown in tables 13, 14 and 15 respectively.

Table 13: Wear Rate values for Pure Aluminium with 2% Red mud of 42 nm particle size at 200 rpm

V_S =3.93 X 10^{-1} m/sec **ρ=2.4380 x 1000 kg/m³**

m_1	m_2	Δm	T	F_f	μ	R.Dx10^{-3}	W_r×10^{-6}	W_v×10^{-12}	W_s×10^{-13}
(gm)	(gm)	(gm)	(sec)	kgf		m	(N/m)	(m³/sec)	(m³/N-m)
6.530	6.424	0.106	3600	0.220	0.073	1.418	0.731	12.039	10.211
6.530	6.384	0.146	7200	0.210	0.070	2.836	0.504	8.298	7.038
6.530	6.344	0.186	10800	0.190	0.063	4.254	0.428	7.051	5.981
6.530	6.304	0.226	14400	0.200	0.067	5.672	0.390	6.428	5.452
6.530	6.274	0.256	18000	0.180	0.060	7.090	0.354	5.826	4.941
6.530	6.234	0.296	21600	0.190	0.063	8.508	0.341	5.614	4.762

Table 14: Wear Rate values for Pure Aluminium with 2% Red mud of 42 nm particle size at 400 rpm

V_s =8.35 X 10^{-1} m/sec **ρ=2.4380 x 1000 kg/m³**

m_1	m_2	Δm	T	F_f	μ	R.Dx10^{-3}	W_r×10^{-6}	W_v×10^{-12}	W_s×10^{-13}
(gm)	(gm)	(gm)	(sec)	kgf		m	(N/m)	(m³/sec)	(m³/N-m)
6.580	6.384	0.196	3600	0.240	0.080	3.027	0.635	22.324	8.912
6.580	6.304	0.276	7200	0.230	0.077	6.054	0.447	15.720	6.275
6.580	6.234	0.346	10800	0.210	0.070	9.081	0.374	13.138	5.245
6.580	6.164	0.416	14400	0.220	0.073	12.108	0.337	11.848	4.730
6.580	6.094	0.486	18000	0.190	0.063	15.135	0.315	11.073	4.420
6.580	6.024	0.556	21600	0.210	0.070	18.162	0.300	10.557	4.214

Table 15: Wear Rate values for Pure Aluminium with 2% Red mud of 42 nm particle size at 600 rpm

V_s =1.244 m/sec **ρ=2.4380 x 1000 kg/m³**

m_1	m_2	Δm	T	F_f	μ	R.Dx10^{-3}	W_r×10^{-6}	W_v×10^{-12}	W_s×10^{-13}
(gm)	(gm)	(gm)	(sec)	kgf		m	(N/m)	(m³/sec)	(m³/N-m)
6.540	6.270	0.270	3600	0.260	0.087	4.399	0.601	30.706	8.228
6.540	6.170	0.370	7200	0.260	0.087	8.798	0.412	21.050	5.640
6.540	6.080	0.460	10800	0.250	0.083	13.197	0.342	17.451	4.676
6.540	5.990	0.550	14400	0.230	0.077	17.596	0.306	15.652	4.194
6.540	5.900	0.640	18000	0.220	0.073	21.995	0.285	14.573	3.905
6.540	5.810	0.730	21600	0.230	0.077	26.394	0.271	13.853	3.712

The Wear rate values for pure aluminium with 4% red mud of 100 µm particle size at 200rpm,400 rpm and 600 rpm is shown in tables 16, 17 and 18 respectively.

Table 16: Wear Rate values for Pure Aluminium with 4% Red mud of 100 µm particle size at 200 rpm

V_S =3.93 X 10^{-1} m/sec **ρ=2.44 x 1000 kg/m³**

m_1	m_2	Δm	T	F_f	µ	R.Dx10^{-3}	W_r×10^{-6}	W_v×10^{-12}	W_s×10^{-13}
(gm)	(gm)	(gm)	(sec)	kgf		m	(N/m)	(m³/sec)	(m³/N-m)
7.100	7.001	0.099	3600	0.270	0.090	1.515	0.640	11.252	9.544
7.100	6.961	0.139	7200	0.260	0.087	3.030	0.450	7.903	6.703
7.100	6.931	0.169	10800	0.250	0.083	4.545	0.364	6.407	5.434
7.100	6.901	0.199	14400	0.270	0.090	6.060	0.322	5.659	4.800
7.100	6.871	0.229	18000	0.240	0.080	7.575	0.296	5.210	4.419
7.100	6.841	0.259	21600	0.250	0.083	9.090	0.279	4.911	4.166

Table 17: Wear Rate values for Pure Aluminium with 4% Red mud of 100 µm particle size at 400 rpm

V_s =8.35 X 10^{-1} m/sec **ρ=2.44 x 1000 kg/m³**

m_1	m_2	Δm	T	F_f	µ	R.Dx10^{-3}	W_r×10^{-6}	W_v×10^{-12}	W_s×10^{-13}
(gm)	(gm)	(gm)	(sec)	kgf		m	(N/m)	(m³/sec)	(m³/N-m)
7.120	6.933	0.187	3600	0.290	0.097	3.010	0.608	21.238	8.478
7.120	6.872	0.248	7200	0.280	0.093	6.020	0.403	14.091	5.625
7.120	6.812	0.308	10800	0.260	0.087	9.030	0.334	11.671	4.659
7.120	6.752	0.368	14400	0.240	0.080	12.040	0.299	10.461	4.176
7.120	6.692	0.428	18000	0.250	0.083	15.050	0.279	9.735	3.886
7.120	6.632	0.488	21600	0.240	0.080	18.060	0.265	9.251	3.693

Table 18: Wear Rate values for Pure Aluminium with 4% Red mud of 100 µm particle size at 600 rpm

V_s =1.244 m/sec **ρ=2.44 x 1000 kg/m³**

m_1	m_2	Δm	T	F_f	M	R.Dx10^{-3}	W_r×10^{-6}	W_v×10^{-12}	W_s×10^{-13}
(gm)	(gm)	(gm)	(sec)	kgf		m	(N/m)	(m³/sec)	(m³/N-m)
6.830	6.595	0.235	3600	0.300	0.100	4.265	0.541	26.777	7.175
6.830	6.505	0.325	7200	0.290	0.097	8.530	0.374	18.511	4.960
6.830	6.425	0.405	10800	0.300	0.100	12.795	0.311	15.377	4.120
6.830	6.345	0.485	14400	0.280	0.093	17.060	0.279	13.809	3.700
6.830	6.265	0.565	18000	0.270	0.090	21.325	0.260	12.869	3.448
6.830	6.185	0.645	21600	0.290	0.097	25.590	0.247	12.242	3.280

The Wear rate values for pure aluminium with 4% red mud of 150 µm particle size at 200rpm,400 rpm and 600 rpm is shown in tables 19, 20 and 21 respectively.

Table 19: Wear Rate values for Pure Aluminium with 4% Red mud of 150 µm particle size at 200 rpm

V_S =3.93 X 10^{-1} m/sec **ρ=2.44 x 1000 kg/m³**

m_1	m_2	Δm	T	F_f	µ	R.Dx10^{-3}	W_r×10^{-6}	W_v×10^{-12}	W_s×10^{-13}
(gm)	(gm)	(gm)	(sec)	kgf		m	(N/m)	(m³/sec)	(m³/N-m)
7.200	7.073	0.127	3600	0.330	0.110	1.516	0.825	14.514	12.311
7.200	7.032	0.168	7200	0.320	0.107	3.032	0.545	9.591	8.135
7.200	6.992	0.208	10800	0.340	0.113	4.548	0.450	7.912	6.711
7.200	6.952	0.248	14400	0.310	0.103	6.064	0.402	7.072	5.999
7.200	6.912	0.288	18000	0.320	0.107	7.580	0.373	6.569	5.571
7.200	6.872	0.328	21600	0.300	0.100	9.096	0.354	6.233	5.286

Table 20: Wear Rate values for Pure Aluminium with 4% Red mud of 150 µm particle size at 400 rpm

V_s =8.35 X 10^{-1} m/sec **ρ=2.44 x 1000 kg/m³**

m_1	m_2	Δm	T	F_f	µ	R.Dx10^{-3}	W_r×10^{-6}	W_v×10^{-12}	W_s×10^{-13}
(gm)	(gm)	(gm)	(sec)	kgf		m	(N/m)	(m³/sec)	(m³/N-m)
6.980	6.743	0.237	3600	0.350	0.117	2.990	0.779	27.030	10.790
6.980	6.653	0.327	7200	0.360	0.120	5.980	0.537	18.638	7.440
6.980	6.573	0.407	10800	0.330	0.110	8.970	0.446	15.461	6.172
6.980	6.493	0.487	14400	0.340	0.113	11.960	0.400	13.873	5.538
6.980	6.413	0.567	18000	0.330	0.110	14.950	0.372	12.920	5.158
6.980	6.333	0.647	21600	0.320	0.107	17.940	0.354	12.284	4.904

Table 21: Wear Rate values for Pure Aluminium with 4% Red mud of 150 µm particle size at 600 rpm

V_s =1.244 m/sec **ρ=2.44 x 1000 kg/m³**

m_1	m_2	Δm	T	F_f	µ	R.Dx10^{-3}	W_r×10^{-6}	W_v×10^{-12}	W_s×10^{-13}
(gm)	(gm)	(gm)	(sec)	kgf		m	(N/m)	(m³/sec)	(m³/N-m)
6.850	6.561	0.289	3600	0.370	0.123	4.496	0.630	32.870	8.808
6.850	6.441	0.409	7200	0.320	0.107	8.992	0.446	23.266	6.234
6.850	6.331	0.519	10800	0.360	0.120	13.488	0.377	19.685	5.275
6.850	6.221	0.629	14400	0.350	0.117	17.984	0.343	17.894	4.795
6.850	6.101	0.749	18000	0.340	0.113	22.480	0.327	17.048	4.568
6.850	5.991	0.859	21600	0.360	0.120	26.976	0.312	16.294	4.366

The Wear rate values for pure aluminium with 4% red mud of 200 µm particle size at 200rpm,400 rpm and 600 rpm is shown in tables 22, 23 and 24 respectively.

Table 22: Wear Rate values for Pure Aluminium with 4% Red mud of 200 µm particle size at 200 rpm

V_S =3.93 X 10^{-1} m/sec **ρ=2.44 x 1000 kg/m³**

m_1	m_2	Δm	T	F_f	µ	R.Dx10^{-3}	W_r×10^{-6}	W_v×10^{-12}	W_s×10^{-13}
(gm)	(gm)	(gm)	(sec)	kgf		m	(N/m)	(m³/sec)	(m³/N-m)
6.760	6.607	0.153	3600	0.380	0.127	1.507	0.998	17.458	14.808
6.760	6.547	0.213	7200	0.370	0.123	3.015	0.694	12.144	10.301
6.760	6.497	0.263	10800	0.350	0.117	4.522	0.571	9.994	8.476
6.760	6.447	0.313	14400	0.360	0.120	6.030	0.510	8.918	7.564
6.760	6.397	0.363	18000	0.330	0.110	7.537	0.473	8.273	7.017
6.760	6.347	0.413	21600	0.350	0.117	9.044	0.448	7.843	6.652

Table 23: Wear Rate values for Pure Aluminium with 4% Red mud of 200 µm particle size at 400 rpm

V_s =8.35 X 10^{-1} m/sec **ρ=2.44 x 1000 kg/m³**

m_1	m_2	Δm	T	F_f	µ	R.Dx10^{-3}	W_r×10^{-6}	W_v×10^{-12}	W_s×10^{-13}
(gm)	(gm)	(gm)	(sec)	kgf		m	(N/m)	(m³/sec)	(m³/N-m)
6.860	6.572	0.288	3600	0.400	0.133	2.990	0.946	32.825	13.104
6.860	6.462	0.398	7200	0.390	0.130	5.980	0.653	22.674	9.051
6.860	6.362	0.498	10800	0.370	0.123	8.970	0.545	18.911	7.549
6.860	6.262	0.598	14400	0.360	0.120	11.960	0.491	17.029	6.798
6.860	6.162	0.698	18000	0.320	0.107	14.950	0.458	15.900	6.347
6.860	6.062	0.798	21600	0.350	0.117	17.940	0.437	15.147	6.047

Table 24: Wear Rate values for Pure Aluminium with 4% Red mud of 200 µm particle size at 600 rpm

V_s =1.244 m/sec **ρ=2.44 x 1000 kg/m³**

m_1	m_2	Δm	T	F_f	µ	R.Dx10^{-3}	W_r×10^{-6}	W_v×10^{-12}	W_s×10^{-13}
(gm)	(gm)	(gm)	(sec)	kgf		m	(N/m)	(m³/sec)	(m³/N-m)
6.850	6.423	0.427	3600	0.430	0.143	4.589	0.912	48.568	13.014
6.850	6.263	0.587	7200	0.410	0.137	9.178	0.627	33.392	8.947
6.850	6.113	0.737	10800	0.390	0.130	13.767	0.525	27.953	7.490
6.850	5.963	0.887	14400	0.420	0.140	18.356	0.474	25.234	6.762
6.850	5.813	1.037	18000	0.370	0.123	22.945	0.443	23.603	6.324
6.850	5.663	1.187	21600	0.390	0.130	27.534	0.423	22.515	6.033

The Wear rate values for pure aluminium with 4% red mud of 42 nm particle size at 200rpm, 400 rpm and 600 rpm is shown in tables 25, 26 and 27 respectively.

Table 25: Wear Rate values for Pure Aluminium with 4% Red mud of 42 nm particle size at 200 rpm

V_S =3.93 X 10^{-1} m/sec **ρ=2.44 x 1000 kg/m³**

m_1	m_2	Δm	T	F_f	μ	R.Dx10^{-3}	$W_r \times 10^{-6}$	$W_v \times 10^{-12}$	$W_s \times 10^{-13}$
(gm)	(gm)	(gm)	(sec)	kgf		m	(N/m)	(m³/sec)	(m³/N-m)
6.530	6.468	0.062	3600	0.190	0.063	1.509	0.404	7.075	6.001
6.530	6.438	0.092	7200	0.180	0.060	3.018	0.300	5.245	4.449
6.530	6.408	0.122	10800	0.190	0.063	4.527	0.265	4.635	3.931
6.530	6.378	0.152	14400	0.170	0.057	6.036	0.247	4.330	3.673
6.530	6.358	0.172	18000	0.150	0.050	7.545	0.224	3.919	3.324
6.530	6.338	0.192	21600	0.170	0.057	9.054	0.208	3.646	3.092

Table 26: Wear Rate values for Pure Aluminium with 4% Red mud of 42 nm particle size at 400 rpm

V_s =8.35 X 10^{-1} m/sec **ρ=2.44 x 1000 kg/m³**

m_1	m_2	Δm	T	F_f	μ	R.Dx10^{-3}	$W_r \times 10^{-6}$	$W_v \times 10^{-12}$	$W_s \times 10^{-13}$
(gm)	(gm)	(gm)	(sec)	kgf		m	(N/m)	(m³/sec)	(m³/N-m)
6.870	6.754	0.116	3600	0.210	0.070	3.020	0.377	13.213	5.274
6.870	6.704	0.166	7200	0.200	0.067	6.040	0.270	9.452	3.773
6.870	6.654	0.216	10800	0.180	0.060	9.060	0.234	8.199	3.273
6.870	6.614	0.256	14400	0.170	0.057	12.080	0.208	7.288	2.909
6.870	6.564	0.306	18000	0.220	0.073	15.100	0.199	6.969	2.782
6.870	6.524	0.346	21600	0.190	0.063	18.120	0.187	6.566	2.621

Table 27: Wear Rate values for Pure Aluminium with 4% Red mud of 42 nm particle size at 600 rpm

V_s =1.244 m/sec **ρ=2.44 x 1000 kg/m³**

m_1	m_2	Δm	T	F_f	μ	R.Dx10^{-3}	$W_r \times 10^{-6}$	$W_v \times 10^{-12}$	$W_s \times 10^{-13}$
(gm)	(gm)	(gm)	(sec)	kgf		m	(N/m)	(m³/sec)	(m³/N-m)
6.720	6.550	0.170	3600	0.220	0.073	4.518	0.369	19.347	5.184
6.720	6.480	0.240	7200	0.200	0.067	9.036	0.260	13.658	3.660
6.720	6.420	0.300	10800	0.170	0.057	13.554	0.217	11.382	3.050
6.720	6.360	0.360	14400	0.190	0.063	18.072	0.195	10.244	2.745
6.720	6.300	0.420	18000	0.180	0.060	22.590	0.182	9.562	2.562
6.720	6.250	0.470	21600	0.190	0.063	27.108	0.170	8.917	2.389

The Wear rate values for pure aluminium with 6% red mud of 100 µm particle size at 200rpm,400 rpm and 600 rpm is shown in tables 28, 29 and 30 respectively.

Table 28: Wear Rate values for Pure Aluminium with 6% Red mud of 100 µm particle size at 200 rpm

V_S =3.93 X 10^{-1} m/sec **ρ=2.45 x 1000 kg/m³**

m_1	m_2	Δm	T	F_f	µ	R.Dx10^{-3}	W_r×10^{-6}	W_v×10^{-12}	W_s×10^{-13}
(gm)	(gm)	(gm)	(sec)	kgf		m	(N/m)	(m³/sec)	(m³/N-m)
7.100	7.027	0.073	3600	0.250	0.083	1.509	0.474	8.267	7.012
7.100	6.997	0.103	7200	0.240	0.080	3.018	0.335	5.834	4.948
7.100	6.967	0.133	10800	0.260	0.087	4.527	0.288	5.023	4.260
7.100	6.937	0.163	14400	0.230	0.077	6.036	0.265	4.618	3.917
7.100	6.917	0.183	18000	0.250	0.083	7.545	0.238	4.148	3.518
7.100	6.887	0.213	21600	0.220	0.073	9.054	0.231	4.023	3.412

Table 29: Wear Rate values for Pure Aluminium with 6% Red mud of 100 µm particle size at 400 rpm

V_s =8.35 X 10^{-1} m/sec **ρ=2.45 x 1000 kg/m³**

m_1	m_2	Δm	T	F_f	µ	R.Dx10^{-3}	W_r×10^{-6}	W_v×10^{-12}	W_s×10^{-13}
(gm)	(gm)	(gm)	(sec)	kgf		m	(N/m)	(m³/sec)	(m³/N-m)
7.120	6.993	0.127	3600	0.260	0.087	2.967	0.420	14.402	5.749
7.120	6.943	0.177	7200	0.240	0.080	5.934	0.293	10.036	4.006
7.120	6.903	0.217	10800	0.230	0.077	8.901	0.239	8.202	3.274
7.120	6.863	0.257	14400	0.260	0.087	11.868	0.212	7.285	2.908
7.120	6.823	0.297	18000	0.230	0.077	14.835	0.196	6.735	2.689
7.120	6.783	0.337	21600	0.250	0.083	17.802	0.186	6.369	2.542

Table 30: Wear Rate values for Pure Aluminium with 6% Red mud of 100 µm particle size at 600 rpm

V_s =1.244 m/sec **ρ=2.45 x 1000 kg/m³**

m_1	m_2	Δm	T	F_f	µ	R.Dx10^{-3}	W_r×10^{-6}	W_v×10^{-12}	W_s×10^{-13}
(gm)	(gm)	(gm)	(sec)	kgf		m	(N/m)	(m³/sec)	(m³/N-m)
6.830	6.647	0.183	3600	0.280	0.093	4.460	0.402	20.722	5.552
6.830	6.577	0.253	7200	0.270	0.090	8.920	0.278	14.329	3.840
6.830	6.517	0.313	10800	0.280	0.093	13.380	0.229	11.820	3.167
6.830	6.457	0.373	14400	0.250	0.083	17.840	0.205	10.566	2.831
6.830	6.397	0.433	18000	0.260	0.087	22.300	0.190	9.813	2.629
6.830	6.337	0.493	21600	0.270	0.090	26.760	0.181	9.311	2.495

The Wear rate values for pure aluminium with 6% red mud of 150 µm particle size at 200rpm,400 rpm and 600 rpm is shown in tables 31, 32 and 33 respectively.

Table 31: Wear Rate values for Pure Aluminium with 6% Red mud of 150 µm particle size at 200 rpm

V_S =3.93 X 10^{-1} m/sec **ρ=2.45 x 1000 kg/m³**

m_1	m_2	Δm	T	F_f	µ	R.Dx10^{-3}	W_r×10^{-6}	W_v×10^{-12}	W_s×10^{-13}
(gm)	(gm)	(gm)	(sec)	kgf		m	(N/m)	(m³/sec)	(m³/N-m)
7.200	7.096	0.104	3600	0.300	0.100	1.498	0.682	11.808	10.015
7.200	7.056	0.144	7200	0.290	0.097	2.996	0.472	8.171	6.931
7.200	7.026	0.174	10800	0.310	0.103	4.494	0.380	6.581	5.582
7.200	6.996	0.204	14400	0.320	0.107	5.992	0.334	5.786	4.908
7.200	6.966	0.234	18000	0.280	0.093	7.490	0.307	5.309	4.503
7.200	6.936	0.264	21600	0.320	0.107	8.988	0.288	4.991	4.234

Table 32: Wear Rate values for Pure Aluminium with 6% Red mud of 150 µm particle size at 400 rpm

V_s =8.35 X 10^{-1} m/sec **ρ=2.45 x 1000 kg/m³**

m_1	m_2	Δm	T	F_f	µ	R.Dx10^{-3}	W_r×10^{-6}	W_v×10^{-12}	W_s×10^{-13}
(gm)	(gm)	(gm)	(sec)	kgf		m	(N/m)	(m³/sec)	(m³/N-m)
6.980	6.781	0.199	3600	0.320	0.107	3.010	0.649	22.577	9.013
6.980	6.711	0.269	7200	0.310	0.103	6.020	0.439	15.257	6.091
6.980	6.651	0.329	10800	0.300	0.100	9.030	0.358	12.439	4.966
6.980	6.591	0.389	14400	0.280	0.093	12.040	0.317	11.030	4.403
6.980	6.521	0.459	18000	0.310	0.103	15.050	0.299	10.411	4.156
6.980	6.461	0.519	21600	0.310	0.103	18.060	0.282	9.810	3.916

Table 33: Wear Rate values for Pure Aluminium with 6% Red mud of 150 µm particle size at 600 rpm

V_s =1.244 m/sec **ρ=2.45 x 1000 kg/m³**

m_1	m_2	Δm	T	F_f	µ	R.Dx10^{-3}	W_r×10^{-6}	W_v×10^{-12}	W_s×10^{-13}
(gm)	(gm)	(gm)	(sec)	kgf		m	(N/m)	(m³/sec)	(m³/N-m)
6.850	6.620	0.230	3600	0.330	0.110	4.590	0.492	26.100	6.994
6.850	6.530	0.320	7200	0.340	0.113	9.180	0.342	18.152	4.864
6.850	6.450	0.400	10800	0.320	0.107	13.770	0.285	15.125	4.053
6.850	6.370	0.480	14400	0.330	0.110	18.360	0.257	13.611	3.647
6.850	6.290	0.560	18000	0.290	0.097	22.950	0.239	12.703	3.404
6.850	6.210	0.640	21600	0.280	0.093	27.540	0.228	12.098	3.242

The Wear rate values for pure aluminium with 6% red mud of 200 µm particle size at 200rpm,400 rpm and 600 rpm is shown in tables 34, 35 and 36 respectively.

Table 34: Wear Rate values for Pure Aluminium with 6% Red mud of 200 µm particle size at 200 rpm

V_S =3.93 X 10^{-1} m/sec **ρ=2.45 x 1000 kg/m³**

m_1	m_2	Δm	T	F_f	µ	R.Dx10^{-3}	$W_r \times 10^{-6}$	$W_v \times 10^{-12}$	$W_s \times 10^{-13}$
(gm)	(gm)	(gm)	(sec)	kgf		m	(N/m)	(m³/sec)	(m³/N-m)
6.760	6.635	0.125	3600	0.350	0.117	1.485	0.825	14.159	12.010
6.760	6.585	0.175	7200	0.340	0.113	2.970	0.578	9.914	8.409
6.760	6.535	0.225	10800	0.360	0.120	4.455	0.495	8.499	7.209
6.760	6.495	0.265	14400	0.340	0.113	5.940	0.437	7.508	6.368
6.760	6.445	0.315	18000	0.330	0.110	7.425	0.416	7.140	6.056
6.760	6.405	0.355	21600	0.320	0.107	8.910	0.391	6.706	5.688

Table 35: Wear Rate values for Pure Aluminium with 6% Red mud of 200 µm particle size at 400 rpm

V_s =8.35 X 10^{-1} m/sec **ρ=2.45 x 1000 kg/m³**

m_1	m_2	Δm	T	F_f	µ	R.Dx10^{-3}	$W_r \times 10^{-6}$	$W_v \times 10^{-12}$	$W_s \times 10^{-13}$
(gm)	(gm)	(gm)	(sec)	kgf		m	(N/m)	(m³/sec)	(m³/N-m)
6.860	6.608	0.252	3600	0.370	0.123	3.013	0.821	28.589	11.413
6.860	6.508	0.352	7200	0.380	0.127	6.026	0.573	19.964	7.970
6.860	6.418	0.442	10800	0.360	0.120	9.039	0.480	16.710	6.671
6.860	6.328	0.532	14400	0.350	0.117	12.052	0.433	15.084	6.021
6.860	6.238	0.622	18000	0.350	0.117	15.065	0.405	14.108	5.632
6.860	6.148	0.712	21600	0.340	0.113	18.078	0.386	13.457	5.372

Table 36: Wear Rate values for Pure Aluminium with 6% Red mud of 200 µm particle size at 600 rpm

V_s =1.244 m/sec **ρ=2.45 x 1000 kg/m³**

m_1	m_2	Δm	T	F_f	µ	R.Dx10^{-3}	$W_r \times 10^{-6}$	$W_v \times 10^{-12}$	$W_s \times 10^{-13}$
(gm)	(gm)	(gm)	(sec)	kgf		m	(N/m)	(m³/sec)	(m³/N-m)
6.850	6.508	0.342	3600	0.390	0.130	4.510	0.744	38.780	10.391
6.850	6.378	0.472	7200	0.380	0.127	9.020	0.513	26.760	7.170
6.850	6.258	0.592	10800	0.370	0.123	13.530	0.429	22.375	5.995
6.850	6.138	0.712	14400	0.350	0.117	18.040	0.387	20.183	5.408
6.850	6.018	0.832	18000	0.350	0.117	22.550	0.362	18.867	5.056
6.850	5.898	0.952	21600	0.360	0.120	27.060	0.345	17.990	4.821

The Wear rate values for pure aluminium with 6% red mud of 42 nm particle size at 200 rpm, 400 rpm and 600 rpm is shown in tables 37, 38 and 39 respectively.

Table 37: Wear Rate values for Pure Aluminium with 6% Red mud of 42 nm particle size at 200 rpm

V_S =3.93 X 10^{-1} m/sec **ρ=2.45 x 1000 kg/m³**

m_1	m_2	Δm	T	F_f	μ	R.Dx10^{-3}	$W_r \times 10^{-6}$	$W_v \times 10^{-12}$	$W_s \times 10^{-13}$
(gm)	(gm)	(gm)	(sec)	kgf		m	(N/m)	(m³/sec)	(m³/N-m)
6.530	6.478	0.052	3600	0.118	0.039	1.353	0.379	5.927	5.027
6.530	6.458	0.072	7200	0.112	0.037	2.706	0.262	4.097	3.475
6.530	6.438	0.092	10800	0.110	0.037	4.059	0.223	3.487	2.958
6.530	6.428	0.102	14400	0.119	0.040	5.412	0.185	2.899	2.459
6.530	6.418	0.112	18000	0.114	0.038	6.765	0.163	2.546	2.159
6.530	6.408	0.122	21600	0.120	0.040	8.118	0.148	2.311	1.960

Table 38: Wear Rate values for Pure Aluminium with 6% Red mud of 42 nm particle size at 400 rpm

V_s =8.35 X 10^{-1} m/sec **ρ=2.45 x 1000 kg/m³**

m_1	m_2	Δm	T	F_f	μ	R.Dx10^{-3}	$W_r \times 10^{-6}$	$W_v \times 10^{-12}$	$W_s \times 10^{-13}$
(gm)	(gm)	(gm)	(sec)	kgf		m	(N/m)	(m³/sec)	(m³/N-m)
6.870	6.769	0.101	3600	0.152	0.051	2.973	0.334	11.476	4.581
6.870	6.729	0.141	7200	0.152	0.051	5.946	0.233	8.006	3.196
6.870	6.699	0.171	10800	0.149	0.050	8.919	0.188	6.471	2.583
6.870	6.659	0.211	14400	0.131	0.044	11.892	0.174	5.987	2.390
6.870	6.629	0.241	18000	0.143	0.048	14.865	0.159	5.470	2.184
6.870	6.599	0.271	21600	0.132	0.044	17.838	0.149	5.125	2.046

Table 39: Wear Rate values for Pure Aluminium with 6% Red mud of 42 nm particle size at 600 rpm

V_s =1.244 m/sec **ρ=2.45 x 1000 kg/m³**

m_1	m_2	Δm	T	F_f	μ	R.Dx10^{-3}	$W_r \times 10^{-6}$	$W_v \times 10^{-12}$	$W_s \times 10^{-13}$
(gm)	(gm)	(gm)	(sec)	kgf		m	(N/m)	(m³/sec)	(m³/N-m)
6.720	6.557	0.163	3600	0.161	0.054	4.820	0.332	18.495	4.956
6.720	6.497	0.223	7200	0.168	0.056	9.640	0.227	12.649	3.389
6.720	6.437	0.283	10800	0.167	0.056	14.460	0.192	10.700	2.867
6.720	6.387	0.333	14400	0.159	0.053	19.280	0.169	9.442	2.530
6.720	6.327	0.393	18000	0.162	0.054	24.100	0.160	8.914	2.389
6.720	6.267	0.453	21600	0.158	0.053	28.920	0.154	8.562	2.294

APPENDIX II – B (WITH HEAT TREATMENT CONDITION)

i) Wear rate tables for pure aluminium with red mud at 10 N load

The Wear rate values for pure aluminium with 6% red mud of 100 µm particle size with 200rpm, at 350^0C, 400^0C and 450^0C are shown in Tables 1, 2 and 3 respectively.

Table 1: Wear Rate values for Pure Aluminium with 6% Red mud of 100 µm particle size at 200 rpm and 350^0C

Vs=4.191 X 10^{-1} m/sec **ρ=2.45 x 1000 kg/m³**

m_1	m_2	Δm	T	F_f	µ	R.Dx10^{-3}	$W_r \times 10^{-6}$	$W_v \times 10^{-12}$	$W_s \times 10^{-13}$
(gm)	(gm)	(gm)	(sec)	kgf		m	(N/m)	(m³/sec)	(m³/N-m)
7.1	7.074	0.026	3600	0.41	0.41	1.509	0.169	2.962	7.062
7.1	7.049	0.051	7200	0.42	0.42	3.018	0.165	2.905	6.931
7.1	7.025	0.075	10800	0.39	0.39	4.527	0.162	2.848	6.798
7.1	7.001	0.099	14400	0.41	0.41	6.036	0.160	2.819	6.727
7.1	6.976	0.124	18000	0.45	0.45	7.545	0.161	2.825	6.741
7.1	6.952	0.148	21600	0.4	0.4	9.054	0.160	2.810	6.704

Table 2: Wear Rate values for Pure Aluminium with 6% Red mud of 100 µm particle size at 200 rpm and 400^0C

Vs=4.191 X 10^{-1} m/sec **ρ=2.45 x 1000 kg/m³**

m_1	m_2	Δm	T	F_f	µ	R.Dx10^{-3}	$W_r \times 10^{-6}$	$W_v \times 10^{-12}$	$W_s \times 10^{-13}$
(gm)	(gm)	(gm)	(sec)	kgf		m	(N/m)	(m³/sec)	(m³/N-m)
7.1	7.075	0.025	3600	0.49	0.49	1.509	0.162	2.848	6.795
7.1	7.051	0.049	7200	0.51	0.51	3.018	0.159	2.791	6.659
7.1	7.027	0.073	10800	0.52	0.52	4.527	0.158	2.772	6.614
7.1	7.003	0.097	14400	0.55	0.55	6.036	0.157	2.762	6.591
7.1	6.979	0.121	18000	0.48	0.48	7.545	0.157	2.757	6.577
7.1	6.954	0.146	21600	0.42	0.42	9.054	0.158	2.772	6.614

Table 3: Wear Rate values for Pure Aluminium with 6% Red mud of 100 µm particle size at 200 rpm and 450^0C

Vs=4.191 X 10^{-1} m/sec **ρ=2.45 x 1000 kg/m³**

m_1	m_2	Δm	T	F_f	µ	R.Dx10^{-3}	$W_r \times 10^{-6}$	$W_v \times 10^{-12}$	$W_s \times 10^{-13}$
(gm)	(gm)	(gm)	(sec)	kgf		m	(N/m)	(m³/sec)	(m³/N-m)
7.1	7.077	0.023	3600	0.55	0.55	1.509	0.149	2.620	6.251
7.1	7.055	0.045	7200	0.57	0.57	3.018	0.146	2.563	6.115
7.1	7.033	0.067	10800	0.54	0.54	4.527	0.145	2.544	6.070
7.1	7.011	0.089	14400	0.53	0.53	6.036	0.144	2.535	6.047
7.1	6.989	0.111	18000	0.48	0.48	7.545	0.144	2.529	6.034
7.1	6.967	0.133	21600	0.51	0.51	9.054	0.144	2.525	6.025

The Wear rate values for pure aluminium with 6% red mud of 100 μm particle size with 200 rpm, at 500^0C and Wear rate values for pure aluminium with 6% red mud of 100 μm particle size at 400 rpm, at 350^0C and 400^0C are shown in Tables 4, 5 and 6 respectively.

Table 4: Wear Rate values for Pure Aluminium with 6% Red mud of 100 μm particle size at 200 rpm and 500^0C

Vs=4.191 X 10^{-1} m/sec **ρ=2.45 x 1000 kg/m³**

m_1 (gm)	m_2 (gm)	Δm (gm)	T (sec)	F_f kgf	μ	R.Dx10^{-3} m	$W_r \times 10^{-6}$ (N/m)	$W_v \times 10^{-12}$ (m³/sec)	$W_s \times 10^{-13}$ (m³/N-m)
7.1	7.076	0.024	3600	0.61	0.61	1.509	0.156	2.734	6.523
7.1	7.053	0.047	7200	0.63	0.63	3.018	0.152	2.677	6.387
7.1	7.03	0.07	10800	0.59	0.59	4.527	0.151	2.658	6.342
7.1	7.007	0.093	14400	0.65	0.65	6.036	0.151	2.649	6.319
7.1	6.984	0.116	18000	0.62	0.62	7.545	0.150	2.643	6.306
7.1	6.961	0.139	21600	0.49	0.49	9.054	0.150	2.639	6.297

Table 5: Wear Rate values for Pure Aluminium with 6% Red mud of 100 μm particle size at 400 rpm and 350^0C

Vs=8.2416 X 10^{-1} m/se **ρ=2.45 x 1000 kg/m³**

m_1 (gm)	m_2 (gm)	Δm (gm)	T (sec)	F_f kgf	μ	R.Dx10^{-3} m	$W_r \times 10^{-6}$ (N/m)	$W_v \times 10^{-12}$ (m³/sec)	$W_s \times 10^{-13}$ (m³/N-m)
7.12	7.078	0.042	3600	0.44	0.44	2.967	0.138	4.785	5.806
7.12	7.037	0.083	7200	0.45	0.45	5.934	0.137	4.728	5.737
7.12	6.996	0.124	10800	0.43	0.43	8.901	0.136	4.709	5.714
7.12	6.955	0.165	14400	0.47	0.47	11.868	0.136	4.699	5.702
7.12	6.914	0.206	18000	0.46	0.46	14.835	0.136	4.694	5.695
7.12	6.873	0.247	21600	0.42	0.42	17.802	0.136	4.690	5.691

Table 6: Wear Rate values for Pure Aluminium with 6% Red mud of 100 μm particle size at 400 rpm and 400^0C

Vs=8.2416 X 10^{-1} m/sec **ρ=2.45 x 1000 kg/m³**

m_1 (gm)	m_2 (gm)	Δm (gm)	T (sec)	F_f kgf	μ	R.Dx10^{-3} m	$W_r \times 10^{-6}$ (N/m)	$W_v \times 10^{-12}$ (m³/sec)	$W_s \times 10^{-13}$ (m³/N-m)
7.12	7.08	0.04	3600	0.53	0.53	2.967	0.132	4.557	5.529
7.12	7.04	0.08	7200	0.52	0.52	5.934	0.132	4.557	5.529
7.12	7.00	0.12	10800	0.51	0.51	8.901	0.132	4.557	5.529
7.12	6.93	0.19	14400	0.55	0.55	11.868	0.157	5.411	6.566
7.12	6.89	0.23	18000	0.53	0.53	14.835	0.152	5.241	6.359
7.12	6.85	0.27	21600	0.57	0.57	17.802	0.148	5.127	6.221

The Wear rate values for pure aluminium with 6% red mud of 100 µm particle size with 400 rpm, at 450^0C and 500^0C and Wear rate values for pure aluminium with 6% red mud of 100 µm particle size at 600 rpm, at 350^0C are shown in Tables 7, 8 and 9 respectively.

Table 7: Wear Rate values for Pure Aluminium with 6% Red mud of 100 µm particle size at 400 rpm and 450^0C

Vs=8.2416 X 10^{-1} m/sec **ρ=2.45 x 1000 kg/m³**

m_1 (gm)	m_2 (gm)	Δm (gm)	T (sec)	F_f kgf	µ	R.Dx10^{-3} m	$W_r \times 10^{-6}$ (N/m)	$W_v \times 10^{-12}$ (m³/sec)	$W_s \times 10^{-13}$ (m³/N-m)
7.12	7.083	0.037	3600	0.59	0.59	2.967	0.122	4.215	5.115
7.12	7.047	0.073	7200	0.58	0.58	5.934	0.120	4.158	5.045
7.12	7.011	0.109	10800	0.62	0.62	8.901	0.120	4.139	5.022
7.12	6.975	0.145	14400	0.61	0.61	11.868	0.119	4.130	5.011
7.12	6.94	0.18	18000	0.57	0.57	14.835	0.119	4.101	4.976
7.12	6.903	0.217	21600	0.59	0.59	17.802	0.119	4.120	4.999

Table 8: Wear Rate values for Pure Aluminium with 6% Red mud of 100 µm particle size at 400 rpm and 500^0C

Vs=8.2416 X 10^{-1} m/sec **ρ=2.45 x 1000 kg/m³**

m_1 (gm)	m_2 (gm)	Δm (gm)	T (sec)	F_f kgf	µ	R.Dx10^{-3} m	$W_r \times 10^{-6}$ (N/m)	$W_v \times 10^{-12}$ (m³/sec)	$W_s \times 10^{-13}$ (m³/N-m)
7.12	7.082	0.038	3600	0.69	0.69	2.967	0.125	4.329	5.253
7.12	7.045	0.075	7200	0.68	0.68	5.934	0.123	4.272	5.184
7.12	7.008	0.112	10800	0.69	0.69	8.901	0.123	4.253	5.161
7.12	6.971	0.149	14400	0.71	0.71	11.868	0.123	4.244	5.149
7.12	6.934	0.186	18000	0.67	0.67	14.835	0.122	4.238	5.142
7.12	6.897	0.223	21600	0.71	0.71	17.802	0.122	4.234	5.138

Table 9: Wear Rate values for Pure Aluminium with 6% Red mud of 100 µm particle size at 600 rpm and 350^0C

Vs=1.2388 m/sec **ρ=2.45 x 1000 kg/m³**

m_1 (gm)	m_2 (gm)	Δm (gm)	T (sec)	F_f kgf	µ	R.Dx10^{-3} m	$W_r \times 10^{-6}$ (N/m)	$W_v \times 10^{-12}$ (m³/sec)	$W_s \times 10^{-13}$ (m³/N-m)
6.83	6.772	0.058	3600	0.46	0.46	4.46	0.127	6.608	5.334
6.83	6.715	0.115	7200	0.47	0.47	8.92	0.126	6.551	5.288
6.83	6.658	0.172	10800	0.45	0.45	13.38	0.126	6.532	5.272
6.83	6.601	0.229	14400	0.44	0.44	17.84	0.125	6.522	5.265
6.83	6.544	0.286	18000	0.51	0.51	22.3	0.125	6.517	5.260
6.83	6.489	0.341	21600	0.48	0.48	26.76	0.125	6.475	5.226

The Wear rate values for pure aluminium with 6% red mud of 100 µm particle size with 600 rpm at 400^0C, 450^0C and 500^0C are shown in Tables 10, 11 and 12 respectively.

Table 10: Wear Rate values for Pure Aluminium with 6% Red mud of 100 µm particle size at 600 rpm and 400^0C

Vs=1.2388 m/sec **ρ=2.45 x 1000 kg/m³**

m_1	m_2	Δm	T	F_f	µ	R.Dx10^{-3}	$W_r \times 10^{-6}$	$W_v \times 10^{-12}$	$W_s \times 10^{-13}$
(gm)	(gm)	(gm)	(sec)	kgf		m	(N/m)	(m³/sec)	(m³/N-m)
6.83	6.775	0.055	3600	0.49	0.49	4.46	0.120	6.266	5.058
6.83	6.721	0.109	7200	0.51	0.51	8.92	0.1196	6.209	5.012
6.83	6.667	0.163	10800	0.53	0.53	13.38	0.1195	6.190	4.996
6.83	6.613	0.217	14400	0.51	0.51	17.84	0.1193	6.181	4.989
6.83	6.559	0.271	18000	0.54	0.54	22.3	0.1192	6.175	4.984
6.83	6.505	0.325	21600	0.52	0.52	26.76	0.1191	6.171	4.981

Table 11: Wear rate values for pure aluminium with 6% red mud of 100 µm particle size at 600 rpm and 450^0C temperature

Vs=1.2388 m/sec **ρ=2.45 x 1000 kg/m³**

m1	m2	Δm	t	F_f	µ	R.Dx1000	$Wr \times 10^{-6}$	$Wv \times 10^{-12}$	$Ws \times 10^{-13}$
(gm)	(gm)	(gm)	(sec)	kgf		m	(N/m)	(m³/sec)	(m³/N-m)
6.83	6.779	0.051	3600	0.55	0.55	4.46	0.112	5.810	4.690
6.83	6.729	0.101	7200	0.56	0.56	8.92	0.111	5.753	4.644
6.83	6.679	0.151	10800	0.59	0.59	13.38	0.110	5.734	4.628
6.83	6.63	0.2	14400	0.54	0.54	17.84	0.1099	5.696	4.598
6.83	6.581	0.249	18000	0.57	0.57	22.3	0.1095	5.674	4.579
6.83	6.54	0.29	21600	0.56	0.56	26.76	0.106	5.506	4.445

Table 12: Wear Rate values for Pure Aluminium with 6% Red mud of 100 µm particle size at 600 rpm and 500^0C

Vs=1.2388 m/sec **ρ=2.45 x 1000 kg/m³**

m_1	m_2	Δm	T	F_f	µ	R.Dx10^{-3}	$W_r \times 10^{-6}$	$W_v \times 10^{-12}$	$W_s \times 10^{-13}$
(gm)	(gm)	(gm)	(sec)	kgf		m	(N/m)	(m³/sec)	(m³/N-m)
6.83	6.776	0.054	3600	0.69	0.69	4.46	0.118	6.152	4.966
6.83	6.723	0.107	7200	0.71	0.71	8.92	0.117	6.095	4.920
6.83	6.67	0.16	10800	0.75	0.75	13.38	0.117	6.076	4.904
6.83	6.617	0.213	14400	0.72	0.72	17.84	0.117	6.067	4.897
6.83	6.564	0.266	18000	0.74	0.74	22.3	0.117	6.061	4.892
6.83	6.514	0.316	21600	0.73	0.73	26.76	0.115	6.000	4.843

The Wear rate values for pure aluminium with 6% red mud of 42nm particle size with 200 rpm, at 350^0C, 400^0C and 450^0C are shown in Tables 13, 14 and 15 respectively.

Table 13: Wear Rate values for Pure Aluminium with 6% Red mud of 42 nm particle size at 200 rpm and 350^0C

Vs=4.191 X 10^{-1} m/sec **ρ=2.45 x 1000 kg/m³**

m_1	m_2	Δm	T	F_f	μ	R.Dx10^{-3}	$W_r \times 10^{-6}$	$W_v \times 10^{-12}$	$W_s \times 10^{-13}$
(gm)	(gm)	(gm)	(sec)	kgf		m	(N/m)	(m³/sec)	(m³/N-m)
7.12	7.101	0.019	3600	0.28	0.28	1.509	0.123	2.164	5.164
7.12	7.082	0.038	7200	0.26	0.26	3.018	0.123	2.164	5.164
7.12	7.064	0.056	10800	0.257	0.257	4.527	0.121	2.126	5.073
7.12	7.045	0.075	14400	0.254	0.254	6.036	0.121	2.136	5.096
7.12	7.027	0.093	18000	0.262	0.262	7.545	0.120	2.119	5.055
7.12	7.008	0.112	21600	0.269	0.269	9.054	0.121	2.126	5.073

Table 14: Wear Rate values for Pure Aluminium with 6% Red mud of 42 nm particle size at 200 rpm and 400^0C

Vs=4.191 X 10^{-1} m/sec **ρ=2.45 x 1000 kg/m³**

m1	m2	Δm	T	F_f	μ	R.Dx10^{-3}	$W_r \times 10^{-6}$	$W_v \times 10^{-12}$	$W_s \times 10^{-13}$
(gm)	(gm)	(gm)	(sec)	kgf		m	(N/m)	(m³/sec)	(m³/N-m)
6.87	6.852	0.018	3600	0.25	0.25	1.509	0.118	2.050	4.892
6.87	6.834	0.036	7200	0.23	0.23	3.018	0.117	2.050	4.892
6.87	6.817	0.053	10800	0.21	0.21	4.527	0.114	2.012	4.802
6.87	6.8	0.07	14400	0.22	0.22	6.036	0.113	1.993	4.756
6.87	6.783	0.087	18000	0.216	0.216	7.545	0.113	1.982	4.729
6.87	6.766	0.104	21600	0.2	0.2	9.054	0.112	1.974	4.711

Table 15: Wear Rate values for Pure Aluminium with 6% Red mud of 42 nm particle size at 200 rpm and 450^0C

Vs=4.191 X 10^{-1} m/sec **ρ=2.45 x 1000 kg/m³**

m1	m2	Δm	T	F_f	μ	R.Dx10^{-3}	$W_r \times 10^{-6}$	$W_v \times 10^{-12}$	$W_s \times 10^{-13}$
(gm)	(gm)	(gm)	(sec)	kgf		m	(N/m)	(m³/sec)	(m³/N-m)
7.02	7.004	0.016	3600	0.21	0.21	1.509	0.107	1.822	4.349
7.02	6.988	0.032	7200	0.206	0.206	3.018	0.104	1.822	4.349
7.02	6.972	0.048	10800	0.199	0.199	4.527	0.104	1.822	4.349
7.02	6.957	0.063	14400	0.209	0.209	6.036	0.102	1.794	4.281
7.02	6.941	0.079	18000	0.213	0.213	7.545	0.102	1.800	4.294
7.02	6.926	0.094	21600	0.204	0.204	9.054	0.101	1.785	4.258

The Wear rate values for pure aluminium with 6% red mud of 42 nm particle size with 200 rpm at 500^0C and wear rate values for pure aluminium with 6% red mud of 42 nm particle size with 400 rpm at 350^0C, and 400^0C are shown in Tables 16, 17 and 18 respectively.

Table 16: Wear Rate values for Pure Aluminium with 6% Red mud of 42 nm particle size at 200 rpm and 500^0C

Vs=4.191 X 10^{-1} m/sec **ρ=2.45 x 1000 kg/m³**

m1	m2	Δm	T	F_f	μ	R.Dx10^{-3}	$W_r \times 10^{-6}$	$W_v \times 10^{-12}$	$W_s \times 10^{-13}$
(gm)	(gm)	(gm)	(sec)	kgf		m	(N/m)	(m³/sec)	(m³/N-m)
6.87	6.852	0.018	3600	0.25	0.25	1.509	0.115	2.050	4.892
6.87	6.835	0.035	7200	0.236	0.236	3.018	0.113	1.993	4.756
6.87	6.818	0.052	10800	0.242	0.242	4.527	0.112	1.974	4.711
6.87	6.801	0.069	14400	0.245	0.245	6.036	0.112	1.965	4.688
6.87	6.784	0.086	18000	0.265	0.265	7.545	0.111	1.959	4.678
6.87	6.767	0.103	21600	0.25	0.25	9.054	0.111	1.955	4.666

Table 17: Wear Rate values for Pure Aluminium with 6% Red mud of 42 nm particle size at 400 rpm and 350^0C

Vs=8.2416 X 10^{-1} m/sec **ρ=2.45 x 1000 kg/m³**

m_1	m_2	Δm	T	F_f	μ	R.Dx10^{-3}	$W_r \times 10^{-6}$	$W_v \times 10^{-12}$	$W_s \times 10^{-13}$
(gm)	(gm)	(gm)	(sec)	kgf		m	(N/m)	(m³/sec)	(m³/N-m)
7.12	7.089	0.031	3600	0.256	0.256	2.967	0.102	3.532	4.285
7.12	7.06	0.06	7200	0.256	0.256	5.934	0.099	3.418	4.147
7.12	7.03	0.09	10800	0.243	0.243	8.901	0.099	3.418	4.147
7.12	7.01	0.11	14400	0.234	0.234	11.868	0.090	3.133	3.801
7.12	6.98	0.14	18000	0.239	0.239	14.835	0.092	3.190	3.870
7.12	6.95	0.17	21600	0.23	0.23	17.802	0.093	3.228	3.916

Table 18: Wear Rate values for Pure Aluminium with 6% Red mud of 42 nm particle size at 400 rpm and 400^0C

Vs=8.2416 X 10^{-1} m/sec **ρ=2.45 x 1000 kg/m³**

m_1	m_2	Δm	T	F_f	μ	R.Dx10^{-3}	$W_r \times 10^{-6}$	$W_v \times 10^{-12}$	$W_s \times 10^{-13}$
(gm)	(gm)	(gm)	(sec)	kgf		m	(N/m)	(m³/sec)	(m³/N-m)
6.87	6.841	0.029	3600	0.236	0.236	2.967	0.095	3.304	4.009
6.87	6.813	0.057	7200	0.21	0.21	5.934	0.094	3.247	3.939
6.87	6.784	0.086	10800	0.18	0.18	8.901	0.094	3.266	3.963
6.87	6.756	0.114	14400	0.209	0.209	11.868	0.094	3.247	3.939
6.87	6.73	0.14	18000	0.205	0.205	14.835	0.092	3.190	3.870
6.87	6.703	0.167	21600	0.186	0.186	17.802	0.092	3.171	3.847

The Wear rate values for pure aluminium with 6% red mud of 42 nm particle size with 400 rpm at 450^0C, 500^0C and wear rate values for pure aluminium with 6% red mud of 42 nm particle size with 600 rpm at 350^0C, are shown in Tables 19, 20 and 21 respectively.

Table 19: Wear Rate values for Pure Aluminium with 6% Red mud of 42 nm particle size at 400 rpm and 450^0C

Vs=8.2416 X 10^{-1} m/sec **ρ=2.45 x 1000 kg/m³**

m_1	m_2	Δm	T	F_f	μ	R.Dx10^{-3}	W_r×10^{-6}	W_v×10^{-12}	W_s ×10^{-13}
(gm)	(gm)	(gm)	(sec)	kgf		m	(N/m)	(m³/sec)	(m³/N-m)
7.02	6.993	0.027	3600	0.226	0.226	2.967	0.089	3.076	3.732
7.02	6.967	0.053	7200	0.219	0.219	5.934	0.087	3.019	3.663
7.02	6.94	0.08	10800	0.2	0.2	8.901	0.088	3.038	3.686
7.02	6.915	0.105	14400	0.17	0.17	11.868	0.086	2.990	3.628
7.02	6.89	0.13	18000	0.213	0.213	14.835	0.085	2.962	3.594
7.02	6.865	0.155	21600	0.207	0.207	17.802	0.085	2.943	3.571

Table 20: Wear Rate values for Pure Aluminium with 6% Red mud of 42 nm particle size at 400 rpm and 500^0C

Vs=8.2416 X 10^{-1} m/sec **ρ=2.45 x 1000 kg/m³**

m_1	m_2	Δm	T	F_f	μ	R.Dx10^{-3}	W_r×10^{-6}	W_v×10^{-12}	W_s ×10^{-13}
(gm)	(gm)	(gm)	(sec)	kgf		m	(N/m)	(m³/sec)	(m³/N-m)
6.87	6.842	0.028	3600	0.236	0.236	2.967	0.091	3.190	3.870
6.87	6.815	0.055	7200	0.22	0.22	5.934	0.090	3.133	3.801
6.87	6.788	0.082	10800	0.216	0.216	8.901	0.090	3.114	3.778
6.87	6.76	0.11	14400	0.205	0.205	11.868	0.090	3.133	3.801
6.87	6.733	0.137	18000	0.223	0.223	14.835	0.090	3.121	3.787
6.87	6.706	0.164	21600	0.215	0.215	17.802	0.090	3.114	3.778

Table 21: Wear Rate values for Pure Aluminium with 6% Red mud of 42 nm particle size at 600 rpm and 350^0C

Vs=1.2388 m/sec **ρ=2.45 x 1000 kg/m³**

m_1	m_2	Δm	T	F_f	μ	R.Dx10^{-3}	W_r×10^{-6}	W_v×10^{-12}	W_s ×10^{-13}
(gm)	(gm)	(gm)	(sec)	kgf		m	(N/m)	(m³/sec)	(m³/N-m)
7.12	7.077	0.043	3600	0.27	0.27	4.46	0.094	4.899	3.954
7.12	7.035	0.085	7200	0.264	0.264	8.92	0.093	4.842	3.908
7.12	6.993	0.127	10800	0.256	0.256	13.38	0.093	4.823	3.893
7.12	6.951	0.169	14400	0.25	0.25	17.84	0.092	4.813	3.885
7.12	6.909	0.211	18000	0.262	0.262	22.3	0.092	4.808	3.881
7.12	6.87	0.25	21600	0.258	0.258	26.76	0.091	4.747	3.831

The Wear rate values for pure aluminium with 6% red mud of 42 μm particle size with 600 rpm, at 400^0C, 450^0C and 500^0C are shown in Tables 22, 23 and 24 respectively.

Table 22: Wear Rate values for Pure Aluminium with 6% Red mud of 42 nm particle size at 600 rpm and 400^0C

Vs=1.2388 m/sec **ρ=2.45 x 1000 kg/m³**

m_1	m_2	Δm	T	F_f	μ	R.Dx10^{-3}	$W_r \times 10^{-6}$	$W_v \times 10^{-12}$	$W_s \times 10^{-13}$
(gm)	(gm)	(gm)	(sec)	kgf		m	(N/m)	(m³/sec)	(m³/N-m)
6.87	6.831	0.039	3600	0.264	0.264	4.46	0.085	4.443	3.586
6.87	6.793	0.077	7200	0.256	0.256	8.92	0.084	4.386	3.540
6.87	6.755	0.115	10800	0.249	0.249	13.38	0.084	4.367	3.525
6.87	6.718	0.152	14400	0.253	0.253	17.84	0.083	4.329	3.494
6.87	6.68	0.19	18000	0.24	0.24	22.3	0.083	4.329	3.494
6.87	6.643	0.227	21600	0.23	0.23	26.76	0.083	4.310	3.479

Table 23: Wear rate values for pure aluminium with 6% red mud of 42 nm particle size at 600 rpm and 450^0C

Vs=1.2388 m/sec **ρ=2.45 x 1000 kg/m³**

m1	m2	Δm	t	F_f	μ	R.Dx1000	Wr×10^{-6}	Wv×10^{-12}	Ws×10^{-13}
(gm)	(gm)	(gm)	(sec)	(kg)		m	(N/m)	(m³/sec)	(m³/N-m)
7.02	6.983	0.037	3600	0.254	0.254	4.46	0.081	4.215	3.402
7.02	6.947	0.073	7200	0.243	0.243	8.92	0.080	4.158	3.356
7.02	6.911	0.109	10800	0.236	0.236	13.38	0.079	4.139	3.341
7.02	6.875	0.145	14400	0.249	0.249	17.84	0.079	4.130	3.333
7.02	6.84	0.18	18000	0.238	0.238	22.3	0.079	4.101	3.310
7.02	6.805	0.215	21600	0.22	0.22	26.76	0.078	4.082	3.295

Table 24: Wear Rate values for Pure Aluminium with 6% Red mud of 42 nm particle size at 600 rpm and 500^0C

Vs=1.2388 m/sec **ρ=2.45 x 1000 kg/m³**

m_1	m_2	Δm	T	F_f	μ	R.Dx10^{-3}	$W_r \times 10^{-6}$	$W_v \times 10^{-12}$	$W_s \times 10^{-13}$
(gm)	(gm)	(gm)	(sec)	kgf		m	(N/m)	(m³/sec)	(m³/N-m)
6.87	6.832	0.038	3600	0.264	0.264	4.46	0.083	4.329	3.494
6.87	6.795	0.075	7200	0.253	0.253	8.92	0.082	4.272	3.448
6.87	6.758	0.112	10800	0.24	0.24	13.38	0.082	4.253	3.433
6.87	6.722	0.148	14400	0.251	0.251	17.84	0.081	4.215	3.402
6.87	6.685	0.185	18000	0.244	0.244	22.3	0.081	4.215	3.402
6.87	6.65	0.22	21600	0.23	0.23	26.76	0.080	4.177	3.372

ii) Wear rate tables for pure aluminium with red mud at 20 N load (Heat Treatment Condition)

The Wear rate values for pure aluminium with 6% red mud of 100 µm particle size with 200rpm, at 350^0C, 400^0C and 450^0C are shown in Tables 1, 2 and 3 respectively.

Table 1: Wear Rate values for Pure Aluminium with 6% Red mud of 100 µm particle size at 200 rpm and 350^0C

Vs=4.191 X 10^{-1} m/sec **ρ=2.45 x 1000 kg/m³**

m_1	m_2	Δm	T	F_f	µ	R.Dx10^{-3}	$W_r \times 10^{-6}$	$W_v \times 10^{-12}$	$W_s \times 10^{-13}$
(gm)	(gm)	(gm)	(sec)	kgf		m	(N/m)	(m³/sec)	(m³/N-m)
7.1	7.072	0.028	3600	0.41	0.205	1.509	0.179	3.175	3.788
7.1	7.047	0.053	7200	0.42	0.210	3.018	0.172	3.004	3.584
7.1	7.023	0.077	10800	0.39	0.195	4.527	0.167	2.910	3.471
7.1	6.999	0.101	14400	0.41	0.205	6.036	0.164	2.863	3.415
7.1	6.974	0.126	18000	0.45	0.225	7.545	0.164	2.857	3.408
7.1	6.950	0.150	21600	0.4	0.200	9.054	0.162	2.834	3.381

Table 2: Wear Rate values for Pure Aluminium with 6% Red mud of 100 µm particle size at 200 rpm and 400^0C

Vs=4.191 X 10^{-1} m/sec **ρ=2.45 x 1000 kg/m³**

m_1	m_2	Δm	T	F_f	µ	R.Dx10^{-3}	$W_r \times 10^{-6}$	$W_v \times 10^{-12}$	$W_s \times 10^{-13}$
(gm)	(gm)	(gm)	(sec)	kgf		m	(N/m)	(m³/sec)	(m³/N-m)
7.1	7.074	0.026	3600	0.49	0.245	1.509	0.171	2.948	3.517
7.1	7.050	0.050	7200	0.51	0.255	3.018	0.162	2.834	3.381
7.1	7.026	0.074	10800	0.52	0.260	4.527	0.160	2.797	3.337
7.1	7.002	0.098	14400	0.55	0.275	6.036	0.159	2.778	3.314
7.1	6.978	0.122	18000	0.48	0.240	7.545	0.159	2.766	3.300
7.1	6.953	0.147	21600	0.42	0.210	9.054	0.159	2.778	3.314

Table 3: Wear Rate values for Pure Aluminium with 6% Red mud of 100 µm particle size at 200 rpm and 450^0C

Vs=4.191 X 10^{-1} m/sec **ρ=2.45 x 1000 kg/m³**

m_1	m_2	Δm	T	F_f	µ	R.Dx10^{-3}	$W_r \times 10^{-6}$	$W_v \times 10^{-12}$	$W_s \times 10^{-13}$
(gm)	(gm)	(gm)	(sec)	kgf		m	(N/m)	(m³/sec)	(m³/N-m)
7.1	7.076	0.024	3600	0.55	0.275	1.509	0.158	2.721	3.246
7.1	7.054	0.046	7200	0.57	0.285	3.018	0.150	2.608	3.111
7.1	7.032	0.068	10800	0.54	0.290	4.527	0.147	2.570	3.066
7.1	7.010	0.090	14400	0.53	0.265	6.036	0.146	2.551	3.043
7.1	6.988	0.112	18000	0.48	0.240	7.545	0.146	2.540	3.030
7.1	6.966	0.134	21600	0.51	0.255	9.054	0.145	2.532	3.021

The Wear rate values for pure aluminium with 6% red mud of 100 µm particle size with 200 rpm at 500^0C and wear rate values for pure aluminium with 6% red mud of 100 µm particle size with 400 rpm at 350^0C, and 400^0C are shown in Tables 4, 5 and 6 respectively.

Table 4: Wear Rate values for Pure Aluminium with 6% Red mud of 100 µm particle size at 200 rpm and 500^0C

Vs=4.191 X 10^{-1} m/sec **ρ=2.45 x 1000 kg/m³**

m_1	m_2	Δm	T	F_f	µ	R.Dx10^{-3}	$W_r \times 10^{-6}$	$W_v \times 10^{-12}$	$W_s \times 10^{-13}$
(gm)	(gm)	(gm)	(sec)	kgf		m	(N/m)	(m³/sec)	(m³/N-m)
7.1	7.075	0.025	3600	0.61	0.305	1.509	0.165	2.834	3.381
7.1	7.052	0.047	7200	0.63	0.315	3.018	0.153	2.664	3.178
7.1	7.029	0.07	10800	0.59	0.295	4.527	0.152	2.646	3.157
7.1	7.006	0.093	14400	0.65	0.325	6.036	0.151	2.636	3.145
7.1	6.983	0.116	18000	0.62	0.310	7.545	0.151	2.630	3.138
7.1	6.960	0.139	21600	0.49	0.245	9.054	0.151	2.627	3.134

Table 5: Wear Rate values for Pure Aluminium with 6% Red mud of 100 µm particle size at 400 rpm and 350^0C

Vs=8.2416 X 10^{-1} m/sec **ρ=2.45 x 1000 kg/m³**

m_1	m_2	Δm	T	F_f	µ	R.Dx10^{-3}	$W_r \times 10^{-6}$	$W_v \times 10^{-12}$	$W_s \times 10^{-13}$
(gm)	(gm)	(gm)	(sec)	kgf		m	(N/m)	(m³/sec)	(m³/N-m)
7.12	7.076	0.044	3600	0.44	0.220	2.967	0.146	4.989	3.027
7.12	7.035	0.085	7200	0.45	0.225	5.934	0.145	4.818	2.923
7.12	6.994	0.126	10800	0.43	0.215	8.901	0.139	4.762	2.889
7.12	6.953	0.167	14400	0.47	0.235	11.868	0.138	4.734	2.872
7.12	6.912	0.208	18000	0.46	0.230	14.835	0.138	4.716	2.861
7.12	6.871	0.249	21600	0.42	0.210	17.802	0.137	4.705	2.854

Table 6: Wear Rate values for Pure Aluminium with 6% Red mud of 100 µm particle size at 400 rpm and 400^0C

Vs=8.2416 X 10^{-1} m/sec **ρ=2.45 x 1000 kg/m³**

m_1	m_2	Δm	T	F_f	µ	R.Dx10^{-3}	$W_r \times 10^{-6}$	$W_v \times 10^{-12}$	$W_s \times 10^{-13}$
(gm)	(gm)	(gm)	(sec)	kgf		m	(N/m)	(m³/sec)	(m³/N-m)
7.12	7.078	0.042	3600	0.53	0.265	2.967	0.140	4.762	2.889
7.12	7.038	0.082	7200	0.52	0.260	5.934	0.136	4.648	2.820
7.12	6.998	0.122	10800	0.51	0.255	8.901	0.134	4.611	2.797
7.12	6.928	0.192	14400	0.55	0.275	11.868	0.159	5.442	3.302
7.12	6.888	0.232	18000	0.53	0.265	14.835	0.153	5.261	3.192
7.12	6.848	0.272	21600	0.57	0.285	17.802	0.150	5.140	3.118

The Wear rate values for pure aluminium with 6% red mud of 100 μm particle size with 400 rpm at 450^0C, 500^0C and wear rate values for pure aluminium with 6% red mud of 100 μm particle size with 600 rpm at 350^0C are shown in Tables 7, 8 and 9 respectively.

Table 7: Wear Rate values for Pure Aluminium with 6% Red mud of 100 μm particle size at 400 rpm and 450^0C

Vs=8.2416 X 10^{-1} m/sec **ρ=2.45 x 1000 kg/m³**

m_1	m_2	Δm	T	F_f	μ	R.Dx10^{-3}	W_r×10^{-6}	W_v×10^{-12}	W_s×10^{-13}
(gm)	(gm)	(gm)	(sec)	kgf		m	(N/m)	(m³/sec)	(m³/N-m)
7.12	7.081	0.039	3600	0.59	0.295	2.967	0.129	4.422	2.683
7.12	7.045	0.075	7200	0.58	0.290	5.934	0.124	4.252	2.580
7.12	7.009	0.111	10800	0.62	0.310	8.901	0.122	4.195	2.545
7.12	6.973	0.147	14400	0.61	0.305	11.868	0.122	4.167	2.528
7.12	6.938	0.182	18000	0.57	0.285	14.835	0.120	4.127	2.504
7.12	6.901	0.219	21600	0.59	0.295	17.802	0.121	4.138	2.510

Table 8: Wear Rate values for Pure Aluminium with 6% Red mud of 100 μm particle size at 400 rpm and 500^0C

Vs=8.2416 X 10^{-1} m/sec **ρ=2.45 x 1000 kg/m³**

m_1	m_2	Δm	T	F_f	μ	R.Dx10^{-3}	W_r×10^{-6}	W_v×10^{-12}	W_s×10^{-13}
(gm)	(gm)	(gm)	(sec)	kgf		m	(N/m)	(m³/sec)	(m³/N-m)
7.12	7.080	0.040	3600	0.69	0.345	2.967	0.132	4.535	2.751
7.12	7.043	0.077	7200	0.68	0.340	5.934	0.127	4.365	2.648
7.12	7.006	0.114	10800	0.69	0.345	8.901	0.126	4.308	2.614
7.12	6.969	0.151	14400	0.71	0.355	11.868	0.125	4.280	2.596
7.12	6.932	0.188	18000	0.67	0.335	14.835	0.124	4.263	2.586
7.12	6.895	0.225	21600	0.71	0.355	17.802	0.124	4.252	2.580

Table 9: Wear Rate values for Pure Aluminium with 6% Red mud of 100 μm particle size at 600 rpm and 350^0C

Vs=1.2388 m/sec **ρ=2.45 x 1000 kg/m³**

m_1	m_2	Δm	T	F_f	μ	R.Dx10^{-3}	W_r×10^{-6}	W_v×10^{-12}	W_s×10^{-13}
(gm)	(gm)	(gm)	(sec)	kgf		m	(N/m)	(m³/sec)	(m³/N-m)
6.83	6.769	0.061	3600	0.46	0.230	4.46	0.134	6.916	2.791
6.83	6.712	0.118	7200	0.47	0.235	8.92	0.130	6.689	2.700
6.83	6.655	0.175	10800	0.45	0.225	13.38	0.128	6.614	2.670
6.83	6.598	0.232	14400	0.44	0.220	17.84	0.128	6.576	2.654
6.83	6.541	0.289	18000	0.51	0.255	22.3	0.127	6.553	2.645
6.83	6.486	0.344	21600	0.48	0.240	26.76	0.126	6.500	2.624

The Wear rate values for pure aluminium with 6% red mud of 100 µm particle size with 600 rpm, at 400^0C, 450^0C and 500^0C are shown in Tables 10, 11 and 12 respectively.

Table 10: Wear Rate values for Pure Aluminium with 6% Red mud of 100 µm particle size at 600 rpm and 400^0C

Vs=1.2388 m/sec **ρ=2.45 x 1000 kg/m³**

m_1	m_2	Δm	T	F_f	µ	R.Dx10^{-3}	$W_r \times 10^{-6}$	$W_v \times 10^{-12}$	$W_s \times 10^{-13}$
(gm)	(gm)	(gm)	(sec)	kgf		m	(N/m)	(m³/sec)	(m³/N-m)
7.1	7.080	0.020	3600	0.49	0.245	1.509	0.127	2.268	0.915
7.1	7.056	0.044	7200	0.51	0.255	3.018	0.143	2.494	1.007
7.1	7.032	0.068	10800	0.52	0.260	4.527	0.147	2.570	1.037
7.1	7.008	0.092	14400	0.55	0.275	6.036	0.150	2.608	1.053
7.1	6.984	0.116	18000	0.48	0.240	7.545	0.151	2.630	1.062
7.1	6.959	0.141	21600	0.42	0.210	9.054	0.153	2.664	1.075

Table 11: Wear Rate values for Pure Aluminium with 6% Red mud of 100 µm particle size at 600 rpm and 450^0C

Vs=1.2388 m/sec **ρ=2.45 x 1000 kg/m³**

m_1	m_2	Δm	T	F_f	µ	R.Dx10^{-3}	$W_r \times 10^{-6}$	$W_v \times 10^{-12}$	$W_s \times 10^{-13}$
(gm)	(gm)	(gm)	(sec)	kgf		m	(N/m)	(m³/sec)	(m³/N-m)
7.1	7.082	0.018	3600	0.55	0.275	1.509	0.118	2.041	0.824
7.1	7.058	0.045	7200	0.57	0.285	3.018	0.146	2.551	1.030
7.1	7.034	0.067	10800	0.54	0.270	4.527	0.145	2.532	1.022
7.1	7.010	0.089	14400	0.53	0.265	6.036	0.145	2.523	1.018
7.1	6.986	0.111	18000	0.48	0.240	7.545	0.144	2.517	1.016
7.1	6.961	0.133	21600	0.51	0.255	9.054	0.144	2.513	1.014

Table 12: Wear Rate values for Pure Aluminium with 6% Red mud of 100 µm particle size at 600 rpm and 500^0C

Vs=1.2388 m/sec **ρ=2.45 x 1000 kg/m³**

m_1	m_2	Δm	T	F_f	µ	R.Dx10^{-3}	$W_r \times 10^{-6}$	$W_v \times 10^{-12}$	$W_s \times 10^{-13}$
(gm)	(gm)	(gm)	(sec)	kgf		m	(N/m)	(m³/sec)	(m³/N-m)
7.1	7.081	0.019	3600	0.61	0.305	1.509	0.125	2.154	0.869
7.1	7.058	0.042	7200	0.63	0.315	3.018	0.136	2.381	0.961
7.1	7.035	0.065	10800	0.59	0.295	4.527	0.141	2.456	0.991
7.1	7.012	0.088	14400	0.65	0.325	6.036	0.143	2.494	1.007
7.1	6.989	0.111	18000	0.62	0.310	7.545	0.144	2.517	1.016
7.1	6.966	0.134	21600	0.49	0.245	9.054	0.145	2.532	1.022

The Wear rate values for pure aluminium with 6% red mud of 42nm particle size with 200 rpm, at 350^0C, 400^0C and 450^0C are shown in Tables 13, 14 and 15 respectively.

Table 13: Wear Rate values for Pure Aluminium with 6% Red mud of 42 nm particle size at 200 rpm and 350^0C

Vs=4.191 X 10^{-1} m/sec **ρ=2.45 x 1000 kg/m³**

m_1	m_2	Δm	T	F_f	μ	R.Dx10^{-3}	$W_r \times 10^{-6}$	$W_v \times 10^{-12}$	$W_s \times 10^{-13}$
(gm)	(gm)	(gm)	(sec)	kgf		m	(N/m)	(m³/sec)	(m³/N-m)
7.12	7.100	0.020	3600	0.28	0.140	1.509	0.131	2.268	2.706
7.12	7.077	0.043	7200	0.26	0.130	3.018	0.140	2.438	2.909
7.12	7.054	0.066	10800	0.257	0.128	4.527	0.143	2.494	2.975
7.12	7.031	0.089	14400	0.254	0.127	6.036	0.145	2.523	3.010
7.12	7.008	0.112	18000	0.262	0.131	7.545	0.146	2.540	3.030
7.12	6.985	0.135	21600	0.269	0.134	9.054	0.146	2.551	3.043

Table 14: Wear Rate values for Pure Aluminium with 6% Red mud of 42 nm particle size at 200 rpm and 400^0C

Vs=4.191 X 10^{-1} m/sec **ρ=2.45 x 1000 kg/m³**

m_1	m_2	Δm	T	F_f	μ	R.Dx10^{-3}	$W_r \times 10^{-6}$	$W_v \times 10^{-12}$	$W_s \times 10^{-13}$
(gm)	(gm)	(gm)	(sec)	kgf		m	(N/m)	(m³/sec)	(m³/N-m)
6.87	6.851	0.019	3600	0.25	0.125	1.509	0.125	2.154	2.570
6.87	6.833	0.037	7200	0.23	0.115	3.018	0.120	2.098	2.503
6.87	6.816	0.054	10800	0.21	0.105	4.527	0.117	2.041	2.435
6.87	6.799	0.071	14400	0.22	0.110	6.036	0.115	2.012	2.400
6.87	6.782	0.088	18000	0.216	0.108	7.545	0.114	1.995	2.380
6.87	6.765	0.105	21600	0.2	0.100	9.054	0.114	1.984	2.367

Table 15: Wear Rate values for Pure Aluminium with 6% Red mud of 42 nm particle size at 200 rpm and 450^0C

Vs=4.191 X 10^{-1} m/sec **ρ=2.45 x 1000 kg/m³**

m_1	m_2	Δm	T	F_f	μ	R.Dx10^{-3}	$W_r \times 10^{-6}$	$W_v \times 10^{-12}$	$W_s \times 10^{-13}$
(gm)	(gm)	(gm)	(sec)	kgf		m	(N/m)	(m³/sec)	(m³/N-m)
7.02	7.003	0.017	3600	0.21	0.105	1.509	0.113	1.927	4.349
7.02	6.987	0.033	7200	0.206	0.103	3.018	0.107	1.871	4.349
7.02	6.971	0.049	10800	0.199	0.100	4.527	0.106	1.852	4.349
7.02	6.956	0.064	14400	0.209	0.104	6.036	0.104	1.814	4.281
7.02	6.940	0.080	18000	0.213	0.106	7.545	0.104	1.814	4.294
7.02	6.925	0.095	21600	0.204	0.102	9.054	0.103	1.795	4.258

The Wear rate values for pure aluminium with 6% red mud of 42 nm particle size with 200 rpm at 500^0C and wear rate values for pure aluminium with 6% red mud of 42 nm particle size with 400 rpm at 350^0C, and 400^0C are shown in Tables 16, 17 and 18 respectively.

Table 16: Wear Rate values for Pure Aluminium with 6% Red mud of 42 nm particle size at 200 rpm and 500^0C

Vs=4.191 X 10^{-1} m/sec **ρ=2.45 x 1000 kg/m³**

m_1	m_2	Δm	T	F_f	μ	R.Dx10^{-3}	$W_r \times 10^{-6}$	$W_v \times 10^{-12}$	$W_s \times 10^{-13}$
(gm)	(gm)	(gm)	(sec)	kgf		m	(N/m)	(m³/sec)	(m³/N-m)
6.87	6.851	0.019	3600	0.25	0.125	1.509	0.122	2.154	2.570
6.87	6.834	0.036	7200	0.236	0.118	3.018	0.117	2.041	2.435
6.87	6.817	0.053	10800	0.242	0.121	4.527	0.115	2.003	2.390
6.87	6.800	0.070	14400	0.245	0.122	6.036	0.114	1.984	2.367
6.87	6.783	0.087	18000	0.265	0.132	7.545	0.113	1.973	2.354
6.87	6.766	0.104	21600	0.25	0.125	9.054	0.113	1.965	2.344

Table 17: Wear Rate values for Pure Aluminium with 6% Red mud of 42 nm particle size at 400 rpm and 350^0C

Vs=8.2416 X 10^{-1} m/sec **ρ=2.45 x 1000 kg/m³**

m_1	m_2	Δm	T	F_f	μ	R.Dx10^{-3}	$W_r \times 10^{-6}$	$W_v \times 10^{-12}$	$W_s \times 10^{-13}$
(gm)	(gm)	(gm)	(sec)	kgf		m	(N/m)	(m³/sec)	(m³/N-m)
7.12	7.087	0.033	3600	0.256	0.128	2.967	0.108	3.741	2.270
7.12	7.058	0.062	7200	0.256	0.128	5.934	0.102	3.515	2.132
7.12	7.028	0.092	10800	0.243	0.122	8.901	0.101	3.477	2.109
7.12	7.008	0.112	14400	0.234	0.117	11.868	0.093	3.175	1.926
7.12	6.978	0.142	18000	0.239	0.120	14.835	0.094	3.220	1.953
7.12	6.948	0.172	21600	0.23	0.115	17.802	0.095	3.250	1.972

Table 18: Wear Rate values for Pure Aluminium with 6% Red mud of 42 nm particle size at 400 rpm and 400^0C

Vs=8.2416 X 10^{-1} m/sec **ρ=2.45 x 1000 kg/m³**

m_1	m_2	Δm	T	F_f	μ	R.Dx10^{-3}	$W_r \times 10^{-6}$	$W_v \times 10^{-12}$	$W_s \times 10^{-13}$
(gm)	(gm)	(gm)	(sec)	kgf		m	(N/m)	(m³/sec)	(m³/N-m)
6.87	6.839	0.031	3600	0.236	0.118	2.967	0.101	3.515	2.132
6.87	6.811	0.059	7200	0.21	0.105	5.934	0.098	3.345	2.029
6.87	6.782	0.088	10800	0.18	0.090	8.901	0.097	3.326	2.018
6.87	6.754	0.116	14400	0.209	0.104	11.868	0.096	3.288	1.995
6.87	6.728	0.142	18000	0.205	0.102	14.835	0.094	3.220	1.954
6.87	6.701	0.169	21600	0.186	0.093	17.802	0.093	3.193	1.937

The Wear rate values for pure aluminium with 6% red mud of 42 nm particle size with 400 rpm at 450^0C, 500^0C and wear rate values for pure aluminium with 6% red mud of 42 nm particle size with 600 rpm at 350^0C, are shown in Tables 19, 20 and 21 respectively.

Table 19: Wear Rate values for Pure Aluminium with 6% Red mud of 42 nm particle size at 400 rpm and 450^0C

Vs=8.2416 X 10^{-1} m/sec **ρ=2.45 x 1000 kg/m³**

m_1	m_2	Δm	T	F_f	μ	R.Dx10^{-3}	$W_r \times 10^{-6}$	$W_v \times 10^{-12}$	$W_s \times 10^{-13}$
(gm)	(gm)	(gm)	(sec)	kgf		m	(N/m)	(m³/sec)	(m³/N-m)
7.02	6.992	0.028	3600	0.226	0.113	2.967	0.094	3.175	1.926
7.02	6.966	0.054	7200	0.219	0.110	5.934	0.089	3.061	1.857
7.02	6.939	0.081	10800	0.2	0.100	8.901	0.089	3.061	1.857
7.02	6.914	0.106	14400	0.17	0.085	11.868	0.088	3.004	1.822
7.02	6.889	0.131	18000	0.213	0.106	14.835	0.087	2.971	1.802
7.02	6.864	0.156	21600	0.207	0.104	17.802	0.086	2.948	1.788

Table 20: Wear Rate values for Pure Aluminium with 6% Red mud of 42 nm particle size at 400 rpm and 500^0C

Vs=8.2416 X 10^{-1} m/sec **ρ=2.45 x 1000 kg/m³**

m_1	m_2	Δm	T	F_f	μ	R.Dx10^{-3}	$W_r \times 10^{-6}$	$W_v \times 10^{-12}$	$W_s \times 10^{-13}$
(gm)	(gm)	(gm)	(sec)	kgf		m	(N/m)	(m³/sec)	(m³/N-m)
6.87	6.841	0.029	3600	0.236	0.118	2.967	0.0966	3.288	1.995
6.87	6.814	0.056	7200	0.22	0.110	5.934	0.0926	3.175	1.926
6.87	6.787	0.083	10800	0.216	0.108	8.901	0.0915	3.137	1.903
6.87	6.759	0.111	14400	0.205	0.102	11.868	0.0918	3.146	1.909
6.87	6.732	0.138	18000	0.223	0.112	14.835	0.0912	3.129	1.898
6.87	6.705	0.165	21600	0.215	0.108	17.802	0.0909	3.118	1.892

Table 21: Wear Rate values for Pure Aluminium with 6% Red mud of 42 nm particle size at 600 rpm and 350^0C

Vs=1.2388 m/sec **ρ=2.45 x 1000 kg/m³**

m_1	m_2	Δm	T	F_f	μ	R.Dx10^{-3}	$W_r \times 10^{-6}$	$W_v \times 10^{-12}$	$W_s \times 10^{-13}$
(gm)	(gm)	(gm)	(sec)	kgf		m	(N/m)	(m³/sec)	(m³/N-m)
7.12	7.075	0.045	3600	0.27	0.135	4.46	0.0998	5.102	2.059
7.12	7.033	0.087	7200	0.264	0.132	8.92	0.0957	4.932	1.991
7.12	6.991	0.129	10800	0.256	0.128	13.38	0.0946	4.875	1.968
7.12	6.949	0.171	14400	0.25	0.125	17.84	0.0940	4.847	1.956
7.12	6.907	0.213	18000	0.262	0.131	22.3	0.0937	4.830	1.949
7.12	6.868	0.252	21600	0.258	0.129	26.76	0.0924	4.762	1.922

The Wear rate values for pure aluminium with 6% red mud of 42 μm particle size with 600 rpm, at 400^0C, 450^0C and 500^0C are shown in Tables 22, 23 and 24 respectively.

Table 22: Wear Rate values for Pure Aluminium with 6% Red mud of 42 nm particle size at 600 rpm and 400^0C

Vs=1.2388 m/sec **ρ=2.45 x 1000 kg/m³**

m_1	m_2	Δm	T	F_f	μ	R.Dx10^{-3}	$W_r \times 10^{-6}$	$W_v \times 10^{-12}$	$W_s \times 10^{-13}$
(gm)	(gm)	(gm)	(sec)	kgf		m	(N/m)	(m³/sec)	(m³/N-m)
6.87	6.829	0.041	3600	0.264	0.132	4.46	0.0902	4.648	1.876
6.87	6.791	0.079	7200	0.256	0.128	8.92	0.0869	4.478	1.807
6.87	6.753	0.117	10800	0.249	0.124	13.38	0.0858	4.422	1.785
6.87	6.716	0.154	14400	0.253	0.126	17.84	0.0847	4.365	1.762
6.87	6.678	0.192	18000	0.24	0.120	22.3	0.0845	4.354	1.757
6.87	6.641	0.229	21600	0.23	0.115	26.76	0.0839	4.327	1.746

Table 23: Wear Rate values for Pure Aluminium with 6% Red mud of 42 nm particle size at 600 rpm and 450^0C

Vs=1.2388 m/sec **ρ=2.45 x 1000 kg/m³**

m_1	m_2	Δm	T	F_f	μ	R.Dx10^{-3}	$W_r \times 10^{-6}$	$W_v \times 10^{-12}$	$W_s \times 10^{-13}$
(gm)	(gm)	(gm)	(sec)	kgf		m	(N/m)	(m³/sec)	(m³/N-m)
7.02	6.981	0.039	3600	0.254	0.127	4.46	0.086	4.422	1.785
7.02	6.945	0.075	7200	0.243	0.122	8.92	0.082	4.252	1.716
7.02	6.909	0.111	10800	0.236	0.118	13.38	0.081	4.195	1.693
7.02	6.873	0.147	14400	0.249	0.124	17.84	0.081	4.167	1.682
7.02	6.838	0.182	18000	0.238	0.119	22.3	0.080	4.127	1.666
7.02	6.803	0.217	21600	0.22	0.110	26.76	0.080	4.100	1.655

Table 24: Wear Rate values for Pure Aluminium with 6% Red mud of 42 nm particle size at 600 rpm and 500^0C

Vs=1.2388 m/sec **ρ=2.45 x 1000 kg/m³**

m_1	m_2	Δm	T	F_f	μ	R.Dx10^{-3}	$W_r \times 10^{-6}$	$W_v \times 10^{-12}$	$W_s \times 10^{-13}$
(gm)	(gm)	(gm)	(sec)	kgf		m	(N/m)	(m³/sec)	(m³/N-m)
6.87	6.830	0.040	3600	0.264	0.132	4.46	0.088	4.535	1.830
6.87	6.793	0.077	7200	0.253	0.126	8.92	0.084	4.365	1.762
6.87	6.756	0.114	10800	0.24	0.120	13.38	0.083	4.308	1.739
6.87	6.720	0.150	14400	0.251	0.126	17.84	0.082	4.252	1.716
6.87	6.683	0.187	18000	0.244	0.122	22.3	0.082	4.240	1.711
6.87	6.648	0.222	21600	0.23	0.115	26.76	0.081	4.195	1.693

iii) Wear rate tables for pure aluminium with red mud at 30 N load (Heat Treatment Condition)

The Wear rate values for pure aluminium with 6% red mud of 100 µm particle size with 200rpm, at 350^0C, 400^0C and 450^0C are shown in Tables 1, 2 and 3 respectively.

Table 1: Wear Rate values for Pure Aluminium with 6% Red mud of 100 µm particle size at 200 rpm and 350^0C

Vs=4.191 X 10^{-1} m/sec **ρ=2.45 x 1000 kg/m³**

m_1	m_2	Δm	T	F_f	µ	R.Dx10^{-3}	$W_r \times 10^{-6}$	$W_v \times 10^{-12}$	$W_s \times 10^{-13}$
(gm)	(gm)	(gm)	(sec)	kgf		m	(N/m)	(m³/sec)	(m³/N-m)
7.1	7.072	0.028	3600	0.41	0.137	1.509	0.182	3.175	2.525
7.1	7.047	0.053	7200	0.42	0.140	3.018	0.172	3.004	2.389
7.1	7.023	0.077	10800	0.39	0.130	4.527	0.167	2.910	2.314
7.1	6.999	0.101	14400	0.41	0.137	6.036	0.164	2.863	2.277
7.1	6.974	0.126	18000	0.45	0.150	7.545	0.164	2.857	2.272
7.1	6.950	0.150	21600	0.4	0.133	9.054	0.162	2.834	2.254

Table 2: Wear Rate values for Pure Aluminium with 6% Red mud of 100 µm particle size at 200 rpm and 400^0C

Vs=4.191 X 10^{-1} m/sec **ρ=2.45 x 1000 kg/m³**

m_1	m_2	Δm	T	F_f	µ	R.Dx10^{-3}	$W_r \times 10^{-6}$	$W_v \times 10^{-12}$	$W_s \times 10^{-13}$
(gm)	(gm)	(gm)	(sec)	kgf		m	(N/m)	(m³/sec)	(m³/N-m)
7.1	7.073	0.027	3600	0.49	0.163	1.509	0.176	3.061	2.434
7.1	7.049	0.051	7200	0.51	0.170	3.018	0.166	2.891	2.299
7.1	7.025	0.075	10800	0.52	0.173	4.527	0.162	2.834	2.254
7.1	7.001	0.099	14400	0.55	0.183	6.036	0.161	2.806	2.232
7.1	6.977	0.123	18000	0.48	0.160	7.545	0.160	2.789	2.218
7.1	6.952	0.148	21600	0.42	0.140	9.054	0.160	2.797	2.225

Table 3: Wear Rate values for Pure Aluminium with 6% Red mud of 100 µm particle size at 200 rpm and 450^0C

Vs=4.191 X 10^{-1} m/sec **ρ=2.45 x 1000 kg/m³**

m_1	m_2	Δm	T	F_f	µ	R.Dx10^{-3}	$W_r \times 10^{-6}$	$W_v \times 10^{-12}$	$W_s \times 10^{-13}$
(gm)	(gm)	(gm)	(sec)	kgf		m	(N/m)	(m³/sec)	(m³/N-m)
7.1	7.074	0.026	3600	0.55	0.183	1.509	0.169	2.948	2.345
7.1	7.052	0.048	7200	0.57	0.190	3.018	0.156	2.721	2.164
7.1	7.030	0.070	10800	0.54	0.180	4.527	0.152	2.646	2.104
7.1	7.008	0.092	14400	0.53	0.177	6.036	0.150	2.608	2.074
7.1	6.986	0.114	18000	0.48	0.160	7.545	0.148	2.585	2.056
7.1	6.964	0.136	21600	0.51	0.170	9.054	0.147	2.570	2.044

The Wear rate values for pure aluminium with 6% red mud of 100 µm particle size with 200 rpm at 500^0C and wear rate values for pure aluminium with 6% red mud of 100 µm particle size with 400 rpm at 350^0C, and 400^0C are shown in Tables 4, 5 and 6 respectively.

Table 4: Wear Rate values for Pure Aluminium with 6% Red mud of 100 µm particle size at 200 rpm and 500^0C

Vs=4.191 X 10^{-1} m/sec **ρ=2.45 x 1000 kg/m³**

m_1 (gm)	m_2 (gm)	Δm (gm)	T (sec)	F_f kgf	µ	R.Dx10^{-3} m	W_r×10^{-6} (N/m)	W_v×10^{-12} (m³/sec)	W_s×10^{-13} (m³/N-m)
7.1	7.073	0.027	3600	0.61	0.203	1.509	0.174	3.061	2.434
7.1	7.050	0.050	7200	0.63	0.210	3.018	0.162	2.834	2.254
7.1	7.027	0.073	10800	0.59	0.197	4.527	0.158	2.759	2.194
7.1	7.004	0.096	14400	0.65	0.217	6.036	0.156	2.721	2.164
7.1	6.981	0.119	18000	0.62	0.207	7.545	0.155	2.698	2.146
7.1	6.958	0.142	21600	0.49	0.163	9.054	0.154	2.683	2.134

Table 5: Wear Rate values for Pure Aluminium with 6% Red mud of 100 µm particle size at 400 rpm and 350^0C

Vs=8.2416 X 10^{-1} m/sec **ρ=2.45 x 1000 kg/m³**

m_1 (gm)	m_2 (gm)	Δm (gm)	T (sec)	F_f kgf	µ	R.Dx10^{-3} m	W_r×10^{-6} (N/m)	W_v×10^{-12} (m³/sec)	W_s×10^{-13} (m³/N-m)
7.12	7.074	0.046	3600	0.44	0.147	2.967	0.153	5.215	2.109
7.12	7.033	0.087	7200	0.45	0.150	5.934	0.144	4.932	1.995
7.12	6.992	0.128	10800	0.43	0.143	8.901	0.141	4.837	1.956
7.12	6.951	0.169	14400	0.47	0.157	11.868	0.140	4.790	1.937
7.12	6.910	0.210	18000	0.46	0.153	14.835	0.139	4.762	1.926
7.12	6.869	0.251	21600	0.42	0.140	17.802	0.138	4.743	1.918

Table 6: Wear Rate values for Pure Aluminium with 6% Red mud of 100 µm particle size at 400 rpm and 400^0C

Vs=8.2416 X 10^{-1} m/sec **ρ=2.45 x 1000 kg/m³**

m_1 (gm)	m_2 (gm)	Δm (gm)	T (sec)	F_f kgf	µ	R.Dx10^{-3} m	W_r×10^{-6} (N/m)	W_v×10^{-12} (m³/sec)	W_s×10^{-13} (m³/N-m)
7.12	7.075	0.045	3600	0.53	0.177	2.967	0.148	5.102	2.064
7.12	7.035	0.085	7200	0.52	0.173	5.934	0.141	4.818	1.949
7.12	6.995	0.125	10800	0.51	0.170	8.901	0.138	4.724	1.911
7.12	6.925	0.195	14400	0.55	0.183	11.868	0.161	5.527	2.235
7.12	6.885	0.235	18000	0.53	0.177	14.835	0.155	5.329	2.155
7.12	6.845	0.275	21600	0.57	0.190	17.802	0.152	5.196	2.102

The Wear rate values for pure aluminium with 6% red mud of 100 µm particle size with 400 rpm at 450^0C, 500^0C and wear rate values for pure aluminium with 6% red mud of 100 µm particle size with 600 rpm at 350^0C are shown in Tables 7, 8 and 9 respectively.

Table 7: Wear Rate values for Pure Aluminium with 6% Red mud of 100 µm particle size at 400 rpm and 450^0C

Vs=8.2416 X 10^{-1} m/sec **ρ=2.45 x 1000 kg/m³**

m_1 (gm)	m_2 (gm)	Δm (gm)	T (sec)	F_f kgf	µ	R.Dx10^{-3} m	$W_r \times 10^{-6}$ (N/m)	$W_v \times 10^{-12}$ (m³/sec)	$W_s \times 10^{-13}$ (m³/N-m)
7.12	7.080	0.040	3600	0.59	0.197	2.967	0.135	4.535	1.834
7.12	7.044	0.076	7200	0.58	0.193	5.934	0.126	4.308	1.742
7.12	7.008	0.112	10800	0.62	0.207	8.901	0.123	4.233	1.712
7.12	6.972	0.148	14400	0.61	0.203	11.868	0.122	4.195	1.697
7.12	6.937	0.183	18000	0.57	0.190	14.835	0.121	4.150	1.678
7.12	6.900	0.220	21600	0.59	0.197	17.802	0.121	4.157	1.681

Table 8: Wear Rate values for Pure Aluminium with 6% Red mud of 100 µm particle size at 400 rpm and 500^0C

Vs=8.2416 X 10^{-1} m/sec **ρ=2.45 x 1000 kg/m³**

m_1 (gm)	m_2 (gm)	Δm (gm)	T (sec)	F_f kgf	µ	R.Dx10^{-3} m	$W_r \times 10^{-6}$ (N/m)	$W_v \times 10^{-12}$ (m³/sec)	$W_s \times 10^{-13}$ (m³/N-m)
7.12	7.080	0.040	3600	0.69	0.230	2.967	0.139	4.535	1.834
7.12	7.043	0.077	7200	0.68	0.227	5.934	0.127	4.365	1.765
7.12	7.006	0.114	10800	0.69	0.230	8.901	0.126	4.308	1.742
7.12	6.969	0.151	14400	0.71	0.237	11.868	0.125	4.280	1.731
7.12	6.932	0.188	18000	0.67	0.223	14.835	0.124	4.263	1.724
7.12	6.895	0.225	21600	0.71	0.237	17.802	0.124	4.252	1.720

Table 9: Wear Rate values for Pure Aluminium with 6% Red mud of 100 µm particle size at 600 rpm and 350^0C

Vs=1.2388 m/sec **ρ=2.45 x 1000 kg/m³**

m_1 (gm)	m_2 (gm)	Δm (gm)	T (sec)	F_f kgf	µ	R.Dx10^{-3} m	$W_r \times 10^{-6}$ (N/m)	$W_v \times 10^{-12}$ (m³/sec)	$W_s \times 10^{-13}$ (m³/N-m)
6.83	6.770	0.060	3600	0.46	0.153	4.46	0.141	6.803	1.831
6.83	6.713	0.117	7200	0.47	0.157	8.92	0.129	6.633	1.785
6.83	6.656	0.174	10800	0.45	0.150	13.38	0.128	6.576	1.769
6.83	6.599	0.231	14400	0.44	0.147	17.84	0.127	6.548	1.762
6.83	6.542	0.288	18000	0.51	0.170	22.3	0.127	6.531	1.757
6.83	6.487	0.343	21600	0.48	0.160	26.76	0.126	6.481	1.744

The Wear rate values for pure aluminium with 6% red mud of 100 μm particle size with 600 rpm, at 400^0C, 450^0C and 500^0C are shown in Tables 10, 11 and 12 respectively.

Table 10: Wear Rate values for Pure Aluminium with 6% Red mud of 100 μm particle size at 600 rpm and 400^0C

Vs=1.2388 m/sec **ρ=2.45 x 1000 kg/m³**

m_1	m_2	Δm	T	F_f	μ	R.Dx10^{-3}	$W_r \times 10^{-6}$	$W_v \times 10^{-12}$	$W_s \times 10^{-13}$
(gm)	(gm)	(gm)	(sec)	kgf		m	(N/m)	(m³/sec)	(m³/N-m)
7.1	7.079	0.021	3600	0.49	0.163	1.509	0.136	2.381	0.641
7.1	7.055	0.045	7200	0.51	0.170	3.018	0.146	2.551	0.686
7.1	7.031	0.069	10800	0.52	0.173	4.527	0.150	2.608	0.702
7.1	7.007	0.093	14400	0.55	0.183	6.036	0.151	2.636	0.709
7.1	6.983	0.117	18000	0.48	0.160	7.545	0.152	2.653	0.714
7.1	6.958	0.142	21600	0.42	0.140	9.054	0.154	2.683	0.722

Table 11: Wear Rate values for Pure Aluminium with 6% Red mud of 100 μm particle size at 600 rpm and 450^0C

Vs=1.2388 m/sec **ρ=2.45 x 1000 kg/m³**

m_1	m_2	Δm	T	F_f	μ	R.Dx10^{-3}	$W_r \times 10^{-6}$	$W_v \times 10^{-12}$	$W_s \times 10^{-13}$
(gm)	(gm)	(gm)	(sec)	kgf		m	(N/m)	(m³/sec)	(m³/N-m)
7.1	7.082	0.018	3600	0.55	0.183	1.509	0.120	2.041	0.549
7.1	7.060	0.040	7200	0.57	0.190	3.018	0.130	2.268	0.610
7.1	7.038	0.062	10800	0.54	0.180	4.527	0.134	2.343	0.630
7.1	7.016	0.084	14400	0.53	0.177	6.036	0.136	2.381	0.641
7.1	6.994	0.106	18000	0.48	0.160	7.545	0.138	2.404	0.647
7.1	6.972	0.128	21600	0.51	0.170	9.054	0.139	2.419	0.651

Table 12: Wear Rate values for Pure Aluminium with 6% Red mud of 100 μm particle size at 600 rpm and 500^0C

Vs=1.2388 m/sec **ρ=2.45 x 1000 kg/m³**

m_1	m_2	Δm	T	F_f	μ	R.Dx10^{-3}	$W_r \times 10^{-6}$	$W_v \times 10^{-12}$	$W_s \times 10^{-13}$
(gm)	(gm)	(gm)	(sec)	kgf		m	(N/m)	(m³/sec)	(m³/N-m)
7.1	7.080	0.020	3600	0.61	0.203	1.509	0.128	2.268	0.610
7.1	7.057	0.043	7200	0.63	0.210	3.018	0.140	2.438	0.656
7.1	7.034	0.066	10800	0.59	0.197	4.527	0.143	2.494	0.671
7.1	7.011	0.089	14400	0.65	0.217	6.036	0.145	2.523	0.679
7.1	6.988	0.112	18000	0.62	0.207	7.545	0.146	2.540	0.683
7.1	6.965	0.135	21600	0.49	0.163	9.054	0.146	2.551	0.686

The Wear rate values for pure aluminium with 6% red mud of 42nm particle size with 200 rpm, at 350^0C, 400^0C and 450^0C are shown in Tables 13, 14 and 15 respectively.

Table 13: Wear Rate values for Pure Aluminium with 6% Red mud of 42 nm particle size at 200 rpm and 350^0C

Vs=4.191 X 10^{-1} m/sec **ρ=2.45 x 1000 kg/m³**

m_1	m_2	Δm	T	F_f	μ	R.Dx10^{-3}	$W_r \times 10^{-6}$	$W_v \times 10^{-12}$	$W_s \times 10^{-13}$
(gm)	(gm)	(gm)	(sec)	kgf		m	(N/m)	(m³/sec)	(m³/N-m)
7.12	7.100	0.020	3600	0.28	0.093	1.509	0.137	2.268	1.804
7.12	7.081	0.039	7200	0.26	0.087	3.018	0.127	2.211	1.758
7.12	7.063	0.057	10800	0.257	0.086	4.527	0.124	2.154	1.713
7.12	7.044	0.076	14400	0.254	0.085	6.036	0.124	2.154	1.713
7.12	7.026	0.094	18000	0.262	0.087	7.545	0.122	2.132	1.696
7.12	7.007	0.113	21600	0.269	0.090	9.054	0.122	2.135	1.698

Table 14: Wear Rate values for Pure Aluminium with 6% Red mud of 42 nm particle size at 200 rpm and 400^0C

Vs=4.191 X 10^{-1} m/sec **ρ=2.45 x 1000 kg/m³**

m_1	m_2	Δm	T	F_f	μ	R.Dx10^{-3}	$W_r \times 10^{-6}$	$W_v \times 10^{-12}$	$W_s \times 10^{-13}$
(gm)	(gm)	(gm)	(sec)	kgf		m	(N/m)	(m³/sec)	(m³/N-m)
6.87	6.850	0.020	3600	0.25	0.083	1.509	0.132	2.268	1.804
6.87	6.832	0.038	7200	0.23	0.077	3.018	0.124	2.154	1.713
6.87	6.815	0.055	10800	0.21	0.070	4.527	0.119	2.079	1.654
6.87	6.798	0.072	14400	0.22	0.073	6.036	0.117	2.041	1.623
6.87	6.781	0.089	18000	0.216	0.072	7.545	0.116	2.018	1.605
6.87	6.764	0.106	21600	0.2	0.067	9.054	0.115	2.003	1.593

Table 15: Wear Rate values for Pure Aluminium with 6% Red mud of 42 nm particle size at 200 rpm and 450^0C

Vs=4.191 X 10^{-1} m/sec **ρ=2.45 x 1000 kg/m³**

m_1	m_2	Δm	T	F_f	μ	R.Dx10^{-3}	$W_r \times 10^{-6}$	$W_v \times 10^{-12}$	$W_s \times 10^{-13}$
(gm)	(gm)	(gm)	(sec)	kgf		m	(N/m)	(m³/sec)	(m³/N-m)
7.02	7.002	0.018	3600	0.21	0.070	1.509	0.119	2.041	1.623
7.02	6.986	0.034	7200	0.206	0.069	3.018	0.111	1.927	1.533
7.02	6.970	0.050	10800	0.199	0.066	4.527	0.108	1.890	1.503
7.02	6.955	0.065	14400	0.209	0.070	6.036	0.106	1.842	1.465
7.02	6.939	0.081	18000	0.213	0.071	7.545	0.105	1.837	1.461
7.02	6.924	0.096	21600	0.204	0.068	9.054	0.104	1.814	1.443

The Wear rate values for pure aluminium with 6% red mud of 42 nm particle size with 200 rpm at 500^0C and wear rate values for pure aluminium with 6% red mud of 42 nm particle size with 400 rpm at 350^0C, and 400^0C are shown in Tables 16, 17 and 18 respectively.

Table 16: Wear Rate values for Pure Aluminium with 6% Red mud of 42 nm particle size at 200 rpm and 500^0C

Vs=4.191 X 10^{-1} m/sec **ρ=2.45 x 1000 kg/m³**

m_1	m_2	Δm	T	F_f	μ	R.Dx10^{-3}	$W_r \times 10^{-6}$	$W_v \times 10^{-12}$	$W_s \times 10^{-13}$
(gm)	(gm)	(gm)	(sec)	kgf		M	(N/m)	(m³/sec)	(m³/N-m)
6.87	6.851	0.019	3600	0.25	0.083	1.509	0.126	2.154	1.713
6.87	6.834	0.036	7200	0.236	0.079	3.018	0.117	2.041	1.623
6.87	6.817	0.053	10800	0.242	0.081	4.527	0.115	2.003	1.593
6.87	6.800	0.070	14400	0.245	0.082	6.036	0.114	1.984	1.578
6.87	6.783	0.087	18000	0.265	0.088	7.545	0.113	1.973	1.569
6.87	6.766	0.104	21600	0.25	0.083	9.054	0.113	1.965	1.563

Table 17: Wear Rate values for Pure Aluminium with 6% Red mud of 42 nm particle size at 400 rpm and 350^0C

Vs=8.2416 X 10^{-1} m/sec **ρ=2.45 x 1000 kg/m³**

m_1	m_2	Δm	T	F_f	μ	R.Dx10^{-3}	$W_r \times 10^{-6}$	$W_v \times 10^{-12}$	$W_s \times 10^{-13}$
(gm)	(gm)	(gm)	(sec)	kgf		M	(N/m)	(m³/sec)	(m³/N-m)
7.12	7.086	0.034	3600	0.256	0.085	2.967	0.114	3.855	1.559
7.12	7.057	0.063	7200	0.256	0.085	5.934	0.104	3.571	1.444
7.12	7.027	0.093	10800	0.243	0.081	8.901	0.102	3.515	1.422
7.12	7.007	0.113	14400	0.234	0.078	11.868	0.093	3.203	1.295
7.12	6.977	0.143	18000	0.239	0.080	14.835	0.094	3.243	1.312
7.12	6.947	0.173	21600	0.23	0.077	17.802	0.095	3.269	1.322

Table 18: Wear Rate values for Pure Aluminium with 6% Red mud of 42 nm particle size at 400 rpm and 400^0C

Vs=8.2416 X 10^{-1} m/sec **ρ=2.45 x 1000 kg/m³**

m_1	m_2	Δm	T	F_f	μ	R.Dx10^{-3}	$W_r \times 10^{-6}$	$W_v \times 10^{-12}$	$W_s \times 10^{-13}$
(gm)	(gm)	(gm)	(sec)	kgf		m	(N/m)	(m³/sec)	(m³/N-m)
6.87	6.838	0.032	3600	0.236	0.079	2.967	0.105	3.628	1.467
6.87	6.810	0.060	7200	0.21	0.070	5.934	0.099	3.401	1.376
6.87	6.781	0.089	10800	0.18	0.060	8.901	0.098	3.364	1.361
6.87	6.753	0.117	14400	0.209	0.070	11.868	0.097	3.316	1.341
6.87	6.727	0.143	18000	0.205	0.068	14.835	0.094	3.243	1.312
6.87	6.700	0.170	21600	0.186	0.062	17.802	0.094	3.212	1.299

The Wear rate values for pure aluminium with 6% red mud of 42 nm particle size with 400 rpm at 450^0C, 500^0C and wear rate values for pure aluminium with 6% red mud of 42 nm particle size with 600 rpm at 350^0C, are shown in Tables 19, 20 and 21 respectively.

Table 19: Wear Rate values for Pure Aluminium with 6% Red mud of 42 nm particle size at 400 rpm and 450^0C

Vs=8.2416 X 10^{-1} m/sec **ρ=2.45 x 1000 kg/m³**

m_1	m_2	Δm	T	F_f	μ	R.Dx10^{-3}	$W_r \times 10^{-6}$	$W_v \times 10^{-12}$	$W_s \times 10^{-13}$
(gm)	(gm)	(gm)	(sec)	kgf		m	(N/m)	(m³/sec)	(m³/N-m)
7.02	6.989	0.031	3600	0.226	0.075	2.967	0.101	3.515	1.422
7.02	6.963	0.057	7200	0.219	0.073	5.934	0.094	3.231	1.307
7.02	6.936	0.084	10800	0.2	0.067	8.901	0.092	3.175	1.284
7.02	6.911	0.109	14400	0.17	0.057	11.868	0.090	3.090	1.250
7.02	6.886	0.134	18000	0.213	0.071	14.835	0.089	3.038	1.229
7.02	6.861	0.159	21600	0.207	0.069	17.802	0.088	3.004	1.215

Table 20: Wear Rate values for Pure Aluminium with 6% Red mud of 42 nm particle size at 400 rpm and 500^0C

Vs=8.2416 X 10^{-1} m/sec **ρ=2.45 x 1000 kg/m³**

m_1	m_2	Δm	T	F_f	μ	R.Dx10^{-3}	$W_r \times 10^{-6}$	$W_v \times 10^{-12}$	$W_s \times 10^{-13}$
(gm)	(gm)	(gm)	(sec)	kgf		m	(N/m)	(m³/sec)	(m³/N-m)
6.87	6.838	0.032	3600	0.236	0.079	2.967	0.105	3.628	1.467
6.87	6.811	0.059	7200	0.22	0.073	5.934	0.098	3.345	1.353
6.87	6.784	0.086	10800	0.216	0.072	8.901	0.095	3.250	1.314
6.87	6.756	0.114	14400	0.205	0.068	11.868	0.094	3.231	1.307
6.87	6.729	0.141	18000	0.223	0.074	14.835	0.093	3.197	1.293
6.87	6.702	0.168	21600	0.215	0.072	17.802	0.092	3.175	1.284

Table 21: Wear Rate values for Pure Aluminium with 6% Red mud of 42 nm particle size at 600 rpm and 350^0C

Vs=1.2388 m/sec **ρ=2.45 x 1000 kg/m³**

m_1	m_2	Δm	T	F_f	μ	R.Dx10^{-3}	$W_r \times 10^{-6}$	$W_v \times 10^{-12}$	$W_s \times 10^{-13}$
(gm)	(gm)	(gm)	(sec)	kgf		m	(N/m)	(m³/sec)	(m³/N-m)
7.12	7.073	0.047	3600	0.27	0.090	4.46	0.103	5.329	1.434
7.12	7.031	0.089	7200	0.264	0.088	8.92	0.098	5.045	1.357
7.12	6.989	0.131	10800	0.256	0.085	13.38	0.096	4.951	1.332
7.12	6.947	0.173	14400	0.25	0.083	17.84	0.095	4.904	1.320
7.12	6.905	0.215	18000	0.262	0.087	22.3	0.094	4.875	1.312
7.12	6.866	0.254	21600	0.258	0.086	26.76	0.093	4.800	1.292

The Wear rate values for pure aluminium with 6% red mud of 42 μm particle size with 600 rpm, at 400^0C, 450^0C and 500^0C are shown in Tables 22, 23 and 24 respectively.

Table 22: Wear Rate values for Pure Aluminium with 6% Red mud of 42 nm particle size at 600 rpm and 400^0C

Vs=1.2388 m/sec **ρ=2.45 x 1000 kg/m³**

m_1	m_2	Δm	T	F_f	μ	R.Dx10^{-3}	$W_r \times 10^{-6}$	$W_v \times 10^{-12}$	$W_s \times 10^{-13}$
(gm)	(gm)	(gm)	(sec)	kgf		m	(N/m)	(m³/sec)	(m³/N-m)
6.87	6.827	0.043	3600	0.264	0.088	4.46	0.095	4.875	1.312
6.87	6.789	0.081	7200	0.256	0.085	8.92	0.089	4.592	1.236
6.87	6.751	0.119	10800	0.249	0.083	13.38	0.087	4.497	1.210
6.87	6.714	0.156	14400	0.253	0.084	17.84	0.086	4.422	1.190
6.87	6.676	0.194	18000	0.24	0.080	22.3	0.085	4.399	1.184
6.87	6.639	0.231	21600	0.23	0.077	26.76	0.085	4.365	1.174

Table 23: Wear Rate values for Pure Aluminium with 6% Red mud of 42 nm particle size at 600 rpm and 450^0C

Vs=1.2388 m/sec **ρ=2.45 x 1000 kg/m³**

m_1	m_2	Δm	T	F_f	μ	R.Dx10^{-3}	$W_r \times 10^{-6}$	$W_v \times 10^{-12}$	$W_s \times 10^{-13}$
(gm)	(gm)	(gm)	(sec)	kgf		m	(N/m)	(m³/sec)	(m³/N-m)
7.02	6.980	0.040	3600	0.254	0.085	4.46	0.089	4.535	1.220
7.02	6.944	0.076	7200	0.243	0.081	8.92	0.084	4.308	1.159
7.02	6.908	0.112	10800	0.236	0.079	13.38	0.082	4.233	1.139
7.02	6.872	0.148	14400	0.249	0.083	17.84	0.081	4.195	1.129
7.02	6.837	0.183	18000	0.238	0.079	22.3	0.081	4.150	1.117
7.02	6.802	0.218	21600	0.22	0.073	26.76	0.080	4.119	1.108

Table 24: Wear Rate values for Pure Aluminium with 6% Red mud of 42 nm particle size at 600 rpm and 500^0C

Vs=1.2388 m/sec **ρ=2.45 x 1000 kg/m³**

m_1	m_2	Δm	T	F_f	μ	R.Dx10^{-3}	$W_r \times 10^{-6}$	$W_v \times 10^{-12}$	$W_s \times 10^{-13}$
(gm)	(gm)	(gm)	(sec)	kgf		m	(N/m)	(m³/sec)	(m³/N-m)
6.87	6.828	0.042	3600	0.264	0.088	4.46	0.092	4.762	1.281
6.87	6.791	0.079	7200	0.253	0.084	8.92	0.087	4.478	1.205
6.87	6.754	0.116	10800	0.24	0.080	13.38	0.085	4.384	1.180
6.87	6.718	0.152	14400	0.251	0.084	17.84	0.084	4.308	1.159
6.87	6.681	0.189	18000	0.244	0.081	22.3	0.083	4.286	1.153
6.87	6.646	0.224	21600	0.23	0.077	26.76	0.082	4.233	1.139

CONCLUSION

The present Appendix-II gives the wear rate tables for pure aluminium with red mud of 10 N, 20 N and 30 N loads at normal condition and heat treatment conditions in two parts i.e., Appendix-II-A and Appendix-II-B. In the Chapter-5, the graphs are plotted for these Appendix II wear rate tables (Figure 5.2-5.19).

APPENDIX - III

INTRODUCTION

The Appendix-III consists of Appendix-III-A and Appendix-III-B parts. The Appendix-III-A consists of wear rate tables for pure aluminium and 4% tungsten carbide with 2%, 4% and 6% red mud of 10 N, 20 N and 30 N loads at normal condition. The Appendix-III-B consists of wear rate tables for pure aluminium and 4% tungsten carbide with 2%, 4% and 6% red mud of 10 N, 20 N and 30 N loads at heat treatment conditions. In Chapter-6 (Figure 6.1-6.9), the graphs are plotted for these Appendix III wear rate tables.

APPENDIX III - A (AT NORMAL CONDITION)

i) Wear rate tables for pure aluminium with red mud and 4% tungsten carbide at 10N load

The Wear rate value for pure aluminium with 4% tungsten carbide and 2% red mud of 100 μm particle size at 600 rpm is shown in Table 1.

Table 1: Wear rate values for pure aluminium with 4% tungsten carbide and 2% red mud of 100 μm particle size at 600 rpm

V_s = 1.256 m/sec **ρ = 4.482 x 1000 kg/m³**

m_1	m_2	Δm	T	F_f	μ	R.Dx10^{-3}	$W_r \times 10^{-6}$	$W_v \times 10^{-12}$	$W_s \times 10^{-13}$
(gm)	(gm)	(gm)	(sec)	kgf		m	(N/m)	(m³/sec)	(m³/N-m)
6.95	6.79	0.16	3600	0.33	0.33	4.5257	0.346	9.893	7.876
6.95	6.63	0.32	7200	0.34	0.34	9.0514	0.346	9.904	7.886
6.95	6.47	0.48	10800	0.34	0.34	13.5771	0.347	9.908	7.889
6.95	6.31	0.64	14400	0.35	0.35	18.1028	0.347	9.910	7.890
6.95	6.15	0.80	18000	0.31	0.31	22.6285	0.347	9.912	7.891
6.95	5.99	0.96	21600	0.32	0.32	27.1542	0.347	9.912	7.892

The wear rate value for pure aluminium with 4% tungsten carbide and 4% and 6% red mud of 100 µm particle size at 600 rpm are shown in Table 2 and 3 respectively. The Wear rate value for pure aluminium with 4% tungsten carbide and 2% red mud of 42 nm particle size at 600 rpm is shown in Table 4.

Table 2: Wear rate value for pure aluminium with 4% tungsten carbide and 4% red mud of 100 µm particle size at 600 rpm

V_s = 1.256 m/sec **ρ= 4.7254 x 1000 kg/m³**

m_1	m_2	Δm	T	F_f	µ	R.Dx10^{-3}	$W_r \times 10^{-6}$	$W_v \times 10^{-12}$	$W_s \times 10^{-13}$
(gm)	(gm)	(gm)	(sec)	kgf		m	(N/m)	(m³/sec)	(m³/N-m)
7.15	7.06	0.09	3600	0.32	0.32	4.5257	0.201	5.451	4.340
7.15	6.96	0.19	7200	0.34	0.34	9.0514	0.209	5.665	4.510
7.15	6.87	0.28	10800	0.33	0.33	13.5771	0.204	5.540	4.411
7.15	6.77	0.38	14400	0.35	0.35	18.1028	0.207	5.625	4.478
7.15	6.68	0.47	18000	0.32	0.32	22.6285	0.205	5.558	4.425
7.15	6.59	0.56	21600	0.3	0.3	27.1542	0.203	5.513	4.390

Table 3: Wear rate value for pure aluminium with 4% tungsten carbide and 6% red mud of 100 µm particle size at 600 rpm

V_s = 1.256 m/sec **ρ= 4.9254 x 1000 kg/m³**

m_1	m_2	Δm	T	F_f	µ	R.Dx10^{-3}	$W_r \times 10^{-6}$	$W_v \times 10^{-12}$	$W_s \times 10^{-13}$
(gm)	(gm)	(gm)	(sec)	kgf		m	(N/m)	(m³/sec)	(m³/N-m)
7.23	7.16	0.07	3600	0.3	0.3	4.5257	0.151	3.930	3.129
7.23	7.08	0.15	7200	0.31	0.31	9.0514	0.162	4.221	3.361
7.23	7.01	0.22	10800	0.35	0.35	13.5771	0.159	4.131	3.289
7.23	6.93	0.30	14400	0.32	0.32	18.1028	0.162	4.226	3.365
7.23	6.86	0.37	18000	0.32	0.32	22.6285	0.160	4.171	3.321
7.23	6.79	0.44	21600	0.31	0.31	27.1542	0.159	4.134	3.291

Table 4: Wear rate value for pure aluminium with 4% tungsten carbide and 2% red mud of 42 nm particle size at 600 rpm

V_s = 1.256 m/sec **ρ= 4.482 x 1000 kg/m³**

m_1	m_2	Δm	T	F_f	µ	R.Dx10^{-3}	$W_r \times 10^{-6}$	$W_v \times 10^{-12}$	$W_s \times 10^{-13}$
(gm)	(gm)	(gm)	(sec)	kgf		m	(N/m)	(m³/sec)	(m³/N-m)
6.95	6.85	0.10	3600	0.29	0.29	4.5257	0.216	6.176	4.917
6.95	6.80	0.15	7200	0.31	0.31	9.0514	0.162	4.637	3.692
6.95	6.75	0.20	10800	0.28	0.28	13.5771	0.144	4.124	3.284
6.95	6.70	0.25	14400	0.28	0.28	18.1028	0.135	3.868	3.080
6.95	6.65	0.30	18000	0.27	0.27	22.6285	0.130	3.714	2.957
6.95	6.60	0.35	21600	0.3	0.3	27.1542	0.126	3.612	2.876

The Wear rate value for pure aluminium with 4% tungsten carbide and 4% and 6% red mud of 42 nm particle size at 600 rpm is shown in Table 5 and 6 respectively.

Table 5: Wear rate value for pure aluminium with 4% tungsten carbide and 4% red mud of 42 nm particle size at 600 rpm

V_s = 1.256 m/sec **ρ= 4.7254 x 1000 kg/m³**

m_1	m_2	Δm	T	F_f	μ	R.Dx10^{-3}	$W_r \times 10^{-6}$	$W_v \times 10^{-12}$	$W_s \times 10^{-13}$
(gm)	(gm)	(gm)	(sec)	kgf		m	(N/m)	(m³/sec)	(m³/N-m)
7.15	7.080	0.070	3600	0.27	0.27	4.5257	0.151	4.095	3.260
7.15	7.027	0.123	7200	0.28	0.28	9.0514	0.133	3.605	2.870
7.15	6.977	0.173	10800	0.29	0.29	13.5771	0.125	3.383	2.694
7.15	6.927	0.223	14400	0.32	0.32	18.1028	0.121	3.272	2.605
7.15	6.877	0.273	18000	0.27	0.27	22.6285	0.118	3.206	2.552
7.15	6.817	0.333	21600	0.26	0.26	27.1542	0.120	3.259	2.595

Table 6: Wear rate value for pure aluminium with 4% tungsten carbide and 6% red mud of 42 nm particle size at 600 rpm

V_s = 1.256 m/sec **ρ= 4.924 x 1000 kg/m³**

m_1	m_2	Δm	T	F_f	μ	R.Dx10^{-3}	$W_r \times 10^{-6}$	$W_v \times 10^{-12}$	$W_s \times 10^{-13}$
(gm)	(gm)	(gm)	(sec)	kgf		m	(N/m)	(m³/sec)	(m³/N-m)
7.23	7.175	0.055	3600	0.27	0.27	4.5257	0.119	3.097	2.466
7.23	7.125	0.105	7200	0.28	0.28	9.0514	0.114	2.959	2.356
7.23	7.075	0.155	10800	0.26	0.26	13.5771	0.112	2.913	2.319
7.23	7.035	0.195	14400	0.31	0.31	18.1028	0.106	2.749	2.188
7.23	6.995	0.235	18000	0.34	0.34	22.6285	0.102	2.650	2.110
7.23	6.945	0.285	21600	0.26	0.26	27.1542	0.103	2.679	2.133

ii) Wear rate tables for pure aluminium with red mud and 4% tungsten carbide at 20 N load

The Wear rate value for pure aluminium with 4% tungsten carbide and 2%, 4% and 6% red mud of 100 μm particle sizes at 600 rpm is shown in Table 1, 2 and 3 respectively.

Table 1: Wear rate values for pure aluminium with 4% tungsten carbide and 2% red mud of 100 μm particle size at 600 rpm

V_s = 1.256 m/sec **ρ = 4.482 x 1000 kg/m³**

m_1 (gm)	m_2 (gm)	Δm (gm)	T (sec)	F_f kgf	μ	R.Dx10^{-3} m	$W_r \times 10^{-6}$ (N/m)	$W_v \times 10^{-12}$ (m³/sec)	$W_s \times 10^{-13}$ (m³/N-m)
6.95	6.66	0.29	3600	0.33	0.165	4.5257	0.618	17.670	7.034
6.95	6.50	0.45	7200	0.34	0.17	9.0514	0.482	13.793	5.491
6.95	6.34	0.61	10800	0.34	0.17	13.5771	0.437	12.501	4.976
6.95	6.18	0.77	14400	0.35	0.175	18.1028	0.415	11.855	4.719
6.95	6.02	0.93	18000	0.31	0.155	22.6285	0.401	11.467	4.565
6.95	5.86	1.09	21600	0.32	0.16	27.1542	0.392	11.208	4.462

Table 2: Wear rate value for pure aluminium with 4% tungsten carbide and 4% red mud of 100 μm particle size at 600 rpm

V_s = 1.256 m/sec **ρ= 4.7254 x 1000 kg/m³**

m_1 (gm)	m_2 (gm)	Δm (gm)	T (sec)	F_f kgf	μ	R.Dx10^{-3} m	$W_r \times 10^{-6}$ (N/m)	$W_v \times 10^{-12}$ (m³/sec)	$W_s \times 10^{-13}$ (m³/N-m)
7.15	6.99	0.16	3600	0.32	0.16	4.5257	0.355	9.627	3.833
7.15	6.89	0.26	7200	0.34	0.17	9.0514	0.286	7.753	3.086
7.15	6.80	0.35	10800	0.33	0.165	13.5771	0.256	6.932	2.760
7.15	6.70	0.45	14400	0.35	0.175	18.1028	0.246	6.669	2.655
7.15	6.61	0.54	18000	0.32	0.16	22.6285	0.236	6.393	2.545
7.15	6.52	0.63	21600	0.3	0.15	27.1542	0.229	6.209	2.472

Table 3: Wear rate value for pure aluminium with 4% tungsten carbide and 6% red mud of 100 μm particle size at 600 rpm

V_s = 1.256 m/sec **ρ= 4.9254 x 1000 kg/m³**

m_1 (gm)	m_2 (gm)	Δm (gm)	T (sec)	F_f kgf	μ	R.Dx10^{-3} m	$W_r \times 10^{-6}$ (N/m)	$W_v \times 10^{-12}$ (m³/sec)	$W_s \times 10^{-13}$ (m³/N-m)
7.23	7.09	0.14	3600	0.3	0.15	4.5257	0.298	7.756	3.087
7.23	7.01	0.22	7200	0.31	0.155	9.0514	0.236	6.134	2.442
7.23	6.94	0.29	10800	0.35	0.175	13.5771	0.208	5.406	2.152
7.23	6.86	0.37	14400	0.32	0.16	18.1028	0.199	5.183	2.063
7.23	6.79	0.44	18000	0.32	0.16	22.6285	0.190	4.936	1.965
7.23	6.72	0.51	21600	0.31	0.155	27.1542	0.183	4.771	1.899

The Wear rate value for pure aluminium with 4% tungsten carbide and 2%, 4% and 6% red mud of 42 nm particle sizes at 600 rpm is shown in Table 4, 5 and 6 respectively.

Table 4: Wear rate value for pure aluminium with 4% tungsten carbide and 2% red mud of 42 nm particle size at 600 rpm

V_s = 1.256 m/sec **ρ= 4.482 x 1000 kg/m³**

m_1 (gm)	m_2 (gm)	Δm (gm)	T (sec)	F_f kgf	μ	R.Dx10^{-3} m	$W_r \times 10^{-6}$ (N/m)	$W_v \times 10^{-12}$ (m³/sec)	$W_s \times 10^{-13}$ (m³/N-m)
6.95	6.77	0.18	3600	0.29	0.145	4.5257	0.391	11.179	4.450
6.95	6.72	0.23	7200	0.31	0.155	9.0514	0.250	7.139	2.842
6.95	6.67	0.28	10800	0.28	0.14	13.5771	0.203	5.792	2.306
6.95	6.62	0.33	14400	0.28	0.14	18.1028	0.179	5.119	2.038
6.95	6.57	0.38	18000	0.27	0.135	22.6285	0.165	4.715	1.877
6.95	6.52	0.43	21600	0.3	0.15	27.1542	0.155	4.446	1.770

Table 5: Wear rate value for pure aluminium with 4% tungsten carbide and 4% red mud of 42 nm particle size at 600 rpm

V_s = 1.256 m/sec **ρ= 4.7254 x 1000 kg/m³**

m_1 (gm)	m_2 (gm)	Δm (gm)	T (sec)	F_f kgf	μ	R.Dx10^{-3} m	$W_r \times 10^{-6}$ (N/m)	$W_v \times 10^{-12}$ (m³/sec)	$W_s \times 10^{-13}$ (m³/N-m)
7.15	7.001	0.149	3600	0.27	0.135	4.5257	0.323	8.759	3.487
7.15	6.948	0.202	7200	0.28	0.14	9.0514	0.219	5.938	2.364
7.15	6.898	0.252	10800	0.29	0.145	13.5771	0.182	4.938	1.966
7.15	6.848	0.302	14400	0.32	0.16	18.1028	0.164	4.438	1.767
7.15	6.798	0.352	18000	0.27	0.135	22.6285	0.153	4.139	1.648
7.15	6.738	0.412	21600	0.26	0.13	27.1542	0.149	4.037	1.607

Table 6: Wear rate value for pure aluminium with 4% tungsten carbide and 6% red mud of 42 nm particle size at 600 rpm

V_s = 1.256 m/sec **ρ= 4.924 x 1000 kg/m³**

m_1 (gm)	m_2 (gm)	Δm (gm)	T (sec)	F_f kgf	μ	R.Dx10^{-3} m	$W_r \times 10^{-6}$ (N/m)	$W_v \times 10^{-12}$ (m³/sec)	$W_s \times 10^{-13}$ (m³/N-m)
7.23	7.125	0.105	3600	0.27	0.135	4.5257	0.227	5.908	2.352
7.23	7.075	0.155	7200	0.28	0.14	9.0514	0.168	4.364	1.737
7.23	7.025	0.205	10800	0.26	0.13	13.5771	0.148	3.850	1.533
7.23	6.985	0.245	14400	0.31	0.155	18.1028	0.133	3.451	1.374
7.23	6.945	0.285	18000	0.34	0.17	22.6285	0.123	3.212	1.279
7.23	6.895	0.335	21600	0.26	0.13	27.1542	0.121	3.147	1.253

iii) Wear rate tables for pure aluminium with red mud and 4% tungsten carbide at 30 N load

The Wear rate value for pure aluminium with 4% tungsten carbide and 2%, 4% and 6% red mud of 100 μm particle sizes at 600 rpm is shown in Table 1, 2 and 3 respectively.

Table 1: Wear rate value for pure aluminium with 4% tungsten carbide and 2% red mud of 100 μm particle size at 600 rpm

V_s = 1.256 m/sec **ρ = 4.482 x 1000 kg/m³**

m_1	m_2	Δm	T	F_f	μ	R.Dx10^{-3}	$W_r \times 10^{-6}$	$W_v \times 10^{-12}$	$W_s \times 10^{-13}$
(gm)	(gm)	(gm)	(sec)	kgf		m	(N/m)	(m³/sec)	(m³/N-m)
6.95	6.54	0.41	3600	0.33	0.110	4.5257	0.887	25.361	6.731
6.95	6.38	0.57	7200	0.34	0.113	9.0514	0.617	17.639	4.681
6.95	6.22	0.73	10800	0.34	0.113	13.5771	0.527	15.064	3.998
6.95	6.06	0.89	14400	0.35	0.117	18.1028	0.482	13.777	3.656
6.95	5.90	1.05	18000	0.31	0.103	22.6285	0.455	13.005	3.451
6.95	5.74	1.21	21600	0.32	0.107	27.1542	0.437	12.490	3.315

Table 2: Wear rate value for pure aluminium with 4% tungsten carbide and 4% red mud of 100 μm particle size at 600 rpm

V_s = 1.256 m/sec **ρ= 4.7254 x 1000 kg/m³**

m_1	m_2	Δm	T	F_f	μ	R.Dx10^{-3}	$W_r \times 10^{-6}$	$W_v \times 10^{-12}$	$W_s \times 10^{-13}$
(gm)	(gm)	(gm)	(sec)	kgf		m	(N/m)	(m³/sec)	(m³/N-m)
7.15	6.92	0.23	3600	0.32	0.16	4.5257	0.507	13.749	3.649
7.15	6.82	0.33	7200	0.34	0.17	9.0514	0.362	9.814	2.605
7.15	6.73	0.42	10800	0.33	0.165	13.5771	0.306	8.306	2.204
7.15	6.63	0.52	14400	0.35	0.175	18.1028	0.284	7.699	2.043
7.15	6.54	0.61	18000	0.32	0.16	22.6285	0.266	7.217	1.915
7.15	6.45	0.70	21600	0.3	0.15	27.1542	0.254	6.896	1.830

Table 3: Wear rate value for pure aluminium with 4% tungsten carbide and 6% red mud of 100 μm particle size at 600 rpm

V_s = 1.256 m/sec **ρ= 4.9254 x 1000 kg/m³**

m_1	m_2	Δm	T	F_f	μ	R.Dx10^{-3}	$W_r \times 10^{-6}$	$W_v \times 10^{-12}$	$W_s \times 10^{-13}$
(gm)	(gm)	(gm)	(sec)	kgf		m	(N/m)	(m³/sec)	(m³/N-m)
7.23	7.03	0.20	3600	0.3	0.15	4.5257	0.443	11.529	3.060
7.23	6.95	0.28	7200	0.31	0.155	9.0514	0.308	8.021	2.129
7.23	6.88	0.35	10800	0.35	0.175	13.5771	0.256	6.664	1.769
7.23	6.80	0.43	14400	0.32	0.16	18.1028	0.235	6.126	1.626
7.23	6.73	0.50	18000	0.32	0.16	22.6285	0.219	5.691	1.510
7.23	6.66	0.57	21600	0.31	0.155	27.1542	0.208	5.400	1.433

The Wear rate value for pure aluminium with 4% tungsten carbide and 2%, 4% and 6% red mud of 42 nm particle sizes at 600 rpm is shown in Table 4, 5 and 6 respectively.

Table 4: Wear rate value for pure aluminium with 4% tungsten carbide and 2% red mud of 42 nm particle size at 600 rpm

V_s = 1.256 m/sec **ρ= 4.482 x 1000 kg/m³**

m_1	m_2	Δm	T	F_f	μ	R.Dx10^{-3}	$W_r \times 10^{-6}$	$W_v \times 10^{-12}$	$W_s \times 10^{-13}$
(gm)	(gm)	(gm)	(sec)	kgf		m	(N/m)	(m³/sec)	(m³/N-m)
6.95	6.69	0.26	3600	0.29	0.145	4.5257	0.565	16.154	4.287
6.95	6.64	0.31	7200	0.31	0.155	9.0514	0.337	9.627	2.555
6.95	6.59	0.36	10800	0.28	0.14	13.5771	0.261	7.451	1.977
6.95	6.54	0.41	14400	0.28	0.14	18.1028	0.223	6.363	1.689
6.95	6.49	0.46	18000	0.27	0.135	22.6285	0.200	5.710	1.515
6.95	6.44	0.51	21600	0.3	0.15	27.1542	0.184	5.275	1.400

Table 5: Wear rate value for pure aluminium with 4% tungsten carbide and 4% red mud of 42 nm particle size at 600 rpm

V_s = 1.256 m/sec **ρ= 4.7254 x 1000 kg/m³**

m_1	m_2	Δm	T	F_f	μ	R.Dx10^{-3}	$W_r \times 10^{-6}$	$W_v \times 10^{-12}$	$W_s \times 10^{-13}$
(gm)	(gm)	(gm)	(sec)	kgf		m	(N/m)	(m³/sec)	(m³/N-m)
7.15	6.922	0.228	3600	0.27	0.135	4.5257	0.494	13.397	3.555
7.15	6.869	0.281	7200	0.28	0.14	9.0514	0.304	8.256	2.191
7.15	6.819	0.331	10800	0.29	0.145	13.5771	0.239	6.484	1.721
7.15	6.769	0.381	14400	0.32	0.16	18.1028	0.206	5.598	1.486
7.15	6.719	0.431	18000	0.27	0.135	22.6285	0.187	5.066	1.344
7.15	6.659	0.491	21600	0.26	0.13	27.1542	0.177	4.810	1.276

Table 6: Wear rate value for pure aluminium with 4% tungsten carbide and 6% red mud of 42 nm particle size at 600 rpm

V_s = 1.256 m/sec **ρ= 4.924 x 1000 kg/m³**

m_1	m_2	Δm	T	F_f	μ	R.Dx10^{-3}	$W_r \times 10^{-6}$	$W_v \times 10^{-12}$	$W_s \times 10^{-13}$
(gm)	(gm)	(gm)	(sec)	kgf		m	(N/m)	(m³/sec)	(m³/N-m)
7.23	7.076	0.154	3600	0.27	0.135	4.5257	0.334	8.692	2.307
7.23	7.026	0.204	7200	0.28	0.14	9.0514	0.221	5.757	1.528
7.23	6.976	0.254	10800	0.26	0.13	13.5771	0.184	4.778	1.268
7.23	6.936	0.294	14400	0.31	0.155	18.1028	0.159	4.148	1.101
7.23	6.896	0.334	18000	0.34	0.17	22.6285	0.145	3.769	1.000
7.23	6.846	0.384	21600	0.26	0.13	27.1542	0.139	3.611	0.958

APPENDIX-III-B (WITH HEAT TREATMENT CONDITIONS)

i) Wear rate tables for pure aluminium with 4% tungsten carbide and red mud at 10 N load

The Wear rate values for pure aluminium with 4% tungsten carbide and 2%, 4% and 6% red mud of 100 μm particle sizes at 600 rpm, at 350^0C are shown in Tables 1, 2 and 3 respectively.

Table 1: Wear Rate values for Pure Aluminium with 4% Tungsten Carbide and 2% Red mud of 100 μm particle size at 600 rpm and 350^0C

Vs=1.256 m/s **ρ=4.482 x10³kg/m³**

m_1	m_2	Δm	T	F_f	μ	R.Dx10^{-3}	$W_r\times10^{-6}$	$W_v\times10^{-12}$	$W_s\times10^{-13}$
(gm)	(gm)	(gm)	(sec)	kgf		m	(N/m)	(m³/sec)	(m³/N-m)
6.95	6.803	0.147	3600	0.31	0.31	4.5257	0.318	9.110	7.247
6.95	6.66	0.29	7200	0.32	0.32	9.0514	0.314	8.986	7.148
6.95	6.52	0.43	10800	0.29	0.29	13.5771	0.310	8.883	7.066
6.95	6.38	0.57	14400	0.28	0.28	18.1028	0.308	8.831	7.025
6.95	6.24	0.71	18000	0.31	0.31	22.6285	0.307	8.800	7.000
6.95	6.1	0.85	21600	0.32	0.32	27.1542	0.307	8.779	6.984

Table 2: Wear Rate values for Pure Aluminium with 4% Tungsten Carbide and 4% Red mud of 100 μm particle size at 600 rpm and 350^0C

Vs=1.256 m/s **ρ = 4.7254x10³ kg/m³**

m_1	m_2	Δm	T	F_f	μ	R.Dx10^{-3}	$W_r\times10^{-6}$	$W_v\times10^{-12}$	$W_s\times10^{-13}$
(gm)	(gm)	(gm)	(sec)	kgf		m	(N/m)	(m³/sec)	(m³/N-m)
7.15	7.066	0.084	3600	0.30	0.30	4.5257	0.182	4.937	3.927
7.15	6.99	0.16	7200	0.31	0.31	9.0514	0.173	4.702	3.740
7.15	6.91	0.24	10800	0.29	0.29	13.5771	0.173	4.702	3.740
7.15	6.83	0.32	14400	0.32	0.32	18.1028	0.173	4.702	3.740
7.15	6.76	0.39	18000	0.29	0.29	22.6285	0.169	4.585	3.647
7.15	6.68	0.47	21600	0.31	0.31	27.1542	0.169	4.604	3.662

Table 3: Wear Rate values for Pure Aluminium with 4% Tungsten Carbide and 6% Red mud of 100 μm particle size at 600 rpm and 350^0C

Vs=1.256 m/s **ρ = 4.924x10³ kg/m³**

m_1	m_2	Δm	T	F_f	μ	R.Dx10^{-3}	$W_r\times10^{-6}$	$W_v\times10^{-12}$	$W_s\times10^{-13}$
(gm)	(gm)	(gm)	(sec)	kgf		m	(N/m)	(m³/sec)	(m³/N-m)
7.23	7.174	0.056	3600	0.28	0.28	4.525	0.121	3.159	2.512
7.23	7.12	0.11	7200	0.29	0.29	9.051	0.119	3.102	2.468
7.23	7.07	0.16	10800	0.30	0.30	13.577	0.115	3.008	2.393
7.23	7.02	0.21	14400	0.31	0.31	18.102	0.113	2.961	2.355
7.23	6.97	0.26	18000	0.30	0.30	22.628	0.112	2.933	2.333
7.23	6.92	0.31	21600	0.29	0.29	27.154	0.111	2.914	2.318

The Wear rate values for pure aluminium with 4% tungsten carbide and 2%, 4% and 6% red mud of 100 µm particle sizes at 600 rpm, at 400^0C are shown in Tables 4, 5 and 6 respectively.

Table 4: Wear Rate values for Pure Aluminium with 4% Tungsten Carbide and 2% Red mud of 100 µm particle size at 600 rpm and 400^0C

Vs=1.256 m/s **ρ=4.482 x10³kg/m³**

m_1	m_2	Δm	T	F_f	µ	R.Dx10^{-3}	$W_r \times 10^{-6}$	$W_v \times 10^{-12}$	$W_s \times 10^{-13}$
(gm)	(gm)	(gm)	(sec)	kgf		m	(N/m)	(m³/sec)	(m³/N-m)
6.95	6.806	0.144	3600	0.30	0.30	4.5257	0.312	8.924	7.099
6.95	6.67	0.28	7200	0.31	0.31	9.0514	0.303	8.676	6.901
6.95	6.53	0.42	10800	0.29	0.29	13.5771	0.303	8.676	6.901
6.95	6.41	0.54	14400	0.30	0.30	18.1028	0.292	8.366	6.655
6.95	6.26	0.69	18000	0.28	0.28	22.6285	0.299	8.552	6.803
6.95	6.13	0.82	21600	0.33	0.33	27.1542	0.296	8.470	6.737

Table 5: Wear Rate values for Pure Aluminium with 4% Tungsten Carbide and 4% Red mud of 100 µm particle size at 600 rpm and 400^0C

Vs=1.256 m/s **ρ = 4.7254x10³ kg/m³**

m_1	m_2	Δm	T	F_f	µ	R.Dx10^{-3}	$W_r \times 10^{-6}$	$W_v \times 10^{-12}$	$W_s \times 10^{-13}$
(gm)	(gm)	(gm)	(sec)	kgf		m	(N/m)	(m³/sec)	(m³/N-m)
7.15	7.067	0.083	3600	0.33	0.33	4.5257	0.179	4.879	3.881
7.15	6.99	0.16	7200	0.35	0.35	9.0514	0.173	4.702	3.74
7.15	6.91	0.24	10800	0.34	0.34	13.5771	0.173	4.702	3.740
7.15	6.83	0.32	14400	0.32	0.32	18.1028	0.173	4.702	3.740
7.15	6.76	0.39	18000	0.34	0.34	22.6285	0.169	4.585	3.647
7.15	6.68	0.47	21600	0.32	0.32	27.1542	0.169	4.604	3.662

Table 6: Wear Rate values for Pure Aluminium with 4% Tungsten Carbide and 6% Red mud of 100 µm particle size at 600 rpm and 400^0C

Vs=1.256 m/s **ρ = 4.924x10³ kg/m³**

m_1	m_2	Δm	T	F_f	µ	R.Dx10^{-3}	$W_r \times 10^{-6}$	$W_v \times 10^{-12}$	$W_s \times 10^{-13}$
(gm)	(gm)	(gm)	(sec)	kgf		m	(N/m)	(m³/sec)	(m³/N-m)
7.23	7.176	0.054	3600	0.31	0.31	4.5257	0.117	3.046	2.423
7.23	7.123	0.107	7200	0.33	0.33	9.0514	0.115	3.018	2.400
7.23	7.07	0.16	10800	0.32	0.32	13.5771	0.115	3.008	2.39
7.23	7.02	0.21	14400	0.30	0.30	18.1028	0.113	2.961	2.355
7.23	6.97	0.26	18000	0.29	0.29	22.6285	0.112	2.933	2.333
7.23	6.92	0.31	21600	0.28	0.28	27.1542	0.111	2.914	2.318

The Wear rate values for pure aluminium with 4% tungsten carbide and 2%, 4% and 6% red mud of 100 μm particle sizes at 600 rpm, at 450^0C are shown in Tables 7, 8 and 9 respectively.

Table 7: Wear Rate values for Pure Aluminium with 4% Tungsten Carbide and 2% Red mud of 100 μm particle size at 600 rpm and 450^0C

Vs=1.256 m/s **ρ=4.482 x10³kg/m³**

m_1	m_2	Δm	T	F_f	μ	R.Dx10^{-3}	$W_r\times10^{-6}$	$W_v\times10^{-12}$	$W_s\times10^{-13}$
(gm)	(gm)	(gm)	(sec)	kgf		m	(N/m)	(m³/sec)	(m³/N-m)
6.95	6.811	0.139	3600	0.34	0.34	4.5257	0.301	8.614	6.852
6.95	6.673	0.277	7200	0.29	0.29	9.0514	0.300	8.583	6.827
6.95	6.54	0.41	10800	0.33	0.33	13.5771	0.296	8.470	6.737
6.95	6.40	0.55	14400	0.32	0.32	18.1028	0.298	8.521	6.778
6.95	6.27	0.68	18000	0.31	0.31	22.6285	0.294	8.428	6.704
6.95	6.14	0.81	21600	0.30	0.30	27.1542	0.292	8.366	6.655

Table 8: Wear Rate values for Pure Aluminium with 4% Tungsten Carbide and 4% Red mud of 100 μm particle size at 600 rpm and 450^0C

Vs=1.256 m/s **ρ = 4.7254x10³ kg/m³**

m_1	m_2	Δm	T	F_f	μ	R.Dx10^{-3}	$W_r\times10^{-6}$	$W_v\times10^{-12}$	$W_s\times10^{-13}$
(gm)	(gm)	(gm)	(sec)	kgf		m	(N/m)	(m³/sec)	(m³/N-m)
7.15	7.07	0.08	3600	0.27	0.27	4.5257	0.173	4.702	3.740
7.15	6.991	0.159	7200	0.28	0.28	9.0514	0.172	4.673	3.717
7.15	6.915	0.235	10800	0.30	0.30	13.5771	0.169	4.604	3.662
7.15	6.84	0.31	14400	0.29	0.29	18.1028	0.167	4.555	3.623
7.15	6.77	0.38	18000	0.31	0.31	22.6285	0.164	4.467	3.553
7.15	6.70	0.45	21600	0.31	0.31	27.1542	0.162	4.408	3.507

Table 9: Wear Rate values for Pure Aluminium with 4% Tungsten Carbide and 6% Red mud of 100 μm particle size at 600 rpm and 450^0C

Vs=1.256 m/s **ρ = 4.924x10³ kg/m³**

m_1	m_2	Δm	T	F_f	μ	R.Dx10^{-3}	$W_r\times10^{-6}$	$W_v\times10^{-12}$	$W_s\times10^{-13}$
(gm)	(gm)	(gm)	(sec)	kgf		m	(N/m)	(m³/sec)	(m³/N-m)
7.23	7.18	0.05	3600	0.30	0.30	4.5257	0.108	2.820	2.243
7.23	7.132	0.098	7200	0.32	0.32	9.0514	0.106	2.764	2.198
7.23	7.084	0.146	10800	0.31	0.31	13.5771	0.105	2.745	2.183
7.23	7.04	0.19	14400	0.29	0.29	18.1028	0.102	2.679	2.131
7.23	7.00	0.23	18000	0.33	0.33	22.6285	0.099	2.595	2.064
7.23	6.96	0.27	21600	0.31	0.31	27.1542	0.097	2.538	2.019

The Wear rate values for pure aluminium with 4% tungsten carbide and 2%, 4% and 6% red mud of 100 μm particle sizes at 600 rpm, at 500^0C are shown in Tables 10, 11 and 12 respectively.

Table 10: Wear Rate values for Pure Aluminium with 4% Tungsten Carbide and 2% Red mud of 100 μm particle size at 600 rpm and 500^0C

Vs=1.256 m/s **ρ=4.482 x10³kg/m³**

m_1	m_2	Δm	T	F_f	μ	R.Dx10^{-3}	$W_r\times10^{-6}$	$W_v\times10^{-12}$	$W_s\times10^{-13}$
(gm)	(gm)	(gm)	(sec)	kgf		m	(N/m)	(m³/sec)	(m³/N-m)
6.95	6.806	0.144	3600	0.30	0.30	4.5257	0.312	8.924	7.099
6.95	6.665	0.285	7200	0.32	0.32	9.0514	0.308	8.831	7.025
6.95	6.52	0.43	10800	0.31	0.31	13.5771	0.310	8.883	7.066
6.95	6.38	0.57	14400	0.33	0.33	18.1028	0.308	8.831	7.025
6.95	6.24	0.71	18000	0.29	0.29	22.6285	0.307	8.800	7.000
6.95	6.13	0.82	21600	0.30	0.30	27.1542	0.296	8.470	6.737

Table 11: Wear Rate values for Pure Aluminium with 4% Tungsten Carbide and 4% Red mud of 100 μm particle size at 600 rpm and 500^0C

Vs=1.256 m/s **ρ = 4.7254x10³ kg/m³**

m_1	m_2	Δm	T	F_f	μ	R.Dx10^{-3}	$W_r\times10^{-6}$	$W_v\times10^{-12}$	$W_s\times10^{-13}$
(gm)	(gm)	(gm)	(sec)	kgf		m	(N/m)	(m³/sec)	(m³/N-m)
7.15	7.068	0.082	3600	0.32	0.32	4.5257	0.177	4.820	3.834
7.15	6.988	0.162	7200	0.30	0.30	9.0514	0.175	4.761	3.787
7.15	6.91	0.24	10800	0.31	0.31	13.5771	0.173	4.702	3.740
7.15	6.83	0.32	14400	0.33	0.33	18.1028	0.173	4.702	3.740
7.15	6.76	0.39	18000	0.29	0.29	22.6285	0.169	4.585	3.647
7.15	6.68	0.47	21600	0.28	0.28	27.1542	0.169	4.604	3.662

Table 12: Wear Rate values for Pure Aluminium with 4% Tungsten Carbide and 6% Red mud of 100 μm particle size at 600 rpm and 500^0C

Vs=1.256 m/s **ρ = 4.924x10³ kg/m³**

m_1	m_2	Δm	T	F_f	μ	R.Dx10^{-3}	$W_r\times10^{-6}$	$W_v\times10^{-12}$	$W_s\times10^{-13}$
(gm)	(gm)	(gm)	(sec)	kgf		m	(N/m)	(m³/sec)	(m³/N-m)
7.23	7.178	0.052	3600	0.35	0.35	4.5257	0.113	2.933	2.333
7.23	7.13	0.1	7200	0.34	0.34	9.0514	0.108	2.820	2.243
7.23	7.08	0.15	10800	0.36	0.36	13.5771	0.108	2.820	2.243
7.23	7.04	0.19	14400	0.37	0.37	18.1028	0.102	2.679	2.131
7.23	7.00	0.23	18000	0.34	0.34	22.6285	0.099	2.595	2.064
7.23	6.96	0.27	21600	0.32	0.32	27.1542	0.097	2.538	2.019

The Wear rate values for pure aluminium with 4% tungsten carbide and 2%, 4% and 6% red mud of 42 nm particle sizes at 600 rpm, at 350^0C are shown in Tables 13, 14 and 15 respectively.

Table 13: Wear Rate values for Pure Aluminium with 4% Tungsten Carbide and 2% Red mud of 42 nm particle size at 600 rpm and 350^0C

Vs=1.256 m/s **ρ=4.482 x10³kg/m³**

m_1	m_2	Δm	T	F_f	μ	R.Dx10^{-3}	$W_r\times10^{-6}$	$W_v\times10^{-12}$	$W_s\times10^{-13}$
(gm)	(gm)	(gm)	(sec)	kgf		m	(N/m)	(m³/sec)	(m³/N-m)
6.95	6.86	0.09	3600	0.28	0.28	4.5257	0.195	5.57	4.436
6.95	6.77	0.18	7200	0.29	0.29	9.0514	0.195	5.577	4.436
6.95	6.682	0.268	10800	0.27	0.27	13.5771	0.193	5.536	4.404
6.95	6.6	0.35	14400	0.25	0.25	18.1028	0.189	5.422	4.313
6.95	6.51	0.44	18000	0.25	0.25	22.6285	0.190	5.453	4.338
6.95	6.43	0.52	21600	0.26	0.26	27.1542	0.187	5.371	4.272

Table 14: Wear Rate values for Pure Aluminium with 4% Tungsten Carbide and 4% Red mud of 42 nm particle size at 600 rpm and 350^0C

Vs=1.256 m/s **ρ = 4.7254x10³ kg/m³**

m_1	m_2	Δm	T	F_f	μ	R.Dx10^{-3}	$W_r\times10^{-6}$	$W_v\times10^{-12}$	$W_s\times10^{-13}$
(gm)	(gm)	(gm)	(sec)	kgf		m	(N/m)	(m³/sec)	(m³/N-m)
7.15	7.098	0.052	3600	0.28	0.28	4.5257	0.112	3.056	2.431
7.15	7.047	0.103	7200	0.29	0.29	9.0514	0.111	3.027	2.408
7.15	7	0.15	10800	0.30	0.30	13.5771	0.108	2.939	2.338
7.15	6.95	0.2	14400	0.29	0.29	18.1028	0.108	2.939	2.338
7.15	6.91	0.24	18000	0.27	0.27	22.6285	0.104	2.821	2.244
7.15	6.86	0.29	21600	0.29	0.29	27.1542	0.104	2.841	2.260

Table 15: Wear Rate values for Pure Aluminium with 4% Tungsten Carbide and 6% Red mud of 42 nm particle size at 600 rpm and 350^0C

Vs=1.256 m/s **ρ = 4.924x10³ kg/m³**

m_1	m_2	Δm	T	F_f	μ	R.Dx10^{-3}	$W_r\times10^{-6}$	$W_v\times10^{-12}$	$W_s\times10^{-13}$
(gm)	(gm)	(gm)	(sec)	kgf		m	(N/m)	(m³/sec)	(m³/N-m)
7.23	7.187	0.043	3600	0.25	0.25	4.5257	0.093	2.425	1.929
7.23	7.15	0.08	7200	0.24	0.24	9.0514	0.086	2.256	1.794
7.23	7.11	0.12	10800	0.29	0.29	13.5771	0.086	2.256	1.794
7.23	7.072	0.158	14400	0.25	0.25	18.1028	0.085	2.228	1.772
7.23	7.04	0.19	18000	0.28	0.28	22.6285	0.082	2.143	1.705
7.23	7.03	0.2	21600	0.27	0.27	27.1542	0.072	1.880	1.495

The Wear rate values for pure aluminium with 4% tungsten carbide and 2%, 4% and 6% red mud of 42 nm particle sizes at 600 rpm, at 400^0C are shown in Tables 16, 17 and 18 respectively.

Table 16: Wear Rate values for Pure Aluminium with 4% Tungsten Carbide and 2% Red mud of 42 nm particle size at 600 rpm and 400^0C

Vs=1.256 m/s **ρ=4.482 x10³kg/m³**

m_1	m_2	Δm	T	F_f	μ	R.Dx10^{-3}	$W_r \times 10^{-6}$	$W_v \times 10^{-12}$	$W_s \times 10^{-13}$
(gm)	(gm)	(gm)	(sec)	kgf		m	(N/m)	(m³/sec)	(m³/N-m)
6.95	6.865	0.085	3600	0.28	0.28	4.5257	0.184	5.267	4.190
6.95	6.78	0.17	7200	0.24	0.24	9.0514	0.184	5.267	4.190
6.95	6.7	0.25	10800	0.26	0.26	13.5771	0.180	5.164	4.108
6.95	6.62	0.33	14400	0.25	0.25	18.1028	0.178	5.113	4.067
6.95	6.54	0.41	18000	0.29	0.29	22.6285	0.177	5.082	4.042
6.95	6.46	0.49	21600	0.23	0.23	27.1542	0.177	5.061	4.026

Table 17: Wear Rate values for Pure Aluminium with 4% Tungsten Carbide and 4% Red mud of 42 nm particle size at 600 rpm and 400^0C

Vs=1.256 m/s **ρ = 4.7254x10³ kg/m³**

m_1	m_2	Δm	T	F_f	μ	R.Dx10^{-3}	$W_r \times 10^{-6}$	$W_v \times 10^{-12}$	$W_s \times 10^{-13}$
(gm)	(gm)	(gm)	(sec)	kgf		m	(N/m)	(m³/sec)	(m³/N-m)
7.15	7.1	0.05	3600	0.28	0.28	4.5257	0.108	2.939	2.338
7.15	7.05	0.1	7200	0.27	0.27	9.0514	0.108	2.939	2.338
7.15	7	0.15	10800	0.26	0.26	13.5771	0.108	2.939	2.338
7.15	6.96	0.19	14400	0.25	0.25	18.1028	0.102	2.792	2.221
7.15	6.92	0.23	18000	0.27	0.27	22.6285	0.099	2.704	2.150
7.15	6.88	0.27	21600	0.27	0.27	27.1542	0.097	2.645	2.104

Table 18: Wear Rate values for Pure Aluminium with 4% Tungsten Carbide and 6% Red mud of 42 nm particle size at 600 rpm and 400^0C

Vs=1.256 m/s **ρ = 4.924x10³ kg/m³**

m_1	m_2	Δm	T	F_f	μ	R.Dx10^{-3}	$W_r \times 10^{-6}$	$W_v \times 10^{-12}$	$W_s \times 10^{-13}$
(gm)	(gm)	(gm)	(sec)	kgf		m	(N/m)	(m³/sec)	(m³/N-m)
7.23	7.192	0.038	3600	0.27	0.27	4.5257	0.082	2.143	1.705
7.23	7.16	0.07	7200	0.29	0.29	9.0514	0.075	1.974	1.570
7.23	7.13	0.1	10800	0.25	0.25	13.5771	0.072	1.880	1.495
7.23	7.1	0.13	14400	0.29	0.29	18.1028	0.070	1.833	1.458
7.23	7.07	0.16	18000	0.27	0.27	22.6285	0.069	1.805	1.435
7.23	7.04	0.19	21600	0.29	0.29	27.1542	0.068	1.786	1.421

The Wear rate values for pure aluminium with 4% tungsten carbide and 2%, 4% and 6% red mud of 42 nm particle sizes at 600 rpm, at 450^0C are shown in Tables 19, 20 and 21 respectively.

Table 19: Wear Rate values for Pure Aluminium with 4% Tungsten Carbide and 2% Red mud of 42 nm particle size at 600 rpm and 450^0C

Vs=1.256 m/s **ρ=4.482 x10³kg/m³**

m_1	m_2	Δm	T	F_f	μ	R.Dx10^{-3}	$W_r\times10^{-6}$	$W_v\times10^{-12}$	$W_s\times10^{-13}$
(gm)	(gm)	(gm)	(sec)	kgf		m	(N/m)	(m³/sec)	(m³/N-m)
6.95	6.868	0.082	3600	0.29	0.29	4.5257	0.177	5.082	4.042
6.95	6.79	0.16	7200	0.28	0.28	9.0514	0.173	4.958	3.943
6.95	6.71	0.24	10800	0.27	0.27	13.5771	0.173	4.958	3.943
6.95	6.632	0.318	14400	0.26	0.26	18.1028	0.172	4.92	3.919
6.95	6.56	0.39	18000	0.25	0.25	22.6285	0.169	4.834	3.845
6.95	6.49	0.46	21600	0.29	0.29	27.1542	0.166	4.751	3.779

Table 20: Wear Rate values for Pure Aluminium with 4% Tungsten Carbide and 4% Red mud of 42 nm particle size at 600 rpm and 450^0C

Vs=1.256 m/s **ρ = 4.7254x10³ kg/m³**

m_1	m_2	Δm	T	F_f	μ	R.Dx10^{-3}	$W_r\times10^{-6}$	$W_v\times10^{-12}$	$W_s\times10^{-13}$
(gm)	(gm)	(gm)	(sec)	kgf		m	(N/m)	(m³/sec)	(m³/N-m)
7.15	7.102	0.048	3600	0.29	0.29	4.5257	0.104	2.821	2.244
7.15	7.06	0.09	7200	0.29	0.29	9.0514	0.097	2.645	2.104
7.15	7.01	0.14	10800	0.31	0.31	13.5771	0.101	2.743	2.182
7.15	6.97	0.18	14400	0.28	0.28	18.1028	0.097	2.645	2.104
7.15	6.93	0.22	18000	0.28	0.28	22.6285	0.095	2.586	2.057
7.15	6.89	0.26	21600	0.27	0.27	27.1542	0.093	2.547	2.026

Table 21: Wear Rate values for Pure Aluminium with 4% Tungsten Carbide and 6% Red mud of 42 nm particle size at 600 rpm and 450^0C

Vs=1.256 m/s **ρ = 4.924x10³ kg/m³**

m_1	m_2	Δm	T	F_f	μ	R.Dx10^{-3}	$W_r\times10^{-6}$	$W_v\times10^{-12}$	$W_s\times10^{-13}$
(gm)	(gm)	(gm)	(sec)	kgf		m	(N/m)	(m³/sec)	(m³/N-m)
7.23	7.194	0.036	3600	0.27	0.27	4.5257	0.078	2.030	1.615
7.23	7.158	0.072	7200	0.29	0.29	9.0514	0.078	2.030	1.615
7.23	7.13	0.1	10800	0.31	0.31	13.5771	0.072	1.880	1.495
7.23	7.1	0.13	14400	0.28	0.28	18.1028	0.070	1.833	1.458
7.23	7.07	0.16	18000	0.25	0.25	22.6285	0.069	1.805	1.435
7.23	7.04	0.19	21600	0.26	0.26	27.1542	0.068	1.786	1.421

The Wear rate values for pure aluminium with 4% tungsten carbide and 2%, 4% and 6% red mud of 42 nm particle sizes at 600 rpm, at 500^0C are shown in Tables 22, 23 and 24 respectively.

Table 22: Wear Rate values for Pure Aluminium with 4% Tungsten Carbide and 2% Red mud of 42 nm particle size at 600 rpm and 500^0C

Vs=1.256 m/s **ρ=4.482 x10³kg/m³**

m_1	m_2	Δm	T	F_f	μ	R.Dx10^{-3}	$W_r\times10^{-6}$	$W_v\times10^{-12}$	$W_s\times10^{-13}$
(gm)	(gm)	(gm)	(sec)	kgf		m	(N/m)	(m³/sec)	(m³/N-m)
6.95	6.866	0.084	3600	0.25	0.25	4.5257	0.182	5.206	4.141
6.95	6.79	0.16	7200	0.24	0.24	9.0514	0.173	4.958	3.943
6.95	6.71	0.24	10800	0.29	0.29	13.5771	0.173	4.958	3.943
6.95	6.64	0.31	14400	0.31	0.31	18.1028	0.167	4.803	3.820
6.95	6.56	0.39	18000	0.28	0.28	22.6285	0.169	4.834	3.845
6.95	6.49	0.46	21600	0.27	0.27	27.1542	0.166	4.751	3.779

Table 23: Wear Rate values for Pure Aluminium with 4% Tungsten Carbide and 4% Red mud of 42 nm particle size at 600 rpm and 500^0C

Vs=1.256 m/s **ρ = 4.7254x10³ kg/m³**

m_1	m_2	Δm	T	F_f	μ	R.Dx10^{-3}	$W_r\times10^{-6}$	$W_v\times10^{-12}$	$W_s\times10^{-13}$
(gm)	(gm)	(gm)	(sec)	kgf		m	(N/m)	(m³/sec)	(m³/N-m)
7.15	7.101	0.049	3600	0.28	0.28	4.5257	0.106	2.880	2.291
7.15	7.06	0.09	7200	0.29	0.29	9.0514	0.097	2.645	2.104
7.15	7.01	0.14	10800	0.27	0.27	13.5771	0.101	2.743	2.182
7.15	6.97	0.18	14400	0.25	0.25	18.1028	0.097	2.645	2.104
7.15	6.93	0.22	18000	0.25	0.25	22.6285	0.095	2.586	2.057
7.15	6.89	0.26	21600	0.27	0.27	27.1542	0.093	2.547	2.026

Table 24: Wear Rate values for Pure Aluminium with 4% Tungsten Carbide and 6% Red mud of 42 nm particle size at 600 rpm and 500^0C

Vs=1.256 m/s **ρ = 4.924x10³ kg/m³**

m_1	m_2	Δm	T	F_f	μ	R.Dx10^{-3}	$W_r\times10^{-6}$	$W_v\times10^{-12}$	$W_s\times10^{-13}$
(gm)	(gm)	(gm)	(sec)	kgf		m	(N/m)	(m³/sec)	(m³/N-m)
7.23	7.193	0.037	3600	0.26	0.26	4.5257	0.080	2.087	1.660
7.23	7.16	0.07	7200	0.25	0.25	9.0514	0.075	1.974	1.570
7.23	7.13	0.1	10800	0.24	0.24	13.5771	0.072	1.880	1.495
7.23	7.1	0.13	14400	0.31	0.31	18.1028	0.070	1.833	1.458
7.23	7.07	0.16	18000	0.25	0.25	22.6285	0.069	1.805	1.435
7.23	7.04	0.19	21600	0.29	0.29	27.1542	0.068	1.786	1.421

ii) Wear rate tables for pure aluminium with 4% tungsten carbide and red mud at 20 N load

The Wear rate values for pure aluminium with 4% tungsten carbide and 2%, 4% and 6% red mud of 100 μm particle sizes at 600 rpm, at 350^0C are shown in Tables 1, 2 and 3 respectively.

Table 1: Wear Rate values for Pure Aluminium with 4% Tungsten Carbide and 2% Red mud of 100 μm particle size at 600 rpm and 350^0C

Vs=1.256 m/s **ρ=4.482 x10³kg/m³**

m_1	m_2	Δm	T	F_f	μ	R.Dx10^{-3}	$W_r\times10^{-6}$	$W_v\times10^{-12}$	$W_s\times10^{-13}$
(gm)	(gm)	(gm)	(sec)	kgf		m	(N/m)	(m³/sec)	(m³/N-m)
6.95	6.796	0.154	3600	0.31	0.155	4.5257	0.334	9.550	3.802
6.95	6.653	0.297	7200	0.32	0.16	9.0514	0.322	9.206	3.665
6.95	6.513	0.437	10800	0.29	0.145	13.5771	0.316	9.030	3.595
6.95	6.373	0.577	14400	0.28	0.14	18.1028	0.313	8.941	3.559
6.95	6.233	0.717	18000	0.31	0.155	22.6285	0.311	8.888	3.538
6.95	6.093	0.857	21600	0.32	0.16	27.1542	0.310	8.853	3.524

Table 2: Wear Rate values for Pure Aluminium with 4% Tungsten Carbide and 4% Red mud of 100 μm particle size at 600 rpm and 350^0C

Vs=1.256 m/s **ρ = 4.7254x10³ kg/m³**

m_1	m_2	Δm	T	F_f	μ	R.Dx10^{-3}	$W_r\times10^{-6}$	$W_v\times10^{-12}$	$W_s\times10^{-13}$
(gm)	(gm)	(gm)	(sec)	kgf		m	(N/m)	(m³/sec)	(m³/N-m)
7.15	7.062	0.088	3600	0.3	0.15	4.5257	0.191	5.180	2.062
7.15	6.986	0.164	7200	0.31	0.155	9.0514	0.178	4.824	1.920
7.15	6.906	0.244	10800	0.29	0.145	13.5771	0.176	4.783	1.904
7.15	6.826	0.324	14400	0.32	0.16	18.1028	0.176	4.763	1.896
7.15	6.756	0.394	18000	0.29	0.145	22.6285	0.171	4.634	1.845
7.15	6.676	0.474	21600	0.31	0.155	27.1542	0.171	4.645	1.849

Table 3: Wear Rate values for Pure Aluminium with 4% Tungsten Carbide and 6% Red mud of 100 μm particle size at 600 rpm and 350^0C

Vs=1.256 m/s **ρ = 4.924x10³ kg/m³**

m_1	m_2	Δm	T	F_f	μ	R.Dx10^{-3}	$W_r\times10^{-6}$	$W_v\times10^{-12}$	$W_s\times10^{-13}$
(gm)	(gm)	(gm)	(sec)	kgf		m	(N/m)	(m³/sec)	(m³/N-m)
7.23	7.171	0.059	3600	0.28	0.14	4.5257	0.127	3.305	1.316
7.23	7.117	0.113	7200	0.29	0.145	9.0514	0.122	3.176	1.264
7.23	7.067	0.163	10800	0.3	0.15	13.5771	0.117	3.057	1.217
7.23	7.017	0.213	14400	0.31	0.155	18.1028	0.115	2.998	1.194
7.23	6.967	0.263	18000	0.3	0.15	22.6285	0.114	2.963	1.179
7.23	6.917	0.313	21600	0.29	0.145	27.1542	0.113	2.939	1.170

The Wear rate values for pure aluminium with 4% tungsten carbide and 2%, 4% and 6% red mud of 100 µm particle sizes at 600 rpm, at 400^0C are shown in Tables 4, 5 and 6 respectively.

Table 4: Wear Rate values for Pure Aluminium with 4% Tungsten Carbide and 2% Red mud of 100 µm particle size at 600 rpm and 400^0C

Vs=1.256 m/s **ρ=4.482 x10³kg/m³**

m_1	m_2	Δm	T	F_f	µ	R.Dx10^{-3}	$W_r \times 10^{-6}$	$W_v \times 10^{-12}$	$W_s \times 10^{-13}$
(gm)	(gm)	(gm)	(sec)	kgf		m	(N/m)	(m³/sec)	(m³/N-m)
6.95	6.799	0.151	3600	0.3	0.15	4.5257	0.328	9.378	3.733
6.95	6.663	0.287	7200	0.31	0.155	9.0514	0.311	8.903	3.544
6.95	6.523	0.427	10800	0.29	0.145	13.5771	0.309	8.828	3.514
6.95	6.403	0.547	14400	0.3	0.15	18.1028	0.297	8.480	3.376
6.95	6.253	0.697	18000	0.28	0.14	22.6285	0.302	8.643	3.441
6.95	6.123	0.827	21600	0.33	0.165	27.1542	0.299	8.546	3.402

Table 5: Wear Rate values for Pure Aluminium with 4% Tungsten Carbide and 4% Red mud of 100 µm particle size at 600 rpm and 400^0C

Vs=1.256 m/s **ρ = 4.7254x10³ kg/m³**

m_1	m_2	Δm	T	F_f	µ	R.Dx10^{-3}	$W_r \times 10^{-6}$	$W_v \times 10^{-12}$	$W_s \times 10^{-13}$
(gm)	(gm)	(gm)	(sec)	kgf		m	(N/m)	(m³/sec)	(m³/N-m)
7.15	7.063	0.087	3600	0.33	0.165	4.5257	0.188	5.098	2.030
7.15	6.986	0.164	7200	0.35	0.175	9.0514	0.177	4.812	1.916
7.15	6.906	0.244	10800	0.34	0.17	13.5771	0.176	4.776	1.901
7.15	6.826	0.324	14400	0.32	0.16	18.1028	0.175	4.758	1.894
7.15	6.756	0.394	18000	0.34	0.17	22.6285	0.171	4.629	1.843
7.15	6.676	0.474	21600	0.32	0.16	27.1542	0.171	4.641	1.848

Table 6: Wear Rate values for Pure Aluminium with 4% Tungsten Carbide and 6% Red mud of 100 µm particle size at 600 rpm and 400^0C

Vs=1.256 m/s **ρ = 4.924x10³ kg/m³**

m_1	m_2	Δm	T	F_f	µ	R.Dx10^{-3}	$W_r \times 10^{-6}$	$W_v \times 10^{-12}$	$W_s \times 10^{-13}$
(gm)	(gm)	(gm)	(sec)	kgf		m	(N/m)	(m³/sec)	(m³/N-m)
7.23	7.173	0.057	3600	0.31	0.155	4.5257	0.123	3.201	1.274
7.23	7.120	0.110	7200	0.33	0.165	9.0514	0.119	3.096	1.232
7.23	7.067	0.163	10800	0.32	0.16	13.5771	0.118	3.060	1.218
7.23	7.017	0.213	14400	0.3	0.15	18.1028	0.115	3.000	1.194
7.23	6.967	0.263	18000	0.29	0.145	22.6285	0.114	2.964	1.180
7.23	6.917	0.313	21600	0.28	0.14	27.1542	0.113	2.940	1.171

The Wear rate values for pure aluminium with 4% tungsten carbide and 2%, 4% and 6% red mud of 100 μm particle sizes at 600 rpm, at 450^0C are shown in Tables 7, 8 and 9 respectively.

Table 7: Wear Rate values for Pure Aluminium with 4% Tungsten Carbide and 2% Red mud of 100 μm particle size at 600 rpm and 450^0C

Vs=1.256 m/s **ρ=4.482 x10³kg/m³**

m_1	m_2	Δm	T	F_f	μ	R.Dx1000	$W_r \times 10^{-6}$	$W_v \times 10^{-12}$	$W_s \times 10^{-13}$
(gm)	(gm)	(gm)	(sec)	kgf		m	(N/m)	(m³/sec)	(m³/N-m)
6.95	6.804	0.146	3600	0.34	0.17	4.5257	0.316	9.035	3.597
6.95	6.666	0.284	7200	0.29	0.145	9.0514	0.308	8.794	3.501
6.95	6.533	0.417	10800	0.33	0.165	13.5771	0.301	8.610	3.428
6.95	6.393	0.557	14400	0.32	0.16	18.1028	0.302	8.627	3.434
6.95	6.263	0.687	18000	0.31	0.155	22.6285	0.298	8.513	3.389
6.95	6.133	0.817	21600	0.3	0.15	27.1542	0.295	8.437	3.359

Table 8: Wear Rate values for Pure Aluminium with 4% Tungsten Carbide and 4% Red mud of 100 μm particle size at 600 rpm and 450^0C

Vs=1.256 m/s **ρ = 4.7254x10³ kg/m³**

m_1	m_2	Δm	T	F_f	μ	$R.Dx10^{-3}$	$W_r \times 10^{-6}$	$W_v \times 10^{-12}$	$W_s \times 10^{-13}$
(gm)	(gm)	(gm)	(sec)	kgf		m	(N/m)	(m³/sec)	(m³/N-m)
7.15	7.066	0.084	3600	0.27	0.135	4.5257	0.182	4.936	1.965
7.15	6.987	0.163	7200	0.28	0.14	9.0514	0.177	4.790	1.907
7.15	6.911	0.239	10800	0.3	0.15	13.5771	0.173	4.682	1.864
7.15	6.836	0.314	14400	0.29	0.145	18.1028	0.170	4.614	1.837
7.15	6.766	0.384	18000	0.31	0.155	22.6285	0.166	4.514	1.797
7.15	6.696	0.454	21600	0.31	0.155	27.1542	0.164	4.448	1.771

Table 9: Wear Rate values for Pure Aluminium with 4% Tungsten Carbide and 6% Red mud of 100 μm particle size at 600 rpm and 450^0C

Vs=1.256 m/s **ρ = 4.924x10³ kg/m³**

m_1	m_2	Δm	T	F_f	μ	$R.Dx10^{-3}$	$W_r \times 10^{-6}$	$W_v \times 10^{-12}$	$W_s \times 10^{-13}$
(gm)	(gm)	(gm)	(sec)	kgf		m	(N/m)	(m³/sec)	(m³/N-m)
7.23	7.178	0.052	3600	0.3	0.15	4.5257	0.113	2.941	1.171
7.23	7.130	0.100	7200	0.32	0.16	9.0514	0.109	2.824	1.124
7.23	7.082	0.148	10800	0.31	0.155	13.5771	0.107	2.786	1.109
7.23	7.038	0.192	14400	0.29	0.145	18.1028	0.104	2.710	1.079
7.23	6.998	0.232	18000	0.33	0.165	22.6285	0.101	2.619	1.043
7.23	6.958	0.272	21600	0.31	0.155	27.1542	0.098	2.559	1.019

The Wear rate values for pure aluminium with 4% tungsten carbide and 2%, 4% and 6% red mud of 100 µm particle sizes at 600 rpm, at 500^0C are shown in Tables 10, 11 and 12 respectively.

Table 10: Wear Rate values for Pure Aluminium with 4% Tungsten Carbide and 2% Red mud of 100 µm particle size at 600 rpm and 500^0C

Vs=1.256 m/s **ρ=4.482 x10³kg/m³**

m_1	m_2	Δm	T	F_f	µ	R.Dx10^{-3}	$W_r \times 10^{-6}$	$W_v \times 10^{-12}$	$W_s \times 10^{-13}$
(gm)	(gm)	(gm)	(sec)	kgf		m	(N/m)	(m³/sec)	(m³/N-m)
6.95	6.799	0.151	3600	0.3	0.15	4.5257	0.328	9.378	3.733
6.95	6.658	0.292	7200	0.32	0.16	9.0514	0.317	9.058	3.606
6.95	6.513	0.437	10800	0.31	0.155	13.5771	0.316	9.034	3.597
6.95	6.373	0.577	14400	0.33	0.165	18.1028	0.313	8.945	3.561
6.95	6.233	0.717	18000	0.29	0.145	22.6285	0.311	8.891	3.540
6.95	6.123	0.827	21600	0.3	0.15	27.1542	0.299	8.546	3.402

Table 11: Wear Rate values for Pure Aluminium with 4% Tungsten Carbide and 4% Red mud of 100 µm particle size at 600 rpm and 500^0C

Vs=1.256 m/s **ρ = 4.7254x10³ kg/m³**

m_1	m_2	Δm	T	F_f	µ	R.Dx10^{-3}	$W_r \times 10^{-6}$	$W_v \times 10^{-12}$	$W_s \times 10^{-13}$
(gm)	(gm)	(gm)	(sec)	kgf		m	(N/m)	(m³/sec)	(m³/N-m)
7.15	7.064	0.086	3600	0.32	0.16	4.5257	0.186	5.044	2.008
7.15	6.984	0.166	7200	0.3	0.15	9.0514	0.180	4.873	1.940
7.15	6.906	0.244	10800	0.31	0.155	13.5771	0.176	4.777	1.902
7.15	6.826	0.324	14400	0.33	0.165	18.1028	0.175	4.759	1.894
7.15	6.756	0.394	18000	0.29	0.145	22.6285	0.171	4.630	1.843
7.15	6.676	0.474	21600	0.28	0.14	27.1542	0.171	4.642	1.848

Table 12: Wear Rate values for Pure Aluminium with 4% Tungsten Carbide and 6% Red mud of 100 µm particle size at 600 rpm and 500^0C

Vs=1.256 m/s **ρ = 4.924x10³ kg/m³**

m_1	m_2	Δm	T	F_f	µ	R.Dx10^{-3}	$W_r \times 10^{-6}$	$W_v \times 10^{-12}$	$W_s \times 10^{-13}$
(gm)	(gm)	(gm)	(sec)	kgf		m	(N/m)	(m³/sec)	(m³/N-m)
7.23	7.176	0.054	3600	0.35	0.175	4.5257	0.118	3.071	1.223
7.23	7.128	0.102	7200	0.34	0.17	9.0514	0.111	2.889	1.150
7.23	7.078	0.152	10800	0.36	0.18	13.5771	0.110	2.866	1.141
7.23	7.038	0.192	14400	0.37	0.185	18.1028	0.104	2.714	1.080
7.23	6.998	0.232	18000	0.34	0.17	22.6285	0.101	2.623	1.044
7.23	6.958	0.272	21600	0.32	0.16	27.1542	0.098	2.562	1.020

The Wear rate values for pure aluminium with 4% tungsten carbide and 2%, 4% and 6% red mud of 42 nm particle sizes at 600 rpm, at 350^0C are shown in Tables 13, 14 and 15 respectively.

Table 13: Wear Rate values for Pure Aluminium with 4% Tungsten Carbide and 2% Red mud of 42 nm particle size at 600 rpm and 350^0C

Vs=1.256 m/s **ρ=4.482 x10³kg/m³**

m_1	m_2	Δm	T	F_f	μ	R.Dx10^{-3}	$W_r \times 10^{-6}$	$W_v \times 10^{-12}$	$W_s \times 10^{-13}$
(gm)	(gm)	(gm)	(sec)	kgf		m	(N/m)	(m³/sec)	(m³/N-m)
6.95	6.855	0.095	3600	0.28	0.14	4.5257	0.205	5.861	2.333
6.95	6.765	0.185	7200	0.29	0.145	9.0514	0.200	5.720	2.277
6.95	6.677	0.273	10800	0.27	0.135	13.5771	0.197	5.631	2.242
6.95	6.595	0.355	14400	0.25	0.125	18.1028	0.192	5.494	2.187
6.95	6.505	0.445	18000	0.25	0.125	22.6285	0.193	5.511	2.194
6.95	6.425	0.525	21600	0.26	0.13	27.1542	0.190	5.419	2.157

Table 14: Wear Rate values for Pure Aluminium with 4% Tungsten Carbide and 4% Red mud of 42 nm particle size at 600 rpm and 350^0C

Vs=1.256 m/s **ρ = 4.7254x10³ kg/m³**

m_1	m_2	Δm	T	F_f	μ	R.Dx10^{-3}	$W_r \times 10^{-6}$	$W_v \times 10^{-12}$	$W_s \times 10^{-13}$
(gm)	(gm)	(gm)	(sec)	kgf		m	(N/m)	(m³/sec)	(m³/N-m)
7.15	7.096	0.054	3600	0.28	0.14	4.5257	0.118	3.200	1.274
7.15	7.045	0.105	7200	0.29	0.145	9.0514	0.114	3.099	1.234
7.15	6.998	0.152	10800	0.3	0.15	13.5771	0.110	2.987	1.189
7.15	6.948	0.202	14400	0.29	0.145	18.1028	0.110	2.975	1.184
7.15	6.908	0.242	18000	0.27	0.135	22.6285	0.105	2.850	1.135
7.15	6.858	0.292	21600	0.29	0.145	27.1542	0.106	2.865	1.141

Table 15: Wear Rate values for Pure Aluminium with 4% Tungsten Carbide and 6% Red mud of 42 nm particle size at 600 rpm and 350^0C

Vs=1.256 m/s **ρ = 4.924x10³ kg/m³**

m_1	m_2	Δm	T	F_f	μ	R.Dx10^{-3}	$W_r \times 10^{-6}$	$W_v \times 10^{-12}$	$W_s \times 10^{-13}$
(gm)	(gm)	(gm)	(sec)	kgf		m	(N/m)	(m³/sec)	(m³/N-m)
7.23	7.185	0.045	3600	0.25	0.125	4.5257	0.0976	2.540	1.011
7.23	7.148	0.082	7200	0.24	0.12	9.0514	0.089	2.314	0.921
7.23	7.108	0.122	10800	0.29	0.145	13.5771	0.088	2.295	0.913
7.23	7.070	0.160	14400	0.25	0.125	18.1028	0.087	2.257	0.898
7.23	7.038	0.192	18000	0.28	0.14	22.6285	0.083	2.167	0.862
7.23	7.028	0.202	21600	0.27	0.135	27.1542	0.073	1.899	0.756

The Wear rate values for pure aluminium with 4% tungsten carbide and 2%, 4% and 6% red mud of 42 nm particle sizes at 600 rpm, at 400^0C are shown in Tables 16, 17 and 18 respectively.

Table 16: Wear Rate values for Pure Aluminium with 4% Tungsten Carbide and 2% Red mud of 42 nm particle size at 600 rpm and 400^0C

Vs=1.256 m/s **ρ=4.482 x10³kg/m³**

m_1	m_2	Δm	T	F_f	μ	R.Dx10^{-3}	$W_r \times 10^{-6}$	$W_v \times 10^{-12}$	$W_s \times 10^{-13}$
(gm)	(gm)	(gm)	(sec)	kgf		m	(N/m)	(m³/sec)	(m³/N-m)
6.95	6.861	0.089	3600	0.28	0.14	4.5257	0.193	5.518	2.197
6.95	6.776	0.174	7200	0.24	0.12	9.0514	0.189	5.393	2.147
6.95	6.696	0.254	10800	0.26	0.13	13.5771	0.184	5.248	2.089
6.95	6.616	0.334	14400	0.25	0.125	18.1028	0.181	5.176	2.060
6.95	6.536	0.414	18000	0.29	0.145	22.6285	0.179	5.132	2.043
6.95	6.456	0.494	21600	0.23	0.115	27.1542	0.178	5.103	2.031

Table 17: Wear Rate values for Pure Aluminium with 4% Tungsten Carbide and 4% Red mud of 42 nm particle size at 600 rpm and 400^0C

Vs=1.256 m/s **ρ = 4.7254x10³ kg/m³**

m_1	m_2	Δm	T	F_f	μ	R.Dx10^{-3}	$W_r \times 10^{-6}$	$W_v \times 10^{-12}$	$W_s \times 10^{-13}$
(gm)	(gm)	(gm)	(sec)	kgf		m	(N/m)	(m³/sec)	(m³/N-m)
7.15	7.098	0.052	3600	0.28	0.14	4.5257	0.113	3.064	1.220
7.15	7.048	0.102	7200	0.27	0.135	9.0514	0.111	3.002	1.195
7.15	6.998	0.152	10800	0.26	0.13	13.5771	0.110	2.981	1.187
7.15	6.958	0.192	14400	0.25	0.125	18.1028	0.104	2.824	1.124
7.15	6.918	0.232	18000	0.27	0.135	22.6285	0.101	2.729	1.086
7.15	6.878	0.272	21600	0.27	0.135	27.1542	0.098	2.666	1.061

Table 18: Wear Rate values for Pure Aluminium with 4% Tungsten Carbide and 6% Red mud of 42 nm particle size at 600 rpm and 400^0C

Vs=1.256 m/s **ρ = 4.924x10³ kg/m³**

m_1	m_2	Δm	T	F_f	μ	R.Dx10^{-3}	$W_r \times 10^{-6}$	$W_v \times 10^{-12}$	$W_s \times 10^{-13}$
(gm)	(gm)	(gm)	(sec)	kgf		m	(N/m)	(m³/sec)	(m³/N-m)
7.23	7.190	0.040	3600	0.27	0.135	4.5257	0.086	2.238	0.891
7.23	7.158	0.072	7200	0.29	0.145	9.0514	0.078	2.022	0.805
7.23	7.128	0.102	10800	0.25	0.125	13.5771	0.073	1.912	0.761
7.23	7.098	0.132	14400	0.29	0.145	18.1028	0.071	1.857	0.739
7.23	7.068	0.162	18000	0.27	0.135	22.6285	0.070	1.824	0.726
7.23	7.038	0.192	21600	0.29	0.145	27.1542	0.069	1.802	0.717

The Wear rate values for pure aluminium with 4% tungsten carbide and 2%, 4% and 6% red mud of 42 nm particle sizes at 600 rpm, at 450^0C are shown in Tables 19, 20 and 21 respectively.

Table 19: Wear Rate values for Pure Aluminium with 4% Tungsten Carbide and 2% Red mud of 42 nm particle size at 600 rpm and 450^0C

Vs=1.256 m/s **ρ=4.482 x10³kg/m³**

m_1	m_2	Δm	T	F_f	μ	R.Dx10^{-3}	$W_r \times 10^{-6}$	$W_v \times 10^{-12}$	$W_s \times 10^{-13}$
(gm)	(gm)	(gm)	(sec)	kgf		m	(N/m)	(m³/sec)	(m³/N-m)
6.95	6.864	0.086	3600	0.29	0.145	4.5257	0.186	5.318	2.117
6.95	6.786	0.164	7200	0.28	0.14	9.0514	0.178	5.076	2.021
6.95	6.706	0.244	10800	0.27	0.135	13.5771	0.176	5.037	2.005
6.95	6.628	0.322	14400	0.26	0.13	18.1028	0.174	4.986	1.985
6.95	6.556	0.394	18000	0.25	0.125	22.6285	0.171	4.881	1.943
6.95	6.486	0.464	21600	0.29	0.145	27.1542	0.168	4.791	1.907

Table 20: Wear Rate values for Pure Aluminium with 4% Tungsten Carbide and 4% Red mud of 42 nm particle size at 600 rpm and 450^0C

Vs=1.256 m/s **ρ = 4.7254x10³ kg/m³**

m_1	m_2	Δm	T	F_f	μ	R.Dx10^{-3}	$W_r \times 10^{-6}$	$W_v \times 10^{-12}$	$W_s \times 10^{-13}$
(gm)	(gm)	(gm)	(sec)	kgf		m	(N/m)	(m³/sec)	(m³/N-m)
7.15	7.100	0.050	3600	0.29	0.145	4.5257	0.109	2.956	1.177
7.15	7.058	0.092	7200	0.29	0.145	9.0514	0.100	2.712	1.080
7.15	7.008	0.142	10800	0.31	0.155	13.5771	0.103	2.788	1.110
7.15	6.968	0.182	14400	0.28	0.14	18.1028	0.099	2.679	1.066
7.15	6.928	0.222	18000	0.28	0.14	22.6285	0.096	2.613	1.040
7.15	6.888	0.262	21600	0.27	0.135	27.1542	0.095	2.570	1.023

Table 21: Wear Rate values for Pure Aluminium with 4% Tungsten Carbide and 6% Red mud of 42 nm particle size at 600 rpm and 450^0C

Vs=1.256 m/s **ρ = 4.924x10³ kg/m³**

m_1	m_2	Δm	T	F_f	μ	R.Dx10^{-3}	$W_r \times 10^{-6}$	$W_v \times 10^{-12}$	$W_s \times 10^{-13}$
(gm)	(gm)	(gm)	(sec)	kgf		m	(N/m)	(m³/sec)	(m³/N-m)
7.23	7.192	0.038	3600	0.27	0.135	4.5257	0.082	2.134	0.850
7.23	7.164	0.066	7200	0.29	0.145	9.0514	0.071	1.857	0.739
7.23	7.134	0.096	10800	0.31	0.155	13.5771	0.069	1.802	0.717
7.23	7.104	0.126	14400	0.28	0.14	18.1028	0.068	1.775	0.706
7.23	7.074	0.156	18000	0.25	0.125	22.6285	0.068	1.758	0.700
7.23	7.044	0.186	21600	0.26	0.13	27.1542	0.067	1.747	0.696

The Wear rate values for pure aluminium with 4% tungsten carbide and 2%, 4% and 6% red mud of 42 nm particle sizes at 600 rpm, at 500^0C are shown in Tables 22, 23 and 24 respectively.

Table 22: Wear Rate values for Pure Aluminium with 4% Tungsten Carbide and 2% Red mud of 42 nm particle size at 600 rpm and 500^0C

Vs=1.256 m/s **ρ=4.482 x10³kg/m³**

m_1	m_2	Δm	T	F_f	μ	R.Dx10^{-3}	$W_r \times 10^{-6}$	$W_v \times 10^{-12}$	$W_s \times 10^{-13}$
(gm)	(gm)	(gm)	(sec)	kgf		m	(N/m)	(m³/sec)	(m³/N-m)
6.95	6.862	0.088	3600	0.25	0.125	4.5257	0.191	5.461	2.174
6.95	6.786	0.164	7200	0.24	0.12	9.0514	0.178	5.086	2.025
6.95	6.706	0.244	10800	0.29	0.145	13.5771	0.176	5.043	2.008
6.95	6.636	0.314	14400	0.31	0.155	18.1028	0.170	4.867	1.937
6.95	6.556	0.394	18000	0.28	0.14	22.6285	0.171	4.885	1.945
6.95	6.486	0.464	21600	0.27	0.135	27.1542	0.168	4.794	1.908

Table 23: Wear Rate values for Pure Aluminium with 4% Tungsten Carbide and 4% Red mud of 42 nm particle size at 600 rpm and 500^0C

Vs=1.256 m/s **ρ = 4.7254x10³ kg/m³**

m_1	m_2	Δm	T	F_f	μ	R.Dx10^{-3}	$W_r \times 10^{-6}$	$W_v \times 10^{-12}$	$W_s \times 10^{-13}$
(gm)	(gm)	(gm)	(sec)	kgf		m	(N/m)	(m³/sec)	(m³/N-m)
7.15	7.099	0.051	3600	0.28	0.14	4.5257	0.111	3.010	1.198
7.15	7.058	0.092	7200	0.29	0.145	9.0514	0.100	2.710	1.079
7.15	7.008	0.142	10800	0.27	0.135	13.5771	0.103	2.787	1.109
7.15	6.968	0.182	14400	0.25	0.125	18.1028	0.099	2.678	1.066
7.15	6.928	0.222	18000	0.25	0.125	22.6285	0.096	2.612	1.040
7.15	6.888	0.262	21600	0.27	0.135	27.1542	0.095	2.569	1.023

Table 24: Wear Rate values for Pure Aluminium with 4% Tungsten Carbide and 6% Red mud of 42 nm particle size at 600 rpm and 500^0C

Vs=1.256 m/s **ρ = 4.924x10³ kg/m³**

m_1	m_2	Δm	T	F_f	μ	R.Dx10^{-3}	$W_r \times 10^{-6}$	$W_v \times 10^{-12}$	$W_s \times 10^{-13}$
(gm)	(gm)	(gm)	(sec)	kgf		m	(N/m)	(m³/sec)	(m³/N-m)
7.23	7.191	0.039	3600	0.26	0.13	4.5257	0.084	2.186	0.870
7.23	7.158	0.072	7200	0.25	0.125	9.0514	0.078	2.024	0.806
7.23	7.128	0.102	10800	0.24	0.12	13.5771	0.074	1.913	0.762
7.23	7.098	0.132	14400	0.31	0.155	18.1028	0.071	1.858	0.740
7.23	7.068	0.162	18000	0.25	0.125	22.6285	0.070	1.825	0.727
7.23	7.038	0.192	21600	0.29	0.145	27.1542	0.069	1.803	0.718

iii) Wear rate tables for pure aluminium with 4% tungsten carbide and red mud at 30 N load

The Wear rate values for pure aluminium with 4% tungsten carbide and 2%, 4% and 6% red mud of 100 μm particle sizes at 600 rpm, at 350^0C are shown in Tables 1, 2 and 3 respectively.

Table 1: Wear Rate values for Pure Aluminium with 4% Tungsten Carbide and 2% Red mud of 100 μm particle size at 600 rpm and 350^0C

Vs=1.256 m/s **ρ=4.482 x10³kg/m³**

m_1	m_2	Δm	T	F_f	μ	R.Dx10^{-3}	$W_r\times10^{-6}$	$W_v\times10^{-12}$	$W_s\times10^{-13}$
(gm)	(gm)	(gm)	(sec)	kgf		m	(N/m)	(m³/sec)	(m³/N-m)
6.95	6.783	0.167	3600	0.31	0.1033	4.5257	0.362	10.3501	2.746
6.95	6.64	0.31	7200	0.32	0.1067	9.0514	0.336	9.606	2.549
6.95	6.5	0.45	10800	0.29	0.0967	13.5771	0.3251	9.296	2.467
6.95	6.36	0.59	14400	0.28	0.0933	18.1028	0.3197	9.141	2.425
6.95	6.22	0.73	18000	0.31	0.1033	22.6285	0.3165	9.048	2.401
6.95	6.08	0.87	21600	0.32	0.1067	27.1542	0.3143	8.986	2.384

Table 2: Wear Rate values for Pure Aluminium with 4% Tungsten Carbide and 4% Red mud of 100 μm particle size at 600 rpm and 350^0C

Vs=1.256 m/s **ρ = 4.7254x10³ kg/m³**

m_1	m_2	Δm	T	F_f	μ	R.Dx10^{-3}	$W_r\times10^{-6}$	$W_v\times10^{-12}$	$W_s\times10^{-13}$
(gm)	(gm)	(gm)	(sec)	kgf		m	(N/m)	(m³/sec)	(m³/N-m)
7.15	7.055	0.0955	3600	0.30	0.1	4.5257	0.207	5.613	1.489
7.15	6.97	0.18	7200	0.31	0.1033	9.0514	0.1951	5.2905	1.404
7.15	6.89	0.26	10800	0.29	0.0967	13.5771	0.1879	5.094	1.351
7.15	6.81	0.34	14400	0.32	0.1067	18.1028	0.1842	4.996	1.325
7.15	6.74	0.41	18000	0.29	0.0967	22.6285	0.1777	4.8202	1.279
7.15	6.66	0.49	21600	0.31	0.1033	27.1542	0.1770	4.8006	1.274

Table 3: Wear Rate values for Pure Aluminium with 4% Tungsten Carbide and 6% Red mud of 100 μm particle size at 600 rpm and 350^0C

Vs=1.256 m/s **ρ = 4.924x10³ kg/m³**

m_1	m_2	Δm	T	F_f	μ	R.Dx10^{-3}	$W_r\times10^{-6}$	$W_v\times10^{-12}$	$W_s\times10^{-13}$
(gm)	(gm)	(gm)	(sec)	kgf		m	(N/m)	(m³/sec)	(m³/N-m)
7.23	7.1668	0.0632	3600	0.28	0.0933	4.5257	0.137	3.565	0.946
7.23	7.12	0.11	7200	0.29	0.0967	9.0514	0.1192	3.102	0.823
7.23	7.07	0.16	10800	0.30	0.1	13.5771	0.1156	3.008	0.798
7.23	7.02	0.21	14400	0.31	0.1033	18.1028	0.1138	2.961	0.785
7.23	6.97	0.26	18000	0.30	0.1	22.6285	0.1127	2.933	0.778
7.23	6.92	0.31	21600	0.29	0.0967	27.1542	0.1120	2.914	0.773

The Wear rate values for pure aluminium with 4% tungsten carbide and 2%, 4% and 6% red mud of 100 µm particle sizes at 600 rpm, at 400^0C are shown in Tables 4, 5 and 6 respectively.

Table 4: Wear Rate values for Pure Aluminium with 4% Tungsten Carbide and 2% Red mud of 100 µm particle size at 600 rpm and 400^0C

Vs=1.256 m/s **ρ=4.482 x10³kg/m³**

m_1	m_2	Δm	T	F_f	µ	R.Dx10^{-3}	$W_r \times 10^{-6}$	$W_v \times 10^{-12}$	$W_s \times 10^{-13}$
(gm)	(gm)	(gm)	(sec)	kgf		m	(N/m)	(m³/sec)	(m³/N-m)
6.95	6.786	0.1638	3600	0.30	0.1	4.5257	0.355	10.151	2.694
6.95	6.65	0.30	7200	0.31	0.1033	9.0514	0.3251	9.296	2.467
6.95	6.51	0.44	10800	0.29	0.0967	13.5771	0.3179	9.089	2.412
6.95	6.39	0.56	14400	0.30	0.1	18.1028	0.30346	8.676	2.302
6.95	6.24	0.71	18000	0.28	0.0933	22.6285	0.3078	8.8006	2.335
6.95	6.11	0.84	21600	0.33	0.11	27.1542	0.30346	8.676	2.302

Table 5: Wear Rate values for Pure Aluminium with 4% Tungsten Carbide and 4% Red mud of 100 µm particle size at 600 rpm and 400^0C

Vs=1.256 m/s **ρ = 4.7254x10³ kg/m³**

m_1	m_2	Δm	T	F_f	µ	R.Dx10^{-3}	$W_r \times 10^{-6}$	$W_v \times 10^{-12}$	$W_s \times 10^{-13}$
(gm)	(gm)	(gm)	(sec)	kgf		m	(N/m)	(m³/sec)	(m³/N-m)
7.15	7.056	0.0941	3600	0.33	0.11	4.5257	0.204	5.531	1.467
7.15	6.98	0.17	7200	0.35	0.1167	9.0514	0.1842	4.996	1.325
7.15	6.9	0.25	10800	0.34	0.1133	13.5771	0.1806	4.898	1.299
7.15	6.82	0.33	14400	0.32	0.1067	18.1028	0.1788	4.849	1.286
7.15	6.75	0.40	18000	0.34	0.1133	22.6285	0.1734	4.702	1.247
7.15	6.67	0.48	21600	0.32	0.1067	27.1542	0.1734	4.702	1.247

Table 6: Wear Rate values for Pure Aluminium with 4% Tungsten Carbide and 6% Red mud of 100 µm particle size at 600 rpm and 400^0C

Vs=1.256 m/s **ρ = 4.924x10³ kg/m³**

m_1	m_2	Δm	T	F_f	µ	R.Dx10^{-3}	$W_r \times 10^{-6}$	$W_v \times 10^{-12}$	$W_s \times 10^{-13}$
(gm)	(gm)	(gm)	(sec)	kgf		m	(N/m)	(m³/sec)	(m³/N-m)
7.23	7.1686	0.0614	3600	0.31	0.1033	4.5257	0.133	3.463	0.919
7.23	7.116	0.114	7200	0.33	0.11	9.0514	0.1236	3.215	0.853
7.23	7.06	0.17	10800	0.32	0.1067	13.5771	0.1228	3.196	0.848
7.23	7.01	0.22	14400	0.30	0.1	18.1028	0.1192	3.102	0.823
7.23	6.96	0.27	18000	0.29	0.0967	22.6285	0.1171	3.046	0.808
7.23	6.91	0.32	21600	0.28	0.0933	27.1542	0.1156	3.008	0.798

The Wear rate values for pure aluminium with 4% tungsten carbide and 2%, 4% and 6% red mud of 100 µm particle sizes at 600 rpm, at 450^0C are shown in Tables 7, 8 and 9 respectively.

Table 7: Wear Rate values for Pure Aluminium with 4% Tungsten Carbide and 2% Red mud of 100 µm particle size at 600 rpm and 450^0C

Vs=1.256 m/s **ρ=4.482 x10³kg/m³**

m_1	m_2	Δm	T	F_f	µ	R.Dx10^{-3}	$W_r\times10^{-6}$	$W_v\times10^{-12}$	$W_s\times10^{-13}$
(gm)	(gm)	(gm)	(sec)	kgf		m	(N/m)	(m³/sec)	(m³/N-m)
6.95	6.792	0.1582	3600	0.34	0.1133	4.5257	0.343	9.804	2.601
6.95	6.654	0.296	7200	0.29	0.0967	9.0514	0.3208	9.172	2.434
6.95	6.52	0.43	10800	0.33	0.11	13.5771	0.3107	8.883	2.357
6.95	6.38	0.57	14400	0.32	0.1067	18.1028	0.3089	8.831	2.343
6.95	6.25	0.70	18000	0.31	0.1033	22.6285	0.3035	8.676	2.302
6.95	6.12	0.83	21600	0.30	0.1	27.1542	0.2999	8.573	2.275

Table 8: Wear Rate values for Pure Aluminium with 4% Tungsten Carbide and 4% Red mud of 100 µm particle size at 600 rpm and 450^0C

Vs=1.256 m/s **ρ = 4.7254x10³ kg/m³**

m_1	m_2	Δm	T	F_f	µ	R.Dx10^{-3}	$W_r\times10^{-6}$	$W_v\times10^{-12}$	$W_s\times10^{-13}$
(gm)	(gm)	(gm)	(sec)	kgf		m	(N/m)	(m³/sec)	(m³/N-m)
7.15	7.059	0.0909	3600	0.27	0.09	4.5257	0.197	5.343	1.417
7.15	6.98	0.17	7200	0.28	0.0933	9.0514	0.1842	4.996	1.325
7.15	6.901	0.249	10800	0.30	0.1	13.5771	0.1799	4.879	1.294
7.15	6.83	0.32	14400	0.29	0.0967	18.1028	0.1734	4.702	1.247
7.15	6.76	0.39	18000	0.31	0.1033	22.6285	0.1691	4.585	1.216
7.15	6.69	0.46	21600	0.31	0.1033	27.1542	0.1662	4.506	1.195

Table 9: Wear Rate values for Pure Aluminium with 4% Tungsten Carbide and 6% Red mud of 100 µm particle size at 600 rpm and 450^0C

Vs=1.256 m/s **ρ = 4.924x10³ kg/m³**

m_1	m_2	Δm	T	F_f	µ	R.Dx10^{-3}	$W_r\times10^{-6}$	$W_v\times10^{-12}$	$W_s\times10^{-13}$
(gm)	(gm)	(gm)	(sec)	kgf		m	(N/m)	(m³/sec)	(m³/N-m)
7.23	7.1733	0.0567	3600	0.30	0.1	4.5257	0.123	3.198	0.848
7.23	7.125	0.105	7200	0.32	0.1067	9.0514	0.1138	2.961	0.785
7.23	7.077	0.153	10800	0.31	0.1033	13.5771	0.1105	2.877	0.763
7.23	7.033	0.197	14400	0.29	0.0967	18.1028	0.1068	2.778	0.562
7.23	6.989	0.241	18000	0.33	0.11	22.6285	0.1045	2.719	0.721
7.23	6.945	0.285	21600	0.31	0.1033	27.1542	0.1030	2.679	0.7109

The Wear rate values for pure aluminium with 4% tungsten carbide and 2%, 4% and 6% red mud of 100 μm particle sizes at 600 rpm, at 500^0C are shown in Tables 10, 11 and 12 respectively.

Table 10: Wear Rate values for Pure Aluminium with 4% Tungsten Carbide and 2% Red mud of 100 μm particle size at 600 rpm and 500^0C

Vs=1.256 m/s **ρ=4.482 x10³kg/m³**

m_1 (gm)	m_2 (gm)	Δm (gm)	T (sec)	F_f kgf	μ	R.Dx10^{-3} m	$W_r\times10^{-6}$ (N/m)	$W_v\times10^{-12}$ (m³/sec)	$W_s\times10^{-13}$ (m³/N-m)
6.95	6.786	0.1638	3600	0.30	0.1	4.5257	0.355	10.151	2.694
6.95	6.645	0.305	7200	0.32	0.1067	9.0514	0.3306	9.451	2.508
6.95	6.5	0.45	10800	0.31	0.1033	13.5771	0.3251	9.296	2.467
6.95	6.36	0.59	14400	0.33	0.11	18.1028	0.3197	9.141	2.425
6.95	6.22	0.73	18000	0.29	0.0967	22.6285	0.3165	9.048	2.401
6.95	6.11	0.84	21600	0.30	0.1	27.1542	0.3035	8.676	2.302

Table 11: Wear Rate values for Pure Aluminium with 4% Tungsten Carbide and 4% Red mud of 100 μm particle size at 600 rpm and 500^0C

Vs=1.256 m/s **ρ = 4.7254x10³ kg/m³**

m_1 (gm)	m_2 (gm)	Δm (gm)	T (sec)	F_f kgf	μ	R.Dx10^{-3} m	$W_r\times10^{-6}$ (N/m)	$W_v\times10^{-12}$ (m³/sec)	$W_s\times10^{-13}$ (m³/N-m)
7.15	7.058	0.0918	3600	0.32	0.1067	4.5257	0.199	5.396	1.432
7.15	6.978	0.172	7200	0.30	0.1033	9.0514	0.1864	5.055	1.341
7.15	6.9	0.25	10800	0.31	0.1033	13.5771	0.1806	4.898	1.299
7.15	6.82	0.33	14400	0.33	0.11	18.1028	0.1788	4.849	1.286
7.15	6.75	0.40	18000	0.29	0.0967	22.6285	0.1734	4.702	1.247
7.15	6.67	0.48	21600	0.28	0.0933	27.1542	0.1734	4.702	1.247

Table 12: Wear Rate values for Pure Aluminium with 4% Tungsten Carbide and 6% Red mud of 100 μm particle size at 600 rpm and 500^0C

Vs=1.256 m/s **ρ = 4.924x10³ kg/m³**

m_1 (gm)	m_2 (gm)	Δm (gm)	T (sec)	F_f kgf	μ	R.Dx10^{-3} m	$W_r\times10^{-6}$ (N/m)	$W_v\times10^{-12}$ (m³/sec)	$W_s\times10^{-13}$ (m³/N-m)
7.23	7.1709	0.0591	3600	0.35	0.1167	4.5257	0.128	3.334	0.884
7.23	7.123	0.107	7200	0.34	0.1133	9.0514	0.116	3.018	0.8009
7.23	7.075	0.155	10800	0.36	0.12	13.5771	0.112	2.914	0.773
7.23	7.027	0.203	14400	0.37	0.1233	18.1028	0.11	2.862	0.759
7.23	6.979	0.251	18000	0.34	0.1133	22.6285	0.1088	2.831	0.751
7.23	6.931	0.299	21600	0.32	0.1067	27.1542	0.1080	2.811	0.746

The Wear rate values for pure aluminium with 4% tungsten carbide and 2%, 4% and 6% red mud of 42 nm particle sizes at 600 rpm, at 350^0C are shown in Tables 13, 14 and 15 respectively.

Table 13: Wear Rate values for Pure Aluminium with 4% Tungsten Carbide and 2% Red mud of 42 nm particle size at 600 rpm and 350^0C

Vs=1.256 m/s **ρ=4.482 x10³kg/m³**

m_1	m_2	Δm	T	F_f	μ	R.Dx10^{-3}	$W_r\times10^{-6}$	$W_v\times10^{-12}$	$W_s\times10^{-13}$
(gm)	(gm)	(gm)	(sec)	kgf		m	(N/m)	(m³/sec)	(m³/N-m)
6.95	6.848	0.1024	3600	0.28	0.0933	4.5257	0.222	6.346	1.684
6.95	6.758	0.192	7200	0.29	0.0967	9.0514	0.2081	5.949	1.578
6.95	6.678	0.272	10800	0.27	0.09	13.5771	0.1965	5.619	1.419
6.95	6.59	0.36	14400	0.25	0.0833	18.1028	0.1951	5.577	1.4801
6.95	6.5	0.45	18000	0.25	0.0833	22.6285	0.1951	5.577	1.4801
6.95	6.42	0.53	21600	0.26	0.0867	27.1542	0.1915	5.474	1.452

Table 14: Wear Rate values for Pure Aluminium with 4% Tungsten Carbide and 4% Red mud of 42 nm particle size at 600 rpm and 350^0C

Vs=1.256 m/s **ρ = 4.7254x10³ kg/m³**

m_1	m_2	Δm	T	F_f	μ	R.Dx10^{-3}	$W_r\times10^{-6}$	$W_v\times10^{-12}$	$W_s\times10^{-13}$
(gm)	(gm)	(gm)	(sec)	kgf		m	(N/m)	(m³/sec)	(m³/N-m)
7.15	7.091	0.0586	3600	0.28	0.0933	4.5257	0.127	3.447	0.914
7.15	7.01	0.110	7200	0.29	0.0967	9.0514	0.1192	3.233	0.858
7.15	6.993	0.157	10800	0.30	0.1	13.5771	0.1134	3.076	0.816
7.15	6.943	0.207	14400	0.29	0.0967	18.1028	0.1122	3.042	0.807
7.15	6.903	0.247	18000	0.27	0.09	22.6285	0.1071	2.903	0.7704
7.15	6.853	0.297	21600	0.29	0.0967	27.1542	0.1073	2.909	0.772

Table 15: Wear Rate values for Pure Aluminium with 4% Tungsten Carbide and 6% Red mud of 42 nm particle size at 600 rpm and 350^0C

Vs=1.256 m/s **ρ = 4.924x10³ kg/m³**

m_1	m_2	Δm	T	F_f	μ	R.Dx10^{-3}	$W_r\times10^{-6}$	$W_v\times10^{-12}$	$W_s\times10^{-13}$
(gm)	(gm)	(gm)	(sec)	kgf		m	(N/m)	(m³/sec)	(m³/N-m)
7.23	7.1811	0.0489	3600	0.25	0.0833	4.5257	0.106	2.758	0.731
7.23	7.144	0.086	7200	0.24	0.08	9.0514	0.0932	2.425	0.643
7.23	7.104	0.126	10800	0.29	0.0967	13.5771	0.091	2.369	0.628
7.23	7.066	0.164	14400	0.25	0.0833	18.1028	0.0889	2.312	0.613
7.23	7.034	0.196	18000	0.28	0.0933	22.6285	0.085	2.211	0.586
7.23	7.024	0.206	21600	0.27	0.09	27.1542	0.0744	1.936	0.513

The Wear rate values for pure aluminium with 4% tungsten carbide and 2%, 4% and 6% red mud of 42 nm particle sizes at 600 rpm, at 400^0C are shown in Tables 16, 17 and 18 respectively.

Table 16: Wear Rate values for Pure Aluminium with 4% Tungsten Carbide and 2% Red mud of 42 nm particle size at 600 rpm and 400^0C

Vs=1.256 m/s **ρ=4.482 x10³kg/m³**

m_1	m_2	Δm	T	F_f	μ	R.Dx10^{-3}	$W_r\times10^{-6}$	$W_v\times10^{-12}$	$W_s\times10^{-13}$
(gm)	(gm)	(gm)	(sec)	kgf		m	(N/m)	(m³/sec)	(m³/N-m)
6.95	6.854	0.0964	3600	0.28	0.0933	4.5257	0.209	5.974	1.585
6.95	6.77	0.18	7200	0.24	0.08	9.0514	0.1951	5.577	1.4801
6.95	6.69	0.26	10800	0.26	0.0867	13.5771	0.1879	5.371	1.425
6.95	6.61	0.34	14400	0.25	0.0833	18.1028	0.1842	5.276	1.4002
6.95	6.53	0.42	18000	0.29	0.0967	22.6285	0.1821	5.206	1.381
6.95	6.45	0.50	21600	0.23	0.0767	27.1542	0.1806	5.164	1.3704

Table 17: Wear Rate values for Pure Aluminium with 4% Tungsten Carbide and 4% Red mud of 42 nm particle size at 600 rpm and 400^0C

Vs=1.256 m/s **ρ = 4.7254x10³ kg/m³**

m_1	m_2	Δm	T	F_f	μ	R.Dx10^{-3}	$W_r\times10^{-6}$	$W_v\times10^{-12}$	$W_s\times10^{-13}$
(gm)	(gm)	(gm)	(sec)	kgf		m	(N/m)	(m³/sec)	(m³/N-m)
7.15	7.094	0.0558	3600	0.28	0.0933	4.5257	0.121	3.2801	0.8705
7.15	7.044	0.106	7200	0.27	0.09	9.0514	0.1149	3.115	0.826
7.15	6.994	0.156	10800	0.26	0.0867	13.5771	0.1127	3.056	0.811
7.15	6.954	0.196	14400	0.25	0.0833	18.1028	0.1062	2.8804	0.7644
7.15	6.914	0.236	18000	0.27	0.09	22.6285	0.1023	2.774	0.736
7.15	6.874	0.276	21600	0.27	0.09	27.1542	0.0997	2.704	0.717

Table 18: Wear Rate values for Pure Aluminium with 4% Tungsten Carbide and 6% Red mud of 42 nm particle size at 600 rpm and 400^0C

Vs=1.256 m/s **ρ = 4.924x10³ kg/m³**

m_1	m_2	Δm	T	F_f	μ	R.Dx10^{-3}	$W_r\times10^{-6}$	$W_v\times10^{-12}$	$W_s\times10^{-13}$
(gm)	(gm)	(gm)	(sec)	kgf		m	(N/m)	(m³/sec)	(m³/N-m)
7.23	7.1871	0.0429	3600	0.27	0.09	4.5257	0.093	2.4201	0.642
7.23	7.155	0.075	7200	0.29	0.0967	9.0514	0.0813	2.115	0.561
7.23	7.125	0.105	10800	0.25	0.0833	13.5771	0.0759	1.974	0.523
7.23	7.095	0.135	14400	0.29	0.0967	18.1028	0.0732	1.903	0.505
7.23	7.065	0.165	18000	0.27	0.09	22.6285	0.0715	1.861	0.493
7.23	7.035	0.195	21600	0.29	0.0967	27.1542	0.0704	1.833	0.486

The Wear rate values for pure aluminium with 4% tungsten carbide and 2%, 4% and 6% red mud of 42 nm particle sizes at 600 rpm, at 450^0C are shown in Tables 19, 20 and 21 respectively.

Table 19: Wear Rate values for Pure Aluminium with 4% Tungsten Carbide and 2% Red mud of 42 nm particle size at 600 rpm and 450^0C

Vs=1.256 m/s **ρ=4.482 x10³kg/m³**

m_1	m_2	Δm	T	F_f	μ	R.Dx10^{-3}	$W_r\times10^{-6}$	$W_v\times10^{-12}$	$W_s\times10^{-13}$
(gm)	(gm)	(gm)	(sec)	kgf		m	(N/m)	(m³/sec)	(m³/N-m)
6.95	6.857	0.0927	3600	0.29	0.0967	4.5257	0.201	5.745	1.524
6.95	6.78	0.17	7200	0.28	0.0933	9.0514	0.1842	5.267	1.4002
6.95	6.7	0.25	10800	0.27	0.09	13.5771	0.1806	5.164	1.3704
6.95	6.622	0.328	14400	0.26	0.0867	18.1028	0.1777	5.082	1.348
6.95	6.55	0.40	18000	0.25	0.0833	22.6285	0.1734	4.958	1.315
6.95	6.48	0.47	21600	0.29	0.0967	27.1542	0.1698	4.854	1.288

Table 20: Wear Rate values for Pure Aluminium with 4% Tungsten Carbide and 4% Red mud of 42 nm particle size at 600 rpm and 450^0C

Vs=1.256 m/s **ρ = 4.7254x10³ kg/m³**

m_1	m_2	Δm	T	F_f	μ	R.Dx10^{-3}	$W_r\times10^{-6}$	$W_v\times10^{-12}$	$W_s\times10^{-13}$
(gm)	(gm)	(gm)	(sec)	kgf		m	(N/m)	(m³/sec)	(m³/N-m)
7.15	7.096	0.0544	3600	0.29	0.0967	4.5257	0.118	3.197	0.848
7.15	7.05	0.1	7200	0.29	0.0967	9.0514	0.1084	2.939	0.779
7.15	7	0.15	10800	0.31	0.1033	13.5771	0.1084	2.939	0.779
7.15	6.96	0.19	14400	0.28	0.0933	18.1028	0.1030	2.792	0.7409
7.15	6.92	0.23	18000	0.28	0.0933	22.6285	0.0997	2.704	0.717
7.15	6.88	0.27	21600	0.27	0.09	27.1542	0.0975	2.645	0.701

Table 21: Wear Rate values for Pure Aluminium with 4% Tungsten Carbide and 6% Red mud of 42 nm particle size at 600 rpm and 450^0C

Vs=1.256 m/s **ρ = 4.924x10³ kg/m³**

m_1	m_2	Δm	T	F_f	μ	R.Dx10^{-3}	$W_r\times10^{-6}$	$W_v\times10^{-12}$	$W_s\times10^{-13}$
(gm)	(gm)	(gm)	(sec)	kgf		m	(N/m)	(m³/sec)	(m³/N-m)
7.23	7.1894	0.0406	3600	0.27	0.09	4.5257	0.088	2.2903	0.607
7.23	7.153	0.077	7200	0.29	0.0967	9.0514	0.0835	2.171	0.576
7.23	7.125	0.105	10800	0.31	0.1033	13.5771	0.0759	1.974	0.523
7.23	7.095	0.135	14400	0.28	0.0933	18.1028	0.0732	1.903	0.505
7.23	7.065	0.165	18000	0.25	0.0833	22.6285	0.0715	1.861	0.493
7.23	7.035	0.195	21600	0.26	0.0867	27.1542	0.0704	1.833	0.486

The Wear rate values for pure aluminium with 4% tungsten carbide and 2%, 4% and 6% red mud of 42 nm particle sizes at 600 rpm, at 500^0C are shown in Tables 22, 23 and 24 respectively.

Table 22: Wear Rate values for Pure Aluminium with 4% Tungsten Carbide and 2% Red mud of 42 nm particle size at 600 rpm and 500^0C

Vs=1.256 m/s **ρ=4.482 x10³kg/m³**

m_1	m_2	Δm	T	F_f	μ	R.Dx10^{-3}	$W_r \times 10^{-6}$	$W_v \times 10^{-12}$	$W_s \times 10^{-13}$
(gm)	(gm)	(gm)	(sec)	kgf		m	(N/m)	(m³/sec)	(m³/N-m)
6.95	6.855	0.0955	3600	0.25	0.0833	4.5257	0.207	5.918	1.5705
6.95	6.78	0.17	7200	0.24	0.08	9.0514	0.1842	5.267	1.397
6.95	6.7	0.25	10800	0.29	0.0967	13.5771	0.1806	5.164	1.3704
6.95	6.63	0.32	14400	0.31	0.1033	18.1028	0.1734	4.958	1.315
6.95	6.55	0.40	18000	0.28	0.0933	22.6285	0.1734	4.958	1.315
6.95	6.48	0.47	21600	0.27	0.09	27.1542	0.1698	4.854	1.288

Table 23: Wear Rate values for Pure Aluminium with 4% Tungsten Carbide and 4% Red mud of 42 nm particle size at 600 rpm and 500^0C

Vs=1.256 m/s **ρ = 4.7254x10³ kg/m³**

m_1	m_2	Δm	T	F_f	μ	R.Dx10^{-3}	$W_r \times 10^{-6}$	$W_v \times 10^{-12}$	$W_s \times 10^{-13}$
(gm)	(gm)	(gm)	(sec)	kgf		m	(N/m)	(m³/sec)	(m³/N-m)
7.15	7.095	0.0554	3600	0.28	0.0933	4.5257	0.120	3.256	0.864
7.15	7.054	0.096	7200	0.29	0.0967	9.0514	0.1040	2.821	0.748
7.15	7.004	0.146	10800	0.27	0.09	13.5771	0.1055	2.8608	0.759
7.15	6.964	0.186	14400	0.25	0.0833	18.1028	0.1008	2.733	0.725
7.15	6.924	0.226	18000	0.25	0.0833	22.6285	0.098	2.657	0.7051
7.15	6.884	0.266	21600	0.27	0.09	27.1542	0.0961	2.606	0.691

Table 24: Wear Rate values for Pure Aluminium with 4% Tungsten Carbide and 6% Red mud of 42 nm particle size at 600 rpm and 500^0C

Vs=1.256 m/s **ρ = 4.924x10³ kg/m³**

m_1	m_2	Δm	T	F_f	μ	R.Dx10^{-3}	$W_r \times 10^{-6}$	$W_v \times 10^{-12}$	$W_s \times 10^{-13}$
(gm)	(gm)	(gm)	(sec)	kgf		m	(N/m)	(m³/sec)	(m³/N-m)
7.23	7.188	0.042	3600	0.26	0.0867	4.5257	0.091	2.369	0.628
7.23	7.155	0.075	7200	0.25	0.0833	9.0514	0.0813	2.115	0.561
7.23	7.125	0.105	10800	0.24	0.08	13.5771	0.0759	1.974	0.523
7.23	7.095	0.135	14400	0.31	0.1033	18.1028	0.0732	1.903	0.505
7.23	7.065	0.165	18000	0.25	0.0833	22.6285	0.0715	1.861	0.493
7.23	7.035	0.195	21600	0.29	0.0967	27.1542	0.0704	1.833	0.486

CONCLUSION

The present Appendix-III gives the wear rate tables for pure aluminium with 2%, 4% and 6% red mud and 4% tungsten carbide of 10 N, 20 N and 30 N loads at normal condition and heat treatment conditions in two parts i.e., Appendix-III-A and Appendix-III-B. In the Chapter-6, the graphs are plotted for these Appendix III wear rate tables (Figure 6.1-6.9).

REFERENCES

1. Aghdam, M.M., Morsali, S.R., Hosseini, S.M.A., Sadighi, M., (2017), "Mechanical behavior of unidirectional SiC/Ti composites subjected to off-axis loading at elevated temperatures" Journal of Materials Science and Engineering, Vol. 688, pp 244-249.
2. Ahamed, H. and Senthil kumar, V. (2010), "Role of nano-size reinforcement and milling on the synthesis of nano-crystalline aluminium alloy composites by mechanical alloying", Journal of alloys and compounds, Vol. 505, pp. 772–782.
3. Alahelisten, A., Bergman, F., Olsson, M. and Hogmark, S. (1993), "On the wear of aluminium and magnesium metal matrix composites", Journal of wear, Vol. 165, no. 2, pp. 221–226.
4. Alan, L. Geiger and Andrew walker, J. (1991), "The processing and properties of discontinuously reinforced Aluminium Composite", Journal of the minerals metals and materials society (JOM), pp. 8-15.
5. Alaneme, K.K. (2011), "Corrosion behaviour of heat-treated Al-6063/SiC composites immersed in 5 wt% NaCl solution", Journal of material science, Vol. 18, pp. 55-64.
6. Alaneme, K.K., Akintunde, I.B., Olubambi, P.A. and Adewale, T.M. (2013), "Fabrication characteristics and mechanical behaviour of rice husk ash-alumina reinforced Al-Mg-Si alloy matrix hybrid composites", Journal of materials research technology, Vol. 2, pp. 60-67.
7. Alidokht, S.A., Alidokht, S. A., Abdollah-zadeh, A., Soleymani, S. and Assadi, H. (2011), "Microstructure and tribological performance of an aluminium alloy based hybrid composite produced by friction stir processing", Journal of materials design, Vol. 32, pp. 27-33.
8. AL-Mosawi, B.T., Wexler, D., Calka, A., (2017), "Characterization and mechanical properties of α-Al_2O_3 particle reinforced aluminium matrix composites, synthesized via uniball magneto-milling and uniaxial hot pressing", Journal of Advanced Powder Technology, Vol. 28 , pp 1054-1064.
9. Amirkhanlou, S., Rezaei, M.R., Niroumand, B. and Toroghinejad, M.R. (2011), "High strength and highly-uniform composites produced by compocasting and cold rolling processes, Journal of materials design, Vol. 32(4), pp. 2085–2090.
10. Baud, S. and Thevenot, F. (2001), "Microstructures and mechanical properties of liquid-phase sintered seeded silicon carbide", Journal of materials chemistry and physics, Vol. 67, pp. 165–174.

11. Beaumont, F.V. (2000), “Aluminum P/M: Past, present and future”, Journal of powder metallurgy, Vol. 36, pp. 41-44.
12. Bhatnagar, A., Vilar, V.J.P., Botelho, C.M.S. and Boaventura, R.A.R. (2011), “A review of the use of red mud as adsorbent for the removal of toxic pollutants from water and waste water”, Journal of environmental technology, Vol. 32, no.3, pp. 231–249.
13. Bobic, B., Mitrovic, S., Bobic, M. and Bobic, I. (2010), “Corrosion of metal matrix composites with aluminium alloy substrate”, Journal of tribology, Vol. 32, pp. 3-11.
14. Brown, K.R., Venice, M.S. and Woods, R.A. (1995), “The increasing use of aluminium in automotive applications”, Journal of materials, Vol. 47, pp. 20-23.
15. Brunori, C., Cremisini, C., Massanisso P., Pinto, V. and Torricelli, L. (2005), “Reuse of a treated red mud bauxite waste: studies on environmental compatibility”, Journal of hazardous materials, Vol. 117, pp. 55–63.
16. Chole Molineux J., Darryl Newport J., Bamdad Ayati, Chuang Wang, Stuart Connop P. and JonE. Green (2016), “Bauxite residue (red mud) as a pulverised fuel ash substitute in the manufacture of light weight aggregate”, Journal of cleaner production, Vol.112, pp.401-408.
17. Das, S.K., Kumar, S. and Ramachadrarao, P. (2000), “Exploitation of iron ore tailing for the development of ceramic tiles”, Journal of waste manage, Vol. 20, pp. 725–729.
18. Deqoyin, I.A., Mohamed, F.A. and Lavernia, E.J. (1991), “Particulate reinforced MMCs - a review”, Journal of material science, Vol. 26, pp. 1137-1156.
19. Deuis, R.L., Subramanian, C. and Yellup, J.M. (1996), “Abrasive wear of Aluminium composites - a review”, Journal of wear, Vol. 201, pp. 132-144.
20. Dolata, A.J., Dyzia, M. and Walke, W. (2012), “Influence of particles types and shape on the corrosion resistance of aluminium hybrid composites”, Journal of solid state phenomena, Vol. 191, pp. 81-87.
21. Doel, T.J.A. and Bowen, P. (1996), “Tensile properties of particulate-reinforced metal matrix composites”, Journal of composites-A, Vol. 27, pp. 655-665.
22. Doychak, J. (1992), “Metal and intermetallic matrix composites for aerospace propulsion and power systems”, Journal of the minerals metals and materials society (JOM), Springer-Verlag, Vol. 44, no.6, pp. 46-51.
23. Éva Ujaczki, Viktória Feigl, Mónika Molnár, Emese Vaszita, Nikolett Uzinger, Attila Erdélyi, Katalin Gruiz (2016), “The potential application of red mud and soil mixture as additive to the surface layer of a landfill cover system”, Journal of Environmental Sciences, Vol. 44, pp 189-196.

24. George, I. and Rack, H.J. (2003), "Powder processing of metal matrix composites in comprehensive composite", Journal of metal matrix composites, Elsevier, Vol. 3, pp. 617-653.
25. Geetha, B. and Ganesan, K. (2015), "The effects of ageing temperature and time on mechanical properties of A356 Aluminium cast alloy with red mud addition and treated by T6 heat treatment", Journal of materials today, Vol. 2, pp.1200-1209.
26. Ghazali, M.J., Rainforth, W.M. and Jones, H. (2007), "The wear of wrought aluminium alloys under dry sliding conditions", Journal of tribology, Vol. 40, pp. 160–169.
27. Giovanni Straffelini, Sergey Verlinski, Piyush Chandra, Verma, Giorgio Valota, Stefano Gialanella, (2016), "Wear and Contact Temperature Evolution in Pin-on-Disc Tribotesting of Low-Metallic Friction Material Sliding Against Pearlitic Cast Iron" Journal of Tribology Letters, Vol. 62, no. 36.
28. Groza, J.R. (1999), "Sintering of nano crystalline powders", Journal of powder metallurgy, Vol. 35, pp. 59-66.
29. Hansen, N. (1969), "Dispersion strengthened aluminium products manufactured by powder blending", Journal of powder metallurgy, Vol. 12 (23), pp. 23–44.
30. Hasheem, F. Ei-Labban., Abdelaziz, M. and Essam R.I. Mahmoud. (2013), "Characterisation of aluminium alloy-based nanocomposites produced by the addition of Al-Ti5-B1 to the matrix melt", American journal of nanotechnology, Vol. 4, pp. 8-15.
31. Hassan Adel Mahamood, Alrashdan Abdalla, Hayajneh Mohammed, T. and Mayyas Ahmad Turki (2009), "Wear behavior of Al–Mg–Cu-based composites containing SiC particles", Journal of tribology, Vol. 42, pp. 1230–1238.
32. Hunt, W.H. (2000), "New directions in aluminum-based P/M materials for automotive applications", Journal of powder metallurgy, Vol. 36, pp. 50-56.
33. John, E., Allison, Gerald and Cole, S. (1993), "Metal matrix composites on the automotive industry opportunities and challenge", Journal of the minerals metals and materials society (JOM), Vol. 45(1), pp. 19-24.
34. Johnson, D.L. (1986), "Solid state sintering", Journal of material science and engineering, Vol. 6, pp. 4520–4525.
35. Khurram S. Munir, Yifeng Zheng, Deliang Zhang, Jixing Lin, Yuncang Li, Cuie Wen, (2017), "Microstructure and mechanical properties of carbon nanotubes reinforced titanium matrix composites fabricated via spark plasma sintering", Journal of Materials Science and Engineering, Vol. 688, pp 505-523.

36. Kondoh, K. (2001), "Effect of Mg on sintering phenomenon of aluminium alloy powder particle", Journal of powder metallurgy, Vol. 44, pp. 161-166.
37. Kumar, Sanjay, Rakesh, Amitav and Bandopadhyay (2006), "Innovative methodologies for the utilisation of wastes from metallurgical and allied industries", Journal of resources conservatives recycling, Vol. 48, pp. 301–314.
38. Kunz, J. M. and Bampton, C.C. (2001), "Challenges to developing and producing MMCs for space applications", Journal of material processing technology, Vol. 53, No. 4, pp. 22-25.
39. Li Zhang, Qudong Wang, Wenjun Liao, Wei Guo, Wenzhen Li, Haiyan Jiang, Wenjiang Ding, (2017), "Microstructure and mechanical properties of the carbon nanotubes reinforced AZ91D magnesium matrix composites processed by cyclic extrusion and compression", Journal of Materials Science and Engineering, Vol. 689, pp 427-434.
40. Liao, C, Z., Shih, K., (2016), "Thermal behavior of red mud and its beneficial use in glass-ceramic production", Journal of Environmental Materials and Waste, pp 525-542.
41. Liu, W., Zhang, X. and Jiang, W. (2011), "Study on particle-size separation pretreatment of Bayer red mud", Journal of environmental engineering, Vol. 5, pp. 921–924.
42. Liu, Y., Lin, C.X. and Wu Y.G. (2007), "Characterization of red mud derived from a combined Bayer process and bauxite calcinations method", Journal of hazardous materials, Vol. 146, pp. 255-261.
43. Lumley, R.N. (1996), "The effect of solubility and particle size on liquid phase sintering", Journal of scripta materialia, Vol. 35, pp. 589-641.
44. Lumley, R.N. (1999), "Surface oxide and the role of magnesium during the sintering of aluminum", Journal of metallurgical and materials transactions A-physical metallurgy and materials science, Vol. 30, pp. 457-464.
45. Maddocks, G., Lin, C. and McConchie, D. (2004), "Effect of bauxite solution and biosolids on soil conditions of acid-generating mine spoil for plant growth", Journal of environment pollution, Vol. 127, pp. 157–167.
46. Martin, J.M. (2002), "Sintering behaviour and mechanical properties of Al-Zn-Mg-Cu alloy containing elemental Mg additions", Journal of powder metallurgy, Vol. 45, pp. 173-178.

47. Meijuan Li, Kaka Ma, Lin Jiang, Hanry Yang, Enrique J. Lavernia, Lianmeng Zhang, Julie M. Schoenung (2016), "Synthesis and mechanical behavior of nanostructured Al 5083/n-TiB_2 metal matrix composites", Journal of Materials Science and Engineering, Vol. 656, pp 241-248.
48. Michael oluwatosin Bodunrin, Kenneth Kanayo Alaneme and Lesley Heath Chown (2015), "Aluminium matrix hybrid composites: a review of reinforcement philosophies, mechanical, corrosion and tribological characteristics", Journal of materials research and technology, Vol.4, pp. 434-445.
49. Mohammad Jahedi, Ehsan Ardjmand, Marko Knezevic, (2017), "Microstructure metrics for quantitative assessment of particle size and dispersion: Application to metal-matrix composites", Journal of Powder Technology, Vol. 311, pp 226-238.
50. Naresh Prasad, Harekrushna Sutar, Subash Chandra Mishra, Santosh Kumar Sahoo and Samir Kumar Acharya (2013), "Dry sliding wear behaviour of aluminium matrix composite using red mud an industrial waste", International research journal of pure and applied chemistry, Vol. 3(1), pp. 59-74.
51. Na Zhang, Xiaoming Liu, Henghu Sun and Longtu Li, (2011), "Evaluation of blends bauxite calcination method red mud with other industrial wastes as a cementitious material: Properties and hydration characteristics", Journal of hazardous materials, Vol. 185, pp. 329–335.
52. Necat Altinkok, Adem Demir and Ibrahim Ozert, (2011), "Processing of Al_2O_3/SiC ceramic preforms and their liquid Al metal infiltration", Journal of composites part- A, Vol. 34, pp. 577-582.
53. Onat, A. (2010), "Mechanical and dry sliding wear properties of silicon carbide particulate reinforced aluminium-copper alloy matrix composites produced by direct squeeze casting method", Journal of alloys compound, Vol. 489, pp. 119-124.
54. Paramguru, R.K., Rath, P.C. and Misra, V.N. (2005), "Trends in red mud utilization-A review", Journal of mineral processing extractive metallurgy, Vol. 26, pp. 1–29.
55. Petrus, M., Wozniak, J., Cygan, T., Adamczyk-Cieslak, B., Kostecki, M., Olszyna A., (2017), "Sintering behaviour of silicon carbide matrix composites reinforced with multilayer grapheme", Journal of Ceramics International, Vol. 43, pp 5007-5013.
56. Poddar, P., Mukherjee, S., and Sahoo, K.L. (2008), "The microstructure and mechanical properties of SiC reinforced magnesium based composites by rheocasting process", Journal of materials engineering performance, Vol. 18, no.7, pp. 849–855.

57. Pramila Bai, B.N., Ramashesh, B.S. and Surappa, M.K. (1992), "Dry sliding wear of A356-Al–SiC composites", Journal of wear, Vol. 157, pp. 295–304.
58. Prasad, S.D. and Krishna, R.A. (2011), "Production and mechanical properties of A356.2/RHA composites", International journal of advance science technology, Vol. 33, pp. 51-58.
59. Qiang Liu, Ruirui Xin, Chengcheng Li, Chunli Xu and Jun Yang (2013), "Application of red mud as a basic catalyst for bio-diesel production", Journal of environmental sciences, Vol. 25, pp.823-829.
60. Qiu, X.R. and Qi, Y.Y. (2011), "Reasonable utilization of red mud in the cement industry", Journal of cement technologies, Vol. 6, pp. 103–105.
61. Ray, S. (1993), "Review - Synthesis of cast metal matrix particulate composites", Journal of material science, Vol. 28, pp. 5397–5413.
62. Reza Rahmany-Gorji, Ali Alizadeh, Hassan Jafari (2016), "Microstructure and mechanical properties of stir cast ZX51/Al_2O_3p magnesium matrix composites", Journal of Materials Science and Engineering, Vol. 674, pp 413-418.
63. Ri-xin Liu, Chi-sun Poon (2016), "Effects of red mud on properties of self-compacting mortar", Journal of Cleaner Production, Vol. 135, pp 1170-1178.
64. Rosenberger, M.R., Schvezov, C.E. and Forlerer, E. (2005), "Wear of different aluminium matrix composites under conditions that generate a mechanically mixed layer", Journal of wear, Vol. 259, pp. 590–601.
65. Sajjad Amirkhanlou and Behzad Niroumand (2012), "Microstructure and mechanical properties of Al 356/SiC cast composites fabricated by a novel technique", Journal of materials engineering and performance, Vol. 22, no.1, pp. 85-93.
66. Sajjadi, S.A., Ezatpour, H.R. and Beygi, H.(2011), "Microstructure and mechanical properties of Al-Al_2O_3 micro and nano composites fabricated by stir casting", Journal of materials science engineering-A, Vol. 528, pp. 8765-8771.
67. Samira Fatma Kurtoğlu, Sezen Soyer-Uzun, Alper Uzun (2016), "Tuning structural characteristics of red mud by simple treatments", Journal of Ceramics International, Vol. 42, pp 17581-17593.
68. Schaffer, G.B. (2001), "Liquid phase sintering of aluminium alloys", Journal of materials chemistry and physics, Vol. 67, pp. 85-87.
69. Senff, L., Hotza, D. and Labrincha, J.A. (2011), "Effect of red mud addition on the rheological behaviour and on hardned state characteristics of cement mortars", Journal of construction and building materials, Vol. 25, pp. 163-170.

70. Senthilvelan, T., Gopalakannan, S., Vishnuvarthan, S. and Keerthivaran, K. (2012), "Fabrication and characterisation of SiC, Al_2O_3 and B_4C reinforced Al-Zn-Mg-Cu alloy (AA 7075) metal matrix composites", Journal of advanced materials research, Vol. 622, pp. 1295-1299

71. Shuai Wang, Shengyu Zhu, Jun Cheng, Zhuhui Qiao, Jun Yang, Weimin Liu, (2017), "Microstructural, mechanical and tribological properties of Al matrix composites reinforced with Cu coated Ti_3AlC_2", Journal of Alloys and Compounds, Vol. 690, pp 612-620.

72. Shuqi Guo, (2016), "Effects of processing temperature on microstructures and mechanical behaviours of reactive hot-pressed SiC(SCS-6)/Ti/ZrB_2–ZrC hybrid composites", Journal of the European Ceramic Society, Vol. 36, pp 3851-3861.

73. Shuo Qin. and Bolin Wu. (2011), "Effect of self glazing on reducing the radioactivity levels of red mud based ceramic materials", Journal of hazardous materials, Vol. 198, pp. 269– 274.

74. Simchi, A. and Veltl, G. (2003), "Investigation of warm compaction and sintering behavior of aluminum alloys", Journal of powder metallurgy, Vol. 46, pp. 159-164.

75. Singh, J. and Chauhan, A. (2015), "Characterization of hybrid aluminum matrix composites for advanced applications – A review", Journal of material research technologies, Vol. 2, pp.116-123.

76. Singh, M., Upadhaya, S.N. and Prasad, P.M. (1997), "Preparation of iron rich cement from red mud", Journal of cement concrete residue, Vol. 27, no.7, pp. 1037–1046.

77. Siva Prasad, D. and Shoba, C. (2014), "Hybrid composites–a better choice for high wear resistant materials", Journal of material research technologies, Vol. 3(2), pp. 172–178.

78. Slipenyuk, A., Kuprin, V., Milman, Y., Goncharuk, V. and Eckert, J. (2006), "Properties of P/M processed particle reinforced metal matrix composites specified by reinforcement concentration and matrix-to-reinforcement particle size ratio", Journal of acta materials, Vol. 54, pp. 157-166.

79. Sneha Samal., Ajoy K. Ray and Amitava Bandopadhyay. (2013), "Proposal for resources, utilization and processes of red mud in India - A review", Journal of mineral processing Vol. 118, pp. 43–55.

80. Songhui Liu, Xuemao Guan, Saisai Zhang, Chi Xu, Haiyan Li, Jianwu Zhang (2017), "Sintering red mud based imitative ceramic bricks with CO_2 emissions below zero", Journal of Materials Letters, Vol. 191, pp 222-224.

81. Srivatsan, T.S. (1996), “Microstructure, tensile properties and fracture behaviour of Al_2O_3 particulate reinforced Al alloy metal matrix composites”, Journal of materials science, Vol. 31, pp. 1375-1388.
82. Tahamtan, S., Halvaee, A., Emamy, M. and Zabihi, M.S. (2013),“Fabrication of Al/A206-Al_2O_3 nano/micro composite by combining ball milling and stir casting technology”, Journal of materials design, Vol. 49, pp. 947-59.
83. Tomasz Cygan, Jaroslaw Wozniak, Marek Kostecki, Mateusz Petrus, Agnieszka Jastrzębska, Wanda Ziemkowska, Andrzej Olszyna, (2017), “Mechanical properties of graphene oxide reinforced alumina matrix composites” Journal of Ceramics International, Vol. 43, pp 6180-6186.
84. Torralba, J. M., Costa, C. E. and Velasco, F. (2003), "P/M aluminum matrix composites; an overview", Journal of material processing technology, Vol. 133, pp. 203 - 206.
85. Uyyuru, R.K., Surappa, M.K. and Brusethaug, S. (2007), “Tribological behaviour of Al–Si–SiCp composites/automobile brake pad system under dry sliding conditions”, Journal of tribology, Vol. 40, pp. 365–373.
86. Venkataraman, B. and Sundararajan, G. (2000), “Correlation between the characteristics of the mechanically mixed layer and wear behaviour of aluminium”, Journal of wear, Vol. 245, pp. 22–38.
87. Wilson, S. and Alpas, A.T. (1997), “Wear mechanism maps for metal matrix composites”, Journal of wear, Vol. 212, pp. 41 –49.
88. Xia Oming Liu Nazhang, Hanghu sun, JixiuZhang, Longtu Li. (2011), “Structural investigation relating to the cementous activity of bauxite residue- red mud”, Journal of cement and concrete research, Vol. 41, no.8, pp. 847-853.
89. Yang, J., Zhang, D., Hou, J., He, B. and Xiao, B. (2008), “Preparation of glass-ceramics from red mud in the aluminium industries”, Journal of ceramics international, Vol. 34, pp. 125-130.
90. Yang, Y. and Li, X. (2004), “Study on bulk aluminium matrix nano-composite fabricated by ultra-sonic dispersion on nano sized SiC particles in molten aluminium alloy”, Journal of materials science and engineering-A, Vol. 38, pp. 378-383.
91. Yanju Liu and Ravi Naidu. (2014), “Hidden values in bauxite residue (red mud): Recovery of metals-review”, Journal of waste management, Vol.34, pp. 2662-2673.

92. Yar, A.A., Montazerian, M., Abdizadeh, H. and Baharvandi, H.R. (2009), "Microstructure and mechanical properties of aluminum alloy matrix composite reinforced with nano-particle MgO", Journal of alloys compound, Vol. 484, pp. 400–404.
93. Yong Liu, Chuxia Lin and Yonggui Wu. (2007), "Characterization of red mud derived from a combined bayer's process and bauxite calcination method", Journal of hazardous materials, Vol. 146, pp. 255–261.
94. Youseffi, M., Showaiter, N. and Martyn, M.T. (2006), "Sintering and mechanical properties of prealloyed 6061 Al powder with and without common lubricants and sintering aids", Journal of powder metallurgy, Vol. 49, pp. 86-95.
95. Youssef, N.F., Shater, M.O., Abadir, M.F. and Ibrahim, O.A. (2002), "Utilization of red mud in the manufacture of ceramic tiles", Journal of engineering materials, Vol. 206, pp. 1775–1778.
96. Yunfeng Su, Yongsheng Zhang, Junjie Song, Litian Hu, (2017), "Tribological behaviour and lubrication mechanism of self-lubricating ceramic/metal composites: The effect of matrix type on the friction and wear properties", Journal of Wear, Vol. 372–373, pp 130-138.
97. ASM Metals Hand Book Volume 21- Composites, Volume Chairs- Daniel B. Miracle and Steven L. Donaldson.
98. Book: Materials Science and Engineering – An Introduction by William D. Callister, Jr., Wiley Publications.
99. Book: Annotated equilibrium diagrams of some aluminum alloy systems by Henry Wilfred Lewis Phillips (1959), The Institute of Metals- Aluminium Alloys, London.
100. Book: Aluminum alloys-structure and properties by Mondolfo, L.F. Butterworths (1976), ISBN: 978-0-408-70932-3, Elsevier Ltd.
101. Book: An Introduction to Metal Matrix Composites, by Clyne, T.W. and Withers, P.J. (1993), Cambridge University Press, Cambridge, UK, pp. 166–217.
102. Book: Composite Materials: Science and Engineering by Krishan K. Chawla, Springer New York Heidelberg Dordrecht London, ISBN: 978-0-387-74365-3.
103. Book: Physical Foundations of Materials Science by Gunter Gottstein, © Springer-Verlag Berlin Heidelberg, ISBN: 978-3-662-09291-0.

PUBLICATIONS

1. C.Neelima Devi, N.Selvaraj, V.Mahesh, "Nano Red Mud – Synthesis and Characterization" 5th International & 26th All India Manufacturing Technology, Design and Research Conference - AIMTDR 2014 on Dec 12-14, 2014 at IIT Guwahati, Assam India.
2. Neelima Devi Chinta, N.Selvaraj, and V. Mahesh, "Evaluation of Mechanical properties and Wear behaviour of Aluminium-Red mud Composite Synthesized by Powder Metallurgy" Journal of Ocean, Mechanical and Aerospace -Science and Engineering by International Society of Ocean, Mechanical and Aerospace Scientists and Engineers - Vol.23, pp.13-18, 2015.
3. Neelima Devi Chinta, N.Selvaraj, and V. Mahesh , "Characterization of Aluminium-Red mud-Tungsten Carbide Hybrid metal matrix Composite" International Conference on Electrical, Electronics and Optimization Techniques (ICEEOT) with IEEE catalog "978-1-4673-9939-5/16 (SCOPUS INDEXED Journal-IEEE Xplore) on March 3-5, 2016.
4. Neelima Devi Chinta, N.Selvaraj, and V. Mahesh, "Dry Sliding Wear behaviour of Aluminium-Red mud-Tungsten Carbide Hybrid Metal Matrix Composite" Journal of Materials Science and Engineering, Vol.149, No.1, pp.1-7, doi:10.1088/1757-899X/149/1/012094 (IOP Publishing, SCOPUS INDEXED, Thomson Reuters, Web of Science), 2016.
5. Neelima Devi Chinta, N.Selvaraj, and V. Mahesh, "Mechanical characterization of Aluminium-Red mud metal matrix composites" Journal of Materials Today: Proceedings Elsevier….to be published in 2017……...……Accepted).
6. Chinta Neelima Devi, N.Selvaraj, and V. Mahesh, "Effect of heat treatment on mechanical and wear properties of Aluminium-Red mud-Tungsten Carbide metal matrix hybrid composites" Proceedings of the 1st International and 18th ISME Conference, February 23rd – 25th, 2017, NIT, Warangal.

BIO-DATA

Name	**NEELIMA DEVI CHINTA**
Date of Birth	**18-08-1982**
Marital Status	**Married**
Present Position	**Assistant Professor** **Department of Mechanical Engineering** **University College of Engineering** **JNTUK-UCEV, Vizianagaram-535003** **Andhra Pradesh, India.**
Qualification	**M.E. (CAD/CAM)**
Permanent Address	**Staff Quarters –F3,** **University College of Engineering** **JNTUK-UCEV, Vizianagaram-535003** **Andhra Pradesh, India.**
E-mail	**cneelima.me@jntukucev.ac.in** **jntukneelima@gmail.com**

ACKNOWLEDGEMENTS

It is beyond my capacity to express deep sense of gratitude to my Supervisor **Prof. N. Selvaraj** for his meticulous guidance, constant encouragement and moral support throughout the course of this research work. I express my sincere gratitude and thanks to my Co-Supervisor **Prof. V. Mahesh**, Principal and Professor of Mechanical Engineering Department, S.R. Engineering College, Warangal for his continuous guidance and encouragement, which lead to the successful completion of this research work. I express my sincere gratitude and heartfelt thanks to **Prof. S. Srinivasa Rao**, Chairman - DSC and Head, Mechanical Engineering Department, National Institute of Technology, Warangal for his valuable guidance and suggestions during the research work.

I express my sincere thanks to **Director**, National Institute of Technology, Warangal for providing the necessary help in completing the research work at the institute. I am very much thankful to **Dr. M. J. Davidson**, Assistant Professor, Department of Mechanical Engineering, **Dr. Asith Kumar Khanra,** Assistant Professor, Department of Metallurgy and Materials Engineering and **Prof. A. R. C. Reddy**, Former Registrar NIT, Warangal and retired Professor of Physics Department, the members of DSC for giving directions and suitable suggestions during the course of study. I express my sincere gratitude and heartfelt thanks to **Prof. C. S. P. Rao**, Professor of Mechanical Engineering Department, National Institute of Technology, Warangal for his valuable guidance and suggestions during the research work

I express my sincere thanks to **all the faculty members** in Mechanical Engineering Department for their support during my research work. I express my sincere thanks to my co-scholars **T. Nagaveni, K. Kishore Kumar and P. Madhukar** for their help in completion of my research work. I wish to extend my sincere thanks to my **parents,** husband **Adepu Ashok Kumar**, only daughter **A. Ananya** and **family members**

for their understanding and continual support during the period of this research work. Finally, I thank everyone who contributed either directly or indirectly in the successful completion of this research work.

(C. Neelima Devi)